



UNIL | Université de Lausanne

Unicentre

CH-1015 Lausanne

<http://serval.unil.ch>

Year : 2013

ON THE ROLE OF PERIOD-2 IN THE ORCADIAN AND HOMEOSTATIC REGULATION OF SLEEP

La Spada Francesco

La Spada Francesco, 2013, ON THE ROLE OF PERIOD-2 IN THE ORCADIAN AND
HOMEOSTATIC REGULATION OF SLEEP

Originally published at : Thesis, University of Lausanne

Posted at the University of Lausanne Open Archive.
<http://serval.unil.ch>

Droits d'auteur

L'Université de Lausanne attire expressément l'attention des utilisateurs sur le fait que tous les documents publiés dans l'Archive SERVAL sont protégés par le droit d'auteur, conformément à la loi fédérale sur le droit d'auteur et les droits voisins (LDA). A ce titre, il est indispensable d'obtenir le consentement préalable de l'auteur et/ou de l'éditeur avant toute utilisation d'une oeuvre ou d'une partie d'une oeuvre ne relevant pas d'une utilisation à des fins personnelles au sens de la LDA (art. 19, al. 1 lettre a). A défaut, tout contrevenant s'expose aux sanctions prévues par cette loi. Nous déclinons toute responsabilité en la matière.

Copyright

The University of Lausanne expressly draws the attention of users to the fact that all documents published in the SERVAL Archive are protected by copyright in accordance with federal law on copyright and similar rights (LDA). Accordingly it is indispensable to obtain prior consent from the author and/or publisher before any use of a work or part of a work for purposes other than personal use within the meaning of LDA (art. 19, para. 1 letter a). Failure to do so will expose offenders to the sanctions laid down by this law. We accept no liability in this respect.



UNIL | Université de Lausanne

Faculté de biologie
et de médecine

Centre Intégréatif de Génomique

ON THE ROLE OF PERIOD-2 IN THE CIRCADIAN AND HOMEOSTATIC REGULATION OF SLEEP

Thèse de doctorat en Neurosciences

présentée à la

Faculté de Biologie et de Médecine
de l'Université de Lausanne

par

Francesco La Spada

Master en Biochimie à l'Université de Genève

Jury

Prof. Jean-Pierre Hornung - Président

Prof. Paul Franken - Directeur

Dr. Frédéric Gachon - Expert

Dr. Christelle Peyron - Expert

Lausanne 2013

***Programme doctoral interuniversitaire en Neurosciences
des Universités de Lausanne et Genève***



UNIL | Université de Lausanne



**UNIVERSITÉ
DE GENÈVE**

**Programme doctoral interuniversitaire en Neurosciences
des Universités de Lausanne et Genève**

Imprimatur

Vu le rapport présenté par le jury d'examen, composé de

Président	Monsieur Prof. Jean-Pierre Hornung
Directeur de thèse	Monsieur Prof. Paul Franken
Co-directeur de thèse	
Experts	Madame Dr Christelle Peyron Monsieur Dr Frédéric Gachon

le Conseil de Faculté autorise l'impression de la thèse de

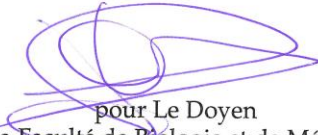
Monsieur Francesco La Spada

Master en biologie de l'Université de Genève

intitulée

**ON THE ROLE OF PERIOD-2 IN THE CIRCADIAN
AND HOMEOSTATIC REGULATION OF SLEEP**

Lausanne, le 29 novembre 2013


pour Le Doyen
de la Faculté de Biologie et de Médecine

Prof. Jean-Pierre Hornung

Remerciements

En premier lieu, je tiens à remercier Paul Franken de m'avoir donné l'opportunité de travailler au sein de son laboratoire avec un sujet de thèse qui, même si il a beaucoup changé et évolué, a toujours été très stimulant et captivant. Je lui suis également reconnaissant pour sa grande disponibilité, son enthousiasme envers la recherche et son sens critique aiguisé. La confiance et l'indépendance témoignées dès le début de mon doctorat ont été précieuses pour me réaliser professionnellement.

J'adresse également mes sincères remerciements à Valérie Mongrain et Thomas Curie pour m'avoir aiguillé au début de ma thèse, ainsi que pour les conseils et méthodes que vous avez su partager avec patience et altruisme.

Merci à Christelle Peyron, Frédéric Gachon, ainsi Jean-Pierre Hornung d'avoir accepté mon invitation à faire partie de mon jury de thèse.

Je remercie également mon mentor académique Béatrice Desvergne pour ses précieuses recommandations lors des moments clés de ma thèse.

Un grand merci à Géraldine Mang, Shanaz Diessler et Cyril Mikhail qui non seulement ont été des collègues exceptionnels sur lesquels j'ai toujours pu compter, mais également des amis bienveillants.

Je remercie également Hannes Richter membre de la plateforme génomique pour ses nombreux conseils en matière de qPCR, Yann Emmenegger et Angélique Vaucher pour leurs collaborations, ainsi que Valérie Hinard et Gérard Didelot pour leurs nombreuses suggestions techniques.

Je remercie tous les membres du groupe de Medhi Tafti, Annick Crevoisier, ainsi que toutes les personnes qui ont contribué à la privation de sommeil de mes souris.

Je voudrais remercier particulièrement Mariano Oppikofer pour ses conseils de vie et de science.

Finalement je souhaite remercier l'ensemble de ma famille qui depuis le début m'a ardemment soutenu. Un merci particulier à Mila, ma fille et Maude, ma femme qui ont su me supporter et m'épauler durant ces derniers mois parfois bien difficiles.

Abstract

Humans spend one third of their life sleeping, then we could raise the basic question: Why do we sleep? Despite the fact that we still don't fully understand its function, we made much progress in understanding at different levels how sleep is regulated. One model suggests that sleep is regulated by two processes: a homeostatic process that tracks the need for sleep and by a circadian rhythm that determines the preferred time-of-day sleep occurs.

At the molecular level circadian rhythms are a property of interlocking transcriptional regulators referred to as clock genes. The heterodimeric transcription factors BMAL1::CLOCK/NPAS2 drive the transcription of many target genes including the clock genes *Cryptochrome1 (Cry1)*, *Cry2*, *Period1 (Per1)*, and *Per2*. The encoded CRY/PER proteins are transcriptional inhibitors of BMAL1::CLOCK/NPAS2 thereby providing negative feedback to their own transcription. These genes seem, however, also involved in sleep homeostasis because the brain expression of clock genes, especially that of *Per2*, increase as a function of time-spent-awake and because mice lacking clock genes display altered sleep homeostasis.

The aim of first part of my doctoral work has been to advance our understanding the link that exists between sleep homeostasis and circadian rhythms investigating a possible mechanism by which sleep deprivation could alter clock gene expression by quantifying DNA-binding of the core-clock genes BMAL1, CLOCK and NPAS2 to their target chromatin loci including the E-box enhancers of the *Per2* promoter. We made use of *chromatin immunoprecipitation (ChIP)* and *quantitative polymerase chain reaction (qPCR)* to show that DNA-binding of CLOCK and BMAL1 to their target genes changes as a function of time-of-day in both liver and cerebral cortex. We then performed a 6h sleep deprivation (SD) and observed a significant decrease in DNA-binding of CLOCK and BMAL1 to *Dbp*. This is consistent with a decrease in *Dbp* mRNA levels after SD. The DNA-binding of NPAS2 and BMAL1 to *Per2* was similarly decreased following SD. However, SD has been previously shown to increase *Per2* expression in the cortex which seems paradoxical. Our results demonstrate that sleep-wake history can affect the molecular clock machinery directly at the level of the chromatin thereby

altering the cortical expression of *Dbp* and *Per2*, and likely other targets. However, the precise dynamic relationship between DNA-binding and mRNA expression, especially for *Per2*, remains elusive.

The second aim of my doctoral work has been to perform an in depth characterization of circadian rhythmicity, sleep architecture, analyze the response to SD in full null-*Per2* knock-out (*Per2*^{-/-}) mice, and *Per1*^{-/-} mice, as well as their double knock-out offspring (*Per1,2*^{-/-}) and littermate wildtype (Wt) mice. The techniques used include locomotor activity recording by *passive infrared* (PIR) sensors, EEG/EMG surgery, recording, and analysis, and cerebral cortex extraction and quantification of mRNA levels by qPCR. Under standard LD12:12 conditions, we found that wakefulness onset, as well as the time courses of clock gene expression in the brain and corticosterone plasma levels were advanced by about 2h in *Per2*^{-/-} mice compared to Wt mice. When released under constant dark conditions almost all *Per2*^{-/-} mice (97%) became arrhythmic immediately. From these observations, we conclude that while *Per2*^{-/-} mice seem to be able to anticipate dark onset, this does not result from a self-sustained circadian clock. Our results suggest instead that the earlier onset of activity results from a labile, not-self sustained 22h rhythm linked to light onset suggesting the existence of a light-driven rhythm. Analyses of sleep under LD12:12 conditions revealed that in both *Per2*^{-/-} and *Per1,2*^{-/-} mice the same sleep phenotypes are observed compared to Wt mice: increased NREM sleep fragmentation and inability to adequately compensate the loss of NREM sleep. That suggests a possible role of PER2 in sleep consolidation and recovery.

Résumé

L'homme passe près un tiers de sa vie à dormir. Ainsi nous pouvons nous poser la question fondamentale : Pourquoi dormons-nous ? Malgré le fait que nous ne saisissons pas encore la fonction du sommeil, beaucoup de progrès ont été faits dans l'étude de sa régulation. Un modèle suggère que le sommeil est régulé par deux processus : un processus homéostatique qui suit le besoin de sommeil et un processus circadien qui détermine à quels moments auront lieu les différents processus biologiques, physiologiques et comportementaux des êtres vivants durant le nycthémère.

Au niveau moléculaire, le rythme circadien est composé de deux boucles principales interconnectées. La première est constituée des hétérodimères BMAL1::CLOCK/NPAS2 qui va entraîner la transcription de nombreux gènes cibles en se fixant à leurs promoteurs E-box. Parmi ces gènes cibles se trouvent, entre autres, les gènes de l'horloge *Cryptochromes* (*Cry1* et *-2*) et *Periodes* (*Per1* et *-2*). Les protéines résultantes vont former les complexes PER/CRY qui vont opérer comme boucle de rétrocontrôle négative en inhibant leur propre transcription. Il a été préalablement démontré qu'une privation de sommeil chez la souris entraîne une altération de l'expression des gènes de l'horloge (en particulier *Per2*) dans le cerveau, suggérant que ces gènes ne sont pas uniquement impliqués dans les rythmes circadiens, mais également dans l'homéostasie du sommeil. Il a également été observé que certaines souris mutées pour un gène de l'horloge possèdent des altérations de leurs marqueurs de l'homéostasie du sommeil.

Le premier objectif de mon travail de thèse a consisté à approfondir le lien existant entre l'homéostasie du sommeil et les rythmes circadiens au niveau même de l'ADN. Nous avons voulu tester l'hypothèse selon laquelle une privation de sommeil (Pds) modifierait l'expression des gènes horloges en altérant la liaison spécifique de trois facteurs de transcriptions clés, à savoir BMAL1, CLOCK et NPAS2, aux séquences promotrices E-box des gènes cibles de l'horloges: *Per1*, *Per2*, *Cry1* et *Dbp*. Pour ce faire, nous avons utilisé comme technique l'immunoprécipitation de la chromatine (ChIP), ainsi que la réaction en chaîne par polymérase quantitative (qPCR). Pour la première fois, nous avons démontré que la liaison de CLOCK et BMAL1 aux gènes cibles variait de manière circadienne dans le

cortex cérébral, comme cela avait préalablement été établi dans le foie. Puis en effectuant 6h de PdS, nous avons observé une diminution significative des liaisons de CLOCK et BMAL1 au promoteur E-box de *Dbp* ; ce qui est cohérent étant donné que l'on observe une baisse de l'ARN de *Dbp* après la PdS. Cependant, nous obtenons également une baisse de la liaison au promoteur de *Per2* de la part de NPAS2 et BMAL1, alors qu'il est connu que l'ARN de *Per2* augmente après PdS, ce qui peut sembler paradoxal de prime abord. Nos résultats démontrent qu'une PdS affecte directement le mécanisme moléculaire de l'horloge lors de la liaison à l'ADN, au niveau cortical. Bien que la relation entre la liaison à l'ADN et l'expression de l'ARN semble comprise pour *Dbp*, la dynamique pour *Per2* reste bien plus compliquée à saisir.

Le second objectif de mon doctorat fut de caractériser de manière approfondie le rythme circadien et l'architecture du sommeil des souris mutantes pour les gènes *Per1*, *Per2*, *Per1,2*, ainsi que leurs réponses homéostatiques à une PdS. Les techniques employées ont été : enregistrements de l'activité locomotrice par capteurs infrarouges, enregistrement électroencéphalographique et la quantification des niveaux d'ARNm par qPCR du cortex cérébral. Nous avons découvert que sous des conditions standard 12h lumière/12h nuit (LD12:12), l'enclenchement de l'activité, l'expression des gènes de l'horloge dans le cortex, ainsi que les taux plasmatiques de corticostérone sont avancés d'environ 2h chez la souris *Per2*^{-/-} comparé aux sauvages (Wt). Dans des conditions d'obscurité constante, 94% des *Per2*^{-/-} deviennent immédiatement arythmiques. Les résultats obtenus ont démontré que bien que les souris *Per2*^{-/-} semblent capables d'anticiper l'obscurité, cela n'est pas le résultat d'une horloge circadienne autonome et fonctionnelle, mais plutôt la conséquence d'un rythme court de 22h induit par l'apparition de la lumière. Les analyses du sommeil en LD12:12 ont, en outre, révélées que les souris *Per2*^{-/-} et *Per1,2*^{-/-} comparées aux Wt avaient un sommeil profond plus fragmenté et étaient incapables de compenser adéquatement la perte de sommeil suite à une PdS. Ceci suggère fortement que PER2 possède un rôle dans la consolidation et la récupération du sommeil.

List of abbreviations

5-HT	: serotonin	DA	: dopamine
aa	: amino acid	DBP	: D-site albumin-promoter binding protein
AASM	: American academy of sleep medicine	DD	: constant dark condition
Ach	: acetylcholine	dDpMe	: dorsal deep mesencephalic reticular nuclei
AMPK1	: AMP-activated protein kinase catalytic subunit alpha-1	DFT	: discrete-Fourier transformation
AMP	: 5'adenosine monophosphate	DMH	: dorsomedial nucleus of the hypothalamus
ARNT	: Aryl hydrocarbon receptor nuclear translocator	DPGi	: dorsal paragigantocellular reticular nucleus
ATP	: adenosine-5'-triphosphate	DRN	: dorsal raphe nucleus
β -TrCP1	: see FBXW1A	DSPS	: delayed sleep-phase syndrome
BF	: basal forebrain	dSPZ	: dorsal subparaventricular zone
bHLH	: basic helix-loop-helix	DYRK1A	: dual specificity tyrosine-phosphorylation-regulated kinase 1A
BMAL1	: brain and muscle ARNT-like 1	E4BP4	: see NFIL3
cAMP	: cyclic adenosine monophosphate	EEF1A	: eukaryotic translation elongation factor 1A
CBP	: CREB binding protein	EEG	: electro-encephalogram
CCG	: clock controlled genes	EMG	: electro-myogram
cDNA	: complementary DNA	EOG	: electro-oculogram
ChIP	: chromatin immunoprecipitation	eVLPO	: extended ventrolateral preoptic area
CIRBP	: cold-inducible RNA-binding protein	EZH2	: enhancer of zest 2
CKI	: casein kinase I	FASPS	: familial advanced sleep-phase syndrome
CLD	: cytoplasm localization domain	FBXL3	: f-box/llr-repeat protein 3
CLOCK	: circadian locomotor output cycles kaput	FBXW1A	: f-box/wd repeat-containing protein 1A
CRE	: cyclic-AMP response element	GABA	: γ -aminobutyric acid
CRY	: cryptochrome	Gal	: galanin
		GAPDH	: glyceraldehyde-3-phosphate dehydrogenase

GC	: glucocorticoids	NA	: noradrenaline
Glu	: glutamate	NAD	: nicotinamide adenine dinucleotide
Gly	: glycine	NEC	: no enzyme control
GR	: glucocorticoid receptor	NES	: nuclear export site
GRE	: glucocorticoid response element	NFIL3	: nuclear factor, interleukin 3 regulated
GSK3 β	: glycogen synthase kinase 3	NLS	: nuclear localization signals
HAT	: histone acetyltransferase	NPAS2	: neuronal PAS domain protein 2
HCRT	: hypocretin/orexin	NREM	: non-rapid eye movement
HDAC3	: histone deacetylase 3	NTC	: no template control
His	: histamin	ORF	: open reading frame
HLH	: helix-loop-helix	PACAP	: pituitary adenylate cyclase-activating poly-peptide
Hprt	: hypoxanthine phosphoribosyltransferase	PAS	: Per-Arnt-Single-minded domain
HSE	: heat-shock element	pCREB	: phosphorylation of cyclic-AMP response element binding protein
HSF	: heat-shock factors	PeF	: perifornical hypothalamus
Ko	: knock-out	PER	: Period
LC	: locus coeruleus	PFP	: pontine reticular formation
LD	: light dark cycle	PIR	: passive infrared sensor
LDT	: laterodorsal tegmentum	PnC	: pontis caudalis
LL	: constant light condition	PnO	: pontis oralis
LTP	: long-term potentiation	POU2F	: POU domain, class 2, transcription factor protein
MCTQ	: Munich chronotype questionnaire	PPT	: pendonculopontine tegmentum
MLL1	: Methyltransferase mixed lineage leukemia 1	PRC	: phase response curve
MOP3	: see BMAL1	pro-rich	: proline rich region
MOP4	: see NPAS2		
MPO	: medial preoptic area		
MSF	: midpoint of sleep on free days		

PVN	: paraventricular nucleus	SLD	: sublaterodorsal tegmental nucleus
qPCR	: quantitative polymerase chain reaction	SWS	: slow-wave sleep
REM	: rapid eye movement	τ	: period length
RHT	: retinohypothalamic tract	TAE	: Tris, Acetate, EDTA
RORE	: retinoic acid-related orphan receptor response element	TBP	: TATA binding protein
RSP9	: Ribosomal protein S9	TK	: Herpes Simplex Virus thymidine kinase
RT	: room temperature	TMN	: tuberomammillary nucleus
SCN	: suprachiasmatic nuclei	vlPAG	: ventrolateral periaqueductal gray
SD	: sleep deprivation	VLPO	: ventrolateral preoptic area
SEM	: standard error of the mean	vPAG	: ventral periaqueductal
SI	: international system of units	vSPZ	: ventral subparaventricular zone
SIRT1	: sirtuin 1	Wt	: wild-type
		ZT	: Zeitgeber time

Table of contents

Remerciements	5
<i>Abstract</i>	6
<i>Résumé</i>	8
<i>List of abbreviations</i>	10
<i>Table of contents</i>	13
<i>List of figures</i>	17
<i>List of tables</i>	20
I. Sleep	24
1. Definition of sleep	24
2. Description of sleep.....	25
3. Neurochemistry of sleep and wakefulness	29
a. Wakefulness	29
b. NREM sleep	31
c. REM sleep.....	32
4. Regulation of sleep.....	33
a. Homeostatic process	33
b. Circadian process.....	35
c. Two-process model	35
II. Circadian Rhythm	36
1. Definition of circadian rhythm	37

2.	Circadian rhythm in animals.....	38
3.	Organization of circadian rhythms	41
4.	Chronotype.....	43
5.	Circadian rhythm at molecular level	45
a.	Core clock loops	46
b.	Secondary clock loop.....	47
c.	Chromatin remodeling	48
d.	Regulation by protein phosphorylation	49
e.	Temperature compensation.....	50
f.	Effect of the redox potential	51
III.	Sleep studies in clock mutant mice	51
1.	<i>Bmal1</i>	52
2.	<i>Clock & Npas2</i>	52
3.	<i>Cry</i>	53
4.	<i>Per</i>	54
5.	<i>Rev-erb</i>	57
IV.	<i>Period 1</i> and <i>Period 2</i>	58
1.	Genes.....	58
2.	Proteins	60
V.	Research outline.....	65
1.	DNA-binding of clock transcription factors as a function of sleep loss.....	65
2.	Circadian rhythms, sleep architecture and homeostasis in <i>Period</i> mutant mice	67

VI.	DNA-binding of clock transcription factors as a function of sleep loss.....	69
1.	Introduction.....	69
2.	Material and methods.....	71
a.	Animals and protocol	71
b.	Chromatin immunoprecipitation (ChIP).....	72
c.	Quantitative PCR	72
d.	Statistical analysis.....	74
3.	Results and discussion.....	75
a.	Rhythmic binding of BMAL1 and CLOCK to selected clock genes	75
b.	Sleep deprivation decreases BMAL1, CLOCK, and NPAS2 binding to specific clock genes ...	78
c.	Core clock transcription factor binding and transcriptional activation	81
4.	Conclusions and perspectives	84
VII.	Circadian rhythms, sleep architecture and homeostasis in <i>Period</i> knock-out mice	86
1.	Introduction.....	86
2.	Materials and methods	90
a.	Animals.....	90
b.	Genotyping.....	91
c.	Locomotor activity recordings and analyses.....	93
d.	EEG and EMG surgery, monitoring and analyses	94
e.	Gene expression in cerebral cortex and corticosterone quantification.....	98
f.	Western blotting	101
g.	Statistical analysis.....	101

3.	Results and discussion.....	103
a.	<i>Per2</i> ^{-/-} mice become immediately arrhythmic in DD despite dark-onset anticipation in LD 103	
b.	Rhythmicity could be triggered <i>Per2</i> ^{-/-} female	104
c.	Clock genes and corticosterone advance of 2h in <i>Per2</i> ^{-/-} mice	107
d.	How can an arrhythmic mouse anticipate dark onset?	110
e.	Altered sleep-wake state distribution in <i>Per</i> knock-out mice	112
f.	NREM sleep is fragmented in mice lacking <i>Per2</i>	114
g.	Quantitative EEG spectral profile in <i>Period</i> knock-out mice	115
h.	<i>Per2</i> ^{-/-} and <i>Per1,2</i> ^{-/-} mice sleep less after a sleep deprivation	117
i.	Homeostatic control of EEG delta power seems not affected by a lack of <i>Per2</i>	119
j.	Missing a central clock gene, <i>Per2</i> ^{-/-} react in the same way to a sleep deprivation at molecular level in the cerebral cortex.....	122
4.	Conclusions and perspectives	125
a.	Circadian characterization.....	125
b.	Sleep regulation analysis.....	132
c.	Others remarks.....	135
VIII.	Concluding remarks.....	138
IX.	References.....	140

List of figures

Figure 1 "Sleep and his half-brother Death" by John William Waterhouse, 1874	22
Figure 2 Typical polygraphic appearance of wakefulness, slow-wave sleep, and REM sleep in the adult mouse and human.....	26
Figure 3 Human hypnogram and sleep distribution in mice.	27
Figure 4 A schematic sagittal view of rodent brain showing the major structures and neurotransmitters involved in the regulation of the vigilance states	30
Figure 5 A schematic diagram of the flip-flop switch model.....	32
Figure 6 Two-process model of sleep regulation.....	35
Figure 7 Real acrograms and phase response curve in mice.....	38
Figure 8 Schematic diagram of synchronized SCN by sunlight.....	41
Figure 9 A schematic diagram to illustrate the several-stage integrator for circadian rhythms	42
Figure 10 Illustration of chronotype	44
Figure 11 Mammal circadian clock is composed of a transcriptional-translational feedback network	47
Figure 12 Chromatin remodeling in the circadian clock.....	48
Figure 13 Circadian rhythms of clock gene expression and clock protein levels in the mouse suprachiasmatic nucleus	51
Figure 14 Comparison between mains domains of PER1 and PER2 proteins and detailed domains and protein interation region for PER2 protein	61
Figure 15 Hypothesis of the DNA-binding project.....	66
Figure 16 Overview of the CHIP time-of-day experiment.....	71
Figure 17 Western blot α-NPAS2.....	72
Figure 18 BMAL1 and CLOCK binding onto the promoter of 4 clock genes in the mouse liver and cerebral cortex.....	74

Figure 19 The effect of time-of-day (ZT) on BMAL1 and CLOCK binding onto the promoter of 4 clock genes in the mouse liver.....	76
Figure 20 The effect of time-of-day (ZT) on BMAL1 and CLOCK binding onto the promoter of 4 clock genes in the mouse cerebral cortex.....	77
Figure 21 The effect of sleep deprivation on BMAL1, CLOCK, and NPAS2 binding onto the promoter of 4 clock genes in the mouse cerebral cortex	78
Figure 22 Overview of the phase relationship between RNA expression and chromatin binding...	82
Figure 23 Generation of <i>Per1</i> ^{-/-} and <i>Per2</i> ^{-/-} knock-out mice.	90
Figure 24 Western blot analysis of PER2 protein in the forebrain and in the cerebral cortex	91
Figure 25 <i>Per1</i> and <i>Per2</i> genotyping samples.....	93
Figure 26 Layout of electrode placements on mouse skull.....	94
Figure 27 Schematic description of the experimental recording setup.....	95
Figure 28 Example of EEG/EMG signals for wakefulness, NREM and REM sleep.....	96
Figure 29 Time-course of expression of house-keeping genes across 12 hours in the cerebral cortex	99
Figure 30 Actograms of <i>Per</i> knock-out male mice under LD12:12 and DD conditions.....	105
Figure 31 Actograms of <i>Per</i> knock-out female mice under LD12:12 and DD conditions	106
Figure 32 Time-course of mRNA expression concentration in cerebral cortex across 12 hours in <i>Per2</i> ^{-/-} and Wt mice.....	108
Figure 33 Time-course of plasma corticosterone concentration across 12 hours in <i>Per2</i> ^{-/-} and Wt mice	109
Figure 34 Effect of lengthening the photoperiod and inverting the LD schedule on activity onset in <i>Per2</i> ^{-/-} mice.....	111
Figure 35 Sleep-wake states across baseline in <i>Per</i> knock-out mice.....	112
Figure 36 Distribution of episode duration for NREM sleep and wakefulness <i>Per</i> knock-out mice.....	115
Figure 37 EEG spectral profiles of 48h baseline for each genotype.....	116

Figure 38 Effect of 6 hours of sleep deprivation (SD) on sleep in <i>Per</i> knock-out mice	118
Figure 39 Time course of EEG delta power during baseline and recovery sleep in <i>Per</i> knock-out mice	120
Figure 40 Effects of 6-h sleep deprivation on slow-wave activity in NREM sleep.....	121
Figure 41 Effect of 6 h sleep deprivation on mRNA level in the cortex of <i>Per2^{-/-}</i> and Wt mice.....	122
Figure 42 Effect of 6 hours of sleep deprivation (SD) on mRNA level in the cortex of Wt mice with or without access to food.....	124

List of tables

Table 1 Summary of all phenotype in clock mutant mice	58
Table 2 All transcripts and protein variants for <i>Per1</i> and <i>Per2</i>	59
Table 3 Main murine Per-Arnt-Sim (PAS) domain superfamily members with associated domains and features. From McIntosh B.E., Hogenesch J.B. & Brad C.A. (2010) [223]	62
Table 4 Primers and probes used for quantitative PCR.....	73
Table 5 Primers used for PCR genotyping.....	93
Table 6 Primers and probes used for quantitative PCR.....	100
Table 7 Summary table of sleep-wake state amounts	113
Table 8 Summary table of sleep-wake state amounts during the recovery.....	119

Insanity: doing the same thing over and over again and expecting different results.

Albert Einstein

Science: doing the same thing over and over again and expecting the same results.

Francesco La Spada

Introduction

Humans spend one third of their life sleeping. The basic question “Why do we sleep?” is a conundrum. For many centuries, sleep was associated to death. For example, in the Greek mythology the act of sleeping was personified by the god Hypnos who was the twin brother of Thanatos, the god of death, both children of Nyx the primordial goddess of the night (Fig.1)[1]. This allegory perfectly summarizes the idea



Figure 1 "Sleep and his half-brother Death" by John William Waterhouse, 1874 (Oil on canvas)

that women and men had of sleep: a mysterious state homologous to death in its stillness, unconsciousness and loss of muscular tone. This similarity between death and sleep has appeared many times in the literature until present day, like the citation of Arthur Schopenhauer: “*Each day is a little life: every waking and rising a little birth, every fresh morning a little youth, every going to rest and sleep a little death.*”[2]. However, this “little death” was considered useless and a waste of time but nevertheless essential to life, especially to the recovery that it provides. The nature of that what recovered is, however, still not understood.

The first important step forward in the description of sleep was made possible by the discovery of the *electro-encephalogram* (EEG) in 1924 by the neurologist Hans Berger with the initial objective to demonstrate his theory on mental telepathy [3]. This technic permitted in 1937 to Alfred Lee Loomins *et al.* to demonstrate that sleep is not a unitary state and they defined the first classification and description of the vigilance states [4]. In 1953, rapid eye movement were discovered by Eugene Aserinsky and Nathaniel Kleitman [5]. However Michel Jouvet discovered in 1959 that specific brain activity and muscle atonia were associated to rapid eye moment and thus he identified a new independent state of alertness called “paradoxical sleep” that could be also named *rapid eye movement*

(REM) sleep [6]. From 2007 the *American academy of sleep medicine* (AASM) proposed technical specification and precise terminology to distinguish five sleep-wake states in human [7].

To understand the function of sleep, Allan Rechtschaffen *et al.* proved in 1989 its necessity showing that a long period of constant sleep deprivation in rats had an enormous impact on metabolism, food intake, immune response, body temperature and provoked the death of the animal [8]. In human long constant sleep deprivation or daily small sleep deprivation decreased the cognitive skills (memories task, reaction time, etc.), increased the hallucination risk and modified the mood and judgment [9]. Unfortunately these observations didn't explain why we sleep. However, based on many observations, many hypotheses were put forward. For example, sleep could be important to restore the balance of energy and metabolites (adenosine and glycogen), altered during wakefulness [10, 11]; to equilibrate the synaptic potentiation accumulated during the wakefulness [12]; to reverse damage caused by oxidative stress in wakefulness [13]; to consolidate learning and memory [14] or on contrary to forget useless information [15].

Despite the fact that we still do not fully understand its function, we made much progress in understanding at different levels how sleep is regulated such as the neurophysiological basis of *non-rapid eye movement* (NREM) and REM sleep and its molecular components and neurotransmitters [16, 17]; and many conceptual models of sleep regulation were proposed as the reciprocal-interaction model of NREM–REM sleep alternation [18], the flip-flop switch model [19], and the two process model [20]. This latter proposes that two main processes contribute to determine the sleep/wake cycle and the sleep structure [21]. The first one is the circadian rhythm (process C) that determines when it is the better moment for wakefulness and sleepiness to occur across a 24h day. The second is the homeostatic process (process S) that tracked the need for sleep that increased during wakefulness and decreased during the sleep. This model assumes that both process S and C are independent and their interaction predicts the sleep/wake distribution. These two processes are considerate as separate at the neuroanatomical and physiological level. In fact, forced desynchrony studies where human were scheduled to a 28h day shown that marker of the process S was inde-

pendent of the process C [21]. Similar conclusion was done in lesion of the *suprachiasmatic nuclei* (SCN, the masterclock of the mammals) studies in several animals [22-25]. In fact, the suppression of circadian rhythm did not affect the dynamic of the process S. However, it was show that these two processes are interconnected by a molecular link. This idea is based on two types of observations. The first one is that mice with disrupted clock genes have changes in the dynamics of the sleep homeostatic process. The second type of observation was that an increase in homeostatic sleep pressure by doing a sleep deprivation increases the expression of certain clock genes [26].

To better understand at which level this link is regulated, the first project of this thesis investigated a possible mechanism by which sleep deprivation could alter clock gene expression at DNA-binding level. To further investigate how this link operated, the second project aimed to characterize scrupulously the circadian and homeostasis aspects of sleep regulation in mice lacking the central clock genes named *Period*.

Before to show my experimental work, some general concepts on sleep and its regulation will be introduced in the next pages, followed by a section dedicated to the role of circadian rhythms at the physiological and molecular level. Moreover, I will specially focus on those aspects that are pertinent to my experiments as circadian and sleep phenotype in clock mutant mice, and finally I will provide a description of the *Period* genes, their function and interactions.

I. Sleep

1. Definition of sleep

Sleep is a basic behavior present in almost all animals studied thus far. However depending on the species, the proprieties of sleep differ. For example, REM sleep is only present in mammals and birds. However, in invertebrates and reptiles the sleep state could not been defined as REM and NREM sleep state, and the term sleep-like state was preferred as in turtles, in drosophila or in honey bee [27, 28]. Unihemispheric NREM sleep has been observed in in cetaceans , seals , and birds [29].

In absence of EEG, the behavioral definition of sleep becomes an immobile state in a species specific body posture with a notable decreased response to various external stimuli. Moreover, this

state has to be quickly reversible, it has to follow a homeostatic regulation, and it has to be required for survival. Indeed, if sleep is prevented death might occur [30]. Although sleep as a behavior can be readily recognized, all previous criteria are needed to distinguish this state from torpor, hibernation and coma.

2. Description of sleep

The standard procedure to analyze sleep in mammals and birds is to use the EEG to measure the electrical activity of the forebrain (more specially the cortex). To gather more information, *electromyogram* (EMG) and *electro-oculogram* (EOG) are often recorded in parallel to detect the muscle tone and eye movements, respectively. Together these signals permit to identify the two sleep states NREM sleep (also called slow-wave sleep, SWS) and REM sleep (also called paradoxical sleep). Note that REM sleep is not detected in cetaceans and only observed in the brainstem of the monotremata family [29]. An alternative and non-invasive technique to collect data on vigilance states in mice is the piezoelectric system that detects animal's movements with high sensitivity permitting to automatically distinguish sleep from wakefulness [31]. In the context of this thesis, I will focus on human and mice studies for the detailed description of different vigilant states.

One protocol currently used in human was standardized by the AASM [7]. It proposes to place non-invasive electrodes in a detailed location on the human scalp and recommended specific EEG derivations between the electrodes to collect the EEG. For the minimal montage in mice, two EEG electrodes were fixed in parietal and frontal bones in the right hemisphere. This placement was chosen to ensure an optimal distinction between the different behavioral states [32]. In fact, the frontal electrode was sited over the frontal cerebral cortex to detect the slow waves oscillations (<5Hz) characteristic of the NREM sleep. The parietal electrode was placed just over the hippocampal structure to capture at best the theta oscillation (5-7Hz) characteristic of the REM sleep. This bipolar acquisition permits to measure the potential difference between the electrodes [33]. These electrodes detect a complex electric signal resulting mainly from summed synaptic currents from the apical dendrites of pyramidal cortical neurons. Synchronized electrical activity in large numbers of these

neurons provides the basis for the changes in extracellular field potentials that underlie the EEG that can be described by amplitudes and frequencies variations [34].

The EEG during wakefulness is composed of irregular signal of small amplitude (mainly alpha rhythm 8–12Hz) often associated with a high and variable muscle tone (EMG) and eye movements (EOG) in both human and mice illustrated in figure 2 [7, 35].

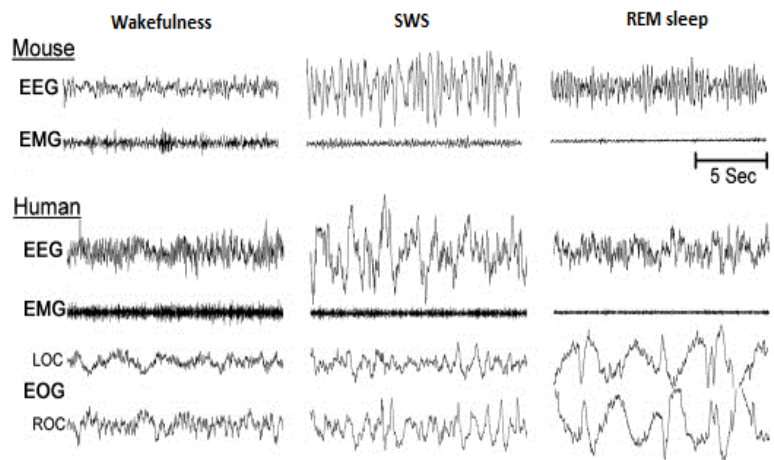


Figure 2 Typical polygraphic appearance of wakefulness (left column), slow-wave sleep (middle column), and REM sleep (right column) in the adult mouse and human. Wakefulness presents low-amplitude and high-frequency EEG waves (sign of activated cortex) and muscles tone. *Slow-wave sleep* (SWS, part of NREM sleep) have high-amplitude, low-frequency EEG waves with slightly reduced muscle tone. During REM sleep, cortical EEG is as activated (low-amplitude, high-frequency waves) as during wakefulness, but with reduction or absence of muscle tone (atonia) and presence of rapid eye movements. Time bar (for all species and states) = 5s. EEG = electroencephalogram; EMG = electromyogram; EOG = electrooculogram. Modified from Datta S. et al. (2007) [35].

NREM sleep in humans is segregated in 3 distinct stages corresponding to increasing depth of NREM sleep. The first one, N1, represent a transition stage with low amplitude and mixed frequency activity (mainly 4-7Hz). Usually the first N1 epoch is considered as the sleep onset. The second stage, N2, is characterized by spindles (a train of distinct waves of 12-14Hz with a maximal duration of 0.5s) and K-complexes (a negative sharp deflection followed by a slower positive component with a maximal duration of 0.5s). The last stage, N3, is characterized by the largest EEG amplitude and prominent slow-wave. For this reason this stage is also called SWS (Fig.3) [7, 34, 35]. Usually NREM sleep is not further subdivided in stages in mice, although similar changes occur between the beginning and the end of the state, such as spindles. NREM sleep has the highest amplitude with predominantly delta activity. Note that no distinction is done between the terms NREM sleep and *slow-wave sleep* (SWS) in mice. Both in man and mouse, NREM sleep is characterized by reduced muscle tone [34, 36]. REM sleep is composed of EEG pattern similar to wakefulness, with low amplitude and high frequency activity. Muscle tone is at the lowest levels of the entire recording (muscle atonia), despite occasional twitches shorter than 0.25s. Irregular and sharply peaked eye movements with an initial deflection usually lasting less than 500ms are present

in human. Due to its smaller size, the EOG recordings are normally not utilized to identify sleep-wake states in mice (Fig.2) [34-36].

In human, the different sleep stages mentioned above are structured in a precise sequence in a regular night. For example, in a normal young adult following a conventional sleep/wake schedule without sleep complaints, the sleep state sequence looks like in figure 3 upper panel [37]. Indeed, sleep was composed by 4 or 5 cycles of approximate length of ca. 90-100min. Each cycle begins with NREM sleep stage N1, followed by stage N2 and, especially in the first half of the night, by stage N3. Thereafter a small moment of stage N2 appear, followed

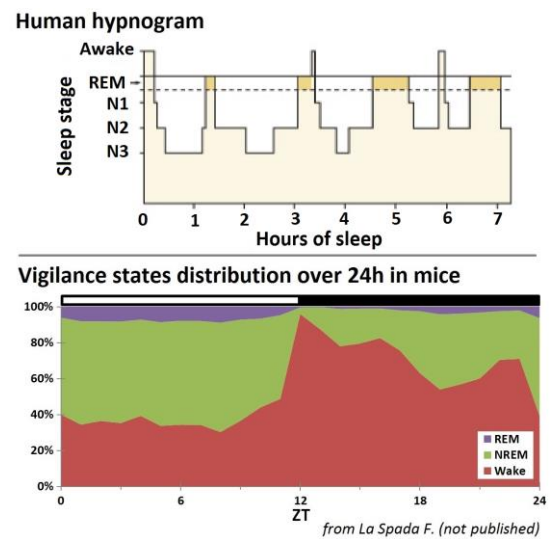


Figure 3 Human hypnogram and sleep distribution in mice. Upper panel Vigilance state distribution in a precise sequence in a normal young adult human night Lower panel Vigilance states distribution over one day in inbred C57BL6/J mice

by REM sleep. After REM sleep's end, a new cycle starts with sometimes a short arousal between. A regular night is structured by 4 to 5 cycles. The first cycles are composed principally by NREM sleep, while the last cycles are composed mainly by REM sleep [37]. Aging affects the sleep architecture and the EEG in humans. In fact, sleep becomes more fragmented, the prevalence of EEG slow waves during NREM sleep decreases and the time spent in NREM sleep stage N3 decreases accordingly as we get older [38].

In C57BL6/J mice the NREM and REM sleep follow a distribution over the day as illustrated in figure 3 lower panel. Note that mice are a nocturnal species and that they sleep mostly during the day, although considerable amounts of sleep are usually present also in the dark period. The usual sequence during sleep in mice is first NREM sleep that is followed sometimes by a REM sleep episode and ends by an arousal. Nevertheless, this order is not strictly respected. In opposition to human whose sleep is monophasic, mice have a polyphasic sleep. In the first part of light period, the sleep is composed by long episode of NREM sleep followed by regular REM sleep episode. It is the most consolidate sleep period. In the second half of this light period, the NREM sleep became more fragment-

ed and less NREM sleep was reported. Some strains of mice are known to take a 'nap' in the second half of the dark period. [32, 36]. The effect of aging is similar in mice compared with human. In fact, the time spent in sleep is smaller in inbred strain mice older than 15 months compared with young of 4 months. Moreover, older mice have less consolidation of sleep and appear to make up this lost sleep over longer time periods [39, 40].

Besides using the EEG to differentiate between different sleep-wake states, the EEG signal contains a lot of information that can be extracted and quantified mathematically. The EEG recorded signal is transformed by a Fast Fourier transformation algorithm to obtain EEG power spectra [41]. This spectrum is divided into the following frequency bands: delta (1–4Hz), theta (5–9Hz), alpha (8–12Hz), sigma (12–15Hz), beta (16–30Hz), low gamma (30-70Hz), and high gamma (70-120Hz) [34, 42]. The reader is reminded that 1 Hertz (Hz) is a SI unit defined as the number of cycles per second to calculate a periodic phenomenon. [43, 44].

During wakefulness, the EEG spectrum is characterized by theta when the animals moving or exploring and with attention and memory task in human (in humans often slower in frequency 2.5-4.0 Hz). The spectrum is also composed of beta and gamma range frequencies (15-120Hz), especially during quiet waking. During relaxed wakefulness, alpha (8-12Hz) rhythms can be observed in humans [34]. SWS is characterized by the largest EEG amplitude and prominent delta (1-4Hz) activity both in human and mice. [7, 34]. Delta activity is typical of the deeper stages of NREM sleep [45-48]. The total power of the EEG signal that occurs within the delta band is called EEG delta power and it is a widely-used marker of the homeostatic sleep need representing the sleep intensity [26]. Changes in delta power can be calculated in mammals based on the sleep/wake distribution especially under sleep deprivation condition. In fact, sleep deprivation increases the delta power [46, 48]. On the other hand, an excess of sleep by nap preceding nighttime sleep prolongs sleep latency and reduces EEG delta power [49]. Unusual higher beta activity in SWS appears in human suffering of primary insomnia resulting from cortical arousal [50]. REM sleep is composed principally by strongly synchronized activity in the theta (5-9Hz) range in rodents that is very similar to wakefulness [34]. However a ge-

netic study suggests that theta generated from hippocampus during REM sleep differ from wakefulness. In fact mice with deficiency in short-chain *acylcoenzyme A dehydrogenase* causes a marked slowing in theta frequency during sleep only. This [51]. In contrast to rodents, theta rhythm is not observed continuously in human, but rather is limited to 1s bouts [34].

3. Neurochemistry of sleep and wakefulness

a. Wakefulness

Wakefulness is one term that encompasses many different behaviors each with their specific brain activity. This following is a very simplified rendition of the complexity that accompanies the initiation and maintenance of wakefulness which only the main players are mentioned. At the neuronal level, it involves multiple redundant structures. Most structures, described below, are dispensable for the maintenance of cortical activation, even though they all contribute. Studies indicated that each structure could be responsible for the waking induction by a specific arousal. For example, new and unexpected external stimulus activate noradrenergic neurons that induce wakefulness and play an important role in alertness; a very lower glucose cerebral level mediate the activation of hypocretin/orexin neurons promoting also waking [52-54]. As illustrated in figure 4, wakefulness is mainly regulated by particular cells groups in the hypothalamus, basal forebrain and brainstem that arouse the thalamus and cerebral cortex in the same way in human and mice. Shortly, histaminergic neurons of the *tuberomammillary nucleus* (TMN) of the posterior hypothalamus project in all central nervous system producing a constant slow activity.

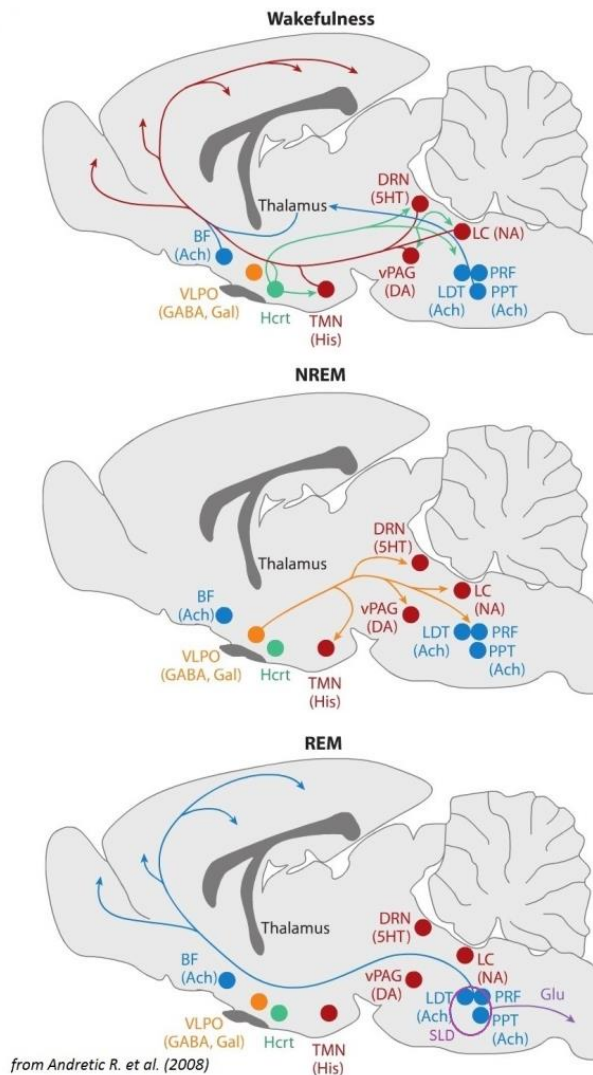


Figure 4 A schematic sagittal view of rodent brain showing the major structures and neurotransmitters involved in the regulation of the vigilance states. **Wakefulness** is maintained by cholinergic (in blue) ascending inputs from the brainstem (PFP, LDT, PPT) to the thalamus, which in turn activates the cortex, and from the BF. Additionally, monoaminergic (in red) such as 5HT from DRN, NA from LC, DA from vPAG, and His from TMN; as well as Hcrt (in green) inputs, contribute to the waking cortical activation. **NREM sleep** may be initiated and maintained by GABA and galanin inhibitory inputs (in orange) from the VLPO to all wakefulness-promoting brain sites. **REM sleep** cortical activation is under the control of cholinergic and non-cholinergic structures arising from SLD in the brainstem, while REM sleep atonia is under the control of the glutamatergic and glycinergic projections to the spinal cord (in purple). Andretic R. et al. (2008) [55]

Neurotransmitters: Ach: acetylcholine; 5HT: serotonin; NA: noradrenaline; DA: dopamine; His: histamin; Hcrt: hypocretin/orexin; GABA: γ -aminobutyric acid; Gal: Galanin; Glu: glutamate; Gly: glycine.

Brain region: PFP: pontine reticular formation; LDT: laterodorsal tegmentum; PPT: pedunculopontine tegmentum; BF: basal forebrain; DRN: dorsal raphe nucleus; LC: locus coeruleus; vPAG: ventral periaqueductal; TMN: tuberomammillary nucleus; VLPO: ventrolateral preoptic nucleus; SLD: sublateralodorsal tegmental nucleus.

Hypocretin/orexin neurons located in *lateral hypothalamus* (LH) project throughout the brain and especially to other wake-promoting centers [16, 55-57]. These neurons have a key role to stabilize the waking state. In fact, deficits in neuropeptides hypocretin/orexin or in their receptors cause the sleep disorder narcolepsy [58-61]. People suffering of this pathology were not able to sustain continually wakefulness and have spontaneous attacks of irresistible sleepiness especially during emotional situations [62]. The *basal forebrain* (BF) is essentially composed by cholinergic, glutamatergic and GABAergic neurons that during wakefulness project to the cortex and thalamus. Cholinergic and glutamatergic neurons directly rouse cortical neurons through nicotinic and glutamatergic receptors as well as indirectly by inhibiting specific thalamic neurons. GABAergic neurons activate the cortical neurons indirectly by inhibiting cortical interneurons. Most of these neurons are responsible of cortical

activation during wake and also REM sleep. [54, 63]. In the brainstem, the *pedunculopontine tegmentum* (PPT) and *laterodorsal tegmentum* (LDT) nuclei, which are also composed of cholinergic neurons, project to the reticular nucleus and to the thalamic-relay nuclei both in the thalamus. These latter nuclei facilitate the activation of the cerebral cortex during wake and REM sleep [54, 57, 64]. Serotonergic neurons from *dorsal raphe nucleus* (DRN or raphe), noradrenergic neurons from *locus coeruleus* (LC), and dopaminergic neurons from *ventral periaqueductal gray matter* (vPAG) project to the cortical region of the brain [55, 57, 65].

b. NREM sleep

During NREM sleep, the wakefulness-promoting brain sites (TMN, PPT, LDT, DRN, LC, vPAG) and hypocretin/orexin neurons in *perifornical hypothalamus* (PeF) are inhibited by GABAergic and galaninergic neurons from the *ventrolateral preoptic nucleus* (VLPO) in the hypothalamus [57, 66, 67]. VLPO cells show their first signs of inhibition activity during drowsiness and continue to discharge throughout NREM sleep and are able to initiate and maintain NREM sleep. While the wake-promoting structures are less active during NREM sleep, they are not completely repressed [55, 57]. Note that VLPO is inhibited by the arousal systems that it inhibits during sleep. In fact, serotonergic neurons from DRN, noradrenergic neurons from LC and GABAergic neurons from TMN inhibit VLPO neurons [57, 68, 69]. Hypocretin/orexin plays a role in the maintenance of the sleep as well. Actually, narcoleptic people do not sleep more than normal individuals but waking more often from sleep at night [56]. The complex circuit containing both inhibitor and activator elements modulate the wakefulness/sleep mechanism seems to follow an electronic flip-flop model, where the production of states are discrete with sharp transitions. In fact, this model tend to avoid transitional states, because when either side begins to overcome the other, the switch 'flips' immediately into the alternative state (Fig.5) [57].

Adenosine is also an important player in sleep regulation [70]. Adenosine is the molecular basis component of *adenosine-5'-triphosphate* (ATP) synthesis. To produce the energy that neurons require, ATP is consumed and degraded in the secondary by-product adenosine which concentration increases in the brain in activity-dependent manner. Thereby adenosine increases with time spent awake [71]. Adenosine binds several receptors which A_1 and A_{2A} are probably promoting sleep. In fact, adenosine inhibits excitatory neurotransmission of neurons in all nervous system by A_1 receptor binding. Moreover, adenosine binds also the A_{2A} receptor present in the VLPO area that contribute to promote sleep as explain above [72]. The most commonly used substance to avoid sleepiness is the caffeine that is an adenosine antagonist increasing wakefulness and sleep latency [73].

c. REM sleep

Brainstem structures are sufficient and necessary to trigger and maintain the REM sleep state [74]. More precisely the REM sleep onset is triggered by neurons in the dorsal part of the *pontis oralis* (PnO) and *caudalis* (PnC) nuclei in cats [74-76]. In rodents, glutamatergic neurons from a specific brainstem region called *sublaterodorsal tegmental nucleus* (SLD) trigger REM sleep and also cause muscle atonia [77, 78]. The inhibition from the VLPO observed in NREM sleep is even more pronounced in REM sleep [55].

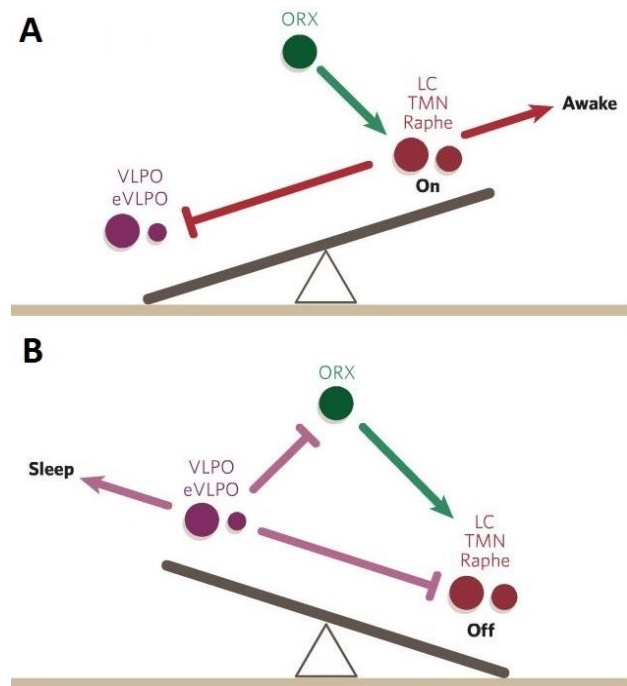


Figure 5 A schematic diagram of the flip-flop switch model. A During wakefulness, the monoaminergic nuclei (LC, TMN, Raphe; red) inhibit the VLPO (purple), thereby relieving the inhibition of the monoaminergic cells, and that of the hypocretin/orexin neurons (ORX; green), and the cholinergic PPT and LDT. Because the VLPO neurons do not have hypocretin/orexin receptors, the hypocretin/orexin neurons serve primarily to reinforce the monoaminergic tone, rather than directly inhibiting the VLPO on their own. **B** During sleep, the firing of the VLPO neurons inhibits the monoaminergic cell groups, thereby relieving their own inhibition. This also allows it to inhibit the hypocretin/orexin neurons, further preventing monoaminergic activation that might interrupt sleep. The direct mutual inhibition between the VLPO and the monoaminergic cell groups forms a classic flip-flop switch, which produces sharp transitions in state, but is relatively unstable. The addition of the hypocretin/orexin neurons stabilizes the switch. VLPO: ventrolateral preoptic nucleus; eVLPO: extended ventrolateral preoptic nucleus; LC: locus coeruleus; TMN: tuberomammillary nucleus; PPT: pedunculopontine tegmentum; LDT: laterodorsal tegmentum. *Saper CB et al. (2005) [57]*

A network model of REM sleep onset and maintenance has been proposed. It suggests that during wake and NREM sleep, specific GABAergic neurons localized in the *ventrolateral periaqueductal gray* (vIPAG) and *dorsal deep mesencephalic reticular nuclei* (dDpMe) inhibits the glutamatergic neurons in the SLD. REM sleep onset would be due to an activation of other GABAergic neurons in an intrinsic manner both the in *dorsal paragigantocellular reticular nucleus* (DPGi) and vIPAG. These latter activate indirectly the SLD by inhibiting both dDpMe and vIPAG neurons. Descending SLD neurons would induce muscle atonia and sensory inhibition, while ascending SLD neurons induce cortical activation *via* thalamic relay neurons in collaboration with cholinergic and glutamatergic neurons from mainly PPT, LDT and *basal forebrain* BF [79]. This cortical activation is responsible for the EEG during REM sleep that closely resembles wakefulness [16]. The exit from REM sleep would be due to the activation of waking systems that inhibits once again GABAergic neurons in DPGi and vIPAG [79].

4. Regulation of sleep

As I mentioned in the beginning of this introduction, the distribution and quality of sleep are principally regulated by two processes, one homeostatic and one circadian that can be illustrated by a model (i.e. “two-process model”) which will be explained in more detail below. One way to distinguish between these two processes is to imagine the oscillation generated by the homeostatic process as an hourglass, every time the sleep/wake state is changed, the hourglass is turned; while the oscillation generated by the circadian process as a self-sustained clock [26]. These two processes work together allowing an optimal adaptation of living organisms to the environment while satisfying their daily need for sleep.

a. Homeostatic process

This process tracks the need for sleep and determines the propensity of an individual to fall asleep during the nycthemeron. During wakefulness the homeostatic process increases exponentially until reaching a maximum (i.e. asymptote). Sleep has the opposite effect; homeostasis sleep decreases until reaching the minimum. Despite the observation that homeostatic process appeared to oscillate with a period of 24h, it is important to realize that this oscillation in propensity is driven by the sleep-

wake distribution which in turn strongly depends on circadian factors [26]. Thus although under normal conditions the sleep homeostatic process follows a circadian time course, the homeostatic process *per se* is completely independent of the circadian process.

Dijk and Czeisler made use of a forced desynchrony protocol in humans to differentiate between circadian and sleep-wake dependent contributions to different aspects of sleep and the EEG [21]. This protocol consisted of scheduling sleep in voluntary subjects in an environment free of time cues for several weeks according to a 28h rest-activity cycle so that sleep episodes of 9.33h occurred at all phases of the endogenous circadian cycle and variations in wakefulness preceding sleep were minimized. They observed that the time course of EEG delta power was mainly sleep/wake driven and varied with very small amplitude to its circadian time suggesting that circadian factors has no or only a small impact on this homeostatic process [21]. Studies in others species such as squirrel monkeys, Siberian hamsters, rats and mice underscored this conclusion. For instance, when the circadian rhythm was abolished by a lesion of the *suprachiasmatic nuclei* (SCN, the central clock pacemaker), these animals became completely arrhythmic. However, their homeostatic process remained unchanged [22-25]. In conclusion, it is now established that circadian rhythm and sleep homeostasis processes are functionally and physiologically separate.

Markers of the sleep homeostatic process are: the total sleep time (or more specifically the duration of NREM and REM sleep), the sleep fragmentation, the EEG theta (4-8Hz) power during wakefulness and, of course, the EEG delta (1-4Hz) power collected during NREM sleep. This latter EEG power represents the sleep intensity [46-48]. Both theta and delta power are so predictable that their time courses can be calculated in mammals based solely on the sleep/wake distribution. [46, 48, 49].

The molecular aspect of the sleep homeostat is also relevant. For instance, the genetic background in mice has a strong impact on the NREM sleep need. In fact, the dynamic of the EEG delta power and NREM sleep duration after a sleep deprivation is specific to the strain [46]. Moreover, it was shown that both NREM sleep intensity (delta power) and NREM sleep duration are regulated

differently between human too [80, 81]. *Homer1a* is the best candidate transcript because its expression follows the sleep/wake distribution in the forebrain. Its expression increase in a very precise way in response to sleep loss and it is also specific of the strain mice. Thus, *Homer1a* is considered a reliable molecular marker of the sleep need as the EEG delta power [45].

b. Circadian process

The circadian process determines when wakefulness and sleep occur across the 24h day. It promotes sleep by decreasing the body temperature and increasing the level of the hormone melatonin to its maximum at a specific time. In contrast, it prevents sleep in other moment of the day by increasing sleep latency. Moreover, it consolidates the vigilance states [21]. There are a several markers that allow the tracing of the circadian process, for instance cortisol and melatonin levels in the blood, the fluctuation of the body temperature and the expression of many clock gene [21, 48]. An entire and complete section will be dedicated below to the circadian rhythm topic.

c. Two-process model

In 1982 Borbély A.A. imagined a model that conceptualizes the wake/sleep cycle named two-process model [20]. The latter has been improved and revisited through the years. [82, 83]. Nowadays, there are many models derived from this model addressing the regulation of fatigue [84], alertness [85, 86] and performance [87]. The original model postulated that both circadian and homeostatic processes were independent as illustrated in figure 6 (upper panel). The process C in blue represents the circadian process that oscillates in a sinusoidal manner across the nycthemeron of 24h. Its H (high) and L (low) thresholds demarcate the boundaries of the process S marked in red. This Process S is based on the dynamics of the EEG delta power and represents the homeostatic process and follows the in-

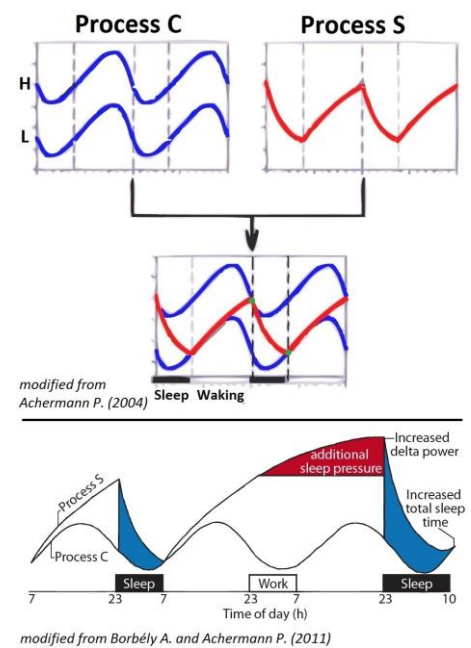


Figure 6 Two-process model of sleep regulation. **Upper panel** Illustration of original two-process model showing the additive effects of circadian (C) and homeostatis (S) processes. Achermann P. (2004) [83] **Lower panel** Prediction of the two-process model of an augmentation of both delta power and total sleep time after sleep deprivation. Borbély A. and Achermann P. (2011) [88]

creased need for sleep during wakefulness which decreases during sleep. Process S increases and decreases in an exponential manner reaching its asymptote. When the process S reaches a blue threshold, the model predicts a change in vigilance state. The EEG delta power is the widely used marker of this process S [83]. Moreover, based on observations, this model was improved to predict the effect of a sleep deprivation (Fig. 6 lower panel), suggesting that a sleep deprivation for 40h would accumulate additional sleep pressure (Process S), resulting in a bigger sleep intensity (EEG delta power) during the recovery night as well an increased total sleep time [88].

The two-process model was successful in predicting alertness and sleepiness for experimental manipulations in a physiological range. However, a challenging task is the modeling of cumulative effects of chronic sleep restriction [83]. In fact, the level of EEG delta power (and Process S) quickly saturated during sleep restriction in accordance with delta power while vigilance and cognitive performance continue to decrease. These data raise the question whether an additional process has to be assumed [89]. Furthermore, additional neurobehavioral measures (such as performance, subjective alertness) , within- and between-subject variability, and cumulative effects need to be addressed to facilitate the development of accurate models [90].

II. Circadian Rhythm

The earth revolves around the sun in one year, creating the seasons. Moreover, it spins on its axis with an angle of 23° creating the nychthemeron (i.e. day/night cycle within 24h). When life emerged, roughly 3.5 billion years ago, it adapted to this predictable variation of temperature, light, humidity, as this was crucial for survival. Indeed, the ability to anticipate these daily changes give an undeniable adaptive advantage because it allows organisms to be more competitive and survive natural selection. For this reason, this internal endogenous timing mechanism is present today in almost all species, from the simplest organisms such as bacteria to more complex ones such as humans, passing through plants and fungi. However, there are exceptions, such as creatures living in ocean trenches or in totally obscure caves [91]. In mammals, most physiological and behavioral processes depend on

this circadian timing. Examples are the body temperature fluctuation [21, 92], metabolism variation [93], cardiovascular activity [94], cognitive performance [92] and of course the sleep/wake cycle [21].

The first scientific observation of the circadian rhythm was made in 1729 by the French scientist Dortous de Mairan, which became the first chronobiologist. He noticed that the daily leaf movements of *mimosa pudica* persisted during several days even in constant obscurity [95]. This simple experiment provided the first evidence that a daily rhythm could be generated by an organism itself. Since then, this biological timekeeper is called circadian clock (from Latin words *circa* and *diem* meaning respectively *about* and *day*). Nevertheless, we had to wait the middle of the twentieth century for the first description of this endogenous clock in an animal and the year 1972 to precisely localize the master-clock in mammals, named SCN, in the anterior part of the hypothalamus above the optic chiasm on either side of the third ventricle [96].

1. Definition of circadian rhythm

A biological rhythm can be called “circadian” if it respects the following properties that were stated by Pittendrigh in 1960 at the XXV Cold Spring Harbor Symposium dedicated to biological clocks [97]:

- Has a period length corresponding to the earth’s rotation with a small variance
- Is endogenous and innate
- Is self-sustained
- Is near-independent of the external temperature (temperature compensation)
- Is light-intensity dependent (period in nocturnal animal was greater in *constant light condition* (LL) than in *constant dark condition* (DD); period in diurnal animal was smaller in LL than in DD)
- Can be entrained by environmental stimuli (called Zeitgeber)

The term *Zeitgeber* (ZT) was first used in 1954 by Jürgen Aschoff (from German words *zeit* and *geber* meaning respectively *time* and *giver*) [98]. This term represents any circadian external or environmental cue (such as light, temperature, social interaction, feeding, and pharmaceutical manipulation)

that can entrain the circadian oscillator of an organism or synchronize circadian oscillators in cultures cells [98, 99].

2. Circadian rhythm in animals

The easiest way to study the circadian rhythm in animals is to record its locomotor activity. In humans, the actiwatch is the most used technique to record activity and light exposure at the same time [100]. In rodents, the running wheel or the *passive infrared sensor* (PIR) are the easiest methods to record locomotor activity [101].

Locomotor activity patterns are commonly represented as a so-called *actogram*, where each day is represented by a horizontal line on which the activity is plotted with vertical black ticks with heights proportional to the activity at a given time. Consecutive days are plotted beneath each other. For clarity, such a graph is often double-plotted so that on each horizontal line two

consecutive days are plotted. In figure 7A, an actogram is illustrated for one mouse that was maintained in a *light-dark* (LD) cycle of 12h on 12h (LD 12:12) for 10 days followed by a DD [101]. This example illustrates the main properties of a circadian rhythm mentioned above. The animal's activity was stably entrained by the LD cycle and then when released in DD, the activity patterns started to 'free-run' with a period slightly less than 24h for the remaining days under DD, demonstrating the endogenous and self-sustained properties of the circadian clock. Note that "free-run" activity is called when the sleep/wake cycle is no longer period entrained by ZT; without temporal cues the activity follow its own internal intrinsic circadian clock.

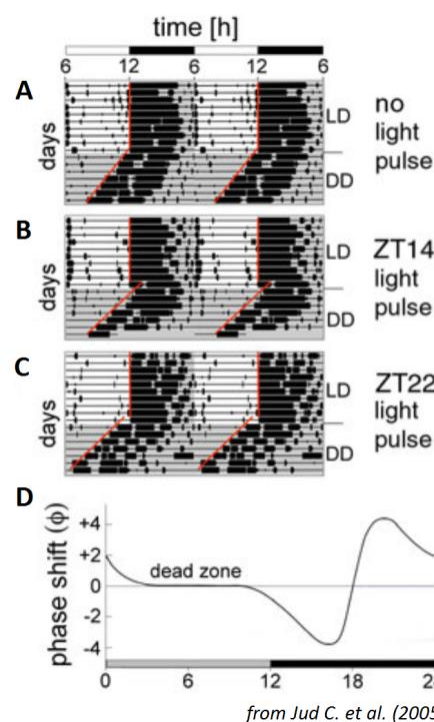


Figure 7 Real actograms and phase response curve in mice. A-C Typical actograms of wild-type mice subjected to an Aschoff type II protocol. Mice were entrained to an LD 12:12 cycle (10 days) before releasing them into DD. The line above "DD" indicates the transition from LD to DD. The grey background represents darkness. **A** Upon release into DD, no light pulse was administered to the mouse, **B** whereas light pulses of 15min were applied to the mouse at ZT14 and **C** at ZT 22. Regression lines (in red) are drawn through the onsets of wheel-running activity in order to calculate the phase shift. **D** Typical light phase response curve (PRC) for nocturnal rodents. The grey and black bars below the PRC indicate subjective day and night, respectively. The X-axis shows the circadian time (CT) at which the light pulse was applied whereas the Y-axis displays the observed phase shift (ϕ) [h]. Light pulses administered between CT11 and CT18 provoke a phase delay (negative values). Light pulses between CT19 and CT3, on the other hand, generate phase advances (positive values). Between CT4 and CT10, no phase shift can be observed (dead zone). Jud C. et al. (2005) [101]

Furthermore, during DD, the phase of this mouse could be shifted by light exposure. The direction of the phase shift in subsequent locomotor activity onset induced by the light pulse, depended on the circadian time light was given (Fig.7B-C) [101]. The relation between the timing of the light signal and its effect is summarized in a so-called *phase response curve* (PRC) whose shape varies depending on species and stimulus. However, this relationship is stereotypic for all organisms (whether diurnal or nocturnal) and characterized by a delay of the phase of activity onset when light is experienced in the evening and early night, an advance in late night and early morning, and a “dead zone”, in which no phase change occurs, corresponding to the midportion of the ‘subjective’ day, i.e. when the animal suppose that this is the light period (Fig.7D) [101, 102].

The response of the circadian clock to these Zeitgeber is a consequence of the plasticity of this mechanism. This can be explained by the fact that day length varies enormously during the year depending on the location of the earth compared to the sun and also depends of the location on the earth. Therefore, it is primordial to have an adaptive mechanism that can be entrained according with the photoperiod or with the food viability [103].

The ability to reset the inner master-clock in a new environment is an opportunity that allows human to resynchronize promptly our physiological functions after a rapid long-distance trans-meridian travel, in spite of some inconveniences called *jet-lag* [104]. Interestingly, if this circadian regulation is not respected due to jet-lag and more so during shift-work, individuals can develop sleep disorders, a decrease in the quality of life, performance, vigilance, negatively affect the mood and even cause irreversible health damage [105, 106].

Circadian clocks play a role in other things as well: changes in the photoperiod of the day supported by the circadian clock enables animals also to anticipate and prepare for seasonal changes in their environment [107]. In fact studies shown that circadian clock are involved to sense changes in day length and to mediate a diverse number of photoperiodic responses in plants [108] as in mammals [109, 110], however this molecular link is controversial topic in insects [107, 111, 112].

The circadian clock is also involved in the navigation. A nice example is the monarch butterfly (*Danaus plexippus*) that undertake a long distance migration from eastern north America to Mexico (about 3600km) maintaining a southwesterly flight as the sun moves across the sky each day using a time-compensated sun compass [113]. Birds (*Columba livia L.*) have also to compensate their sun compass for the apparent movement of the sun with the help of their internal clock during homing [114].

It was observed that aberrant expression of circadian clock genes could have important consequences on expression of downstream targets gene that control the cell cycle and on the ability of cells to undergo apoptosis. This may lead to genomic instability and accelerated cellular proliferation potentially promoting carcinogenesis [115]. For instance, tumors grew two to three times faster in mice with SCN lesions than in sham-operated mice [116]. Moreover, it was reported that arrhythmic *Bmal1*^{-/-} mice have reduced lifespans and display various symptoms of premature aging including sarcopenia, cataracts, less subcutaneous fat and organ shrinkage [117]. Conversely, *Cry1,2*^{-/-} mice had no predisposition to cancer due to γ -radiation induction and were indistinguishable from *wild-type* (Wt) mice [118]. More surprisingly, it was shown that *Cry1,2*^{-/-} *p53*^{-/-} mice had a reduced cancer risk compared to *p53*^{-/-} mice [119]. The *Per2* knock-out mice that a used in unspecified 129/C57BL6 mixed background develop lymphomas at a higher rate than Wt mice after γ -radiation exposure due to partial impairment of p53-mediated apoptosis. For this reason, it has been proposed that PER2 functions as a tumor suppressor [120]. To resume, the effect of circadian clock disruption on cellular response to DNA damage and cancer predisposition may depend on the mechanism by which the clock is disrupted, and elucidation of this mechanism warrants further investigation [115].

3. Organization of circadian rhythms

As mentioned above, in mammals the master-clock of our circadian rhythm is in the SCN, located in the anterior part of the hypothalamus (Fig.8C). The SCN is composed of two nuclei containing *circa* 10'000 neurons each, and subdivided in two parts: the core and the shell [121, 122]. The SCN has several input and output mechanisms. The principal input is visible light especially around 460-500nm (Fig.8A). These wavelengths pass through the eye lens to hit the retina where photopigments transform this electromagnetic signal into bioelectrical signal. The photopigments in

humans are three cone opsins in cone cells, rhodopsin in rod cells and, of particular importance, melanopsin in the retinal ganglion cells (fig.8B) [123]. Melanopsin is not used for image forming but importantly contributes to circadian physiology and pupillary reflex. All five opsins must be disrupted to completely prevent the synchronization of the SCN by light [124]. These melanopsin-containing retinal ganglion cells project monosynaptically *via* the *retinohypothalamic tract* (RHT) to the SCN by glutamate and *pituitary adenylate cyclase-activating polypeptide* (PACAP) release (Fig.8C)[125]. This release leads to membrane depolarization, elevated calcium and cAMP levels, phosphorylation of *cyclic-AMP response element binding protein* (pCREB) and its binding to *cyclic-AMP response elements* (CRE) on the DNA, finally allowing the transcription of the *Period* genes. Given that *Per1* is already induced after 5–15min of a light pulse and is involved directly in the core clock feedback loop, its induction is thought to be largely responsible for resetting the clock [126-128].

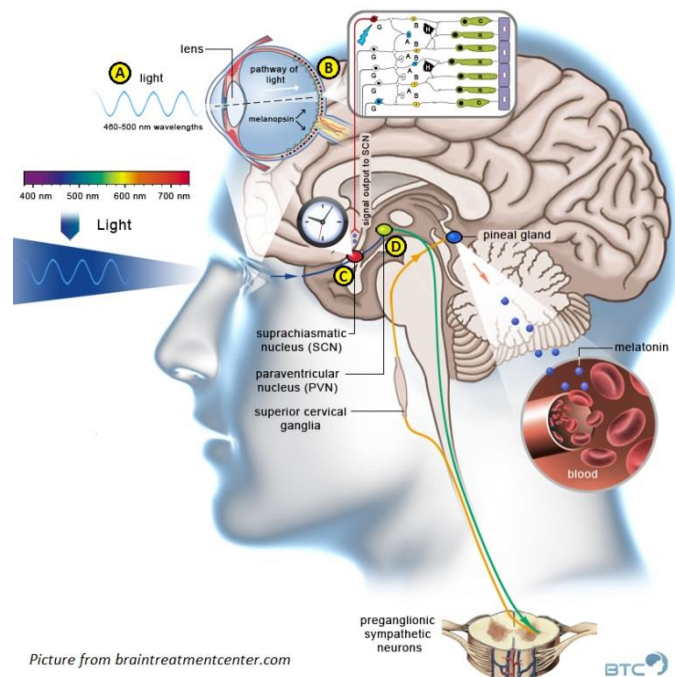


Figure 8 Schematic diagram of synchronized SCN by sunlight during daytime that projected to different brain area to activate in proper timing diverse physiological functions. Here for instance light synchronized the SCN that project to PVN neurons that activated preganglionic sympathetic neurons of the spinal cord, which in turn modulated the activity of the superior cervical ganglia that finally projected to the pineal gland to regulate the melatonin secretion. *Braintreatmentcenter.com*

In a second step, the SCN output pathways are responsible for proper timing of diverse physiological functions, such as thermoregulation, sleep/wake cycle, corticosteroid and melatonin release, and feeding at the neuronal level, as schematized in figure 9. The SCN projects to the *ventral* and *dorsal subparaventricular zone* (vSPZ, dSPZ). dSPZ neurons are crucial for rhythms of body temperature *via* the *medial preoptic area* (MPO), whereas vSPZ relay the information to the *dorsomedial nucleus of the hypothalamus* (DMH) that drives circadian sleep cycles *via* GABAergic neurons in the VLPO to promote sleep and *via* hypocretin/orexins neurons in *lateral hypothalamic* (LH) to promote wakefulness. The LH also contains melanin-concentrating neurons that are involved in feeding behavior. Finally, the DMH projects to the *paraventricular nucleus* (PVN) which is responsible for the cyclic release of corticosteroid and melatonin [57, 121]. In the case of melatonin, PVN activates preganglionic sympathetic neurons of the spinal cord, which in turn modulated the activity of the superior cervical ganglia that finally projected to the pineal gland to regulate the melatonin secretion (Fig. 8).

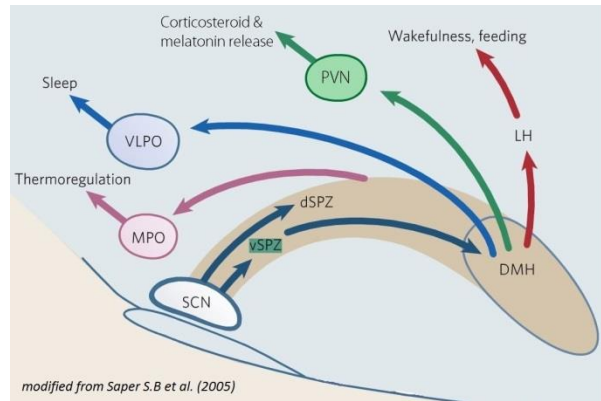


Figure 9 A schematic diagram to illustrate the several-stage integrator for circadian rhythms. The suprachiasmatic nucleus (SCN) serves as a biological master-clock to regulate other systems (e.g. thermoregulation, sleep, corticosteroid release). Most of SCN output goes into the region in light brown, which includes the ventral (vSPZ) and dorsal (dSPZ) subparaventricular zone, and the dorsomedial nucleus of the hypothalamus (DMH). Neurons in the vSPZ relay information necessary for organizing daily cycles of wake-sleep, whereas dSPZ neurons are crucial for rhythms of body temperature. Outputs from the SPZ are integrated in the DMH with other inputs, and DMH neurons drive circadian cycles of sleep, activity, feeding and corticosteroid secretion. Cycles of body temperature are maintained by dSPZ projections back to the medial preoptic area (MPO), whereas the DMH is the origin of projections to the VLPO for sleep cycles, to the corticotropin-releasing hormone neurons of the paraventricular nucleus (PVH) for corticosteroid cycles, and to the lateral hypothalamic (LH) hypocretin/orexin and melanin-concentrating hormone neurons for wakefulness and feeding cycles. Saper CB et al. (2005) [57]

Not only in the SCN circadian rhythms are generated, but in all cells, tissues and organs of our body, that are considered as peripheral clocks (including brain). The SCN sets the phase directly the rhythm of these peripheral clocks as well as many physiological functions as discussed above (temperature, feeding, sleep/wake cycle, etc.). However, some behavioral changes such as food and medication intakes or changes in sleep/wake distribution act as Zeitgebers for specific peripheral clock, and then can shift their oscillations [122]. At the cellular level, individual cells of peripheral tissues, like NIH3T3 fibroblast maintained in culture, are not synchronized among themselves. Their

circadian rhythm could be synchronized for few days with a serum shock of dexamethasone, however after several days, each cell continues to oscillate with its own period and the culture lost its synchrony [99]. However, if these fibroblasts were in co-culture with SCN neurons, their synchrony was constantly maintained [129]. How the SCN exactly synchronizes peripheral clocks is still poorly understood. Nevertheless, neuronal and humoral pathways, such as glucocorticoids, are the best candidate. Indeed, *Period* genes contains *glucocorticoid response element* (GRE) sequences which allow their transcription in presence of glucocorticoid [99]. The synchronization by temperature fluctuation is also another possibility. In fact *Per2* also contains *heat-shock element* (HSE) in its promoter that were activated by *heat-shock factors* (HSF), mediated themselves by temperature fluctuation [130].

The hierarchic organization in non-mammalian vertebrates such as birds, fish, reptiles and amphibians, is significantly different, in that they have multiple photic inputs other than the eyes, such as the pineal gland and deep-brain photoreceptors [131]. Most of these species, in addition to the SCN [131-133], also use the pineal organ (which in mammals has only a secretory role) and the retina as circadian pacemakers. All these structures communicate together to provide a single synchronized output. Significant variation occurs among these species in the relative roles that SCN, pineal gland and eyes in respect to the regulation of the circadian system [131].

4. Chronotype

The phase of rhythms generated by the SCN needs to be synchronized to the external light-dark cycle every day, mainly through the eye exposure to the light. In the absence of such entrainment, the oscillation of the inner clock would follow its own rhythm depending of the endogenous period of the species and the strain [134]. For instance, most laboratory mice have a period somewhat shorter than 24h, while humans have a period of 24.2h [135, 136]. Despite the fact that light is the main synchronizer of our master-clock, other nonphotic Zeitgebers are also important, such as social and environmental factors, work-related constraints and food restriction. It has been shown that mice that had access to food only between ZT3-7 (light period when mice usually do not eat), were able to anticipate it and were awake before this access period. This held true in a normal light/dark cycle or in

constant dark condition. It was shown that in response to this feeding restriction, the expression of circadian genes in the forebrain was affected [137]. However, these nonphotic entrainments are not sufficient to regulate the master-clock. In fact, rhythms in the SCN are ‘immune’ to feeding cycles and completely dissociate from rhythms elsewhere in the body, thus this food-anticipatory behavior is not organized in the SCN. Consistently, most totally blind people suffer from a “non-24h sleep/wake disorder” (subjects with ‘free-running’ circadian rhythms) can be treated with melatonin to adjust the phase of its circadian clock, as regular meals and other environmental constrains are not sufficient [138-140]. The usual treatment used for people suffering of circadian rhythm sleep disorders is the chronotherapy which take into account the body’s natural rhythms, along with bright light therapy. As example, *familial advanced sleep-phase syndrome* (FASPS) in human is circadian disorder characterized by a very short circadian period with early sleep and early morning awakening time as a result. Strategy attempts to cause the body of these patients is to use bright light tables to delaz the sleep phase backwards [141]. FASPS is a human circadian disorder characterized by a very short circadian period with early sleep and early morning awakening time as a result [142]. In two families

FASPS was found to be caused by two autosomal dominant mutations: a single amino-acid missense mutation (S662G) in the *period 2* (*per2*) gene that decreases PER2 phosphorylation preventing the proteolysis of PER2 [143], and a mutation (T44A) within the *casein kinase 1δ* (*CK1δ*), normally responsible for PER2 phosphorylation [144], which therefore reduces PER2 phosphorylation that decreases substantially its enzymatic activity preventing an effective rate of PER2 proteolysis. In contrast, *delayed sleep-phase syndrome* (DSPS) is

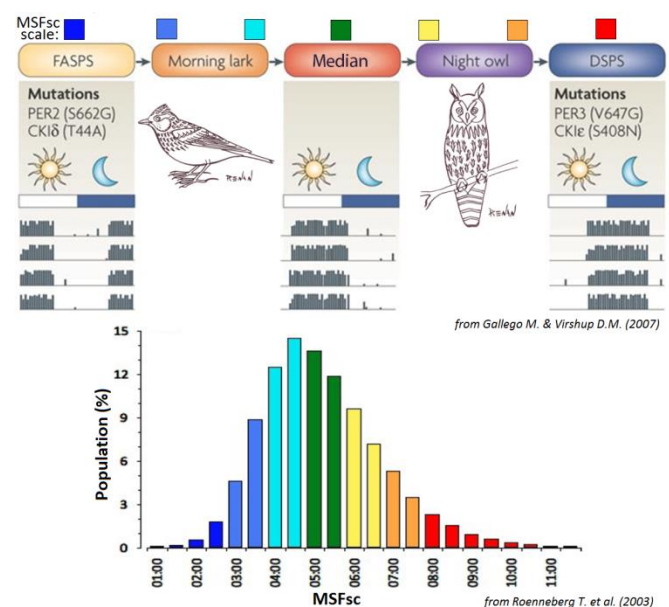


Figure 10 Illustration of chronotype. Upper panel Activity rhythms to individuals affected by FASPS, DSPS or normal people. “Morning-type” people tend to wake up early the morning (like larks) and “evening-type” people tend to sleep late in the evening (like owls). Gallego M. and Virshup D.M. (2007) [147] Lower panel Graphic representing a population (100'000 people) distribution on Munich chronotype questionnaire (MCTQ) based on their sleep habits. Roenneberg T. (2003) [149]

characterized by a late sleep and awaking onset. The cause has not been precisely identified, but mainly two polymorphisms were associated with this disease. The first one is a variant of the human CK1 ϵ (S408N) that is significantly more present in normal population rather than in DSPS patients [145]. While the second polymorphism is in the human PER3 gene (V647G) has been linked to the pathogenesis of DSPS patient [146]. Note that this residue 647 locates in a region similar to the CK1 ϵ -binding region of PER1 and PER2, close to the serine residue in PER2 that is disrupted in FASPS patient. Therefore, this polymorphism might alter the CK1 ϵ -dependent phosphorylation of human PER3 [147].

The chronotype reflects the moment of the day when our physical functions, such as cognitive faculties, eating and sleeping, are most active specific to each individual. FASPS and DSPS people are greatly delayed in these physical functions and belong to the extremes shown in figure 10. Between the extremes formed by FASPS and DSPS subjects lie “morning-type” people who tend to wake up early the morning (like larks) and “evening-type” people who tend to sleep late in the evening (like owls) [147]. This scale could be correlated with the *Munich chronotype questionnaire* (MCTQ) used already to calculate the chronotype of 100'000 people using the *midpoint of sleep on working days* (MSF) which was corrected for “oversleep” on free days (MSFsc). The distribution of the population seemed a Gaussian distribution with the maximum at MSFsc=4.5 [148, 149].

5. Circadian rhythm at molecular level

The first genetic discovery of the circadian loop at molecular level was made in the fruit fly *Drosophila melanogaster*. In 1971, three mutants fly have been isolated according to short, long or no (arrhythmic) period, in both pupal eclosion and locomotor activity, led to the discovery of a crucial gene named *Period (Per)* for the circadian rhythmicity [150]. It was sequenced and characterized ten years after [151, 152], and in 1990 the rhythmic expression in both transcript and protein was measured [153]. This discovery led the suggestion that *Period* gene is involved in a negative auto-regulatory feedback loop. In parallel, this forward genetic and also mutagenesis approach to identify genes responsible for particular circadian behavioral phenotypes was applied to other species like fungi (e.g.

neurospora crassa) [154], plants (e.g. *arabidopsis thaliana*) [155], and, of course, mammals (e.g. *mus musculus*) [156]. All species were found to have similar circadian machineries at the molecular level. In short, the circadian rhythm is composed of a positive limb allowing the transcription of many target genes. More importantly, some of these targets form a negative limb that inhibits their own transcription, as well as some targeted genes by the positive limb. The co-existence of such positive and negative limbs is thought to be the key for the formation of an endogenous biological cycle. Indeed, this positive limb in association with the negative feedback loop (described below) are essentially responsible for the oscillation of all downstream genes involved behavioral and metabolic pathway [157]. Given the scope of this thesis, only the mammalian clock will be detailed further.

a. Core clock loops

The molecular mechanism involved in the circadian rhythms in mammals is well understood. The principal positive limb is composed by the hetero-dimerization of *brain and muscle ARNT-like 1* (BMAL1 also called ARNTL or MOP3) with *circadian locomotor output cycles kaput* protein (CLOCK) or *neuronal PAS domain protein 2* protein (NPAS2 also called MOP4) (Fig.11A). All three contain both a *basic helix-loop-helix* (bHLH) and *Per-Arnt-Single-minded* (PAS) domains [158]. NPAS2 is a homologue to CLOCK but intriguingly it is only expressed in neuronal tissue, such as brain and spinal cord [159]. This hetero-dimerization allow the transcription of many *clock controlled genes* (CCG) by binding the promoter elements E-boxes (5'-CACGTG-3') and E'-boxes (5'-CACGTT-3') [160, 161]. Among the multitude of activated genes, specific targets such as *Cry1* & -2 and *Per1* & -2 genes provides a subsequent negative limb. The resulting PER and CRY proteins bind together and translocate into the nucleus to inhibit their own transcription by interfering with the complexes BMAL1:CLOCK/NPAS2 [162]. This is the main core feedback loop of the circadian rhythm. If all homologues of these genes are removed, the mutants became completely arrhythmic (e.g. *Bmal1*^{-/-} [163], *Clock*^{-/-}*Npas2*^{-/-} [136], *Cry1*^{-/-}*Cry2*^{-/-} [164], and *Per1*^{-/-}*Per2*^{m/m} [165]). This negative feedback loop is essential for the endogenous oscillation of all downstream CCG [26].

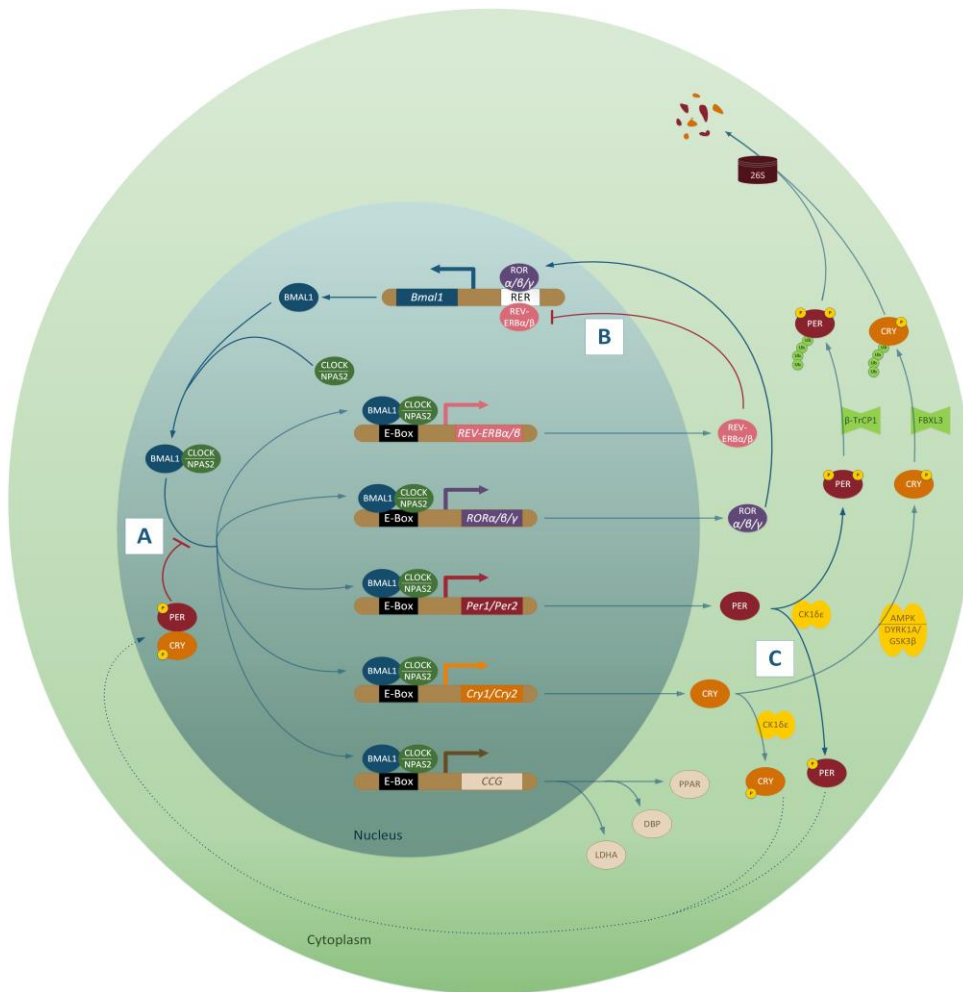


Figure 11 Mammal circadian clock is composed of a transcriptional-translational feedback network. A Main loop composed by the positive limb BMAL1:CLOCK/NPAS2 and its negative feedback by PER:CRY **B** Auxiliary loop reinforcing the main loop via *Bmal1* expression controlled by the positive factors ROR $\alpha/\beta/\gamma$ and by the negative factors Rev-erba/ β **C** PER and CRY regulation by kinase phosphorylation that have an important role for the period length of the rhythm. This phosphorylation contribute to the PER and CRY degradation and also to contribute to their nucleus translocation. Note that PPAR, DBP and LDHA were only three proteins example of the clock controlled gene (CCG) expression tuned by the clock machinery

b. Secondary clock loop

In parallel, an additional regulatory loop involves *Bmal1* through its *retinoic acid-related orphan receptor response element* (RORE) promoter (Fig.11B). In fact, the two orphan nuclear receptors ROR $\alpha/\beta/\gamma$ and *Rev-Erba/β*, induced by the dimer BMAL1:CLOCK/NPAS2, act, respectively, as an activator and an inhibitor [166]. ROR and REV-ERB proteins were in part responsible of the cyclic expression of *Bmal1* [167, 168]. Mutation of ROR α was shown to reduce *Bmal1* amplitude both in SCN and fibroblasts [169, 170] and a deletion of all ROR $\alpha/\beta/\gamma$ did not abolish the *Bmal1* rhythmicity in fibroblasts [168], while *Rev-Erba* deletion resulted in a higher *Bmal1* transcription levels [171] and both *Rev-Erba/β* depletion abolish the *Bmal1* oscillation in fibroblast [168]. However even *Bmal1* did not cycle anymore, that seems not to affect the oscillation of other clock genes such as *Per2* [168]. Moreover, deficiencies in ROR/REV/*Bmal1* loop only produces modest clock phenotypes [167, 169,

171], suggesting that secondary loop provides a “stabilizing” function. An recent study shown that despite the severe activity and metabolism defects observed in *Rev-erba*^{lox/lox}*Rev-erbβ*^{lox/lox} mice, this mutant still maintained a short circadian rhythm in constant dark, confirming the accessory nature of this loop [167].

Even though the basic mechanism of the circadian rhythms at molecular level is now well understood, it remains a very simplified rendition. A lot of the crucial regulation is post-transcriptional and post-translation and involves chromatin remodeling, protein phosphorylation and degradation; and *oxidation/reduction* (redox) potential. Although a lot is known about clock genes and circadian rhythms, very basic question on how it encodes a period length close to 24h, or how temperature compensation is achieved is largely unknown. Some of these hypotheses will be discussed.

c. Chromatin remodeling

Chromatin remodeling is also an essential mechanism for transcriptional regulation of circadian genes (Fig.12). In fact, histones (H3 and H4) from specific target genes (as *Per* and *Cry*) are acetylated and deacetylated in a circadian fashion with the recruitment of multiprotein complexes [172, 173]. For instance, when the dimer BMAL1:CLOCK binds the E-boxes, CLOCK acquired *histone acetyltransferase* (HAT) activity specifically on histone H3, and this contributes to opening of the chromatin fiber which stimulates the rhythmic transcription of the target genes. Other HATs, such as p300 and *CREB binding protein* (CBP), seems to bind this complex on CLOCK as well and contrib-

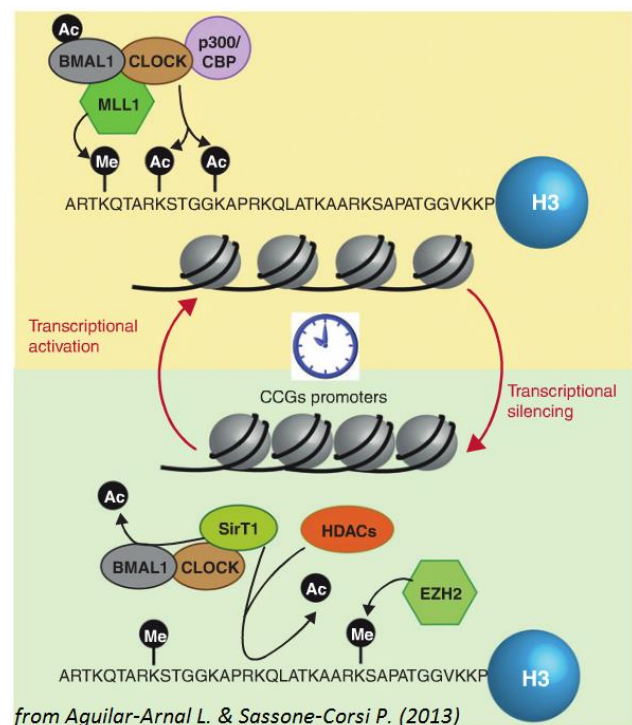


Figure 12 Chromatin remodeling in the circadian clock. Chromatin modifying enzymes act in synchrony for fine-tuning clock-controlled gene expression. Transcriptional activators coordinate rhythmic histone hyperacetylation and H3K4 trimethylation at circadian gene promoters, thereby inducing transcription. Conversely, repressors remove acetylation marks and promote a closed state of the chromatin fiber at the clock controlled gene promoters to inhibit transcription. Thus, activator and repressor enzymes act in a very precise synchrony leading to the circadian transcription. Aguilar-Arnal L. and Sassone-Corsi P. (2013) [173]

utes to histone acetylation [173]. *Methyltransferase mixed lineage leukemia 1* (MLL1) also interacts with this complex to trimethylate the actual methylation residue to promote the transcriptional activation [174]. In contrast, in association with the inhibition brought by the complex PER:CRY, repressors such as the *histone deacetylase 3* (HDAC3) and the NAD⁺-dependent enzyme *sirtuin 1* (SIRT1) promote histone deacetylation, while the *enhancer of zest 2* (EZH2) methylates histones and ultimately promotes a closed chromatin state [175-177]. Together, these observations highlight the crucial role of the clock in maintaining tissue homeostasis by epigenetic control of gene expression [173].

d. Regulation by protein phosphorylation

Another key point of this clock mechanism is protein phosphorylation. This post-transcriptional regulation of PER2 and CRY is important for the period length of the rhythm that modifies the delay in the negative-feedback loop. If after the synthesis of the both repressor proteins, PER and CRY, would directly translocated to the nucleus to repress BMAL1:CLOCK/NPAS2, the whole cycle would take just a few hours rather than one day. To maintain the daily oscillations of clock proteins, a significant delay between the activation and repression of transcription is required. One way to ensure precisely this regulation is through post-translational modifications. Reversible phosphorylation regulates important processes such as nuclear entry, formation of protein complexes and protein degradation. Each of these can individually contribute to introduce the delay that keeps the period at about 24h (Fig.11C) [147]. These post-translational modifications seem to be more important than *Bmal1* clock core gene oscillation. As shown previously, a constitutive BMAL1 expression did not affect *Per2* oscillation in fibroblast [168]. In mammals, the phosphorylation of PER and CRY is mediated by *Casein kinase 1δ* and *ε* (CKIδ and CKIε) (Fig.11C), that ensure many roles in the circadian clock. One main function of PER and CRY phosphorylation is to control its protein stability. In fact, when one or two distinct sites on PER1 or PER2 were phosphorylated by CKIδ/ε, these latter PER proteins are proteolyzed in a second step by the proteasome [178-180]. CRY1 and CRY2 are respectively phosphorylated by *AMP-activated protein kinase catalytic subunit alpha-1* (AMPK1) and by a sequential *dual*

specificity tyrosine-phosphorylation-regulated kinase 1A/glycogen synthase kinase 3 (DYRK1A/GSK3 β) cascade [158]. Subsequently, phosphorylated-PER and -CRY are polyubiquitinated respectively by *f-box/wd repeat-containing protein 1A* (FBXW1A also called β -TrCP1) and *f-box/llr-repeat protein 3* (FBXL3), and are finally degraded by the 26S proteasome [181]. These PER and CRY degradations can reset the clock, allowing the BMAL1:CLOCK/NPAS2 complex to become active. A second central function of protein phosphorylation by kinases is the subcellular localization. In fact, when PER1,-2,-3 are phosphorylated, their *nuclear localization signals* (NLS) become unmasked allowing the nucleus translocation [180, 182, 183].

e. Temperature compensation

As mentioned above, one property of the circadian rhythm is to generate a stable oscillation regardless of the body or ambient temperature [158]. This is very important given that most enzymatic reactions are directly dependent on the temperature. The phosphorylation rates by CKI δ/ϵ of the clock proteins remain stable at different ambient temperature [184]. While the mechanism for temperature compensation is still under investigation, it has been suggested that *heat-shock factors* (HSF) play a role in this process, as well in the cells synchronization by temperature rhythm [130]. It was shown that SCN is resistant to temperature resetting, that is not the case for peripheral tissues [130, 185]. This differential sensitivity to temperature allows the SCN to drive circadian rhythms in body temperature which can then act as a universal cue for the entrainment of others oscillators throughout the body [130, 186]. However, *Per2* that contains a *heat-shock element* (HSE) in its promoter, shown an impairment in temperature compensation both in SCN and in pituitary cells in mice when HSF was pharmacologically blocked [130]. This suggests that HSF is also implicated in this temperature compensation in mammals. Another candidate for temperature compensation might be the *cold-inducible RNA-binding protein* (CIRBP) that is essential to sustain high amplitude in the circadian gene expression in fibroblasts. CIRBP binds several RNA encoding circadian protein such as CLOCK, and is thought to confer robustness to circadian oscillators through regulation of CLOCK expression [187].

f. Effect of the redox potential

The redox state in the cell is mainly represented by the ratio of oxidized and reduced forms of *nicotinamide adenine dinucleotide* (NAD(P)⁺/NAD(P)H) and is thought to play a role in the circadian circuitry as well. Indeed, binding of the dimers BMAL1:CLOCK/NPAS2 to DNA is regulated by the redox state *in vitro*. The reduced form of NAD enhanced DNA-binding, while the oxidized form prevents it [188]. Moreover, the activity of the NAD-dependent histone deacetylase SIRT1 is modulated by the redox state and, as mentioned above, is important for PER2 regulation [177]. Therefore SIRT1 links the redox state of the cell and NAD availability to regulation of circadian rhythms.

To summarize, the different mechanisms described above

are orchestrated in synergy. The resulting effect is the expression of target genes (clock gene *per se* but also CCG) in a stable oscillatory manner with near-24h period (Fig.13). Surprisingly, circadian regulation can affect both gene transcription and mRNA translation taking place at different phases. In fact, all *Per* and *Cry* did not reach at the exact same time. For instance, *Per1* maximum was reached 3h before the *Cry1* in SCN mouse. However *Per* and *Cry* oscillation could be considered in the same phase and in anti-phase with *Bmal1*. All resulting PER, CRY and BMAL1 protein were translated about 6h after the RNA expression [189].

III. Sleep studies in clock mutant mice

As previously discussed, sleep is regulated by both homeostatic and circadian components. Although these two processes were considered as separate at neuroanatomical and physiological level, it was observed that the circadian and homeostatic somehow share the same molecular components. This notion is based on clock gene knock-out studies and also mRNA changes after *sleep deprivation* (SD).

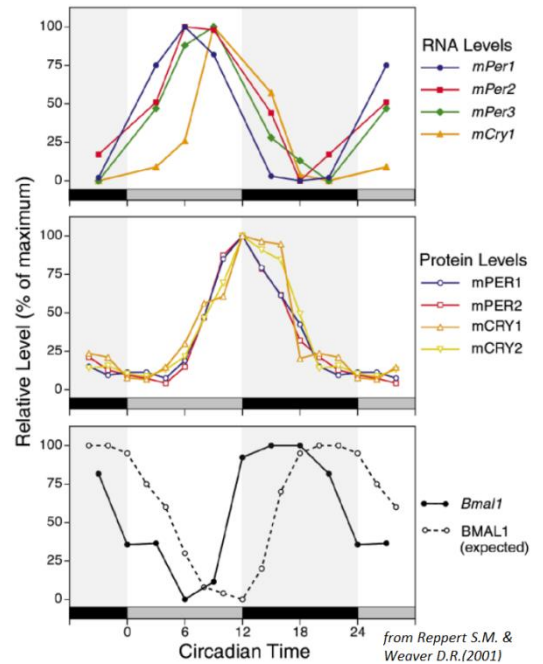


Figure 13 Circadian rhythms of clock gene expression and clock protein levels in the mouse suprachiasmatic nucleus. **Top** Rhythmic abundance of *Per1*, -2, -3, and *Cry1* RNAs; **Middle** PER1, -2, and CRY1, -2 proteins; **Bottom** *Bmal1* RNA (solid line) and hypothetical data (dashed line) represent the expected rhythmic variations in BMAL1 protein. Gray bar represent the subjective day rather than black bar is the subjective night. Reppert S.M. and Weaver D.R. (2001) [189]

If the circadian rhythm was perturbed *via* the mutation or deletion of an important component of the clock machinery, such as the double *Cryptochrome (Cry)-1-2* Ko or the *brain and muscle ARNT-like 1 (Bmal1)* Ko, the delta power was affected [190, 191]. A significant modification on the homeostatic process, such as SD, can impact the expression of some clock genes (*Per2*, increased) or clock controlled gene expression (*D-site albumin-promoter binding protein (Dbp)*, decreased) [192]. However, this molecular link remains poorly understood. The reader is reminded that if circadian rhythm was disrupted by e.g. lesion of the SCN, the delta power was not affected [22-25].

In order to better understand this molecular link, it is interesting to record sleep in mice with different disrupted clock genes. In this chapter, I will therefore review sleep and locomotor phenotypes of several mice mutant for a given circadian gene.

1. *Bmal1*

As mentioned above, *Bmal1*^{-/-} mice are completely arrhythmic in DD. In addition, its activity distribution was also severely altered under LD [163]. The sleep pattern of *Bmal1*^{-/-} in C57Bl/6J background is also greatly perturbed. First, sleep distribution was affected in that this mutant mice showed more NREM and REM sleep across the 24h day but was also more fragmented compared with Wt mice [190]. Moreover, the daily amplitude distribution of sleep and body temperature is null in DD [190]. When sleep intensity was monitored by the EEG delta power, these mice had flat EEG delta power amplitude under baseline condition, and this is in accordance with the NREM sleep distribution [190]. Inspecting the sleep recovery after 6h SD revealed that the EEG delta power in *Bmal1*^{-/-} was lower than the Wt mice suggesting an altered homeostatic regulation of sleep [190].

In summary, the deleting of the central clock component *Bmal1* of the positive limb of the circadian machinery, abolish circadian rhythms and leads to profound differences in time spent asleep, the sleep-wake distribution, and also in the sleep homeostasis.

2. *Clock & Npas2*

The knock-out *Clock*^{-/-} and *Npas2*^{-/-} mice in C57BL/6J background had statistically no changes in the period of locomotor activity in DD compared with the Wt mice. However, the double knock-out

Clock^{-/-}Npas2^{-/-} mice become directly arrhythmic in DD. Moreover, double knock-out mice were entrained under LD with in irregular manner [136]. Intriguingly, in the same C57BL/6J background, *Npas2^{-/-}* mice displayed a shorter period [103], while, the hypomorphic mutant *Clock^{m/m}* mice had a longer period [193]. Given that no sleep studies were done in *Clock^{-/-}Npas2^{-/-}* mice, only *Clock^{m/m}* and *Npas2^{-/-}* single mutant mice were investigated.

In baseline, *Npas2^{-/-}* mice slept less at the end of the second half dark period, while Wt mice typically take a “nap” at this time of the day (i.e. significant decrease of wakefulness from ZT18-22) [103, 194]. After 6h of SD, *Npas2^{-/-}* mice regained less NREM and REM sleep in the following recovery dark period. Moreover, just after the SD, the EEG delta power was smaller in the knock-out mice. Simulation analysis estimating the rate at which EEG delta power increases during wakefulness, showed that delta power in *Npas2^{-/-}* mice increases at a slower rate than in Wt mice, implying that homeostatic regulation was affected [194].

On the other hand, *Clock^{m/m}* mice under baseline condition are characterized by higher wakefulness amount than Wt mice, and a decrease of NREM sleep amount which was also more fragmented. The sleep architecture and the amount of sleep were thus affected by the mutation. EEG delta power and NREM sleep quantity of the *Clock^{m/m}* mice responded in the exact same way after a SD than Wt mice, suggesting that in this case homeostatic regulation of the NREM sleep and sleep intensity was not affected. Nevertheless, the REM sleep homeostasis is affected by the mutation, being smaller after a SD in mutant mice compared with Wt [193].

To summarize, NPAS2 affects the homeostatic regulation of NREM sleep but not the homeostatic regulation of REM sleep, while in *Clock^{m/m}* mice the opposite effect was observed.

3. *Cry*

In the C57BL/6J background, the *Cry1^{-/-}* mice had a shorter period than Wt mice while *Cry2^{-/-}* mice had a longer period [195]. The double *Cry1,2^{-/-}* knock-out mice become directly arrhythmic in DD [196].

Despite this opposite effect on period duration, both single *Cry1*^{-/-} and *Cry2*^{-/-} knock-out mice had no phenotype in the EEG delta power in baseline and after a SD. This suggests that these genes have redundant roles at both sleep and circadian level [195].

In baseline, double *Cry1,2*^{-/-} knock-out mice had more NREM sleep than Wt, and the NREM sleep episodes were longer suggesting a more consolidated sleep. However, their EEG delta power was constantly higher in comparison with Wt. Based on simulation analysis estimating the rate at which EEG delta power increases during wakefulness; the dynamic of delta power in *Cry1,2*^{-/-} mice increased faster than Wt, suggesting that homeostatic regulation was inversely affected compared to *Npas2*^{-/-} mice (see above) [191].

4. *Per*

To assess the role of *Period* genes, several constructs have been made to generate mice with a non-functional *Per1*, -2 and -3 gene in various genetic backgrounds. For instance, three *Per1*^{-/-} mouse lines were considered as full knock-out mice because PER1 protein was not detected: *Per1*^{tm1Drw} (sometimes also called *Per1*^{Ldc}) [197], *Per1*^{tm1Brd} [165] and *Per1*^{tm1Saco} [198]. Surprisingly, these lines did not display the exact same locomotor activity profile. The majority of the *Per1*^{tm1Drw} mice in 129S4/SvJae maintained labile rhythmicity for about 10-14 days, followed with a severe and gradual loss of amplitude in *Per1*^{tm1Drw} mice to finally became arrhythmic [197]. *Per1*^{tm1Saco} in mixed C57BL/6-129S2/SvPas background (94% and 6%, respectively) had a shorter period (23.2h±0.2) than Wt mice (23.7h±0.1)[198]. Finally, *Per1*^{tm1Brd} had a period of 22.6h±0.2 in 129S7/SvEvBrd shorter than Wt (23.7h±0.1) [165].

Concerning *Per2* mutant mice, two constructs can be found in the literature: *Per2*^{tm1Drw} (sometimes called *Per2*^{Ldc}) and *Per2*^{tm1Brd}. Despite the mutation, these mice still express a mutant transcript that could be translated [197, 199]. Under DD conditions, *Per2*^{tm1Drw} on a 129S4/SvJae background, initially displayed a shorter period (23.0h±0.3) than Wt mice (23.1±0.1) and then became arrhythmic. The duration and extent of rhythm persistence in DD was variable [197]. However, when backcrossed onto a C57BL6/J genetic background, these mice remained rhythmic throughout

DD with a normal period (data not shown) demonstrating the dramatic effect that genetic background has on the circadian phenotype [200]. On the other hand, *Per2*^{tm1Brd} mice of 129S7/SvEvBrd x C57BL6 mixed background displayed a period of 22.1h±0.1; i.e., shorter than Wt mice (23.7h±0.1). Moreover some mutant mice became arrhythmic between 2-18 days in a under DD conditions [199]. Double mutant *Per1,2*^{tm1Drw} mice were arrhythmic under DD, demonstrating their redundancy and its importance within circadian machinery [197, 201].

A full null-*Per2* mutant mouse was generated: *Per2*^{tm1Clc}. This latter was never characterized and only one paper mentioned that this construct had the same circadian phenotype that *Per2*^{tm1Brd} in mixed 129(not precisely specified)/C57BL6 background, despite the fact that PER2 protein could not be detected in these mice [120]. One part of this thesis is then based on circadian characterization in *Per2*^{tm1Clc} mice.

A *Per3* mutant mice (*Per3*^{tm1Drw}) was constructed in 129S4/SvJae background. No PER3 protein was detected in *Per3*^{tm1Drw}, while *Per3* transcript was still present and rhythmically expressed but larger than Wt mice. *Per3*^{tm1Drw} had a shorter period (23.3h±0.2) compared with Wt mice (23.8h±0.1) [202]. In spite of this difference, it was concluded that *Per3*^{tm1Drw} only shown a subtle circadian phenotype contrasting with previous *Per1*^{tm1Drw} and *Per2*^{tm1Drw}. In fact these latter had important changes in circadian clock gene expression, that was not the case pour *Per3*^{tm1Drw} [202]. Moreover, the double mutant mice *Per1,3*^{tm1Drw} and *Per2,3*^{tm1Drw} had not a stronger circadian phenotype [197]. Therefore it was concluded that *Per3* does not play an important role in the circadian clock mechanism [197, 202].

Two studies investigated sleep in *Period* mutant mice. The first one done by Kopp *et al.* using *Per1*^{tm1Brd} and *Per2*^{tm1Brd} mice backcrossed to a C57BL6/J background [203], and the second by Shiromani *et al.* using *Per1*^{tm1Drw}, *Per2*^{tm1Drw}, *Per3*^{tm1Drw} and double mutant *Per1,2*^{tm1Drw} mice under an unspecified 129/Sv background (probably 129S4/SvJae background as it was used by the strain creators) [201].

Kopp *et al.* demonstrated that although daily amount of sleep did not differ in mutant mice, the distribution of sleep was affected: *Per1^{tm1Brd}* mice slept less than Wt in the second half of the dark period while *Per2^{tm1Brd}* mice slept less before the dark onset. After a 6h SD, an increase of the amount of sleep was noted in the *Per2^{tm1Brd}* mice recovery in comparison with Wt mice. Both mutant mice lines had also higher amount of REM sleep in the light period of the recovery. Furthermore, lower levels of EEG delta power were reached during recovery sleep immediately following the SD. Despite these changes in sleep distribution and recovery, it was concluded that *Per1^{tm1Brd}* and *Per2^{tm1Brd}* mice have intact sleep homeostasis [203].

The study done by Shiromani *et al.* confirmed that *Per1^{tm1Drw}* and *Per2^{tm1Drw}* had an altered sleep-wake distribution. Concerning the EEG delta power after 6h SD, the rebound was lasting longer in *Per1^{tm1Drw}* and in double mutant *Per1,2^{tm1Drw}* mice. On the other hand, EEG delta power seem to be higher in the *Per1^{tm1Drw}* and in *Per1,2^{tm1Drw}* mice than Wt mice [201]. This ascertainment was in perfect opposition with the previous study done by Kopp *et al.* [203]. Nevertheless, the authors argued that deletion of the *Per* genes do not affect sleep homeostasis [201].

In this thesis, I will show that even that the sleep intensity does not change; the sleep duration is affected differently between the *Per1^{-/-}*, *Per2^{-/-}*, *Per1,2^{-/-}* and Wt mice after 6h SD. I would like to remember also that both sleep intensity and sleep duration were involved in sleep homeostasis.

Shiromani *et al.* showed that *Per3^{tm1Brd}* had no differences in both sleep distribution and EEG delta power during recovery after 6h SD [201]. In contrast, a subsequent study done in C57BL6/J background did find differences in the relative REM sleep rebound during the recovery from 6h SD; due to REM sleep difference under baseline. However, EEG delta power after SD was the same in *Per3^{-/-}* and Wt mice. Given that under baseline the EEG delta power was higher in *Per3^{-/-}* mice, despite the same amount of vigilance state, a homeostatic sleep phenotype was suggested [204].

5. *Rev-erb*

In C57BL6/J background *Rev-erba*^{-/-} had a shorter period than *Rev-erba*^β^{-/-} and Wt mice. Given that the double mutant mice were not viable, a conditional system had to be used. As mentioned above, *Rev-Erba*^{lox/lox}*RevErba*^β^{lox/lox} showed severe activity defects but maintained a short circadian rhythm under DD condition [167]. Sleep studies were not already published on these mice, however *Rev-erba*^{-/-} in mix 129/C57BL6 background showed altered sleep/wake distribution. Moreover, EEG delta power levels were lower at sleep onset under baseline and after 6h SD compared to Wt mice, establishing that sleep homeostasis was affected in the *Rev-erba*^{-/-} mutant mice [205].

In conclusion, it is important to keep in mind that the genetic background can have a huge impact on the activity profile, as well as on sleep patterns [206]. However, it is clear that knock-out of a clock gene belonging to the master-clock generates completely arrhythmic mice, which can also display perturbation of the homeostatic sleep regulation. Some single mutation were enough to modify the homeostatic process such as *Npas2*^{-/-}, *Rev-erba*^{-/-}, rather others had not effect such as *Clock*^{-/-}, *Cry1*^{-/-}, *Cry2*^{-/-}, *Per1*^{-/-}. For the single knock-out *Per2*^{-/-} or *Per3*^{-/-} the results were not so clear and the exact readout could depend from the way the studies were designed and analyzed. All phenotype in clock mutant mice were summarized in table 1.

Clock mutant mice	period	Baseline		SD condition		Background	References
		Sleep/wake distribution	Sleep consolidation	EEG delta power	NREM/REM sleep duration		
<i>Bmal1</i> ^{tm1Brn}	arrhythmic	altered	less	altered	n.a.	C57BL/6J	163, 190
<i>Clock</i> ^{tm1Rep}	normal	-	n.a.	n.a.	n.a.	C57BL/6J	136
<i>Clock</i> ^{tm1Jt}	longer	altered	yes	-	less REM	C57BL/6J	193
<i>Npas2</i> ^{tm1SIm}	shorter	-	-	altered	less NREM/REM	C57BL/6J	103, 194
<i>Clock</i> ^{tm1Rep} <i>Npas2</i> ^{tm1SIm}	arrhythmic	altered	n.a.	n.a.	n.a.	C57BL/6J	136
<i>Cry1</i> ^{tm1Asn}	shorter	altered	-	-	n.a.	C57BL/6J	195
<i>Cry2</i> ^{tm1Asn}	longer	altered	-	-	n.a.	C57BL/6J	195
<i>Cry1</i> ^{tm1Asn} <i>Cry2</i> ^{tm1Asn}	arrhythmic	altered	more	altered	less REM	C57BL/6J	191, 196
<i>Per1</i> ^{tm1Drw}	progressively arr.	affected	-	affected	-	129S4/SvJve	197, 201
<i>Per1</i> ^{tm1Saco}	shorter	-	-	-	-	C57BL/6-129S2/SvPas	198
<i>Per1</i> ^{tm1Brd}	shorter	-	-	-	-	129S7/SvEvBrd	165
	-	affected	-	affected	-	C57BL/6J	203
<i>Per2</i> ^{tm1Drw}	shorter, prog. arr.	altered	n.a.	altered	n.a.	129S4/SvJve	197, 201
	-	-	n.a.	n.a.	n.a.	C57BL/6J	200
<i>Per2</i> ^{tm1Brd}	shorter, prog. arr.	n.a.	n.a.	n.a.	n.a.	129S7/SvEvBrd-C57BL/6	199
	n.a.	altered	n.a.	altered	n.a.	C57BL/6J	203
<i>Per1,2</i> ^{tm1Drw}	arrhythmic	altered	n.a.	altered	n.a.	129S4/SvJve	197, 201
<i>Per3</i> ^{tm1Drw}	shorter	-	n.a.	-	-	129S4/SvJve	202
	n.a.	altered	more	-	-	C57BL/6J	204
<i>Per1</i> ^{tm1Ccl}	shorter	affected	-	-	-	C57BL/6J	present study
<i>Per2</i> ^{tm1Ccl}	arrhythmic	affected	less	-	less NREM/REM	C57BL/6J	present study
<i>Per1,2</i> ^{tm1Ccl}	arrhythmic	affected	less	-	less NREM	C57BL/6J	present study

Table 1 Summary of all phenotype in clock mutant mice n.a: not available data; - : as the Wt mice

IV. *Period 1* and *Period 2*

To understand better the phenotype of mice lacking *Per1* and/or *Per2* genes, it is important to know the possible interactions of these proteins, but also their role in functions other than the circadian machinery. Moreover, by which other way than circadian pathway these genes could be regulated is another important topic of further investigation. Afterward, in this chapter, I will describe the *Per1* and *Per2* genes in further details, as well as their respective proteins and their functions.

1. Genes

In mice *Per1* is located on the chromosome 11 (69'095'217 - 69'109'960b). It has 6 splice variants with 5 having an *open reading frame* (ORF) permitting protein translation (table 2). In mice *Per2* is located on chromosome 1 (91'415'984 - 91'459'330b), it only has one transcript which is translated in a single protein.

Name	Transcript ID	Length (bp)	Exon	Coding exon	Protein ID	Length (aa)	Biotype
Per1-001	ENSMUST0000021271	4671	23	22	ENSMUSP0000021271	1291	Protein coding
Per1-201	ENSMUST00000166748	4636	23	22	ENSMUSP00000132635	1291	Protein coding
Per1-002	ENSMUST00000102605	4537	22	22	ENSMUSP00000099665	1271	Protein coding
Per1-003	ENSMUST00000101004	3507	18	17	ENSMUSP00000098566	827	Protein coding
Per1-005	ENSMUST00000132462	496	3	2	ENSMUSP00000122164	106	Protein coding
Per1-004	ENSMUST00000142392	2972	15	13	ENSMUSP00000121713	572	Nonsense mediated decay
Per2-201	ENSMUST00000069620	5837	23	22	ENSMUSP00000066620	1257	Protein coding

Table 2 All transcripts and protein variants for *Per1* and *Per2*

Per genes have several promoter regions. The most important are the E-box and E'-box that allow the binding of proteins having a *basic helix-loop-helix* (bHLH) such as BMAL1, CLOCK and NPAS2 but also many other such as neurogenin, which are involved in neuronal differentiation [207]. The *glucocorticoid response element* (GRE) is also present in the *Per* promoter region and is induced by the *glucocorticoids* (GC). The principal endogenous GC in rodents is corticosterone which is associated with stress during sleep deprivation [208]. Corticosterone is thought to be important for synchronization of peripheral rhythms [209]. Another interesting GC in rodents is the primary female sex hormone estrogen. In the SCN, estrogen advanced the acrophase of *Per2* only, while no effect was observed in the cortex. On the other hand, only *Per1* expression is changed by estrogen in liver and kidney, whereas acrophase in both genes were advanced in the reproductive tissues uterus. This suggested that the effects of estrogen are tissue specific [210]. In culture cells, the most widely used GC is dexamethasone, a synthetic drug, had similar effect on cells synchronization and *Pers* expression that corticosterone [99]. However, gene induction *via* GC did not work in the exactly same way for *Per1* and *Per2*. In fact, only GC combined with *glucocorticoid receptor* (GR) is enough to induce the *Per1* expression, this is not the case for *Per2*. This latter requires the transcription factor BMAL1 for binding the GRE probably due to an overlapping of GRE and E-box that is specific of the *Per2* promoter [211].

The *cAMP response element* (CRE) is another *Per1* and *-2* promoter element, and is activated by *phosphorylated CRE binding protein* (pCREB) [212]. pCREB was found to be particularly highly expressed in the cerebral cortex and hippocampus after staying awake for a few hours or after sleep deprivation [213]. Light exposure induced *via* RHT a release of glutamate and PACAP in the SCN, which produced high level of cAMP and pCREB, ultimately allowing the expression of *Per1* and *Per2*

(but not *Per3*) in the SCN [125, 214, 215]. D-box is another element present in the promoter of *Per1* and *-2* genes, it allows induction by the clock controlled gene *Dbp* and inhibition by *nuclear factor, interleukin 3 regulated* (NFIL3 also called E4BP4) which both plays an important role in determining the period length [216]. As explained above, the *Per2* promoter contains a HSE that responds to warm exposure *via* HSF permitting cells synchronization *in vitro* [130, 186] but also to have a purpose role in the temperature compensation process [130]. *Pers* genes also have a TATA-box (5'-TATAAA-3') in their promoters that is targeted by the *TATA binding protein* (TBP) -like *POU domain, class 2, transcription factor protein* (POU2F) [217]. Of course the TATA-box is a very common element present at the promoters of about 24% of human genes and therefore has many roles outside the circadian regulation [218].

2. Proteins

The *Per1* gene produces 5 functional translated proteins (table 2). However, PER1-001 and PER1-201 are exactly the same protein composed by 1291 *amino-acid* (aa). The other 3 proteins are truncations, but could still be functional. PER2 is 1257aa long. PER1 and PER2 are very similar in their main domain composition as shown in the comparison view in figure 14 (upper panel) suggesting that the more precisely view of the PER2 domains (Fig.14 lower panel [219, 220]) it is also in part true for PER1.

The first domain found in PER2 from the N-terminal is the helix-loop-helix (HLH) motif; however this probably does not have the ability to bind the E-boxes due to the non-basic aa preceding it [219]. Within this HLH, the first *nuclear export signal* (NES1) is located. The second, NES2, is located just after the proline-rich (pro-rich) sequence, and the third (NES3) follows the cytoplasmic localization domain (CLD). These latter two domains (NES and CLD) are responsible for protein exportation into the cytosol [221]. PER1 and -2 have NES motifs enabling their exit from the nucleus as well as a *nuclear export site* (NLS) that can be masked by binding of CKIε, thus controlling the rate at which PER1 enters the nucleus [178, 222].

Both PER1 and PER2 contain two distinct *Per-Arnt-Sim* (PAS) domains in the N-terminal region. PAS domains are conserved in all life kingdoms and are composed of 275aa containing two ~70aa repeat sections called PAS A (or 1) and PAS B (or 2). Members of this family are often found in pathways that regulate responses to environmental change. In mammals these include the hypoxia, circadian (*Per* gene), and dioxin response pathways (*Arnt* gene). PAS domains are also found in proteins involved in the development of the central nervous system (*Sim* gene) [223]. Most relevant mammalian proteins with PAS

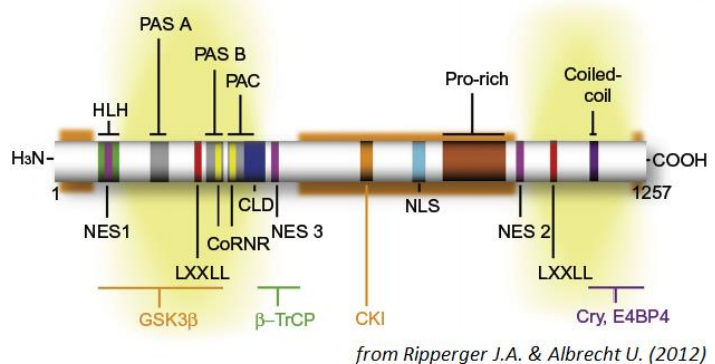
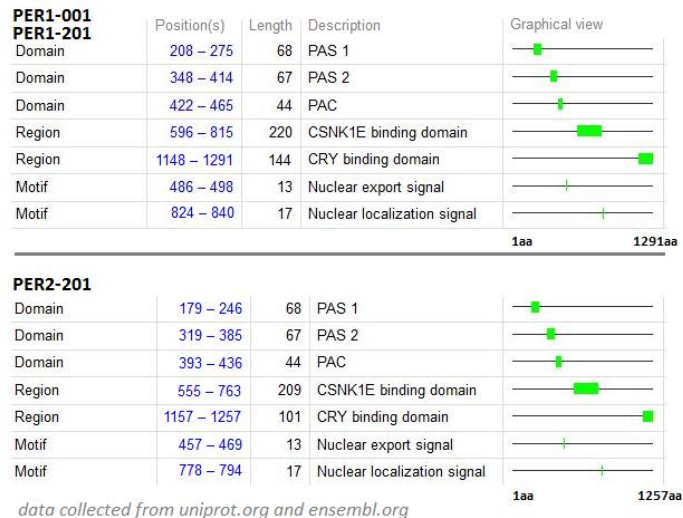


Figure 14 Comparison between main domains of PER1 and PER2 proteins (Upper panel). From Uniprot.org and ensembl.org **Detailed domains and protein interaction region for PER2 protein (Lower panel).** NES: nuclear export site; HLH: helix-loop-helix; PAS: Per-Arnt-Sim domain; NLS: nuclear localization site; CLD: cytoplasm localization domain; CKI: casein kinase 1; pro-rich: proline rich region. Ripperger J.A. and Albrecht U. (2012) [220]

domain are reported in table 3. Phylogenetic analysis of the PAS domain in mice showed that PAS A & B are highly conserved with an identity ratio of 35% and 31%, respectively. Based on this data, mouse PAS domains were grouped into distinct clades: *basic helix-loop-helix* (bHLH) transcriptional regulators involved in neuronal and vascular development; circadian transactivators *Clock* and *Npas2*; *Arnt*, *Bmal1*, and their paralogs; and finally homologs of *Per* which act as transcriptional repressors. Given their ability to bind and sense small molecules, PAS domain-containing proteins are important to mediate environmental adaptation. Small molecules can be used as cofactors, but can also mediate protein-protein interactions [223]. The PAC motif is present at the C-terminal of all known PAS motifs and contributes to the folding of PAS [224]. Thus PAS domains in PERIOD protein allow its dimerization (with BMAL1, CLOCK and NPAS2 for example), but also protein-protein interac-

Gene symbol	Aliases	Chrm.	Peptide length (aa)	bHLH (cd00083, cl00081)	PAS	PAS A (cd00130, cl02459)	PAS B (cd00130, cl02459)	PAC (smart00086)
<i>Hif1a</i>	<i>Mop1, Aip</i>	12	836	17–71	80–345	80–155	228–298	302–345
<i>Epas1</i>	<i>Hif2a, Mop2, Hlf</i>	17	874	15–68	84–357	84–154	230–300	304–347
<i>Hif3a</i>	<i>Mop7, Ipas, Nepas</i>	7	662	12–66	80–340	80–150	225–295	299–340
<i>Ahr</i>	<i>Dioxin receptor</i>	12	805	12–80	116–359	116–179	269–336	342–380
<i>Ahrr</i>		13	701	13–79	106–176	106–176	na	na
<i>Arnt</i>	<i>Drnt, Hif1b</i>	3	776	75–128	147–451	147–223	334–405	409–451
<i>Arnt2</i>	<i>Hif-28</i>	7	712	64–117	134–441	134–209	323–393	398–441
<i>Arntl</i>	<i>Arnt3, Mop3, Bmal1</i>	7	626	80–133	150–451	150–222	333–403	408–451
<i>Arntl2</i>	<i>Bmal2, Clif, Mop9</i>	6	579	49–102	119–414	119–190	296–366	371–414
<i>Clock</i>		5	855	35–85	107–379	107–177	262–332	336–379
<i>Npas2</i>	<i>Mop4</i>	1	816	10–60	82–354	82–152	237–301	311–354
<i>Per1</i>	<i>Per, m-rigui</i>	11	1291	na	208–465	208–275	348–414	422–465
<i>Per2</i>		1	1257	na	179–436	179–246	319–385	393–436
<i>Per3</i>		4	1113	na	120–376	120–187	250–324	333–376
<i>Sim1</i>		10	765	1–54	77–335	77–147	218–288	292–335
<i>Sim2</i>		16	657	1–54	77–335	77–147	218–288	292–335
<i>Npas1</i>	<i>Mop5</i>	7	594	46–99	135–409	135–205	289–360	366–409
<i>Npas3</i>	<i>Mop6</i>	12	925	59–116	152–441	152–222	324–394	398–441
<i>Npas4</i>	<i>Nxf</i>	19	802	1–52	70–319	70–144	203–275	280–319

Table 3 Main murine Per-Arnt-Sim (PAS) domain superfamily members with associated domains and features. From McIntosh B.E., Hogenesch J.B. & Brad C.A. (2010) [223]

tions with other PER proteins [220]. It was also reported that the kinase GSK3 β interact with the PAS domains of PER2 (but not PER1) [183]. It is interesting to note that the PAS A domain of NPAS2 is able to bind heme and a point mutation this PAS A domain that disrupts this heme binding and then inhibits its partnering with BMAL1 [225]. The PAS A domain of PER2 likewise binds heme and can exchange this heme with NPAS2, suggesting similar mechanism of interactions [226]. Moreover, it was proposed that the PAS domain enables PER2 to sense the redox state by this heme interaction [227]. It was also shown that mice lacking the PAS B/PAC domain in PER2 had an altered response to light [228].

PER2 possess some elements also found in coactivators and corepressors proteins as LXXLL motifs (also called NR boxes; L=leucine, X= any aa) and consensus sequence named CoNR boxes. It let us postulate that PER2 is able to interact with different nuclear receptors as other protein containing the same boxes (such as progesterone, estrogen and peroxisome proliferator-activated receptors) [219]. In fact, a study showed that PER2 interacts with some nuclear receptors such as PPAR α and REV-ERB α , serving as a coregulator of nuclear receptor-mediated transcription and thus

modulating the expression of nuclear receptor target genes such as *Bmal1*, *Hnf1 α* , and *Glucose-6-phosphatase*. Thereby PER2 propagates clock information to metabolic pathways [229].

PER1,-2 also contain a pro-rich sequence. This sequence is responsible for a less structured aa chain, preventing helice α structures, and so dividing PER protein into two separate structural entities that could interact with two different protein. Therefore, PER protein could serve as a scaffold. These two structural entities could also fold back on themselves and interact with only one other protein [219].

At its carboxy-terminal, the PER2 protein contains a coiled-coil (a small helix form) that allows the dimerization with other protein in possession of this helix structure [219]. In addition, it was reported that this surrounding area of PER1 and -2, able to bind CRY1 and -2 [230]. It was shown that NFIL3 binds PER2 in the same region [231]. In the figure 14, the yellow-shaded areas represent these potential protein-binding domains [219].

Several kinases can bind PER, as GSK3 β stated above (specifically PER2)[183] and also CKI ϵ (and probably also CKI δ) which as an important role in PER1 and -2 phosphorylation by the binding of CSNK1E domain (see chapter II.5.d) [178-180]. In the figure 14, the orange-shaded areas represent these potential phosphorylation sites [219].

It was shown that FBXW1A (also called β -TrCP1) binds PER protein to leads its polyubiquitination permitting its proteolysis [181].

Given the remarkable size of the PER proteins, it is possible that additional domains and function remain to be discovered. In fact, a cistrome analysis in the mice liver identified about 4600 and 7300 genomic-binding sites for PER1 and PER2, respectively. Motif analysis showed that these factors are specially enriched for E-box sites as well as nuclear receptor binding sites [232].

Science never solves a problem without creating ten more

George Bernard Shaw

Thesis Project

V. Research outline

During my doctoral work I had two main projects both related to circadian rhythm and sleep research, with a particular focus on the *Per2* gene. Given that these two projects address fundamentally different questions, I separated them in two distinct sections.

The aim of my first project has been to advance our understanding of the link between sleep homeostasis and circadian rhythms. In particular, I investigated a possible mechanism by which sleep deprivation could alter clock gene expression by quantifying DNA-binding of the core-clock genes BMAL1, CLOCK and NPAS2 to their target chromatin loci including the E-box enhancers of the *Per2* promoter. To further investigate the nature of this link, my second project aimed at studying locomotor activity and sleep architecture of mice lacking *Period1* and *-2*. I characterized the recovery period after sleep deprivation, and finally assessed the repercussion on the expression of other clock genes.

1. DNA-binding of clock transcription factors as a function of sleep loss

Increasing evidence suggest that clock genes contribute to the homeostatic aspect of sleep regulation [233]. Increasing homeostatic sleep pressure by means of a SD affects the expression of some clock genes in the brain. On the other hand, mutation of some clock genes alters the markers of sleep homeostasis. The goal of my first project was to investigate a possible mechanism by which SD could alter clock gene expression focusing on the DNA-binding of the transcription factors involved in the positive limb of the circadian machinery (i.e. BMAL1, CLOCK and NPAS2). The hypothesis is that changing in sleep/wake behavior performing a SD might contribute to driven transcription through clock machinery (Fig.15).

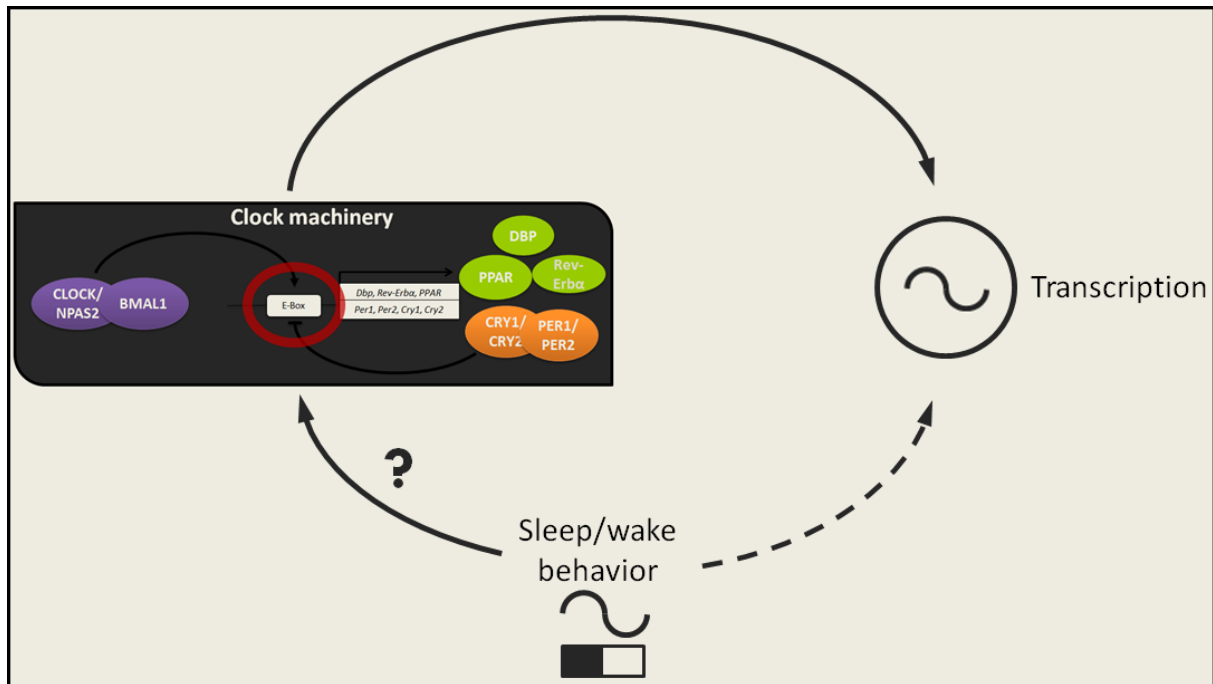


Figure 15 Hypothesis of the project: changing in sleep/wake behavior preforming a SD might contribute to driven transcription through clock machinery

I made use of *chromatin immunoprecipitation* (ChIP) and *quantitative polymerase chain reaction* (qPCR). To validate these methodologies, the experiments were first performed on liver tissue, and we showed that DNA-binding of CLOCK and BMAL1 to their target genes changes as a function of time-of-day as published earlier [234-237]. Subsequently, we performed the same experiment on the cerebral cortex. This has never been done before and we demonstrated that, like in the liver, the DNA-binding pattern of core clock genes varied as a function of time-of-day. We then performed a 6h SD and observed a significant decrease in DNA-binding of CLOCK and BMAL1 to *Dbp*. This is consistent with a decrease in *Dbp* mRNA levels after SD. The DNA-binding of NPAS2 and BMAL1 to *Per2* was similarly decreased following SD. However, SD has been previously shown to increase *Per2* expression in the cortex which seems paradoxical [48, 238, 239]. It could be argued that the *Per2* increase after SD is not driven by BMAL1::CLOCK/NPAS2 but rather, among others, through glucocorticoids and/or *cAMP response element binding protein* (CREB) binding to the *Per2* promoter [240], another pathway that has been linked to sleep regulation [241]. Our results demonstrate that sleep-wake history can affect the molecular clock machinery directly at the level of the chromatin thereby altering the cortical expression of *Dbp* and *Per2*, and likely other targets. However, the precise dy-

namic relationship between DNA-binding and mRNA expression, especially for *Per2*, remains elusive. This work has been published in 2011 in PLoS One [242], where I contributed as co-first author with Valérie Mongrain, performing all experiments, analyzing the data and writing the paper. Refer to chapter VI.

2. Circadian rhythms, sleep architecture and homeostasis in *Period* mutant mice

The molecular organization of circadian rhythms is based on interlocking transcriptional feedback loops involving the core clock genes: *Bmal1*, *Clock*, *Npas2*, *Cry1*, *Cry2*, *Per1*, and *Per2*, among others [158]. These genes seem also to be involved in sleep homeostasis [26, 233]. Indeed, the brain expression of clock genes, especially that of *Per2*, increases as a function of time-spent-awake and mice lacking clock genes display altered sleep homeostasis. However, *Per2* mutant (*Per2^{m/m}*; i.e., *Per2^{tm1Brd}* or *Per2^{tm1Drw}*) mice might be an exception because homeostatic sleep regulation was found to be largely unaffected [201, 203]. For my second project I performed an in depth characterization of circadian rhythmicity, sleep architecture, EEG analysis, and response to SD in full null-*Per2* knock-out (*Per2^{-/-}*; i.e., *Per2^{tm1Ccl}*) mice, and *Per1* knock-out (*Per1^{-/-}*; i.e., *Per1^{tm1Brd}*) mice, as well as their double knock-out offspring and littermate Wt mice. The techniques used include locomotor activity recording by PIR, EEG/EMG surgery, recording, and analysis, and cerebral cortex extraction and quantification of mRNA levels by qPCR. I found that although several aspects of sleep and circadian rhythmicity are shared between *Per2^{-/-}* and *Per2^{m/m}* mice, the arrhythmicity tendency under DD was clearly more severe in the *Per2^{-/-}* mice and proved to be sex-dependent. Under standard LD12:12 conditions, I found that wakefulness onset was advanced by about 2h in *Per2^{-/-}* mice compared to Wt mice. The time courses of clock gene expression in the brain and corticosterone plasma levels were equally advanced. When released under constant dark conditions (DD) almost all *Per2^{-/-}* mice (97%) became arrhythmic immediately. From these observations, we conclude that while *Per2^{-/-}* mice seem to be able to anticipate dark onset, this does not result from a self-sustained circadian clock. Our results suggest instead that the earlier onset of activity results from a labile, not-self sustained 22h rhythm linked to light onset. Analyses of sleep under LD12:12 conditions revealed that in both *Per2^{-/-}* and

Per1,2^{-/-} mice the same sleep phenotypes are observed compared to Wt mice: increased NREM sleep fragmentation and less compensation of NREM sleep time lost. That suggests a possible role of PER2 in sleep consolidation and recovery. This work is currently in preparation and will be submitted the coming months; I contributed as first author by performing the experiments, analyzing the data and writing the paper. Refer to chapter VII.

VI. DNA-binding of clock transcription factors as a function of sleep loss

1. Introduction

Sleep loss has a profound, negative impact on cognition, learning, mood, and diverse aspects of mental health [243]. Although chronic sleep debt is a growing problem in our society, the molecular and cellular sources of its deleterious effects remain poorly understood. Sleep is known to be regulated by the tight interaction between two main processes [106, 244]: a sleep homeostat that tracks sleep need according to the duration of time spent awake and asleep, and a circadian timing system that determines the propensity for wakefulness according to an about 24h rhythm.

At the molecular level, the regulation of the circadian timing system has been extensively studied and it is now well-established that circadian rhythms originate from interacting transcriptional-translational feedback loops involving clock genes and their protein products [245]. In contrast, the molecular wiring of the sleep homeostat remains to be defined. The function of the core clock transcription factors CLOCK, NPAS2, and BMAL1 resides in their hetero-dimerization and binding to E-box (CANNTG) or E-box like (E'-box) elements of target genes from which transcription is initiated [236, 246]. Some specific targets such as *Per-1* and *-2*, and *Cry-1* and *-2* genes subsequently provide negative feedback by interfering with the CLOCK::BMAL1 or NPAS2::BMAL1 transcriptional complexes thereby inhibiting their own transcription [245]. In addition, other target genes such as the orphan nuclear receptor families *Rev-Erb* and *Ror*, respectively suppress and promote the expression of *Npas2*, *Bmal1*, and *Cry1*. These feedback loops, in combination with diverse post-translational mechanisms, result in a rhythmic (about 24h) expression of clock genes, of their protein product, and of a number of output genes (or clock controlled genes) governing a multitude of physiological functions.

It was initially reported that rhythmic gene expression did not depend on rhythmic binding of BMAL1 and CLOCK to the E-box element of a target gene, that of *Per1* in particular [247]. More recent reports clearly demonstrate, however, that BMAL1 and CLOCK bind to clock genes, notably to *Per1*, *Per2*, *Cry1*, *Cry2*, and *Dbp*, in a time-of-day dependent manner in the mouse liver [234-237].

These data imply that, at least for some clock genes, changes in binding of the core clock transcription factors to their genomic sequence play a role in the circadian modulation of their expression.

In addition to their well-established role in generating circadian rhythms, clock genes also play a circadian-independent role in sleep homeostasis [26]. First, mutations in some clock gene change the EEG and molecular markers of sleep pressure in mice [137, 238, 248-250]. For instance, *Npas2*^{-/-} mice show an attenuated EEG delta power response to SD, revealed between 1- 2Hz, compared to Wt littermates [238], whereas this marker of sleep intensity is greatly increased during normal sleep in *Cry1,2*^{-/-} mice [250]. Secondly, an increase in sleep pressure achieved by SD changes the expression of several clock genes in the forebrain of various inbred mouse strains, notably that of *Per1*, *Per2* and *Dbp* [250-252]. Moreover, although some of these sleep/wake-dependent changes, especially those of *Per1* and *Per3*, were driven by the corticosterone surge associated with the SD, the increase in *Per2* expression and the decrease in *Dbp* expression were largely independent of corticosterone [239]. This last finding suggest that the SD-induced changes in the expression of these two clock genes are likely caused by modifications in the activity of the core clock transcription factors (i.e. BMAL1, CLOCK, and NPAS2) upon their respective promoter. The fact that the SD-mediated increase in *Per2* in the brain is reduced in *Npas2*^{-/-} mice [238] and increased in *Cry1,2*^{-/-} mice [252] further supports such notion.

In this project we investigated the potential role of changes in DNA-binding activity of core clock transcription factors in the modulation of clock gene expression observed with elevated sleep pressure. Specifically, we hypothesized that SD modifies the binding of clock transcription factors to the E-box and/or E'-box sequences of specific clock genes, especially that of *Per2* and *Dbp*, in the mouse cerebral cortex. Using ChIP of cortical tissue, we first observed that the binding of clock transcription factors to several clock genes depended on time-of-day in the mouse cortex in a way comparable to the time course previously described for liver [235-237]. Importantly, we found that SD alters the binding of clock transcription factors to their target genes. This effect was both transcription factor and target gene specific. Our findings thus reveal that sleep pressure, in addition to internal time-of-

day, can modify the DNA-binding properties of core clock proteins in the brain, providing a mechanism by which clock components can sense homeostatic sleep need.

2. Material and methods

a. Animals and protocol

C57BL/6J mice originally purchased from Jackson Laboratory (Bar Harbor, ME, USA) were bred on site and maintained under standard animal housing conditions (free access to food and water, 12h-light/12h-dark cycle, 23°C ambient temperature). Males between 11 and 15 weeks at the time of the experiments were used in this study. For the time-of-day experiment (Fig.16), mice were sacrificed at ZT0 (Zeitgeber time 0: lights ON), ZT6, ZT12 (lights OFF), and ZT18 by cervical dislocation and the liver and cerebral cortex were immediately removed and fixed (within 1min), and processed for chromatin extraction. For the sleep deprivation (SD) experiment, mice were sleep-deprived for 6h starting at

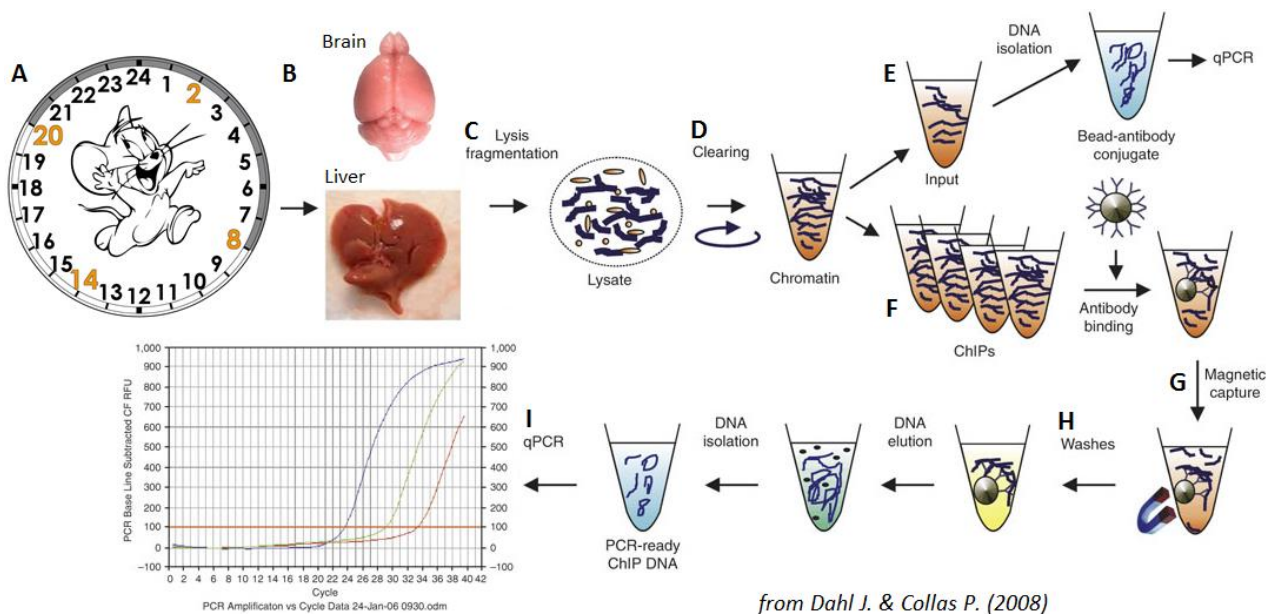


Figure 16 Overview of the time-of-day experiment with **A** sacrifice at 4 different points (in orange), **B** harvest of both liver and brain, **C** chromatin extraction and sonication, **D** pre-clearing step, **E** collection of the input **F** antibody addition except in control no-antibody condition, **G** purification by magnetic bead, **H** wash, elution and DNA isolation, **I** quantification by qPCR. Modified from *Dahl J. & Collas P. (2008)*

ZT0 by gentle handling [253], and sacrificed at ZT6 together with non-sleep-deprived controls. Cerebral cortices were immediately sampled, fixed and processed for chromatin extraction. Experiments were performed 4 to 6 times with 2 to 4 animals per time (ZT) and condition (SD vs. control). Samples were processed randomly. All experiments were approved by the cantonal veterinary office of Vaud.

b. Chromatin immunoprecipitation (ChIP)

Chromatin extraction and immunoprecipitation was performed with the Magna ChIP G commercial kit (Millipore Corporation, Billerica, MA, USA) according to the manufacturer's instructions. Briefly, cortices were chopped in small pieces and incubated for 10min in 1% formaldehyde followed by a 5min glycyl-quinching. After washes and cellular and nuclear lysis, chromatin breakdown was performed with a Bioruptor UCD-200TO (Diagenode SA, Liège, Belgium) to achieve a range of 300-1000bp chromatin lengths as determined by ethidium bromide agarose gel electrophoresis (cycles 30sec ON-30sec OFF at maximum intensity for 15min). A pre-clear step was performed (1h at 4°C with 40µl of magnetic beads) before overnight incubation of chromatin and beads with antibodies. Anti-BMAL1 antibody was from Abcam (Cambridge, England, product #ab3350), and anti-CLOCK from Abcam (product #ab461) or Santa Cruz Biotechnologies (product #sc-6927). These commercial antibodies have been used by independent groups for circadian rhythm research including for ChIP [254-256]. Custom anti-NPAS2 antibodies were produced from rabbit immunization using a peptide directed against amino acids 796 to 810 of the C-terminal domain of NPAS2 (accession #NP_032745) by Lucerna-Chem AG (Lucerne, Switzerland). The specificity of this antibody was verified by ELISA (by the company) and Western blot (Fig. 17) on cortical cortex protein extracts (91kDa). All samples were also identically submitted to a no-antibody condition (mock condition) used to take into account nonspecific binding. DNA purification was performed using the silica columns provided with the kit (Magna ChIP G, Millipore).

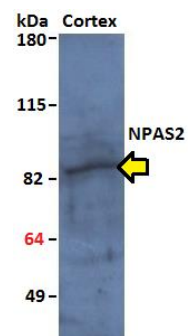


Figure 17 Western blot 1/1000 α -NPAS2 in mouse cortical cortex. 8 % gel, PVDF membrane. Specific band at 91kDa.

c. Quantitative PCR

Quantitative PCR was performed according to Applied Biosystems protocol using a 7900HT Fast Real-time PCR System with SDS2.3 software (Applied Biosystems, Foster City, CA, USA). For each qPCR reaction, purified immunoprecipitated DNA was slightly diluted (4/5) and mixed with 0.9µM of each primers, 0.25µM of probe and MasterMix reagent (Applied Biosystems) or FastStart Universal Probe Master (Roche Diagnostic GmbH, Mannheim, Germany). The qPCR was performed under standard

cycling conditions (i.e., 50°C for 2min, 95°C for 10min, followed by 45 cycles of 95°C for 15sec and 60°C for 1min). Each qPCR reaction was done in triplicate. Primers and probes were designed with Primer Express v2.0 (Applied Biosystems) to amplify E-boxes and E'-boxes containing genomic regions of the four target clock genes (*Cry1*, *Dbp*, *Per1* and *Per2*). More precisely, the amplicons targeted functional sequences located in the promoter region: most proximal E-box (CACGTG) and E'-box (CACGTT) of *Cry1* (similar to [234], same as [257]), the most proximal E-box (CATGTG) of *Dbp* [236], the first E-box (CACGTG) of *Per1* [246, 258], and two E-boxes (CAGATG, CATTG) of *Per2* [258]. As an additional negative control, an amplicon targeting a non-CLOCK::BMAL1 target (i.e., exon 5 of *peripheral myelin protein 22 as Pmp22*) was also amplified for liver samples and for half of cortical samples. The oligonucleotide sequences and their source are provided in table 4. Primers were purchased from Invitrogen or Microsynth (Balgach, Switzerland) and probes from Eurogentec SA (Seraing, Belgium).

Gene		Sequence (5' --> 3')	Accession
<i>Cry1</i>	<i>Forward</i>	CCC CGG CTT CTC ATT GG	NCBIM37:10
	<i>Reverse</i>	CAG TGT AGT AAA CAC ACT TCA GAA ACG T	:84593000:8
	<i>Probe</i>	FAM-CCC CAC GTG ACC ACC GGC A-BQH	4647800:1
<i>Dbp</i>	<i>Forward</i>	ACA CCC GCA TCC GAT AGC	NCBIM37:7:
	<i>Reverse</i>	CCA CTT CGG GCC AAT GAG	52959000:52
	<i>Probe</i>	FAM-CGC GCA AAG CCA TGT GCT TCC-TAMRA	965561:1
<i>Per1</i>	<i>Forward</i>	AGC TTT AGC CAC GTG ACA GTG A	
	<i>Reverse</i>	GGC AAG TGA AGA GGC CAA CA	AB030818
	<i>Probe</i>	FAM-TGC ACT TAA CAG CTG ATT ATG TCA GCC GC-BHQ	
<i>Per2</i>	<i>Forward</i>	AGA AAA GCC CTG CTG TTC CA	
	<i>Reverse</i>	CCA AAT GCG GTG GTG TAG TTT	AF491941
	<i>Probe</i>	FAM-CCG CTT CCA TAG TTC CTG TAA GGT-BQH	
<i>Pmp22</i>	<i>Forward</i>	TTC GTC AGT CCC ACA GTT TTC TC	
	<i>Reverse</i>	ACT CGC TAG TCC CAA GGG TCT A	NM_008885
	<i>Probe</i>	FAM-CGG TCG GAG CAT CAG GAC GAG C-BHQ	

Table 4 Primers and probes used for quantitative PCR

d. Statistical analysis

Tissue sampled from each animal was treated separately and data from the repeated experiments were combined. Similar to what was performed previously [234-237], binding was initially analyzed as a fold relative to input chromatin in both liver and cerebral cortex. However, we observed that non-specific binding (no-antibody condition) varied and was influenced by time-of-day for liver (Fig.18). Thus, data were expressed in fold-change relative to the no-antibody negative control condition, as performed in other studies [259, 260], in order to control for non-specific binding and also for between-experiment differences. The number of biological replicates (i.e., the number of individual mice) contributing to each data point is indicated in each figure. Numbers vary because of data loss and removal of outliers; i.e. values more than two standard deviations away from the mean (<6% of

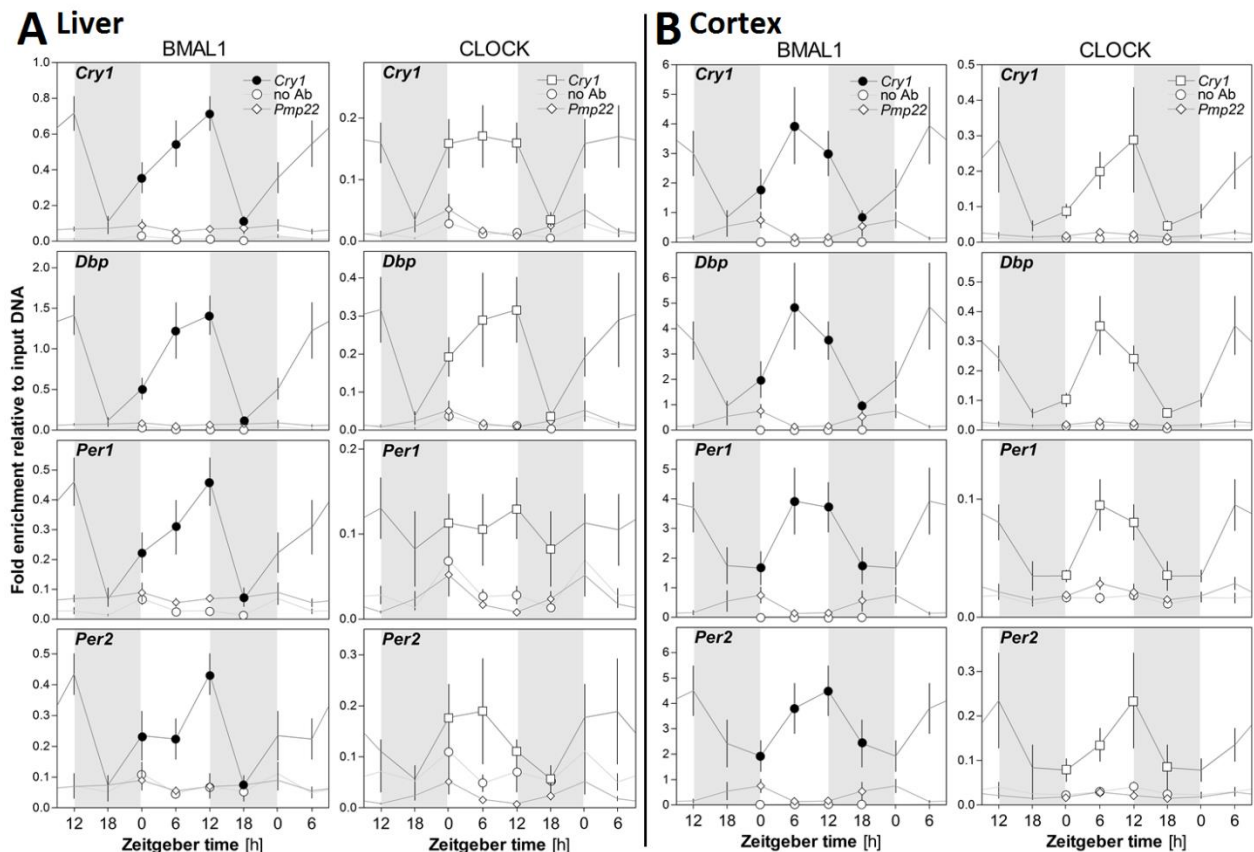


Figure 18 BMAL1 and CLOCK binding onto the promoter of 4 clock genes in the mouse liver (A) and cerebral cortex (B). Mice were sacrificed every 6 hours for 24 hours, and brain cortices were rapidly processed. Chromatin immunoprecipitation (ChIP) was performed using antibodies against BMAL1 and CLOCK or no antibody (negative control), and enrichment of putative promoter sequences of *Cry1*, *Dbp*, *Per1* and *Per2*, and of a non-CLOCK::BMAL1 target, *Pmp22*, was measured using quantitative PCR. Data were expressed relative to input DNA. **A** Time-of-day affected non-specific binding (no antibody) to *Cry1* ($F_{3,23} = 4.2$, $p < 0.05$), *Dbp* ($F_{3,22} = 3.9$, $p < 0.05$), and *Per1* ($F_{3,22} = 3.9$, $p < 0.05$), all plotted in both BMAL1 and CLOCK columns), but not that of BMAL1 or CLOCK to the control gene *Pmp22*. **B** Time-of-day did not significantly affect non-specific binding (no antibody), neither that of BMAL1 or CLOCK to the control gene *Pmp22*. Data are presented as mean \pm SEM ($n = 5, 5, 5, 5$ for all genes for BMAL1; *Cry1* $n = 5, 6, 5, 6$; *Dbp* and *Per2* $n = 5, 5, 5, 5$; *Per1* $n = 6, 6, 5, 5$ for CLOCK for ZT0, -6, -12, and -18, respectively). Grey lines connect double-plotted data, and light grey areas represent 12 h dark periods.

all values). Fold enrichments were calculated as a ratio of the power of Ct between sample and the respective no-antibody control (i.e. fold enrichment = $\frac{2^{-Ct \text{ sample}}}{2^{-Ct \text{ no-antibody}}}$). The effect of time-of-day on chromatin binding was assessed by one-way ANOVA, and significant effects were decomposed using Tukey tests. For assessing the SD effect on chromatin-binding, between-experiment differences were taken into account by expressing each SD enrichment level in percent of the enrichment level of a non-sleep deprived control processed in the same batch ($\frac{\text{fold enrichment SD}}{\text{fold enrichment control}} * 100$). The effect of SD was then analyzed using two-tailed single sample t-tests. Statistical analyses were performed with GraphPad Prism 4 (GraphPad Software Inc., San Diego, CA) or Statistica (Statsoft Inc., Tulsa, OK). The threshold for statistical significance was set to ≤ 0.05 and results are reported as mean \pm SEM.

3. Results and discussion

a. Rhythmic binding of BMAL1 and CLOCK to selected clock genes

We have previously shown that SD does not uniformly affect the expression of all clock genes in the brain [48, 238, 239, 250-252, 261]. For the present chromatin binding study, we selected *Cry1* which shows either no change or a small amplitude decrease or increase following SD, *Dbp* for which mRNA consistently decreases after SD, and *Per1* and *Per2* which mRNA are increased by SD. To validate our technique, we first confirmed rhythmic binding of CLOCK and BMAL1 to the E-box or E'-box elements of the promoter of the four selected clock genes in the mouse liver. Livers collected at 4 different times of day (ZT0, -6, -12, and -18) were processed using ChIP. Consistent with the literature [234-236], we observed that the binding of BMAL1 and CLOCK to *Cry1* and *Dbp* was higher at ZT6 (i.e., 6h after lights on) than at ZT18 (i.e. 6h after lights off) or ZT0. A similar phase was observed for BMAL1 and CLOCK binding to *Per1* and *Per2* promoters (Fig.19).

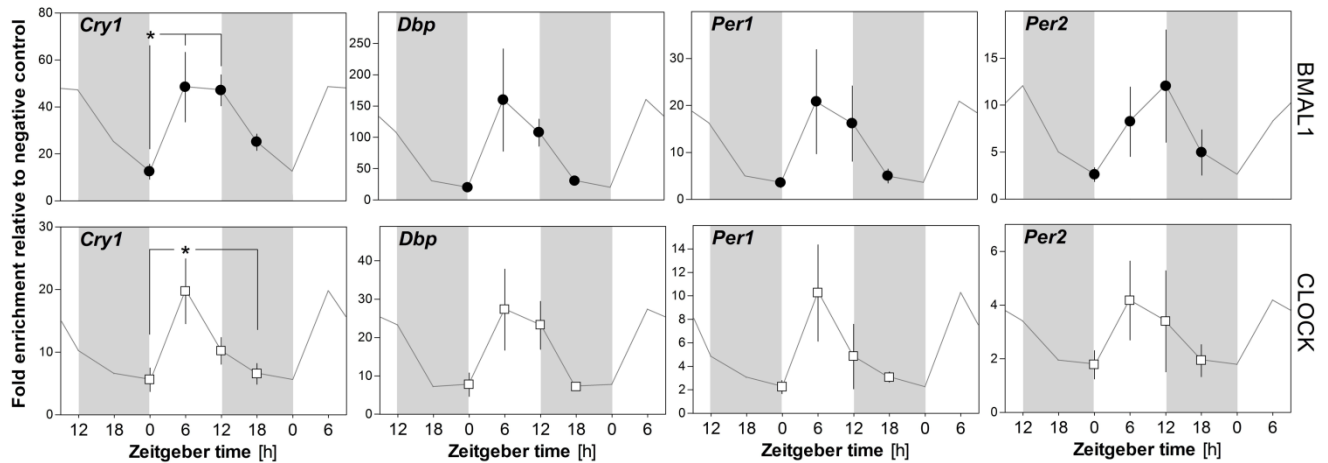


Figure 19 The effect of time-of-day (ZT) on BMAL1 and CLOCK binding onto the promoter of 4 clock genes in the mouse liver. Mice were sacrificed every 6 hours for 24 hours (ZT0=Lights ON), and livers were rapidly sampled and processed. Chromatin immunoprecipitation (ChIP) was performed using antibodies against BMAL1 and CLOCK, and enrichment of E-box or E'-box containing sequences of the putative promoter region of *Cry1*, *Dbp*, *Per1*, and *Per2* was measured using quantitative PCR. Data were normalized to a negative control condition (no-antibody). Time-of-day significantly affected the binding of BMAL1 ($F_{3,19}=4.3$, $p<0.05$) and that of CLOCK ($F_{3,21}=4.1$, $p<0.05$) to *Cry1*. Similar trends were also observed regarding binding to *Dbp* (BMAL1: $F_{3,19}=2.4$, $p=0.1$, n.s.; CLOCK: $F_{3,19}=2.7$, $p=0.08$, n.s.) and CLOCK binding to *Per1* ($F_{3,21}=2.0$, $p=0.1$, n.s.). Data are presented as mean \pm SEM ($n=5, 5, 5, 5$ for all genes for BMAL1; *Cry1* $n=5, 6, 5, 6$; *Dbp* and *Per2* $n=5, 5, 5, 5$; *Per1* $n=6, 6, 5, 5$ for CLOCK for ZT0, -6, -12, and -18, respectively). Grey lines connect double-plotted data, and light grey areas represent 12 h dark periods. (*: $p<0.05$ between indicated points; post-hoc Tukey comparisons).

Daily changes in chromatin binding of core clock transcription factors to the target genes of interest have not been assessed in the mammalian brain. Therefore, to put the eventual changes incurred by the SD into context (see below), we determined the time-of-day variations in DNA-binding of BMAL1 and CLOCK to the four selected clock genes in the mouse cerebral cortex. Cortical tissue from the same 4 different times of day (ZT0, -6, -12, and -18) were analyzed using ChIP. The binding of both core clock transcription factors to their four target genes exhibited highly similar time-of-day variations (Fig.20). Specifically, CLOCK bound to the four target genes in a time-of-day-dependent manner with maximum binding reached at ZT6 and lowest binding at ZT18 or -0 for *Cry1* (one-way ANOVAs: $F_{3,48}=3.9$, $p=0.01$), *Dbp* ($F_{3,49}=6.8$, $p<0.001$), and *Per2* ($F_{3,59}=4.6$, $p<0.01$), while the binding to *Per1* peaked at ZT12 and reached a minimum at ZT18 ($F_{3,54}=3.8$, $p<0.02$). BMAL1 binding showed a similar pattern with maximal levels reached at ZT6 and a minimum at ZT18 or -0 for *Cry1* ($F_{3,56}=4.3$, $p<0.01$) and *Dbp* ($F_{3,56}=2.9$, $p<0.05$), whereas, although similar, the time-of-day changes in *Per1* and *Per2* binding did not reach statistical significance ($F_{3,60}=1.7$, $p=0.2$, n.s. for *Per1*; $F_{3,67}=2.2$, $p=0.09$, n.s. for *Per2*).

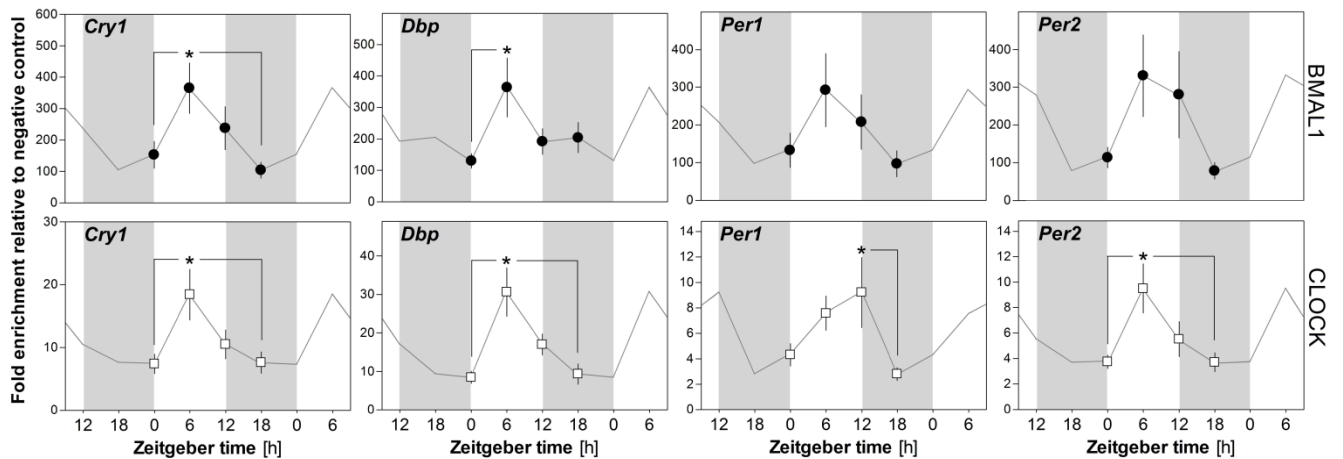


Figure 20 The effect of time-of-day (ZT) on BMAL1 and CLOCK binding onto the promoter of 4 clock genes in the mouse cerebral cortex. Mice were sacrificed every 6 hours for 24 hours (ZT0=Lights ON), and cerebral cortices were rapidly sampled and processed. Chromatin immunoprecipitation (ChIP) was performed using antibodies against BMAL1 and CLOCK, and enrichment of E-box or E'-box containing sequences of the putative promoter region of *Cry1*, *Dbp*, *Per1*, and *Per2* was measured using quantitative PCR. Data were normalized to a negative control condition (no-antibody). Time-of-day significantly affected the binding of BMAL1 to *Cry1* and *Dbp* genes, and the binding of CLOCK to all 4 target genes. Data are presented as mean \pm SEM (*Cry1* n= 14, 16, 14, 13; *Dbp* n= 14, 15, 13, 15; *Per1* n= 16, 16, 14, 15; *Per2* n= 16, 18, 17, 17 for BMAL1; *Cry1* n= 13, 13, 12, 11; *Dbp* n= 12, 14, 11, 13; *Per1* n= 15, 14, 12, 14; *Per2* n= 14, 15, 15, 16 for CLOCK for ZT0, -6, -12, and -18, respectively). Grey lines connect double-plotted data, and light grey areas represent 12 h dark periods. (*: $p < 0.05$ between indicated points; post-hoc Tukey comparisons).

We here demonstrate, that in the cerebral cortex, the binding of BMAL1 and CLOCK to the targeted clock genes varies in function of time of day. These observations are similar to the only other study having assessed BMAL1 binding in the mouse brain [262], which showed a higher binding of BMAL1 to the clock gene *Rev-Erba* and to *Maoa* at ZT6 than at ZT18. Our data, in particular for *Cry1* and *Dbp*, are also consistent with the observations made in the liver where ChIP for BMAL1 and CLOCK also resulted in a higher level of amplified *Cry1* and *Dbp* promoters at ZT6 compared to ZT18 [234-237]. The phase positions of maximum and minimum RNA levels are similar between the brain and liver for the different transcripts targeted (see Fig.22 for a review). Therefore, for each target, similar DNA-binding rhythms between the two tissues were expected. We observed a similar phase regarding the binding of clock transcription factors to *Per1* and *Per2* promoters in the cortex. This rhythm seemed, however, less robust as it did not reach statistical significance for BMAL1. In the liver, one study showed that BMAL1 and CLOCK binding to *Per1* promoter did not vary with time-of-day [247], while another study indicated an inverse phase for *Per2* binding by CLOCK (i.e., higher at ZT15 than at ZT6) although binding was not quantified [263]. A recent study indicates, however, that BMAL1 binding to both *Per1* and *Per2* in the mouse liver appears to peak at ZT6 [235], similar to our

findings in the cortex. In the fruit fly, a highly rhythmic binding of CLOCK to *Per*, with a peak centered around ZT12, was reported and was shown to be closely linked to the rhythm of *Per* mRNA levels [260, 264, 265]. Given the variable results obtained in mice for DNA-binding to *Per1* and *Per2*, it is possible that transcriptional rhythms of mammalian *Per* genes depend less on a highly rhythmic DNA-binding of CLOCK and BMAL1 compared to those of *Cry1* and *Dbp* or that of *Per* in *Drosophila*.

b. Sleep deprivation decreases BMAL1, CLOCK, and NPAS2 binding to specific clock genes

To assess the effect of sleep loss on the binding activity of core clock transcription factors to the targeted clock genes, we measured the impact of a 6h SD performed between ZT0 and -6 on the binding of BMAL1 and CLOCK to the promoter of clock genes in the mouse cerebral cortex (Fig.21). We observed that SD specifically decreased the binding of BMAL1 to the promoter of *Dbp* and *Per2* (t-tests: $t=-3.0$, $p<0.01$ and $t=-3.7$, $p<0.01$, respectively), whereas binding to *Cry1* and *Per1* genes was not affected by SD ($p>0.5$, n.s.). The binding of CLOCK to *Dbp* was also significantly decreased by SD ($t=-2.2$, $p=0.05$) while CLOCK binding to the other clock genes assessed (i.e. *Cry1*, *Per1*, and *Per2*) was not affected ($p>0.5$, n.s.).

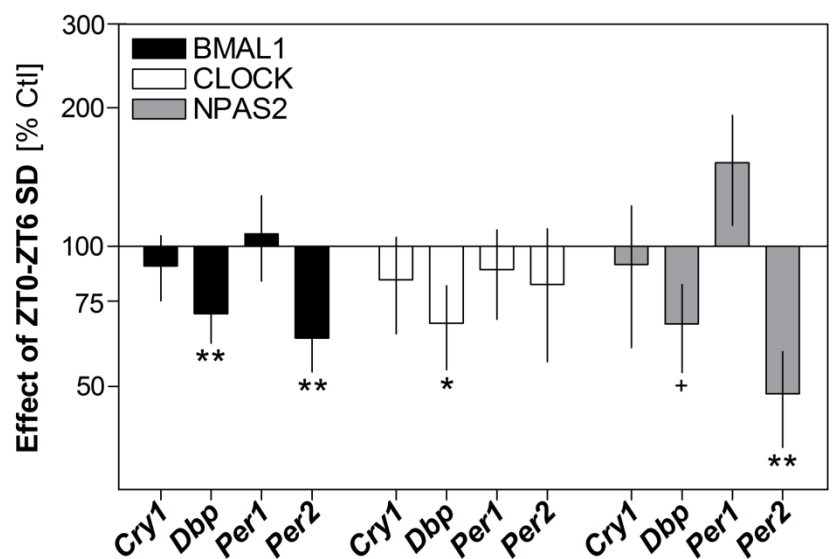


Figure 21 The effect of sleep deprivation (SD) on BMAL1, CLOCK, and NPAS2 binding onto the promoter of 4 clock genes in the mouse cerebral cortex. SD was performed between ZT0 and -6 after which cerebral cortices were rapidly sampled and processed together with non-sleep deprived controls. Chromatin immunoprecipitation (ChIP) was performed using antibodies against BMAL1, CLOCK, and NPAS2, and enrichment of E-box or E'-box containing sequences of the putative promoter regions of *Cry1*, *Dbp*, *Per1*, and *Per2* was measured using quantitative PCR. Data were normalized to a negative control condition (no-antibody) and expressed relative to the control non-sleep deprived sample performed in parallel. SD significantly decreased the binding of BMAL1 to *Dbp* and *Per2*, the binding of CLOCK to *Dbp* gene, and the binding of NPAS2 onto *Per2*. Data are presented as the mean SD/control percentage ratio (\pm SEM of the ratio; $n=18, 17, 16, 14$ for BMAL1; $n=10, 10, 9, 8$ for CLOCK; $n=9, 8, 8, 6$ for NPAS2 for *Cry1*, *Dbp*, *Per1*, and *Per2*, respectively). Please note logarithmic scaling of y-axis (+: $p<0.07$, *: $p=0.05$, **: $p<0.01$; t-tests).

Since BMAL1 binding to *Per2* and not that of CLOCK was decreased by SD, we hypothesized that the SD-mediated change in BMAL1 binding on the promoter of *Per2* could be mediated by the interaction of BMAL1 with its alternative partner, NPAS2. NPAS2, a CLOCK homolog, can associate

with BMAL1 and perform a similar role in regulating clock genes transcription [266]. In addition, NPAS2 is predominantly expressed in the brain, particularly in the cerebral cortex and thalamus [267], and was shown to be involved in the response to sleep deprivation including the increase in EEG slow waves, in NREM sleep duration, and in *Per2* mRNA [238]. We therefore also quantified the effect of SD on the binding of NPAS2 to the chromatin of clock genes in the mouse cerebral cortex (Fig.21, right grey columns). We observed that SD significantly decreased the binding of NPAS2 to *Per2* ($t=-4.6$, $p<0.01$). A similar tendency was observed regarding the binding of NPAS2 to *Dbp* ($t=-2.2$, $p<0.07$, n.s.), while, again, no change in NPAS2 binding was observed upon *Cry1* and *Per1* genes ($p>0.2$, n.s.).

We thus revealed that elevated sleep pressure changes the binding of the three core clock transcription factors (i.e. BMAL1, NPAS2, and CLOCK) to specific clock genes. As expected, significant SD-dependent changes in DNA-binding were observed only for *Dbp* and *Per2*, the two clock genes showing a response mostly independent of the glucocorticoids surge associated with SD [239]. Regarding the DNA-binding to *Cry1*, the observed absence of changes following SD is consistent with the lack of a clear SD effect upon *Cry1* mRNA expression. Also for *Per1*, we did not observe a change in DNA-binding following SD although SD clearly increases *Per1* expression in the mouse brain [239, 250, 251, 261]. We recently showed that this SD-induced increase in *Per1* expression is mediated through a surge in glucocorticoids [239], which combined with the present observations suggest that changes in *Per1* expression following SD are largely due to modifications in its transcription via the activation of a GRE present in its promoter [268], and not through activation involving the core clock components.

Our results specifically show that SD decreases the binding of CLOCK, NPAS2, and BMAL1 to *Dbp* in the mouse brain. Since we previously observed that the SD-dependent decrease in *Dbp* expression was not affected by the glucocorticoid surge [239], and since core clock transcription factors are known to be the main transcriptional regulators of *Dbp* [235, 236], the decreased binding of BMAL1 and CLOCK, and to some extent also that of NPAS2, might be sufficient to explain the de-

crease in *Dbp* expression after SD. However, the present findings cannot exclude the contribution of other pathways in mediating the SD-dependent decrease in *Dbp* expression. For instance, TNF α was recently shown to decrease *Dbp* expression via a TNFR1 and calcium-dependent pathway [269]. These authors also showed that TNF α could increase *Per1* expression, which could contribute, in combination with a GRE-mediated response [239], to the SD-dependent increase in *Per1*. The TNF α pathway is relevant to sleep regulation as reduced sleep duration was associated with increased TNF α in humans and rodents [270, 271], and inactivation of TNF α or TNFR1/IL1R1 alters sleep amounts and EEG [272, 273]. Hence, core clock transcription factors are most likely not the sole contributors to the SD-dependent changes in clock gene expression, and future studies aiming at assessing the SD-dependent changes in clock gene expression in animals bearing mutations of core clock transcription factors will be required to understand their specific contribution.

The observation of a SD-dependent decrease in NPAS2 binding and a lack of effect of SD upon CLOCK binding on *Per2* was unexpected given the overlapping roles of CLOCK and NPAS2 in the maintenance of circadian rhythmicity in behavior and gene expression [266, 274]. In peripheral tissues expected brain and cortical spin, the presence of CLOCK was shown, however, to be required for the persistence of rhythmic gene expression [275]. The sequence of CLOCK and NPAS2 are similar except for the presence of an extra 43aa at the carboxy end of CLOCK. In addition, NPAS2 also lacks an acetyl-CoA binding motif (656-664aa) and a poly-glutamine sequence (753-776aa) compared to CLOCK. The acetyl-CoA binding motif has been involved in conferring CLOCK with a HAT activity [276]. These sequence differences might prevent elevated sleep pressure from changing CLOCK binding to *Per2*, whereas allowing it for *Dbp*. This indicates that, within the same tissue, the effect of elevated sleep pressure on clock gene expression involves complex and different patterns of transcriptional regulation which are highly specific to each clock gene.

We observed that the increase in *Per2* expression following SD [239, 250, 251, 261] was accompanied by a decrease in binding of BMAL1 and NPAS2 to its promoter, which seems paradoxical. It could be argued that the SD-dependent increase in *Per1* and *Per2* mRNA followed by an increase in

protein [48] would not initially be driven by BMAL1::CLOCK/NPAS2 but rather, among others, through glucocorticoids::glucocorticoid receptor binding to GRE and/or CREB binding to CRE [240], another pathway that has been linked to sleep regulation [241]. Subsequently, increase in nuclear PER2 could decrease the DNA binding activity of core clock transcription factors and subsequently mRNA levels of their target genes like *Dbp*. This possibility is supported by our observation that *Per1* and *Per2* mRNA levels are increased as early as after 1h of SD whereas the *Dbp* decrease occurs after 3 to 6h of SD [251]. To address this possibility, the detailed time course of core clock transcription factors binding and of glucocorticoid receptors binding to the target DNA regions of *Per1* and *Per2* and their relation to nuclear levels of PER1 and PER2 protein levels will need to be assessed over the course of SD. To further complicate matters, BMAL1 and CLOCK were recently shown to be able to repress glucocorticoids-mediated transcription [277].

c. Core clock transcription factor binding and transcriptional activation

To clarify the link between DNA binding and mRNA levels, we examined the relationship between the two in the mouse liver and brain. We first observed that during the time when SD is usually performed (i.e. between ZT0 and -6), the binding of BMAL1 and CLOCK to all clock genes assessed gradually increases during control conditions when animals are mainly asleep (Fig.19 and 20). Increased DNA-binding during this time is not always linked to a mRNA increase of the corresponding gene. For instance, while the expression of *Dbp* is increasing during that interval, the mRNA levels of *Cry1*, *Per1*, and *Per2* are decreasing [251, 261]. The current literature indeed supports a range of phase relationships between the two rhythms (Fig.22). For *Cry1*, the peak in chromatin binding is in anti-phase with the peak in mRNA levels for both liver and cortex (about 12h apart). This contrasts the data regarding *Dbp* for which the peak in chromatin binding and mRNA expression coincide. Regarding *Per1* and *Per2*, there is a phase delay of about 6h such that when BMAL1 and CLOCK binding begin to decrease, the mRNA levels reach their peak. These observations are consistent with a recent report that assessed both the time-of-day rhythm of BMAL1 binding to these clock genes and the mRNA expression rhythms in the mouse liver [235]. Accordingly, elevated or decreased BMAL1 and

CLOCK DNA-binding are not directly linked to increased or decreased mRNA levels, respectively, and this seems especially true for *Cry1*, *Per1*, and *Per2*, and in both the cerebral cortex and liver.

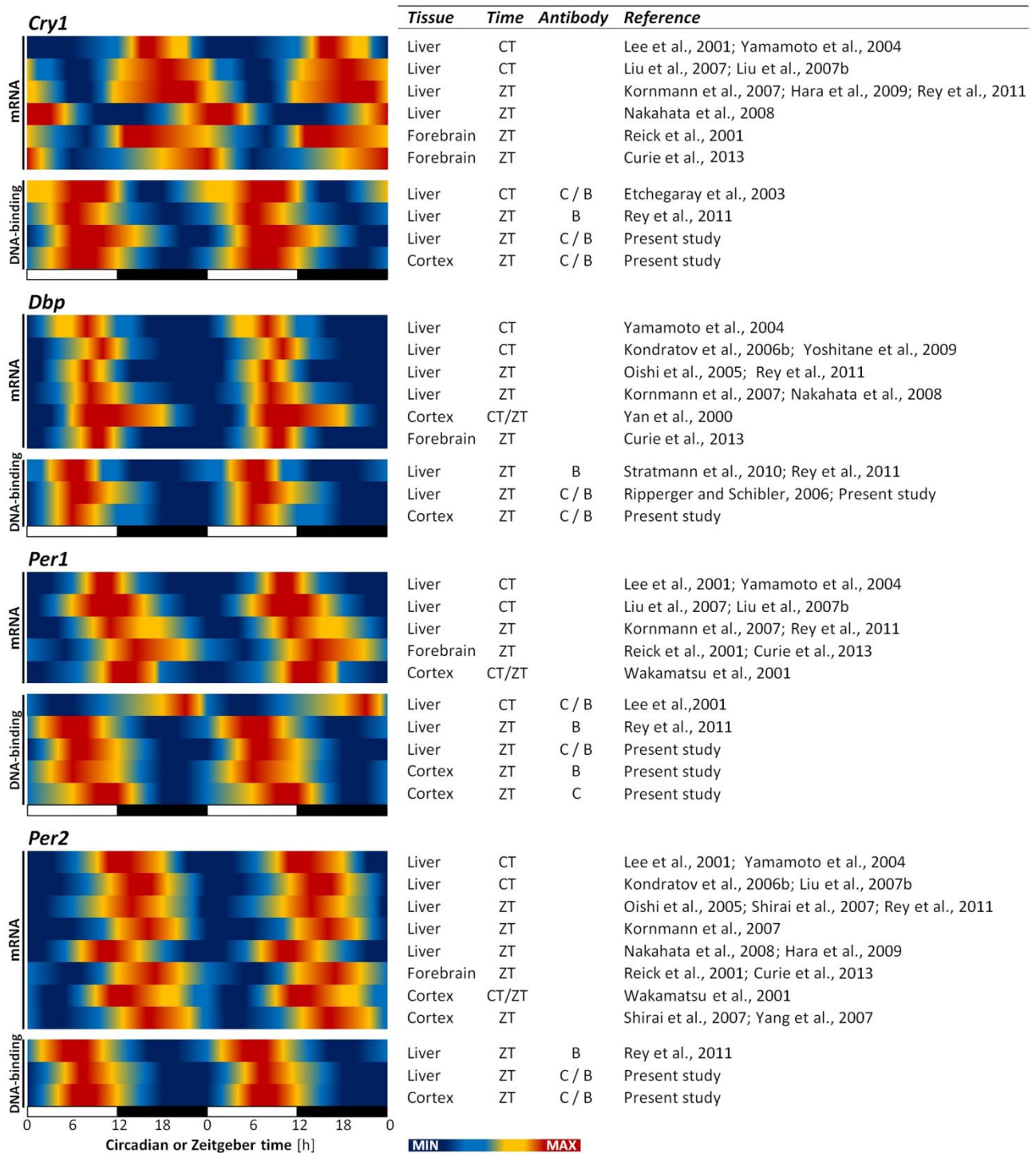


Figure 22 Overview of the phase relationship between RNA expression and chromatin binding. Time-of-day or circadian variations in mRNA expression for the selected clock genes (i.e. *Cry1*, *Dbp*, *Per1*, and *Per2*) for liver and brain samples from selected literature together with variations in DNA-binding of CLOCK (C) and BMAL1 (B) onto these clock genes shown from all previous literature in mice (i.e. liver) and the present study. Relative heat scales go from blue (minimum) to red (maximum). ZT: Zeitgeber time with ZT12=dark onset; CT: Circadian time with CT12=activity onset. For *Cry1*, RNA expression and DNA-binding seem to be in antiphase for both liver and brain, whereas the two rhythms are always in-phase for *Dbp*. Regarding *Per1* and *Per2*, the peak in DNA-binding precedes by several hours that of RNA expression for both tissues.

Previous work described several molecular mechanisms likely to contribute to the delay between chromatin binding and gene expression. For instance, it has been suggested that the phase of some transcripts is due to the interplay between several different transcriptional regulators acting on their promoter [278]. Similarly, Rey et al. [235] proposed that the higher the dependence on BMAL1 transcriptional regulation, the smaller the time lag between chromatin binding and gene expression. In particular, REV-ERB α could prevent the recruitment of RNA polymerase II to the *Cry1* promoter at CT6, thereby interfering with CLOCK::BMAL1 transcriptional activation [234]. Furthermore, the CLOCK::BMAL1 complex itself was shown to repress *Cry1* gene expression when CRY1 bound to the complex [279]. In *Drosophila*, the regulation of *Per* and *Tim* expression was shown to depend on the delicate balance between the binding of CLOCK and that of the repressor PER [264], which was suggested to drive two phases of repression: an ON-DNA phase and an OFF-DNA phase. Also other regulators such as the repressor DEC1, can affect *Per* expression [280]. Such mechanisms might be relevant to our observation of a decrease binding to *Per2* simultaneous to an increase mRNA level after SD, and stress the complex transcriptional regulation of clock genes by clock elements in addition to their regulation by non-clock elements (see above). Also, chromatin state importantly contributes to the relationship between DNA-binding and transcriptional activation as transcription is possible only when chromatin is in a permissive configuration. As mentioned earlier, CLOCK is a HAT required for rhythmic expression of *Dbp* and *Per1* independent of DNA-binding [276]. Furthermore, MLL1, a histone methyltransferase, was recently identified as a protein partner of CLOCK and an essential component to both *Dbp* and *Per2* rhythmic expression [281]. These mechanisms are likely to contribute also to the highly specific transcriptional regulation of individual clock genes. This specificity seems to be similarly reflected at the level of the so-called circadian and the sleep pressure-dependent changes, since the various phase relationships between rhythms of chromatin binding and gene expression (antiphase, in-phase, delayed) are also linked to a specific response to SD in terms of mRNA levels (*Cry1* no distinct change, *Dbp* decrease, *Per* genes increase, respectively) and core clock transcription factor binding.

In the present study, the effect of SD on DNA binding was assessed at the time when the binding of core clock transcription factors peaks (i.e. ZT6; Fig.20). This could have biased our results towards emphasizing decreases in binding as opposed to increases. To address this issue one could assess the effects of SD on DNA-binding at different circadian phases. Moreover, it is possible that the SD protocol could have shifted the phase of core clock transcription factors binding to the DNA of their specific targets, namely that of *Dbp* and *Per2*. This could occur either through a direct effect of wakefulness on the cerebral cortex molecular clock machinery or via resetting of the suprachiasmatic nucleus clock, which was shown to respond to behavioral stimulation (arousal and locomotor activity) [282]. Along this line, it is of interest to note that the main normal waking episode in mice, occurring between ZT12 and -18, is also accompanied by a decrease in *Per2* DNA binding by clock transcription factors and increased levels of *Per2* mRNA (Fig.22). Thus, the distribution of sleep and waking under baseline conditions might contribute to the so-called circadian changes in DNA-binding and gene expression in the mouse brain as we recently modeled in detail [48].

4. Conclusions and perspectives

Neuronal plasticity and neuroprotection are among the functions likely to be direct correlates of sleep need [12, 239, 261]. Clock genes have been shown to be involved in plasticity, particularly *Per* genes and *Npas2* [283, 284]. For example, impaired hippocampal LTP was observed in *Per2* mutant mice [285], and decreased long-term memory of courtship and waking experience-dependent increase in sleep in *Per* mutant flies [286, 287]. Therefore, clock genes could modulate cortical synchrony and synaptic equilibrium associated with vigilance states, which is further illustrated by the effect of clock-gene mutations on sleep homeostasis [288]. Combining ChIP with high throughput sequencing of cerebral cortex sampled either after sleep or SD could help to identify further targets of BMAL1 and CLOCK/NPAS2 relevant to synaptic plasticity.

The transcriptional response to SD depends on brain area [289, 290]. Also the change in *Per* expression after SD was shown to express a characteristic neuroanatomical pattern, with elevated sleep pressure producing more pronounced increases in the cerebral cortex [251, 252]. In the pre-

sent study, the SD-dependent changes in chromatin binding were specifically assessed in the cerebral cortex to more closely investigate their role in the recovery aspect of sleep which is known to be linked to EEG activity in slow frequencies [12, 106]. Nonetheless, the role of clock genes could extend to other, non-cortical brain areas. Also, we measured the binding of BMAL1, CLOCK, and NPAS2 to a single E/E'-box containing sequence. It is believed that the number of different E/E'-box containing sites bound by those transcription factor complexes within a gene will strengthen transcriptional control [235]. Accordingly, characterization of the SD effect upon binding to several sites in the promoter and intronic regions of our genes of interest will be useful to clarify the detailed molecular mechanisms governing SD-dependent changes in clock genes expression.

In conclusion, we reported that in the mouse cerebral cortex, core clock transcription factors bind to the DNA of target clock genes in function of time-of-day. Moreover, we revealed that extended wakefulness changes the binding of core clock transcription factors to the promoter of specific clock genes; specifically, SD decreased CLOCK binding to the promoter of *Dbp*, and decreased BMAL1 and NPAS2 binding to *Per2* and *Dbp*. These sleep-wake dependent changes in DNA-binding are likely contributing to the observed alterations in gene expression following SD, and also to changes observed with time-of-day. Together, our data further support a role for clock genes in the homeostatic regulation of sleep. An avenue we are currently following up on, is how elevated sleep pressure changes the multi-clock protein complex associated to the BMAL1::CLOCK/NPAS2 dimers. Also, future research studying the link between clock genes and sleep homeostasis should focus on the involvement of post-translational modifications, for instance on the acetylation status of the core clock proteins that was shown to tightly regulate their function [291, 292].

VII. Circadian rhythms, sleep architecture and homeostasis in *Period* knock-out mice

1. Introduction

Sleep is regulated by the tight interaction between the homeostatic process and the circadian process introduced above [106, 244, 293]. The regulation of this circadian process has been widely studied and is largely understood at the molecular level [160, 161]. The circadian clock is generated principally by a positive limb involving the hetero-dimerization of BMAL1 with CLOCK or NPAS2 allowing, via E-box sequence binding, the transcription of many target genes. The resulting proteins of specific targets such as *Cry1* and *Cry2* genes and *Per1* and *Per2* genes form complexes and move back into the nucleus to inhibit the transcription of their respective genes by interfering with the BMAL1::CLOCK/NPAS2 dimers [162]. This negative feedback in association with the positive limb is essentially responsible for the endogenous oscillation of all downstream genes (as *Dbp*, *REVERB*, *ROR*, *PPAR*, *LDHA*, etc.) [26]. In contrast, the molecular wiring of sleep homeostasis remains to be defined.

Mutations in core clock genes can impact period length like in *Npas2*^{-/-} [103], *Clock*^{m/m} [193], *Cry1*^{-/-} and *Cry2*^{-/-} mice [195] or can induce arrhythmicity like in *Bmal1*^{-/-} [163], *Clock*^{-/-}*Npas2*^{-/-} [136] and *Cry1,2*^{-/-} double mutant mice [196]. Intriguingly, the effects of *Per* mutant mice are less straightforward. Many studies were performed using *Per1* and *Per2* mutant mice, using different constructs targeting these genes on various genetic backgrounds, producing conflicting results. Both *Per1*^{tm1Brd} on a 129S7/SvEvBrd background [165] and *Per1*^{tm1Saco} on a mixed 94%C57BL/6-6%129S2/SvPas background [198] remained rhythmic albeit with a shorter period (22.6h±0.2 and 23.2h±0.2, respectively) compared to Wt mice (23.7h±0.1 for both strain) under DD, while the majority of *Per1*^{tm1Drw} mice on a 129S4/SvJae background lost their rhythmicity (22.6±0.3h) after about 10-14 days [197]. In this study, I used *Per1*^{tm1Brd} mice on a C57BL6/J background which I will refer to as *Per1*^{-/-} for simplicity, hereafter.

Per2^{tm1Drw} mice on a 129S4/SvJae background initially displayed a period (23.0h±0.3) similar to Wt mice (23.1±0.1), before becoming arrhythmic under DD conditions [197]. However, when backcrossed onto a C57BL6/J background, these mice remained rhythmic with a normal period throughout DD [200]. *Per2*^{tm1Brd} on a 129S7/SvEvBrd x C57BL6 mixed background displayed a short period of 22.1h±0.1, shorter than Wt mice which have a period of 23.7h±0.1. Moreover, some mutant mice became arrhythmic between 2-18 days under DD conditions [199]. These examples powerfully demonstrate the profound effects genetic background has on circadian phenotypes and how background can “rescue” the effects of gene mutations.

Importantly, all *Per2* mutant mice presented above still produce a mutant transcript that can be translated. *Per2*^{tm1Drw} mice produce several *Per2* transcripts that can generate truncated proteins from the first four exons. These exons encode the first 147 residues of PER2 but lack the entire PAS domain [197]. PAS domains in PER2 allow, *inter alia*, its protein dimerization with BMAL1, CLOCK and NPAS2, but also protein-protein interactions with other PER proteins [220]. However, a relatively rare transcript was detected in which exon 4 was spliced directly to exon 7. This splicing event maintains the reading frame as in native PER2 and the resulting transcript could, if translated, form a mutant PER2 protein lacking only the 108 amino acids of the PAS domain encoded by exons 5 and 6 (residues 148–255) [197]. Regarding *Per2*^{tm1Brd}, the presence of a mutant transcript was also detected that if translated, would generate a protein with a deletion of 87 amino acids in the PAS domain [199]. Thus both *Per2*^{tm1Drw} and *Per2*^{tm1Brd} mice cannot be considered as full null-*Per2* mutants. Even if the PAS domain is dysfunctional, it is impossible to predict the implication that the mutant transcript would have if translated. For instance, the domain permitting the binding of the CKIε and CKIδ [294] or the N-terminal domain of the PER2 protein which bind CRY1 and -2 [230] are still present. Note that double mutant *Per1,2*^{tm1Drw} mice on a 129S4/SvJae background were arrhythmic under DD, demonstrating central role of both PER1 and -2 within the circadian machinery [197, 201]. In conclusion, most of *Per1* and *Per2* mutant mice had a shorter period than Wt and several *Per2*^{m/m} became arrhythmic under dark constant condition. In addition not all individuals carrying a specific construct on same

background behave the same phenotype, some were arrhythmic and some were not; that suggests a variability in genetic penetrance.

In addition to the partial deletion mutation described above and used in most of the literature, a full null-*Per2* mutant mouse was generated: *Per2*^{tm1Ccl} by Cheng Chi Lee. These mice have not been widely used or characterized. It was only mentioned that they display a similar circadian phenotype as *Per2*^{tm1Brd} on a mixed 129/C57BL6 background, while completely lacking all PER2 polypeptide [120]. For my work I used *Per2*^{tm1Ccl} mice which I will refer to as *Per2*^{-/-}, hereafter.

Per2 seems to have a particular importance in the circadian circuitry. Several different pathways activate *Per2* transcription to fine tune period length or to reset phase. For instance, the glucocorticoid pathway (such as stress hormone corticosterone [208], female hormone estrogen [210] or synthetic drug dexamethasone [99]) *via* the GRE domain in the *Per2* promoter are important for synchronization of circadian rhythms in peripheral tissues [209]. Light *via* activation of the CRE domain can induce *Per1* and -2 in the SCN [125, 212, 214, 215]. Changes in temperature *via* HSE domains permit cells to synchronize *in vitro* [130]. Finally DBP and its antagonist E4BP4 *via* D-box domains [216]. PER2 is also responsible of the period length in human. Patients suffering from FASPS or DSPS have mutations in the CSNK1-binding domain of PER2 or in the CKIε/δ kinase responsible of the phosphorylation of PER2. All these mutations decreases substantially CKIε/δ enzymatic activity altering PER2 protein stability its translocation into nucleus [147].

In addition to their well-established role in generating circadian rhythms, clock genes seems to play also a circadian-independent role in sleep homeostasis [26]. Some single clock gene mutation were enough to modify the homeostatic process; examples are *Npas2*^{-/-} [194], *Bmal1*^{-/-} [46] and *Rev-erba*^{-/-} [205]. Moreover, when pairs of redundant clock genes were removed altered homeostatic sleep regulation was observed as well, like in *Cry1,2*^{-/-} [191]. However, for both studies done in *Per2*^{m/m} [201, 203] and also *Per1,2* double mutant mice [201], it was concluded that sleep homeostasis regulation of sleep is not affected because EEG delta power responded in the same way in all gen-

otypes after a sleep deprivation, despite the fact that they observed lowest EEG delta power in response to a SD in *Per1^{m/m}* and *Per2^{m/m}* mice compared with the Wt mice [203].

As mentioned above, genetic background has an effect on the phenotype such as the homeostatic process [36, 46] and could also modulates the effects of a gene mutation (e.g. *Per2^{tm1Drw}* x 129S4/SvJae mice become arrhythmic under DD [197] while *Per2^{tm1Drw}* x C57BL6/J mice remain rhythmic [200]). For these reasons, in my project I backcrossed between 7-11 times *Per1^{-/-}* and *Per2^{-/-}* mice onto C57BL6/J inbred mice to have at least 99.2% of recipient genome. Most mice used were backcrossed 9+ times and were considered as congenic mice.

In this project I recorded locomotor activity, EEG/EMG signals and measured gene expression of *Per1^{-/-}*, *Per2^{-/-}*, *Per1,2^{-/-}* and Wt mice. Locomotor activity was used to characterize the circadian clock, while the EEG/EMG recordings were used to determine sleep architecture and the sleep homeostat. In mice kept under LD12:12 conditions I observed that lack of *Per2* advanced activity onset of clock gene expression and corticosterone levels. Although, earlier activity onset could be interpreted to indicate the presence of a circadian rhythm allowing the animals to anticipate dark onset, the immediate loss of circadian organization of locomotor activity upon release in DD in 94% of the mice studied indicates that self-sustained rhythms are not present under LD12:12 and that instead these changes are light-dark driven. Moreover, I found that NREM sleep is less consolidated both in *Per2^{-/-}* and *Per1,2^{-/-}* mice. In addition, although the homeostatic regulation of sleep intensity did not differ between genotypes, the homeostatic regulation of sleep duration did importantly differ and during the first 5h of recovery after a 6h SD, mice lacking *Per2* expressed *less* sleep than during baseline.

2. Materials and methods

a. Animals

Per1^{-/-} mice were described in Zheng *et al* [165]. Fifteen exons (from exon 4 included) of the *Per1* gene were replaced by a *hypoxanthine phosphoribosyltransferase (Hprt)* mini-gene deleting the entire PAS domain and preventing protein translation due to a shift in the reading frame. The *Per1*^{-/-} construct is considered a null allele [165]. *Per2*^{-/-} mice were generated by Cheng Chi Lee and colleagues and were mentioned for the first time in [120]. The entire PAS-B domain (from the 9th exon to 11th included) of the *Per2* gene was deleted generating a reading frame shift which prevents PER2 translation (Fig.23).

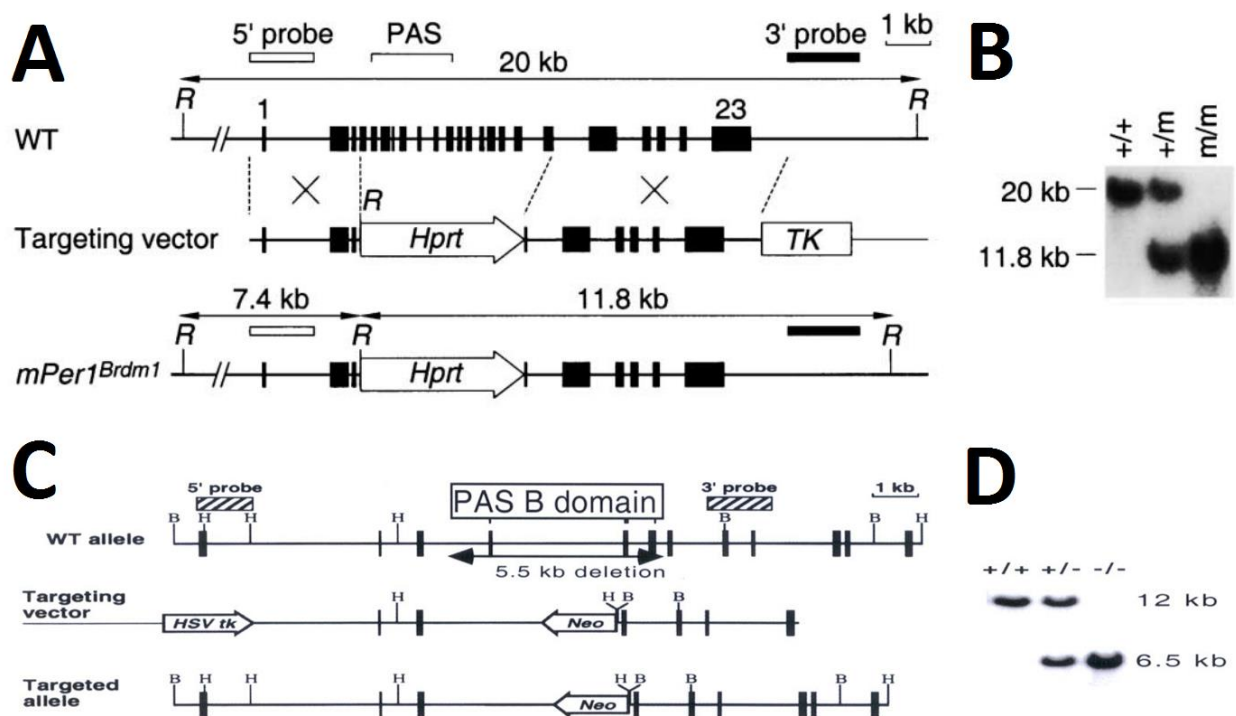


Figure 23 Generation of *Per1*^{-/-} and *Per2*^{-/-} knock-out mice. **A** Genomic structure of the murine *Per1* gene, the targeting vector, and the predicted structure of the targeted allele. Exons are indicated by vertical black bars with the first and last exons numbered. WT: wild-type; R: EcoRI; *Hprt*: hypoxanthine phosphoribosyltransferase gene; *TK*: Herpes Simplex Virus thymidine kinase gene. A 1.6 kb 3' external probe that detects a 20 kb wild-type EcoRI fragment and an 11.8 kb mutant EcoRI fragment were used to detect targeted ES cell clones and to genotype test mutant mice. A 1.5 kb 5' internal probe that detects a 20 kb wild-type EcoRI fragment and a 7.4 kb mutant EcoRI fragment were used to confirm correct targeting at the 5' homology region (data not shown). **B** Southern analysis of F2 littermates obtained from intercrosses between (C57BL/6Tyr^{c-Brd} x 129S7) F1 heterozygous mice using the 3' probe and EcoRI digestion. +: wild-type allele; m: mutant allele. Southern analysis with a probe within the deleted region confirmed the deletion in homozygous mutants (data not shown). **C** The targeting vector and the predicted structure of the targeted allele. A replacement vector is designed to delete the exons 9–11 in the *Per2* gene, which encode the entire PAS-B domain. When spliced, the mutant *Per2* mRNA is out-frame with the wild-type mRNA in the sequence 3' to exon 11 due to frame-shifting, so that the targeted *Per2* allele is a null allele. **D** Southern blot analysis of Bam HI digested genomic DNA obtained from F2 littermates using the 5' probe. AB: from Zheng B. *et al.* (2001) [165]; CD Fu L. *et al.* (2002) [120].

Western blot analysis showed no PER2 protein signal in cerebral cortex and forebrain of *Per2*^{-/-} mice (Fig.24). The antibody used bound the C-terminal part of the protein. Furthermore, Cheng Chi Lee confirmed that no PER2 protein was detected by western (data not shown). Moreover, no *Per2* mRNA was detected by qPCR (Fig.32, 41). The primers used amplified the

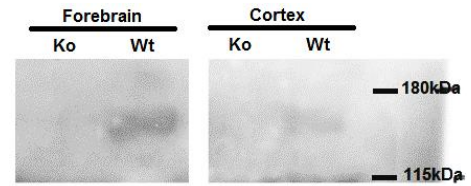


Figure 24 Western blot analysis of PER2 protein in the forebrain and in the cerebral cortex. The PER2 protein was only observed in the Wt mice at the expected weight of 140 kDa, while no PER2 protein was detected in *Per2*^{-/-} mice in both forebrain and cortex.

11th exon of *Per2* (see table 5). Both *Per1*^{-/-} and *Per2*^{-/-} original breeding kept on an unknown mixed background were kindly sent to us by Cheng Chi Lee. *Per1*^{-/-} and *Per2*^{-/-} knockout mice were backcrossed at least 7 times to C57BL/6J mice purchased from Jackson Laboratory (Bar Harbor, ME, USA) to have a purity of minimum 99%. Their offspring were then crossed to obtain double mutant (*Per1,2*^{-/-}) mice. Usually coupling was done with *Per* heterozygote female and C57BL/6J male mice, but to prevent any genetic anomaly in mitochondria, once in a while mice were backcrossed to C57BL/6J females. *Wild-type* (Wt) mice used as control were littermates with homozygous for *Per1*^{-/-} and *Per2*^{-/-} mice. When heterozygote *Per1*^{+/-} (or *Per2*^{+/-}) were backcrossed together, we obtained 25% of *Per1*^{-/-} (full knock-out), 50% *Per1*^{+/-} (heterozygote) and 25% *Per1*^{+/+} mice. Wt mice from the same litter were used as control mice for *Per1*^{-/-} and *Per2*^{-/-} mice. Given the fact that is statistically too difficult to obtain enough double knock-out (*Per1,2*^{-/-}) and Wt mice in the same litter, I used a group of Wt animals composed by 50% from *Per1* litter and 50% from *Per2* litter. No statistical difference was observed among the 3 groups of Wt (*Per1*^{+/+}, *Per2*^{+/+} and 50%*Per1*^{+/+} 50%*Per2*^{+/+}) mice, and thus the datasets were merged. All mice were bred on site and maintained under standard animal housing conditions (food and water *ad libitum*, 12h-light/12h-dark cycle (LD), 23-25°C ambient temperature). All experiments were approved by the cantonal veterinary office of canton Vaud.

b. Genotyping

Mouse ears were punched to have small piece of skin of about 0.3mm diameter and put in a sample with 350µl Tail buffer at pH=8 (50mM Tris-Cl, 100mM EDTA, 100mM NaCl, 1% SDS) supplemented with 300 µg of proteinase K (Promega, Madison, WI, USA). Then, tubes were vortexed and incubated

overnight at 55°C expecting the total tissue dissolution. Subsequently, 175µl NaCl 6M was added at *room temperature* (RT), mixed energetically by hand, incubated 5min on ice and then centrifuged at >8000g 20min 4°C. The supernatant (450µl) was placed in a new tube with 50µg Ribonuclease A (Sigma-Aldrich, St.Louis, MO, USA) and incubated 15min at 37°C. Then, DNA precipitated adding 450µl isopropanol at RT, gently mixed by hand and then centrifuged again at >8000g 20min 4°C. Subsequently, supernatant was discarded and 800µl ice cold EtOH 70% was added. The tubes was centrifuged at >8000g 15min 4°C. Then the supernatant was discarded carefully taking care to not remove the DNA pellet. The tubes were completely dried at 55°C (take about 1h). 50µl TE buffer at pH=8 (10mM Tris-Cl, EDTA 1mM) was added and incubated 1h at 65°C. After a quick spun, DNA quantification was performed on a Nanodrop ND1000 (Wilmington, DE, USA) with a consistent 260/280 ratio between 1.8 and 2.1. DNA was diluted in nuclease free water to have a final concentration between 10 and 20ng/µl.

Then DNA was amplified by *polymerase chain reaction* (PCR). For each reaction, 2.5µl of the diluted DNA was supplemented with 0.125µl HotStar Taq DNA polymerase (5u/µl from Qiagen, Hilden, Germany), 2.5µl Buffer 10x containing MgCl₂ 15mM, 1µl dNTP (5mM each one) and 10pM of each four primers for a total reaction mix of 25µl. The *Per1* PCR reaction was performed under following cycling conditions: 95°C for 15sec, followed by 35 cycles of 94°C for 1min, 58°C for 1min and 72°C for 1min; to conclude at 72°C for 10min. For the *Per2* PCR reaction, the annealing step temperature was fixed at 56°C instead 58°C. The primers sequences used can be found in table 5. Primers were purchased from Eurogentec (Seraing, Belgium).

Gene	Genotype		Sequence (5' --> 3')
<i>Per1</i>	Wt	Forward	CCT CAC CTT AGC CTG TTC CTT CT
		Reverse	ACA ACT CAC TCA CCC TGA ACC TG
<i>Per1</i>	Ko	Forward	TGA ATC TTT GTC AGC AGT TCC CT
		Reverse	CTC ACC ATC ACT TTA TAC CCC CA
<i>Per2</i>	Wt	Forward	TGG GAG GAA CTC TTG TAA GCA GA
		Reverse	AGC ATC ATG GCT GCA ACA CA
<i>Per2</i>	Ko	Forward	TGT CTA AAG CAT CCC TAG CTG CT
		Reverse	GTT GGC TAC CCG TGA TAT TGC T

Table 5 Primers used for PCR genotyping

Then loading buffer was added to PCR reactions, before to be loaded on a 2% agarose gel with TAE buffer supplemented with Midori Green DNA Stain (10µl for 100ml, Nippon Genetics, Dueren, Germany). As you can see in figure 25A, for the *Per1* Wt fragment size appeared at 400bp, while *Per1* ko at 290bp. *Per2*

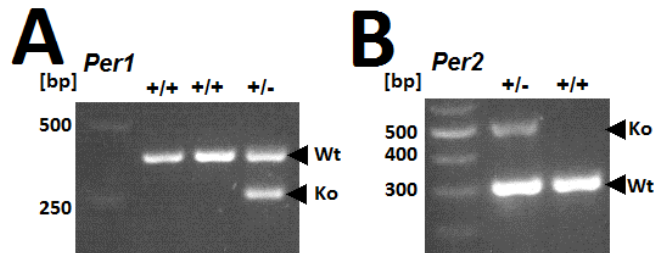


Figure 25 *Per1* and *Per2* genotyping samples. **A** *Per1* Wt and ko fragments appeared at 400bp and 290bp, respectively. The first two lanes were full Wt mice, and the third was a heterozygote mouse. **B** *Per2* Wt and ko fragments appeared at 310bp and 510bp, respectively. The first lane was heterozygote mouse and the second was a full Wt mouse.

Wt fragment size appeared at 310bp, while *Per2* ko at 510bp (Fig.25B).

c. Locomotor activity recordings and analyses

Locomotor activity was recorded in both males and females of each genotype (*Per1*^{-/-}, *Per2*^{-/-}, *Per1,2*^{-/-} and Wt; n=4/4, 21/11, 11/3, and 5/3, respectively, for males/females). All mice were between 11 and 15 weeks old. Locomotor activity was measured using PIR sensor (Visonic, Tel Aviv, Israel) and recorded and analyzed with Clocklab (Natick, MA, USA). Animals were recorded for at least 12 days under standard LD conditions before being released to DD condition for at least 21 days to determine period length (tau, τ) of its “free running” circadian rhythm. Subsequently, LD conditions were reinstated to study re-synchronization of the free-running rhythms to the Zeitgeber. Presence and period of rhythms during freerunning were determined by a chi²-periodogram analysis (Clocklab) after removing the first 3 days under DD [295, 296]. Periodogram analysis assesses the period of rhythmicity in a data set by fitting the data set to candidate periods within a specified range. To be defined as

rhythmic, an animal must show a major and statistically significant ($p < 0.01$) peak in the circadian range ($24\text{h} \pm 4\text{h}$) with periodogram analysis. Animals with only ultradian rhythms (shorter than 18h) or with many small significant peaks but with lacked a major significant peak in the circadian range were considered as arrhythmic.

d. EEG and EMG surgery, monitoring and analyses

EEG and EMG surgery and recording methods were previously described by Mang and Franken [32]. Briefly, from 10 to 13 weeks old *Per1*^{-/-}, *Per2*^{-/-}, *Per1,2*^{-/-}, and Wt male mice (n=10, 9, 10, and 21, respectively) were implanted with EEG and EMG electrodes under deep anesthesia done by 1ml/kg body weight intraperitoneal injection of a mixture containing 75mg/ml of ketamine (Ketazol-100, Graeub, Bern, Switzerland) and 10mg/ml xylazine (Rompun 2%, Provet, Lyssach, Switzerland) in 0.55% NaCl. The mixture had to be protected from light and injected at least at 25°C.

After making a longitudinal incision using a scissor, along the midline of the scalp, the skull periosteum was removed and skull was thoroughly cleaned with ethanol. It's very important that at any time of surgery the cranium was clean and dry. Then five holes were drilled cautiously into the skull at precise location for the EEG screws

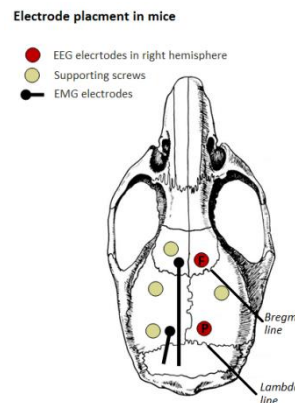


Figure 26 Layout of electrode placements on mouse skull.

Two EEG screws electrodes were positioned over the right cerebral hemisphere in red (F: frontal; P: parietal). Four anchor screws were represented in beige. Two EMG gold-wires were inserted into the neck muscle. Modified from Mang G.M. and Franken P. (2012) [32]

and anchor screws (Fig.26). These latter were placed first, then two gold-plated screws EEG electrode were fixed in the right hemisphere. The frontal EEG electrode was placed at 1.7mm right from the midline and at 1.5mm anterior to the bregma; the parietal at 1.7mm right of midline and at 1.0mm anterior to lambda (Fig.26). This placement was chosen to ensure an optimal distinction between the different behavioral states [32]. The frontal electrode was sited over the frontal cerebral cortex to detect the slow waves oscillations ($< 5\text{Hz}$) characteristic of NREM sleep. The parietal electrode was placed just over the hippocampal structure to capture the theta oscillation (5-7Hz) characteristic of the REM sleep. This bipolar acquirement permits to measure the potential difference between the

electrodes [33]. Then two gold-wires used as EMG electrodes were inserted into the neck muscle to record muscle tone. Adhesive resin (3M ESPE, Rüsclikon, Switzerland) was added to cover the electrodes and to fix to the assembly to the skull. When the cement was exposed to UV light, the skin was stitched in front and in the back of the cement. Then a connector plug was soldered to the EEG and EMG electrode ends taking care that the solder does not short circuit any electrodes. Finally all visible contacts were covered with dental cement (Paladur, Heraeus Kulzer, Hanau, Germany). After surgery, mice were individually housed under standard conditions and were allowed a minimum of 10 days of post-surgical recovery before to start the recording. EEG and EMG signals were recorded between 11 to 14 weeks of age.

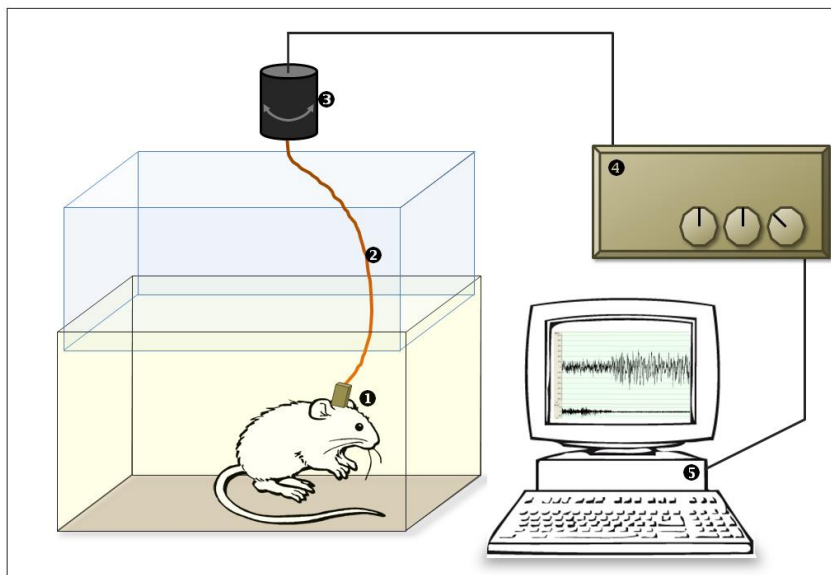


Figure 27 Schematic description of the experimental recording setup. The mouse has been implanted with EEG/EMG electrodes and connected to a head-mounted connector (1). The connector was attached to a recording cable (2) that is linked to a commutator (3) which transfers the signal to the acquisition unit (4). The processed signal is then transferred to a computer installed with a specific EEG/EMG acquisition and analyses software (5). Drawing by La Spada F. in Mang G.M. and Franken P. (2012) [32]

After two days of baseline, mice were sleep deprived for 6h between ZT0-6 (Zeitgeber time or ZT0 = light onset; ZT12 = dark onset usually coinciding with activity onset) by gentle handling [253]. The subsequent 18h were considered recovery. At least 6 days before the recording time, mice were connected to the recording leads which allows the mouse to habituate to the cable. This latter was connected to a swivel contact (3) allowing the tethered animal to move unconstrainedly as you can see in the schematic description in figure 27. The swivel connector was linked to a commutator which transfers the signal to the acquisition unit (Fig.27.4). In fact the recorded EEG and EMG signals were filtered, amplified, and analog-to-digital (AD) converted using Embla (Flaga, Reykjavík, Island) for hardware acquisition. To perform this AD conversion, the theoretically sampling rate should be at

least twice that of the frequency of the EEG activity of interest, although oversampling is recommended. In fact, inappropriate filtering and sampling rates can lead to artifacts in subsequent signal analysis. The signal was digitized at 2000Hz (i.e., a sampling interval of 0.0005 sec) and then down-sampled at 200Hz and a high-pass filter at 0.0625 Hz was set to reject DC signal. A 50-Hz notch filter was used to eventually discard like-artefacts activity caused by interference from surrounding electrical equipment. The processed signal was then transferred to a computer installed with a specific EEG/EMG acquisition and analyses software (Fig.27.5). The acquisition software used was Somnologica 3 (Embla). The EEG signal was transformed with a *Discrete-Fourier Transformation* (DFT) yielding power spectra between 0 and 100 Hz with a 0.25 Hz frequency and 4-sec time resolution (corresponding to one epoch) [32]. We chose this window function of 4-sec which matches the resolution at which we determine behavioral state. By visual inspection of the digitized EEG and EMG traces, each 4s-epoch was classified as wakefulness, NREM sleep, or REM sleep (Fig.28). Artefacts were marked and removed from subsequent EEG analyses.

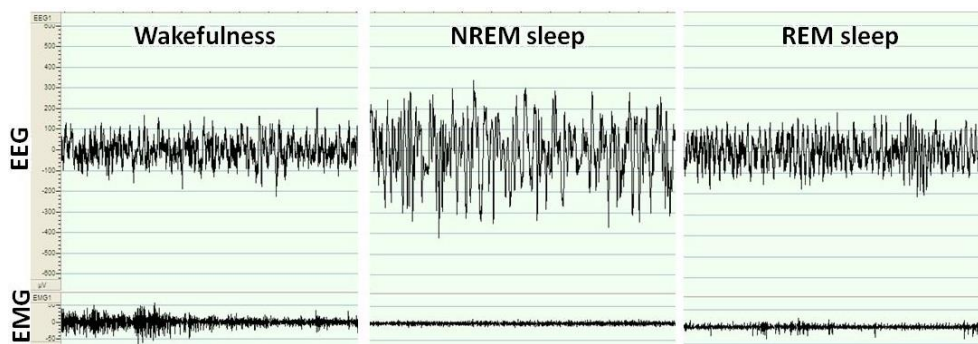


Figure 28 Example of EEG/EMG signals for wakefulness, NREM and REM sleep. During wakefulness, the EEG trace is composed of mixed frequencies, and muscle tone is present on the EMG. NREM sleep is characterized by high amplitude and low frequency from 1 to 4 Hz in EEG, while muscle tone is low in EMG. During REM sleep, EEG shows regular theta waves (6 to 9 Hz) and EMG is flat except for rhythmic heart-rate artifact.

Briefly, wakefulness is characterized by a small amplitude EEG signal with irregular signal coupled with high and variable muscle tone (EMG). NREM sleep is characterized by high amplitude and low frequency < 5 Hz EEG, while muscle tone is low. REM sleep is composed by very regular theta (6 to 9Hz) waves, while its EMG signal is especially low flat (muscle atonia). However occasional twitches can sometimes be observed.

Time spent in each sleep-wake state was summed over the light period, the dark period and over 24h. To determine NREM sleep fragmentation, the amount of different time intervals of NREM sleep was accounted during 48h of baseline. Time intervals: 4sec, 8-12sec, 16-28sec, 32-60sec, 64-124sec, 128-252sec, 256-508sec, 512-1020sec, >1024sec.

EEG power spectra quantify the contribution of the various frequencies in EEG signal. EEG spectra were calculated for each behavioral state for each genotype for 48h of baseline. The frequency range depends on the sampling rate (for instance a sampling rate of 200Hz, the full frequency range will be between 0-100Hz) and the frequency resolution depends on the window size (with a 4-sec window the frequency resolution will be 0.25Hz). EEG spectral density analysis was limited to 0.75 – 45.0Hz with a resolution 0.25Hz. Mean EEG spectra was calculated for each state by adding all the artifact-free 4-sec windows scored as that state, the power density in each frequency bin, and then dividing by the total number of windows obtained for each state and animal. It's necessary to correct inter-individual differences in EEG amplitude by a normalization using a reference value, because absolute EEG values can vary due to e.g., electrode placement. To calculate such a reference value, EEG power was summed and averaged and the weighted according to the contribution of wakefulness, NREM sleep and REM sleep. The reference did not statistically vary with genotype (1-way ANOVA; $p = 0.89$; *Per1*^{+/+} 30.4 ± 2.3 ; *Per2*^{+/+} 28.8 ± 3.1 ; *Per1,2*^{+/+} 28.8 ± 2.4). Note that the *Per1,2*^{-/-} group was reduced to $n=9$, as one mouse had to be rejected from this analysis due to a high number of EEG artifacts.

EEG delta power was calculated as the power in only the 1 to 4Hz range. A time course of EEG delta power was constructed by selecting 12 intervals during the light period, 6 during the dark period, and 8 for sleep recovery in the light period, to which an equal number of 4s NREM sleep epochs contributed (i.e., percentiles). The number of intervals selected within a given recording section was determined by NREM sleep prevalence. Besides NREM sleep EEG activity in the delta frequency range, full EEG spectral profiles were calculated for each sleep-wake state over the 48h of baseline recording to assess genotype differences in the contribution of the various frequency com-

ponents to rhythmic brain activity. Only EEG spectra of 4s-epochs in between two epochs of the same state and artifact free were included in the analyses.

e. Gene expression in cerebral cortex and corticosterone quantification

For the SD experiment, *Per2*^{-/-} and Wt mice were sleep-deprived 6h by gentle handling [253] (between ZT0 and -6), then quickly anesthetized with isoflurane (Minrad Inc., Buffalo, NY, USA), and immediately sacrificed by decapitation at ZT6 together with the corresponding non-sleep-deprived control mice. Cerebral cortex were quickly harvested and immediately put in liquid nitrogen to be stored at -80°C. For the 12h time-course experiment, 4-6 *Per2*^{-/-} and Wt mice were sacrificed every 2h starting at ZT2 and ending at ZT14. At each time point, the cortical cortex was harvested and roughly 500µl of blood were supplemented with 10µl heparin (2units/µl) (Sigma-Aldrich) at 4°C; after centrifugation at 1700g for 5min, the plasma (supernatant) was recovered. Blood plasma were frozen in liquid nitrogen and stored at -80°C.

Corticosterone levels in plasma blood were quantified by enzyme immune assay using a Corticosterone EIA kit (Enzo Life SciencesAG, Lausen, Switzerland) according to manufacturer's instructions. Test samples were diluted 40 times in the provided buffer and the optical density was measured with Safire² (Tecan, Grödig, Austria) at 405nm using Magellan 6.6 software (Tecan).

Total mRNA were extracted from 30mg of cortical tissue (if bigger, it was divided in two parts and pooled after purification) using the RNeasy Mini kit (Qiagen) following the manufacturer's protocol. Briefly, each sample was homogenized by pestle using 350µl of RLT buffer (supplemented with β-mercaptoethanol from Sigma-Aldrich instead DTT) on ice and passed on a QIAshredder column (Qiagen). Contaminating DNA was removed with DNase I (Qiagen). RNA quantification was performed on a Nanodrop ND1000 with a consistent 260/280 ratio between 1.8 and 2.1.

Reverse transcription from 500ng of RNA was performed using the SuperScript II Reverse Transcriptase (Invitrogen, Carlsbad, NM, USA) following manufacturer's instructions. The *complementary* DNA (cDNA) was diluted 10 times in DNase free water. Reactions without enzyme (NEC) and without the template (NTC) were performed in parallel as negative controls.

qPCR was performed according to the Applied Biosystems protocol using a 7900HT Fast Real-time PCR System with SDS 2.3 software (Applied Biosystems, Foster City, CA, USA). For each reaction, 7.2 μ l of the diluted cDNA was supplemented with 18 μ l FastStart Universal Probe Master 2x (Roche Diagnostic GmbH, Mannheim, Germany), 0.9 μ M of each primers and 0.25 μ M of probe for a total reaction mix of 36 μ l. The qPCR was performed under standard cycling conditions (50°C for 2min, 95°C for 10min, followed by 45 cycles of 95°C for 15sec and 60°C for 1min). Each qPCR reaction was performed in triplicate. The oligonucleotide sequences used can be found in table 6. Primers and probes were purchased from Invitrogen or Eurogentec and all probes were dual-labeled with 5'FAM/3'BHQ as fluorophore and quencher. *Ribosomal protein S9 (Rsp9)*, *eukaryotic translation elongation factor 1A (Eef1a)* and *glyceraldehyde-3-phosphate dehydrogenase (Gapdh)* were used as endogenous control genes (Fig.29) to normalize qPCR experiments. Briefly, for every control gene we determined the

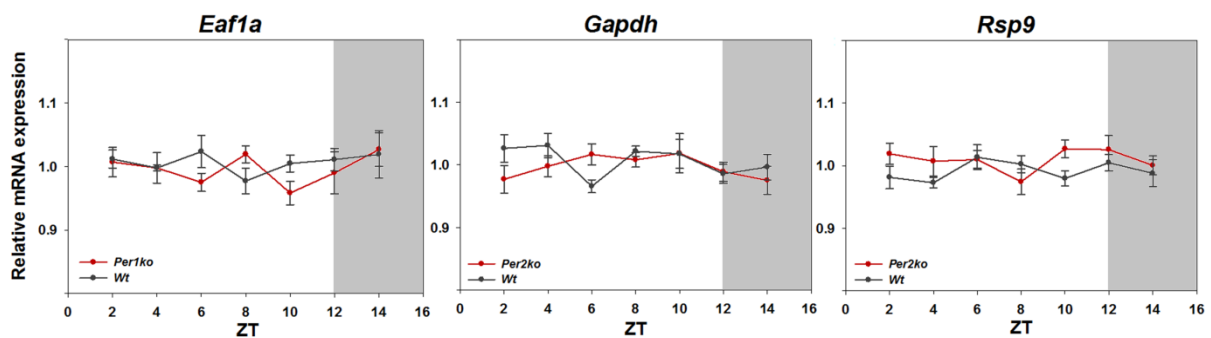


Figure 29 Time-course of expression of house-keeping genes across 12 hours in the cerebral cortex. Relative expression of the house-keeping genes *Rsp9*, *Eef1a*, and *Gapdh* in the cortex of *Per2^{-/-}* and *Wt* mice across 12h starting at ZT2 at 2h intervals. For each time point 4 to 6 mice were used. Data are presented as mean \pm 1SEM. White and grey areas represent light and dark period, respectively. For none of the transcripts was a significant effect observed (2-way ANOVA, factors 'genotype' and 'ZT' P=0.44; 0.49; 0.19, respectively).

pairwise variation with other two control genes as the standard deviation of the logarithmically transformed expression ratios, and defined the internal control gene-stability measure *M* as the average pairwise variation of a particular gene with all other control genes. The systematic variation was also calculated as the pairwise variation, *V*, for repeated RT-PCR experiments on the same gene, reflecting the inherent machine, enzymatic and pipet variation. *M* and *V* values had to be lower than 0.5 and 0.2, respectively, to consider the housekeeping gene stable enough to be used as control genes [297]. Then the normalization factor calculation was based on the geometric mean of the three control genes. Geometric mean was chosen because its controls better for possible outlying

values and abundance differences between the different genes [297]. Finally, the relative quantification was calculated with a modified $\Delta\Delta C_t$ method [298]. All stability calculation, normalization and quantification were performed using qbase^{PLUS} 1.5 (Biogazelle, Machelen, Belgium).

Gene		Sequence (5' --> 3')	Accession
<i>Eef1a1</i>	<i>Forward</i>	CCT GGC AAG CCC ATG TGT	NM_010106.2
	<i>Reverse</i>	TCA TGT CAC GAA CAG CAA AGC	
	<i>Probe</i>	TGA GAG CTT CTC TGA CTA CCC TCC ACT TGG T	
<i>Gapdh</i>	<i>Forward</i>	TCC ATG ACA ACT TTG GCA TTG	NM_001001303.1
	<i>Reverse</i>	CAG TCT TCT GGG TGG CAG TGA	
	<i>Probe</i>	AAG GGC TCA TGA CCA CAG TCC ATG C	
<i>Rps9</i>	<i>Forward</i>	GAC CAG GAG CTA AAG TTG ATT GGA	NM_029767.2
	<i>Reverse</i>	TCT TGG CCA GGG TAA ACT TGA	
	<i>Probe</i>	AAA CCT CAC GTT TGT TCC GGA GTC CAT ACT	
<i>Bmal1</i>	<i>Forward</i>		NM_007489.4
	<i>Reverse</i>	Mm00500226_m1 (Invitrogen)	
	<i>Probe</i>		
<i>Clock</i>	<i>Forward</i>		NM_007715.5
	<i>Reverse</i>	Mm00455950_m1 (Invitrogen)	
	<i>Probe</i>		
<i>Npas2</i>	<i>Forward</i>		NM_008719.2
	<i>Reverse</i>	Mm00500848_m1 (Invitrogen)	
	<i>Probe</i>		
<i>Per1</i>	<i>Forward</i>	ACC AGC GTG TCA TGA TGA CAT AC	NM_011065.4
	<i>Reverse</i>	CTC TCC CGG TCT TGC CTT CAG	
	<i>Probe</i>	CCG TCC AGG GAT GCA GCC TCT	
<i>Per2</i>	<i>Forward</i>	ATG CTC GCC ATC CAC AAG A	NM_011066.3
	<i>Reverse</i>	GCG GAA TCG AAT GGG AGA AAT	
	<i>Probe</i>	ATC CTA CAG GCC GGT GGA CAG CC	
<i>Cry1</i>	<i>Forward</i>	GTT GGC CGG CTC TTC CA	NM_007771.3
	<i>Reverse</i>	CAA GAT CCT CAA GAC ACT GAA GCA	
	<i>Probe</i>	CGT GGG CAT CAA CAG GTG GCG	
<i>Cry2</i>	<i>Forward</i>	CCG CCT GGA CAA GCA CTT	NM_009963.4
	<i>Reverse</i>	GCA TTC ATC CGA GGT CTC TCA	
	<i>Probe</i>	CGG AAG GCC TGG GTT GCC AAC T	
<i>Dbp</i>	<i>Forward</i>	CGT GGA GGT GCT TAA TGA CCT TT	NM_016974.3
	<i>Reverse</i>	CAT GGC CTG GAA TGC TTG A	
	<i>Probe</i>	AAC CTG ATC CCG CTG ATC TCG CC	
<i>Homer1a</i>	<i>Forward</i>	GCA TTG CCA TTT CCA CAT AGG	NM_011982.2
	<i>Reverse</i>	ATG AAC TTC CAT ATT TAT CCA CCT TAC TT	
	<i>Probe</i>	ACA CAT TCA ATT CAG CAA TCA TGA	

Table 6 Primers and probes used for quantitative PCR

f. Western blotting

To verify the absence of PER2 in the brain of *Per2* knock-out mice, both *Per2*^{-/-} and Wt mice were quickly anesthetized by isoflurane inhalation and sacrificed by cervical dislocation at ZT16.5 and cortical cortex or forebrain (that implies whole brain without cerebellum) were harvested. At this time, maximum expression of PER2 protein was expected [299, 300]. Tissues were immediately immersed in gentleMACS tubes (Miltenyi Biotec, Bergisch Gladbach, Germany) containing ice cold RIPA buffer (5ml for forebrain, 2ml for cortex) supplemented with protease inhibitor cocktail (Roche, Mannheim, Germany), 1% NP40 (AppliChem, Darmstadt, Germany) and 1% sodium deoxycholate (AppliChem). Subsequently, tissues were grinded in a gradual manner for 35sec with Dispomix Drive (Medic tools, Zug, Switzerland). Then the tubes were gently spun on a wheel for 30min 4°C, centrifuged at 1700g 20min 4°C, the supernatant was placed in a new tube and centrifuged again at >8000g 10min 4°C and finally the supernatant containing the total protein fraction was recovered. The protein concentration was quantified by BCA protein assay kit (Thermo scientific, Rockford, IL, USA) and the absorbance was read on a Safire² (Tecan) instrument using Magellan 6.6 software (Tecan). 90µg of protein were supplemented with Laemmli buffer 5x, heated at 95°C for 5min, loaded on a 6.5% SDS-page gel (BioRad, Mississauga, ON, USA) and transferred onto a PVDF membrane (Whatman, Sanford, ME, USA) [301]. Antibodies used were: α-PER2 rabbit antibody (1/1000; αPER2 antibody kindly provided by David Gatfield) and α-rabbit HRP-conjugated antibody (1/2000, P0448, Dako, Glostrup, Danmark). Membranes were revealed with Amersham ECL Prime Western Blotting Detection Reagent (GE Healthcare, Buckinghamshire, UK) and Amersham Hyperfilm ECL (GE Healthcare), and developed with a SRX-101A (Konica Minolta, Tokyo, Japan).

g. Statistical analysis

To evaluate statistical differences on time-spent-awake and -asleep, we performed a 1-way ANOVA with as main factor 'genotype' (*Per1*^{-/-}, *Per2*^{-/-}, *Per1,2*^{-/-} and Wt). Post-hocs Holm-Sidak tests were used to contrast the results in knock-out mice to Wt. To evaluate the time course of waking, NREM, and REM sleep, and for the SD effect, we performed 2-way ANOVAs with the factors 'genotype' and

'time' (from ZT1 to 24 in baseline and from ZT6 to 24 in recovery period after a SD). For the comparison between all knock-out mice with the Wt at each ZT, Holm-Sidak was used as post-hoc tests. Within each genotype the effect of SD was also evaluated by performing t-tests between knockout and Wt mice for each 1h increment in order to assess the accumulation of the recovery-to- baseline differences in NREM sleep starting at ZT6 after the SD; i.e., the start of recovery sleep. NREM sleep fragmentation was determined using a 2-way ANOVA comparing all genotypes with different time intervals. Holm-Sidak was used as post-hoc test to compare all knock-out with Wt mice for each time interval. A 2-way ANOVA was performed to compare all genotypes with the ZT for the EEG delta power. Holm-Sidak was used as post-hoc test for the comparison between all knock-out and Wt mice at each ZT. The threshold for statistical significance was set to $p < 0.05$ and the results are reported as mean \pm SEM. A 2-way ANOVA was performed to compare *Per2*^{-/-} and Wt mice with control and SD conditions for the effect on mRNA level in the cortex of the 6h period SD. Holm-Sidak was used as post-hoc test. A 2-way ANOVA was performed to compare *Per2*^{-/-} and Wt mice as well as different time points (ZT). Holm-Sidak was used as post-hoc test for the time-course experiment monitoring corticosterone level and mRNA expression across 12h. Additionally, for the EEG spectral analysis, t-tests were performed to compare power density measured for each frequencies bin of all knock-out mice to the Wt. All data were managed with Pascal and Microsoft Excel (Redmond, WA, USA), the statistical analysis and graphical representation were performed with SigmaPlot v12.3 (Systat Software, Erkrath, Germany).

3. Results and discussion

a. *Per2*^{-/-} mice become immediately arrhythmic in DD despite dark-onset anticipation in LD

Circadian rhythms in locomotor activity were characterized in both male and female mice of the 4 genotypes (*Per1*, *Per2*, *Per1,2*, and their Wt controls) (Fig.30 and 31). All mice were entrained to a 12/12 light/dark (LD) cycle which was confirmed by periodogram analyses yielding a period length (τ) of 24h (Fig.30 H_A LD). Under DD, Wt and *Per1*^{-/-} mice had a specific free-running pattern which allows the calculation of the endogenous τ . Within each genotype, sex did not affect the results (analyses not shown) and the datasets were therefore merged. It was previously reported that *Per1*^{-/-} mice on a 129S7/SvEvBrd background had a shorter τ (22.6h \pm 0.2) compared with Wt mice (23.7h \pm 0.1) [165]. However, in our hands, the shortening of τ in *Per1*^{-/-} mice on a C57BL6/J background were significant but not as marked (23.4h \pm 0.1, n=8) compared to Wt mice (23.8h \pm 0.0, n=14; $p < 0.05$ t-test; Fig.30E,F). All *Per1,2*^{-/-} mice became immediately arrhythmic under DD (n=8; Fig.30G, Fig.31G). Confirming previous observations, the double mutant *Per1,2*^{tm1Drw} mice on a 129S4/SvJae background [197, 201]. *Per2*^{-/-} mice on a C57BL6/J background have not been studied and only one publication mentioned that *Per2*^{-/-} mice were similar to *Per2*^{tm1Brd} mice (both on a mixed 129S7/Sv x C57BL6 background) in that both lines had a short τ (22.1h) in the beginning of the DD and then became arrhythmic after a range of 2 to 18 days.

In stark contrast to *Per2*^{tm1Brd} and *Per2*^{tm1Drw} mice, 94% of *Per2*^{-/-} mice kept under LD 12:12 became directly arrhythmic when released under DD. 90.5% (n=21) of the *Per2*^{-/-} males became and remained arrhythmic throughout DD (Fig.30A,C). Only two male *Per2*^{-/-} mice did not follow in this pattern; one displayed a circadian rhythm of short period throughout DD (τ =22.8h; Fig.30D) with activity onset free-running from the activity onset during LD12:12, while a second male maintained an unusual circadian component of wild-type period length (τ =23.7h) but of small amplitude with activity onset not following activity onset observed during the preceding LD12:12 but about 5h earlier (at ZT5 instead ZT10; Fig.30B). Apparently, *Per2*^{-/-} mice on a C57BL/6J background had a stronger phenotype than *Per2*^{tm1Brd} in 129S7/Sv x C57BL6 mixed background. Moreover, *Per2*^{tm1Brd} mice showed an

earlier locomotor activity onset before the dark period under LD 12:12 conditions. Both male and female were used without distinction [199]. This advanced locomotor activity onset was also found in our *Per2*^{-/-} mice under LD12:12 in both sexes without statistic distinction (2-way ANOVA, factors 'genotype' and 'sex'; genotype effect: $p < 0.001$), and was set at $ZT = 10.6 \pm 0.1h$ ($n = 32$) in the mice; i.e., advanced by about 1.5h ($p < 0.001$ with Holm-Sidak as post-hoc test) compared to Wt, *Per1*^{-/-} and double knock-out mice for which the following activities onset values were found $ZT = 12.0 \pm 0.0$ ($n = 14$), $ZT = 12.3 \pm 0.1$ ($n = 8$), and $ZT = 12.7 \pm 0.1$ ($n = 8$), respectively.

b. Rhythmicity could be triggered *Per2*^{-/-} female

100% ($n = 11/11$) of the females became completely and immediately arrhythmic upon release into DD. Surprisingly, they became rhythmic at the same time with a short τ (21.9 ± 0.2 , $n = 6$; Fig.31A,B) throughout the remainder of DD after several days under DD. Only in one female we observed second loss of rhythmicity (Fig.31C). The event triggering this rhythmicity was associated with checking the status of the mice under DD. The trigger signal could be one of many; e.g., fresh food, noise, odor, red dim light (Fig.31A,B,C). When female mice were not disturbed, they remained arrhythmic until the end of the DD ($n = 4$; Fig.31D). To conclude, *Per2*^{-/-} males and undisturbed *Per2*^{-/-} females maintained arrhythmicity throughout DD despite the fact that they seem able to anticipate the dark onset under LD12:12 conditions and that when disturbed, females could display self-sustained rhythm. The 1.5h earlier onset under LD is consistent with an intrinsic period of 22h observed in females and the 1 male although, this rhythm under LD cannot be considered circadian because it is not self-strained.

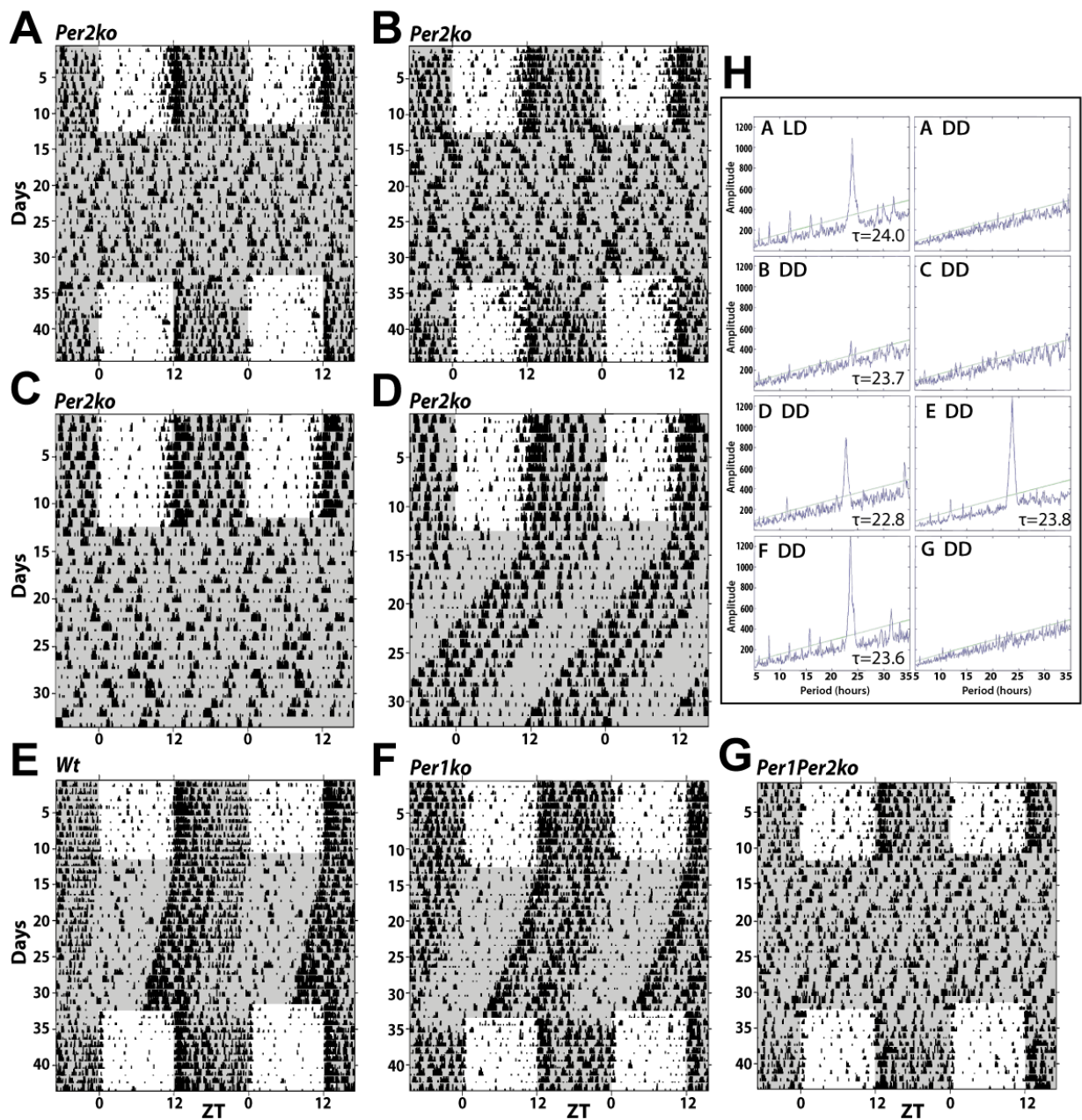


Figure 30 Actograms of *Per* knock-out male mice under LD12:12 and DD conditions. A-G. The locomotor activity is represented in black and double-plotted. Mice were kept on a LD cycle (time of lights off indicated by grey shading) and then put in constant darkness (DD) for a minimum of 21 days and finally put again in LD. A,C Activity record of two representative *Per2^{-/-}* mice (19 out of 21) that became immediately arrhythmic under DD. B,D Two unexpected *Per2^{-/-}* mice that displayed circadian components. E,F,G Activity record of a representative *Wt* (E, $\tau=23.8$ h), *Per1^{-/-}* (F, $\tau=23.6$ h), and *Per1,2^{-/-}* mouse (G, arrhythmic). All mice had a period (τ) of 24h in LD. H panel. Chi² statistical graphics determined with at least 8 days for LD and 18 days for DD. Total number of male mice recorded: *Per1^{-/-}* (n=4), *Per2^{-/-}* (n=21), *Per1,2^{-/-}* (n=11) and *Wt* (n=5).

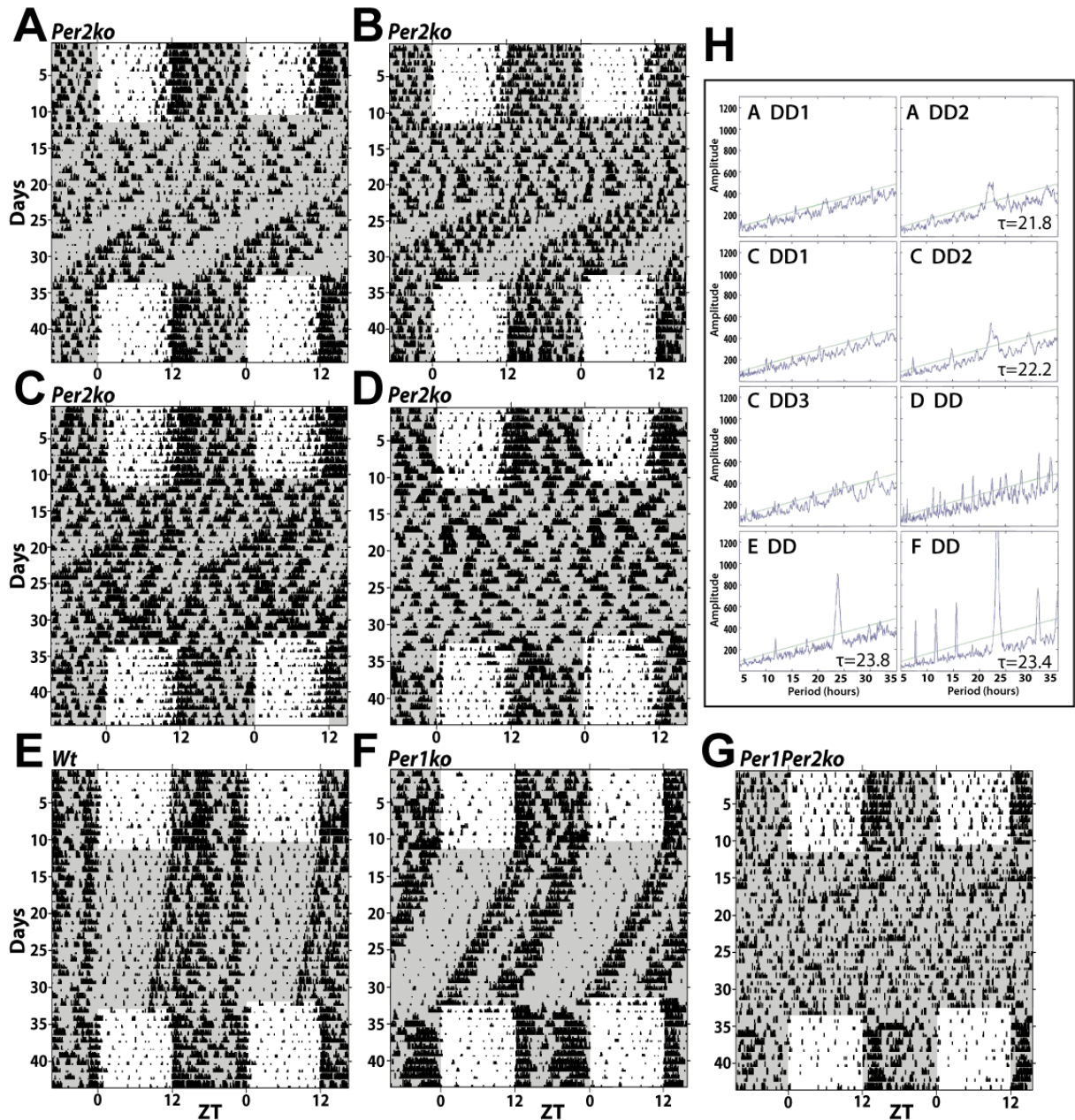


Figure 31 Actograms of *Per* knock-out female mice under LD12:12 and DD conditions. **A,B** Activity recordings of two representatives *Per2*^{-/-} females that became immediately arrhythmic in first part of the DD (11 out of 11) and thereafter became rhythmic with a τ of roughly 22h . **C** One *Per2*^{-/-} female became immediately arrhythmic under DD for 7 days, and then became rhythmic ($\tau=22.2$ h) for 7 days and again arrhythmic for the last 8 days. **D** If *Per2*^{-/-} females were not disturbed (no feeding and health check) mice remained arrhythmic throughout DD. **E,F,G** Activity record of a representative *Wt* (**E**, $\tau=23.8$ h), *Per1*^{-/-} (**F**, $\tau=23.4$ h), and *Per1,2*^{-/-} mouse (**G**, arrhythmic). All mice had a period (τ) of 24h in LD. **H** panel. χ^2 statistical graphics determined with at least 7 days in DD for mice in panels A-D. Some DD period was split in two or three parts when the rhythms appeared, and were numerated DD1,-2 or -3. Total number of mice recorded: *Per1*^{-/-} (n=4), *Per2*^{-/-} (n=11), *Per1,2*^{-/-} (n=3) and *Wt* (n=3). See figure 25 for further details.

c. Clock genes and corticosterone advance of 2h in *Per2*^{-/-} mice

To verify whether the advance of activity onset under LD12:12 conditions was paralleled by an advance of their circadian markers we determined clock gene expression in *Per2*^{-/-} mice in cerebral cortex over a 12h time span covering activity onset in *Per2*^{-/-} mice; i.e. ZT2-14. I quantified the expression of *Bmal1*, *Clock*, *Npas2*, *Cry1*, *Cry2*, *Per1*, and *Per2*, as well as the controlled clock gene *Dbp*, the circadian marker corticosterone and the molecular marker of sleep intensity *Homer1a* transcript [45, 158].

In the brain, *Bmal1*, *Clock* and *Npas2* usually peak at ZT0-6 and reach minimum levels at ZT12-16 [302, 303]. *Per1*, *Per2*, *Cry1*, *Cry2*, and *Dbp*, on the other hand, are usually more or less in antiphase peaking at ZT12-16 and reaching minimum levels at ZT6, except for *Dbp* at ZT0 [48, 242, 302, 304] (Fig.32). *Homer1a* followed sleep-wake distribution decreasing progressively from ZT0 to ZT12 when animals predominantly sleep and increasing from ZT12 to ZT14 when mice are most active and awake [45, 48] (Fig.35A). Although I only sampled half of the 24h cycle, preferring to promote the resolution instead a large scale, the observed time course fits well those described by others.

With the exception of *Clock*, all the time course of all transcripts differed between *Per2*^{-/-} and Wt mice (2-way ANOVA, factors 'genotype' and 'ZT', Fig.32 upper panel) and levels differed at many points (*Bmal1* at ZT 2,4,10,12,14; *Npas2* at ZT2,4,14; *Per1* at ZT12,14; *Cry1* at ZT 0,6,8,10,12,14; *Cry2* at ZT6,12; *Dbp* at ZT2,4,6,12,14; and *Homer1a* at ZT4,12,14 (p<0.05 with Holm-Sidak as post-hoc). *Per2* was not detected in *Per2*^{-/-} mice.

Despite all these differences, in both genotypes mRNA expression followed a similar curve. Assuming, based on the earlier activity onset (Fig.35A), that in *Per2*^{-/-} mice also the mRNA changed were advanced by about 2h, delaying the *Per2*^{-/-} mice data by 2h should yield a better match with the Wt time course. The curves for *Bmal1*, *Clock*, *Npas2*, *Cry2*, *Dbp*, and *Homer1a* now matched for the two genotypes (Fig.32 lower panel) and statistical differences were no longer observed for *Npas2* and *Cry2*. Some statistically changes were noted between *Per2*^{-/-} and Wt mice (2-way ANOVA, factors

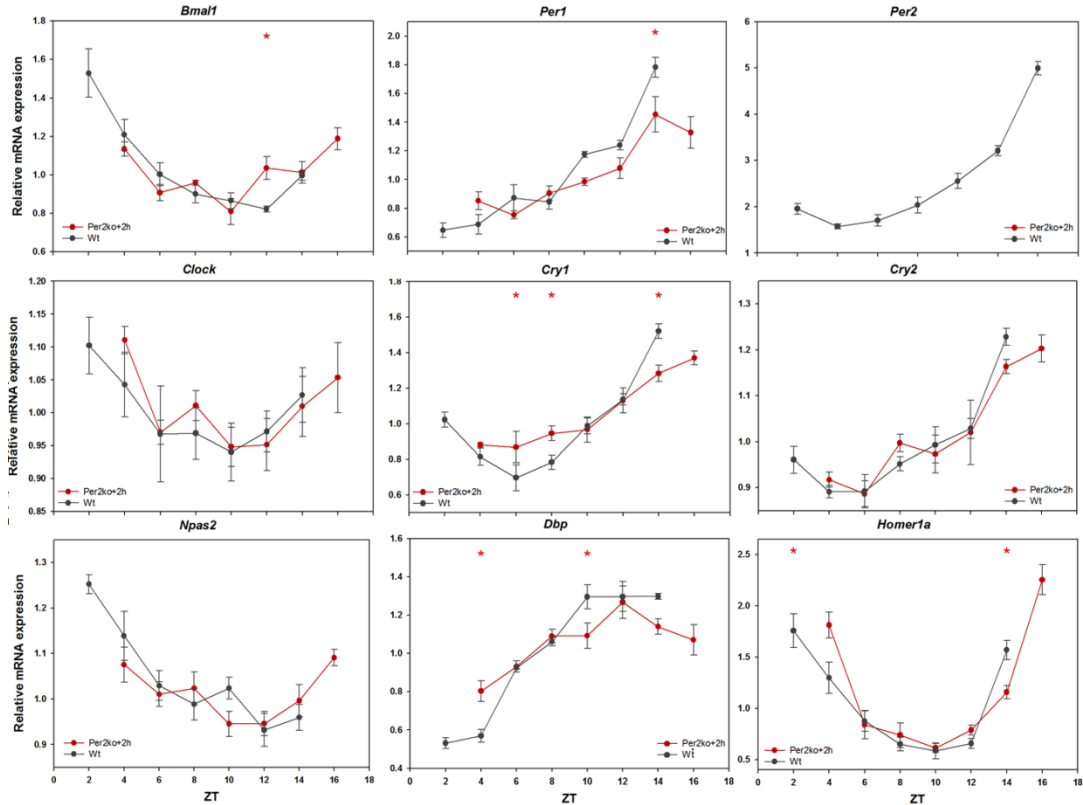
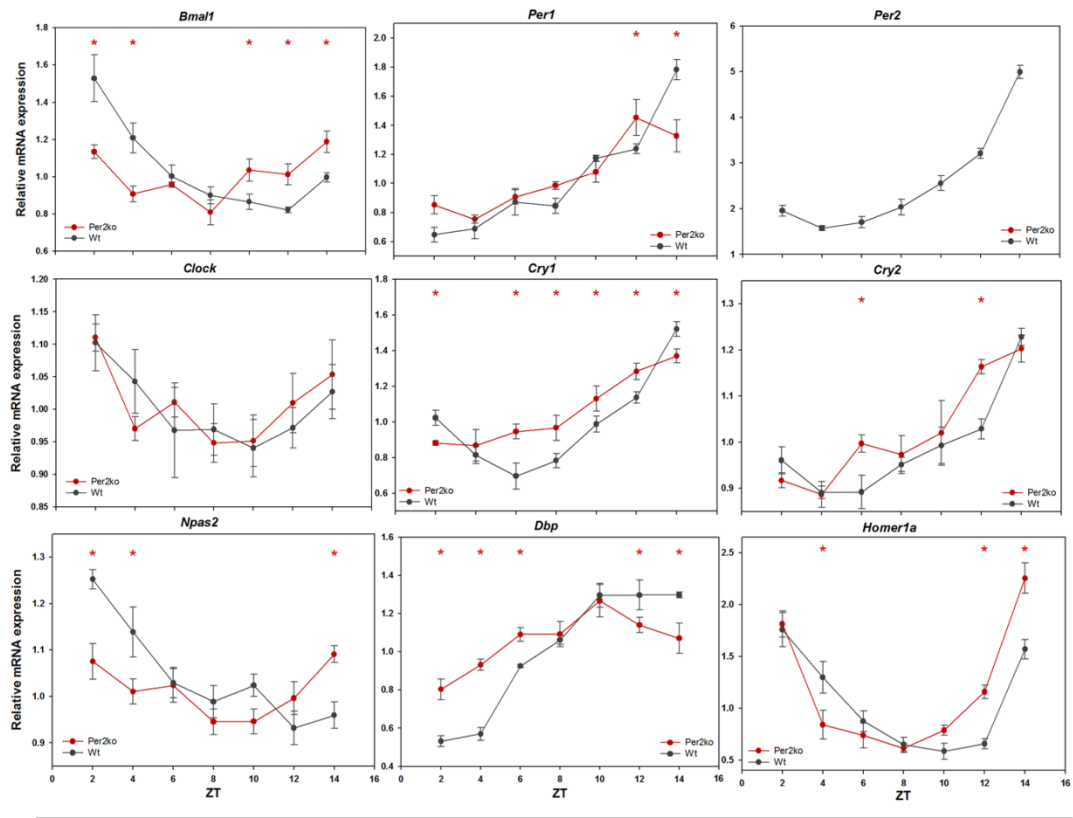


Figure 32 Time-course of mRNA expression concentration in cerebral cortex across 12 hours in *Per2*^{-/-} and Wt mice. Upper panel Relative expression of *Bmal1*, *Clock*, *Npas2*, *Per1*, *Per2*, *Cry1*, *Cry2*, *Dbp* and *Homer1a* across 12 hours started at ZT2 and finished at ZT14 with a point every 2h in cerebral cortex of *Per2*^{-/-} (red) and Wt (grey) mice. 2-way ANOVA: factors 'genotype' and 'ZT', interaction: $p < 0.001$ for all gene except for *Cry2* ($p < 0.05$) and *Clock*. *: $p < 0.05$ with Holm-Sidak as post-hoc test between *Per2*^{-/-} mice and Wt. For each point 4 to 6 mice were used. Lower panel Comparison between Wt and *Per2*^{-/-} 2h-delayed data. Relative expression of *Bmal1*, *Clock*, *Npas2*, *Per1*, *Per2*, *Cry1*, *Cry2*, *Dbp* and *Homer1a* across 12 hours started at ZT2 and finished at ZT14 with a point every 2h in cerebral cortex. The data for *Per2*^{-/-} mice were delayed of 2h and being compared with Wt mice. Two-way ANOVA: 'genotype'- 'ZT', with interaction ($p < 0.03$) for all gene except for *Clock*, *Cry2*, *Npas2*, *Rsp9*, *Eaf1a* and *GADPH*. *: $p < 0.05$ with Holm-Sidak as post-hoc test between *Per2*^{-/-} mice and Wt. For each point 4 to 6 mice were used. Controls genes (*Rsp9*, *Eaf1a*, *Gapdh*) were reported in Fig.29

'genotype' and 'ZT'; Fig.32 lower panel) for instance *Bmal1* at ZT14; *Per1* at ZT14; *Cry1* at ZT6,8,14; *Dbp* at ZT4,10; and *Homer1a* at ZT4,14 ($p < 0.05$ with Holm-Sidak as post-hoc). Despite these statistical changes the curve tendency was in complete accordance between the genotype in *Bmal1*, *Dbp* and *Homer1a*. *Per1* and *Cry1* matched also but it seems that they possessed lower amplitude and minimal values reached seem higher in the *Per2^{-/-}* mice. However to confirm this assumption, a complete 24h cycle should have been sampled. A reduction in the amplitude of *Per1* transcript oscillation was also observed in the *Per2^{m/m}* mice of a previous study [197, 199]. We also hypothesized that there is also a phase advance at the molecular level due to a shorter period in the *Per2^{-/-}* mice.

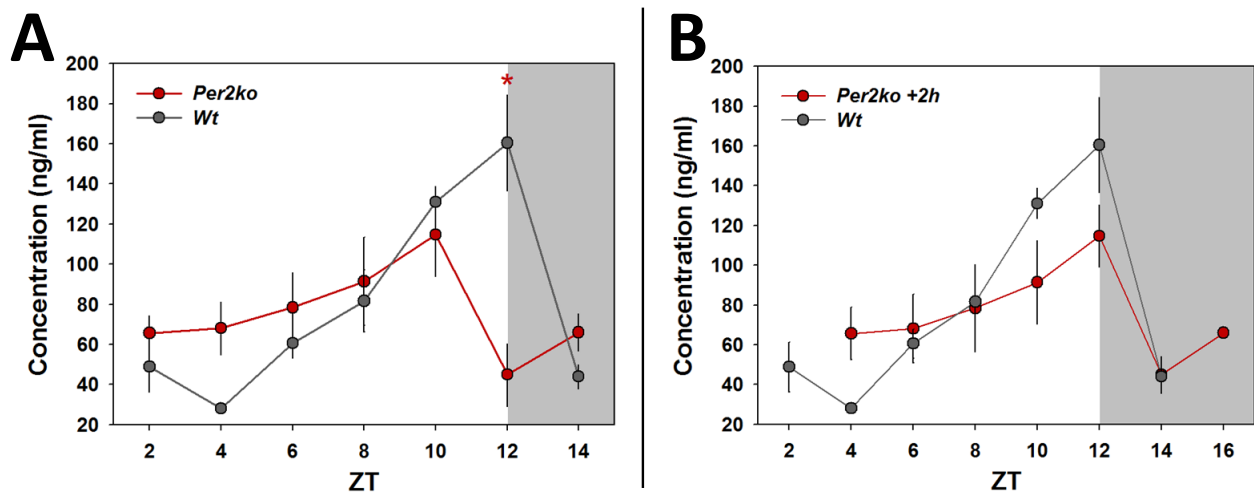


Figure 33 Time-course of plasma corticosterone concentration across 12 hours in *Per2^{-/-}* and *Wt* mice. **A** Corticosterone measurements (mean \pm SEM) started at ZT2 and finished at ZT14 with a 2h resolution. 2-way ANOVA: factors 'genotype' and 'ZT', interaction: $p < 0.001$. *: $p < 0.05$ with Holm-Sidak as post-hoc test between *Per2^{-/-}* and *Wt* mice. **B** Comparison between *Wt* and *Per2^{-/-}* 2h-delayed data. Corticosterone concentration across 12 hours started at ZT2 and finished at ZT14 with a point every 2h in plasma blood. The data for *Per2^{-/-}* mice were delayed of 2h and been compared with *Wt* mice. There is no statistical difference by 2-way ANOVA: factors 'genotype' and 'ZT' between *Per2^{-/-}* and *Wt* mice.

To have an idea if this advance of the circadian machinery at the molecular level was also present at the physiological level, I looked at the time course of plasma corticosterone levels. I chose this hormone because it is important glucocorticoid expressed in a circadian manner with a very stable peak reaching between ZT10-12 just before the dark onset and can set phase of circadian clock [48, 305]. Peak cortisol level is used in human studies as a circadian phase marker [306, 307].

Wt mice showed the predicted time course reaching maximum levels at ZT12 directly followed by a rapid decrease again reaching low levels at ZT14 (Fig.33A). *Per2^{-/-}* mice shown a different distribution peaking at ZT10 followed again by a rapid decrease (2-way ANOVA: factors 'genotype'

and 'ZT'; interaction: $p < 0.001$; red star: $p < 0.05$ with Holm-Sidak as post-hoc test; Fig.33A). If the *Per2*^{-/-} data were also delayed by 2h as the mRNA expression shown above, an almost perfect match was observed (Fig.33B) suggesting that also this circadian marker was advanced of 2h in mice lacking *Per2*. Nevertheless, the amplitude seemed to be reduced in the *Per2*^{-/-} mice. Together these three data sets (behavior, molecular, and hormonal changes) demonstrate that the circadian machinery is coherently advanced in *Per2*^{-/-} mice in accordance with the shorter period length observed in females and in one males. The big unanswered question is why *Per2*^{-/-} mice become arrhythmic when during the preceding LD12:12 a circadian rhythm appear to be present.

d. How can an arrhythmic mouse anticipate dark onset?

To understand this paradoxical phenotype, the following hypothesis could be forwarded. It is possible that in the *Per2*^{-/-} mice under LD12:12 conditions light onset initiates a rhythm each day of about 22h, but that this rhythm is not self-sustained; i.e. light driven, because rhythmicity is lost immediately when light is not present. To test this idea we performed two experiments. First we verified whether the earlier activity onset is associated to dark onset (i.e., anticipation) or to light onset (light driven) by delaying dark onset by 6h thus extended the photoperiod from 12h to 18h (LD 18:6). If light driven, we expect activity onset to stay close to ZT10. If, on the other hand, activity onset results from truly entrained circadian rhythm, activity onset would trail the new dark onset time and thus delay by about 6h. Wt mice had an activity onset under LD 12:12 at ZT12.0h \pm 0.0 (n=3) and at ZT17.9h \pm 0.0 under LD 18:6 as can be seen in the upper half of figure 34 (experiment 1). They behaved as expected from mice with a true circadian clock and needed about 4 days to re-entrain activity onset (first blue line) to dark onset. The activity onset of *Per2*^{-/-} mice was set at ZT10.80 \pm 0.2 (green line, n=5) under LD 12:12 and shorter than that observed in Wt mice (2-way Anova; factors 'genotype' and 'photoperiod'; with both genotype, photoperiod effect and interaction: $p = < 0.001$), while the new activity onset of *Per2*^{-/-} mice in LD18:6 was set at ZT12.2 \pm 0.2 (pink line); i.e., 2h later than the expected ZT10 (green line) but not as much as expected when it was associated with the dark period onset at ZT18.

In the second experiment, the same mice were re-entrained to standard LD12:12 conditions and thereafter put under DD for 48h and then exposed to an inverted LD12:12 cycle. The expectation here is that if the rhythm in *Per2*^{-/-} mice is light driven, we expect to have an activity onset again at ZT10 (old ZT22 on the axis; pink line) from the first day. If truly circadian we expected that mice needed several days of adaptation before to be able follow new schedule as Wt mice (represented by the blue line, figure 34 experiment 2). The results support the light driven hypothesis. In fact activity onset of the first day of the new schedule was set at ZT10.5±0.1 in *Per2*^{-/-} mice. These two experiments show that despite the fact that *Per2*^{-/-} male mice the 2h advance of activity, clock gene expression, and corticosterone do not result from a self-sustained functional circadian clock, but is associated with light onset and thus per definition not circadian [97].

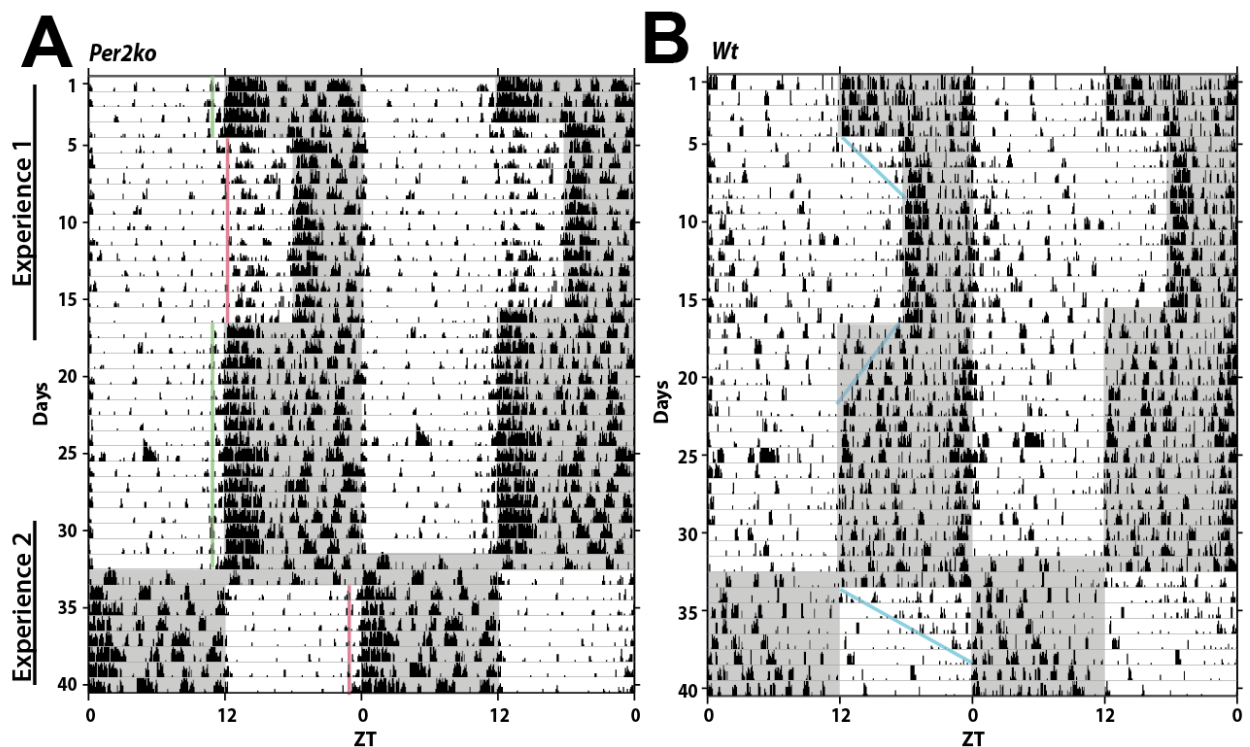


Figure 34 Effect of lengthening the photoperiod and inverting the LD schedule on activity onset in *Per2*^{-/-} mice. In experiment 1: mice were kept on a LD cycle (12:12; dark periods indicated by the grey bars behind actograms) for the first 4 days and then put under LD18:6 for 12 days. In experiment 2: same mice were kept under LD12:12 and then put in constant dark condition for 48h and then submitted to an inverted LD12:12 cycle (light onset at old ZT12) for at least 7 days. The important locomotor activity at ZT6 on day 25 followed delivery of fresh food. **A** Actogram of one representative *Per2*^{-/-} male mouse with activity onset (green lines) at ZT10 under LD12:12, at ZT12 (rose line in experiment 1) under LD18:6, and ZT22 (new ZT10; rose line in experiment 2) under the inverted LD12:12 cycle. **B** Activity record of one representative Wt male mouse. When the schedule is modified, Wt mice need several days of re-entrain activity onset (blue lines). Total number of mice recorded: *Per2*^{-/-} (n=5) and Wt (n=3).

e. Altered sleep-wake state distribution in *Per* knock-out mice

The distribution of each the three sleep-wake state wakefulness, NREM sleep and REMS sleep was computed across the two baseline days. Sleep analyses are a so intensive labor that only male mice were investigated. The overall distribution over the day was similar among the 4 genotypes with sleep being more prevalent in the light phase of the LD12:12 cycle and wakefulness being prevalent during the dark (Fig.35). Nevertheless, the time course and duration of the 3 sleep-wake states importantly varied with genotype (2-way ANOVA, factors 'genotype' and 'ZT'; interaction: $p < 0.001$; Fig.35).

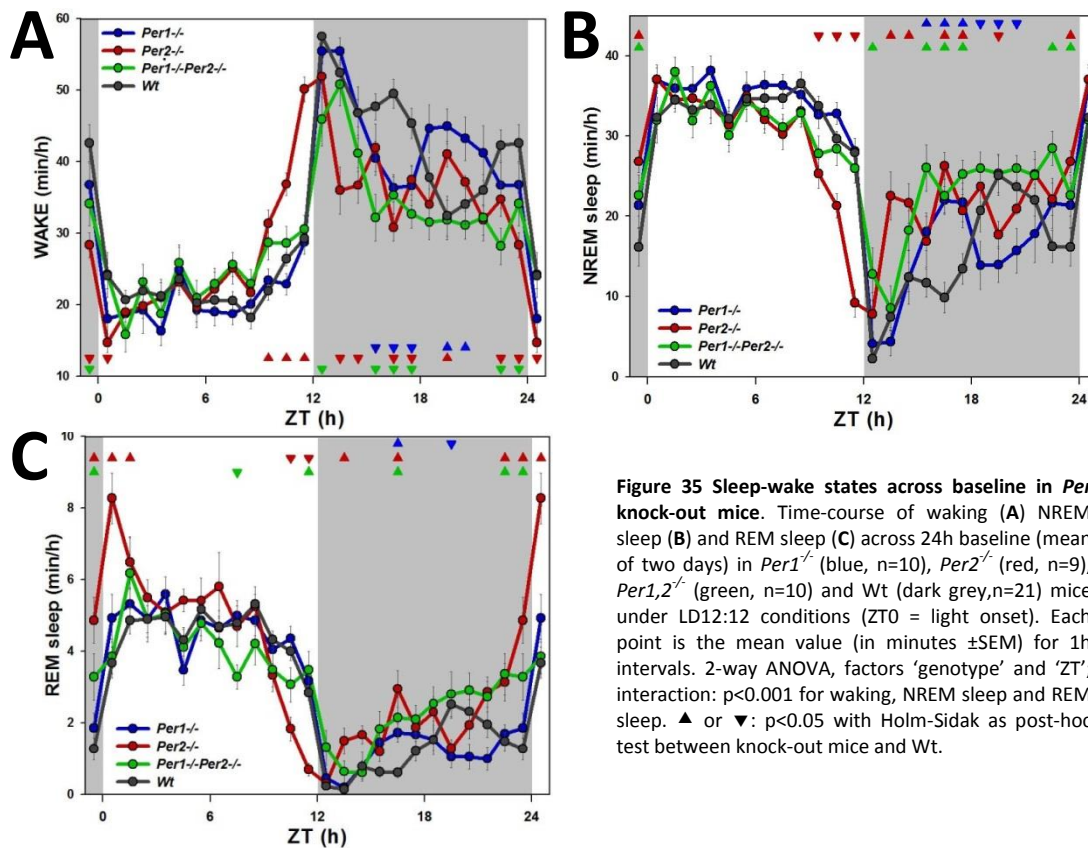


Figure 35 Sleep-wake states across baseline in *Per* knock-out mice. Time-course of waking (A) NREM sleep (B) and REM sleep (C) across 24h baseline (mean of two days) in *Per1*^{-/-} (blue, n=10), *Per2*^{-/-} (red, n=9), *Per1,2*^{-/-} (green, n=10) and Wt (dark grey, n=21) mice under LD12:12 conditions (ZT0 = light onset). Each point is the mean value (in minutes \pm SEM) for 1h intervals. 2-way ANOVA, factors 'genotype' and 'ZT'; interaction: $p < 0.001$ for waking, NREM sleep and REM sleep. ▲ or ▼: $p < 0.05$ with Holm-Sidak as post-hoc test between knock-out mice and Wt.

Of the numerous differences I observed in this distribution, I will here focus specifically the effects of genotype on NREM sleep. Its main periods of wakefulness are at the first 6h from the beginning of dark period and the last 2h of just before the dark light transition. In contrast to humans that have one consolidated bout of sleep (monophasic), Wt mice have many sleep episodes during 24h (polyphasic). A 'nap' normally appeared in the second part of the dark period in C57BL6/J [36]. As previously described by Kopp *et al.* using the same *Per1* knock-out mice also on a C57BL6/J genetic back-

ground [203], after the first 3h of the dark period *Per1*^{-/-} (n=10) mice showed an increase the NREM sleep during 3h followed by an important fall (p<0.05; Fig.35B). It thus seems that the nap was advanced by about 3h compared to Wt (n=21) mice. Otherwise, no large differences in the NREM sleep distribution between *Per1*^{-/-} and Wt mice in the light period. Note that contrast to what was been reported previously in our *Per1*^{-/-} mice where no NREM sleep increase was observed prior to the light-dark and dark-light transitions [203]. Furthermore, the amount of each sleep/wake state (table 7) and NREM sleep and REM sleep fragmentation were not affected in *Per1*^{-/-} mice (Fig.36).

		<i>Per1</i> ^{-/-}	<i>Per2</i> ^{-/-}	<i>Per1,2</i> ^{-/-}	Wt
12h light	Wake [min]	256 (10)	312 (10) ↗	295 (10)	275 (8)
	NREM [min]	409 (9)	351 (12) ↘	375 (11)	392 (9)
	REM [min]	55 (2)	57 (4)	50 (4)	54 (2)
12h dark	Wake [min]	512 (14)	434 (10) ↘	420 (15) ↘	518 (11)
	NREM [min]	193 (13)	259 (10) ↗	273 (13) ↗	187 (10)
	REM [min]	15 (2)	27 (2) ↗	27 (3) ↗	15 (1)
24h	Wake [min]	768 (14)	746 (13) ↘	715 (8) ↘	793 (12)
	NREM [min]	603 (14)	610 (17)	648 (12) ↗	579 (12)
	REM [min]	69 (3)	84 (5) ↗	77 (6)	68 (2)

Table 7 Summary table of sleep-wake state amounts (in min) for the 12h light period, 12h dark period, and 24h for all genotypes. The mean of two days was used (SEM). 1-way ANOVA: factor 'genotype' for Wake, NREM sleep and REM sleep: p<0.001. ↘ or ↗: p<0.05 with Holm-Sidak as post-hoc test between knock-out and Wt. Number of mice used: *Per1*^{-/-} (n=10), *Per2*^{-/-} (n=9), *Per1,2*^{-/-} (n=10) and Wt (n=21).

Baseline sleep in *Per2*^{-/-} mice (n=9) displayed, as was already observed in *Per2*^{m/m} mice [203], an earlier onset of the main wake bout before the dark onset. The wakefulness onset in *Per2*^{-/-} mice was ZT=9.9 ± 0.2h (n=9); i.e., advanced by about 2h (Kruskal-Wallis One Way, factor 'genotype': p<0.05) compared to Wt, *Per1*^{-/-} and double knock-out mice, which had values set at ZT=12.0±0.0 (n=21), 12.0±0.1 (n=10), and ZT=11.8±0.1 (n=10), respectively. These results confirm the locomotor activity onset results described above. Moreover, wake onset appeared 43min before locomotor activity onset (t-test, p<0.01) in *Per2*^{-/-} mice. In addition, *Per2*^{-/-} mice was a relevant increase of the NREM sleep in the first half of the dark period due to its earlier and shorter wake period (p<0.001; Fig.35B). Nevertheless, the total amount of the NREM sleep did not differ from Wt mice although a decrease in total amount of wakefulness was revealed (p=0.029, table 7). This decrease in wakefulness was balanced by an increase in total amount of REM sleep (p=0.015) whose the hourly main values appeared at the dark-light transition (p<0.05, Fig.35C).

Per1,2^{-/-} mice (n=10) had an increase in the total time spent in NREM sleep in baseline ($p=0.002$), due to an excess of NREM sleep during most of the dark period compared with to Wt mice ($p<0.05$ with Holm-Sidak as post-hoc test; Fig.35B; $p<0.001$ with Holm-Sidak as post-hoc; table 7). Previous studies found no statistical changes in sleep amount among *Per1^{-/-}*, *Per2^{m/m}*, *Per3^{-/-}*, *Per1,2^{m/m}* and Wt mice on a 129S4/SvJae background and between *Per1^{-/-}*, *Per2^{m/m}* and Wt mice on a C57BL6/J background, both under LD cycle [201, 203]. *Per1,2^{-/-}* mice thus show a stronger phenotype compared with *Per1,2^{m/m}* mice [201].

f. NREM sleep is fragmented in mice lacking *Per2*

Besides sleep duration, I was also interested in quantifying and comparing the quality of sleep among genotypes and therefore analyzed episode duration of the three sleep/wake states. Both *Per2^{-/-}* and *Per1,2^{-/-}* mice had more short NREM sleep episodes (between 8 to 60 seconds length) (2-way ANOVA, factors 'genotype' and 'episode length'; interaction: $p<0.001$; $p<0.03$ with Holm-Sidak as post-hoc test; Fig.36 upper panel). In addition, in both *Per2^{-/-}* and *Per1,2^{-/-}* mice more of the total NREM sleep was spent in shorter episodes (significant for 32 to 60s category) and less in long episodes (128 to 252s) (2-way ANOVA: factors 'genotype' and 'episode duration'; interaction: $p<0.001$; $p<0.001$ with Holm-Sidak as post-hoc; Fig.36 middle panel). Similarly, both *Per2^{-/-}* and *Per1,2^{-/-}* mice were unable to sustain long waking episodes (>1024s) a category in which most time spent awake occurs (2-way ANOVA: 'genotype' and 'length time'; interaction: $p<0.001$; $p<0.001$ with Holm-Sidak as post-hoc; Fig.36 lower panel). No genotype changes were observed for REM sleep episodes (not shown). To resume, these findings show that *Per2* specifically is needed for the consolidation of NREM sleep and wakefulness a phenotype not reported on earlier.

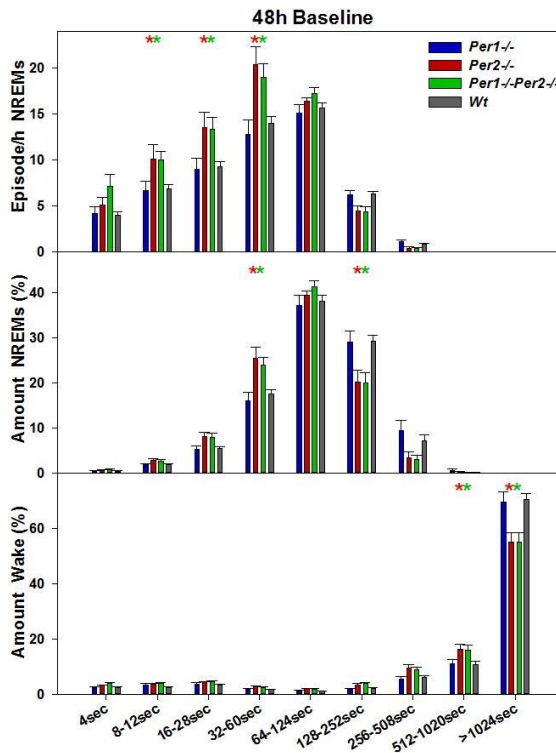


Figure 36 Distribution of episode duration for NREM sleep and wakefulness *Per* knock-out mice. **Upper panel** Relative frequency distribution of NREM sleep episode duration (4sec to >1024sec) during 48h baseline. Values were expressed per h of NREM sleep. 2-way ANOVA; factors 'genotype' and 'episode duration'; interaction: $p < 0.001$. *: $p < 0.001$ with Holm-Sidak as post-hoc test between knock-out and Wt mice. **Middle panel** NREM sleep time spent in each category as % of total time spent in NREM sleep. 2-way ANOVA; factors 'genotype' and 'episode duration'; interaction: $p < 0.001$. *: $p < 0.001$ with Holm-Sidak as post-hoc test between knock-out and Wt mice. **Lower panel** Same as middle panel for wakefulness. 2-way ANOVA; factors 'genotype' and 'episode duration'; interaction: $p < 0.001$. *: $p < 0.001$ with Holm-Sidak as post-hoc test between knock-out and Wt mice. Number of mice used: *Per1*^{-/-} (blue, n=10), *Per2*^{-/-} (red, n=9), *Per1,2*^{-/-} (green, n=10) and Wt (dark grey, n=21).

g. Quantitative EEG spectral profile in *Period* knock-out mice

In the previous section we make use of EEG analysis to determine sleep-wake state distribution, duration and consolidation, to get a fine architecture of sleep and wakefulness. However, EEG signal itself contains valuable information concerning rhythmic brain activity that can be quantified (qEEG) using spectral analysis

To remind the reader, the EEG during wakefulness in Wt mice encompasses a variety of behaviors, each with their characteristic EEG pattern. For instance, during drowsiness delta waves (1–4Hz) can intrude, during an exploratory behavior theta waves (5–9Hz) are characteristic, during quiet wakefulness with eyes closed alpha waves (8–12 Hz) were typical, and during the attention process gamma waves (>30Hz) were prominent [7, 35]. The EEG pattern of NREM sleep is characterized by a widespread synchronous activity in the delta (1–4Hz) frequency range and by spindle oscillations in the sigma (12–15Hz) range [34, 36]. The structures implicated in the generation of these two mutually exclusive rhythms include the thalamus and the entire cerebral cortex [308]. The EEG profile of REM sleep is characterized by theta oscillations (4–12Hz) that can be observed in several regions of the limbic system, including the septum where it is thought to be generated [309, 310].

Both REM sleep and wakefulness are considered activated brain states that share common EEG characteristics, such as the absence of delta and spindle activity and the presence of coherent gamma activity (>30Hz) [34-36].

During waking, *Per2*^{-/-} mice showed an important increase in the β range (15-30Hz), while *Per1,2*^{-/-} mice had a decrease in the γ range (30-45Hz) compared to Wt mice ($p < 0.05$, t-tests; Fig.37). β and γ range are a prominent feature of the EEG during quiet wakefulness [34]. No statistical changes were observed among genotypes for the θ range (5-10Hz) that is associated exploratory behavior, learning and memory and which, in rodents, also dominates the EEG during REM sleep [34].

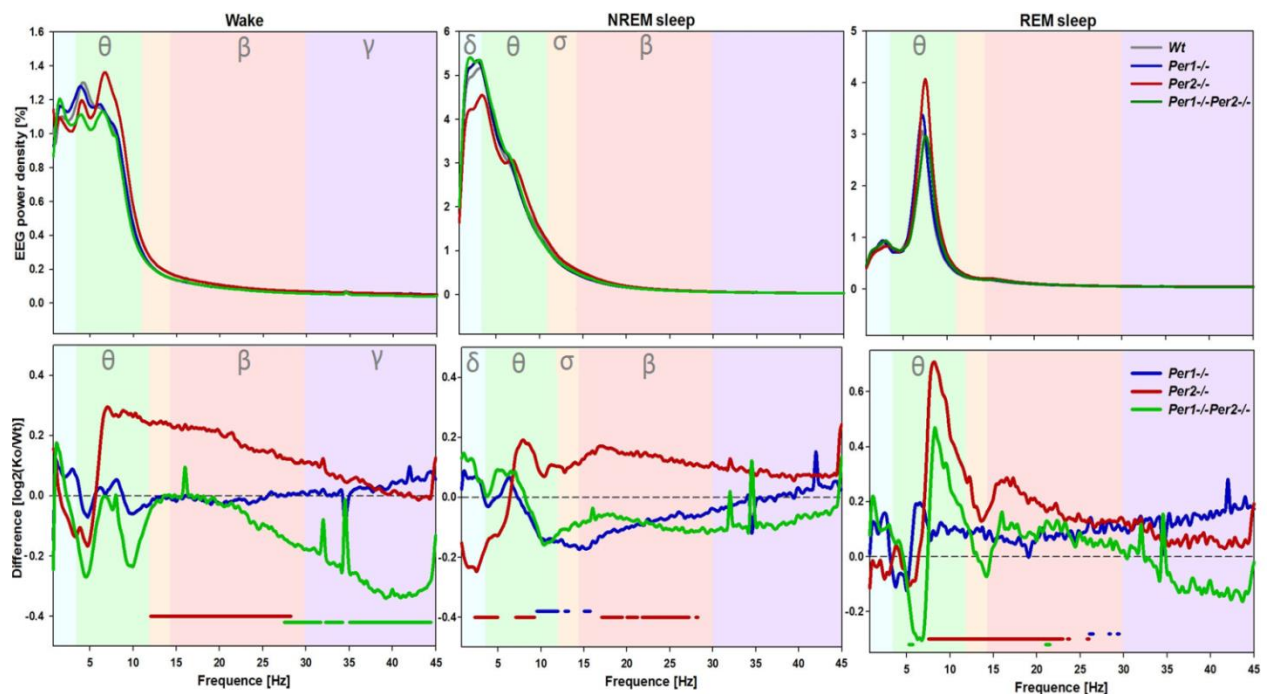


Figure 37 EEG spectral profiles of 48h baseline for each genotype. Upper panels EEG spectral profiles under 48h baseline conditions averaged for all 4s epochs scored as Waking (Left), NREM sleep (Middle), or REM sleep (Right) for *Per1*^{-/-} (n=10), *Per2*^{-/-} (n=9), *Per1,2*^{-/-} (n=9), and Wt mice (n=21). Lower panel Average EEG spectra normalized to total EEG power. Significant genotype differences are indicated by colored bars ($p < 0.05$, by t-tests). Spectral differences as percent change for *Per1,2*^{-/-} versus Wt mice (in γ range for waking state) and more especially in *Per2*^{-/-} versus Wt mice (in all vigilance state). The reference is statistically similar for each genotype permitting the statistical comparison between them (see material and method).

Concerning the NREM sleep EEG, only *Per2*^{-/-} mice showed consistent deviations from Wt mice having a decrease in δ range (2-4Hz). δ oscillations are typical of deeper stages of NREM sleep and reflect the sleep homeostatic process [26]. Moreover EEG activity in the β range was increased in *Per2*^{-/-} mice. These two EEG effects combined with their fragmented NREM sleep point a more superficial NREM sleep and increased cortical arousal. Note that unusual higher β activity during NREM

sleep is also characteristic of NREM sleep in humans suffering of primary insomnia often attributed to increased cortical arousal [50].

Per2^{-/-} mice has significant spectral differences in REM sleep. However, together with *Per1,2*^{-/-} mice had not important changes in the θ range. In rodent, these frequencies were generated within the hippocampal network [311]. Nevertheless in both *Per2*^{-/-} and *Per1,2*^{-/-} mice the peak in theta activity was faster than in Wt mice ($p < 0.001$, $p = 0.005$ respectively by t-test). These delays were responsible of the huge spike in the ratio graphic.

h. *Per2*^{-/-} and *Per1,2*^{-/-} mice sleep less after a sleep deprivation

To study the implication of *Per* genes in the sleep homeostasis, we investigated the response to 6h of sleep deprivation (from ZT0-6) both in terms of sleep intensity and duration. In this section, I analyzed the impact on time spent asleep. Both amount and distribution of NREM and REM sleep were differently affected by the SD according to the genotype (1-way ANOVA, factor 'genotype', $p < 0.05$; 2-way ANOVA, factors 'genotype' and 'ZT'; interaction: $p < 0.001$). The effects of SD on NREM and REM sleep in *Per1*^{-/-} mice did not differ from the observed in Wt mice. In both genotypes both NREM and REM sleep increased from the end of SD and were predominant until the end of the recovery light period, then minimum level was reached followed by a second increase from the 3rd hour of the dark recovery period, to finally decrease again before the dark-light transition (Fig.38A,B). Moreover the NREM and REM sleep amount between *Per1*^{-/-} and Wt mice did not differ (table 8). To better appreciate the recovery dynamics, I determined the hour-by-hour accumulation of the recovery-to-baseline differences in sleep amount after the SD (Fig.38C,D). This analysis revealed that despite differences in distribution of sleep in baseline and during recovery between *Per1*^{-/-} Wt mice their respective recovery patterns overlapped, indicating that lack of *Per1* does not affect the homeostatic regulation of sleep duration.

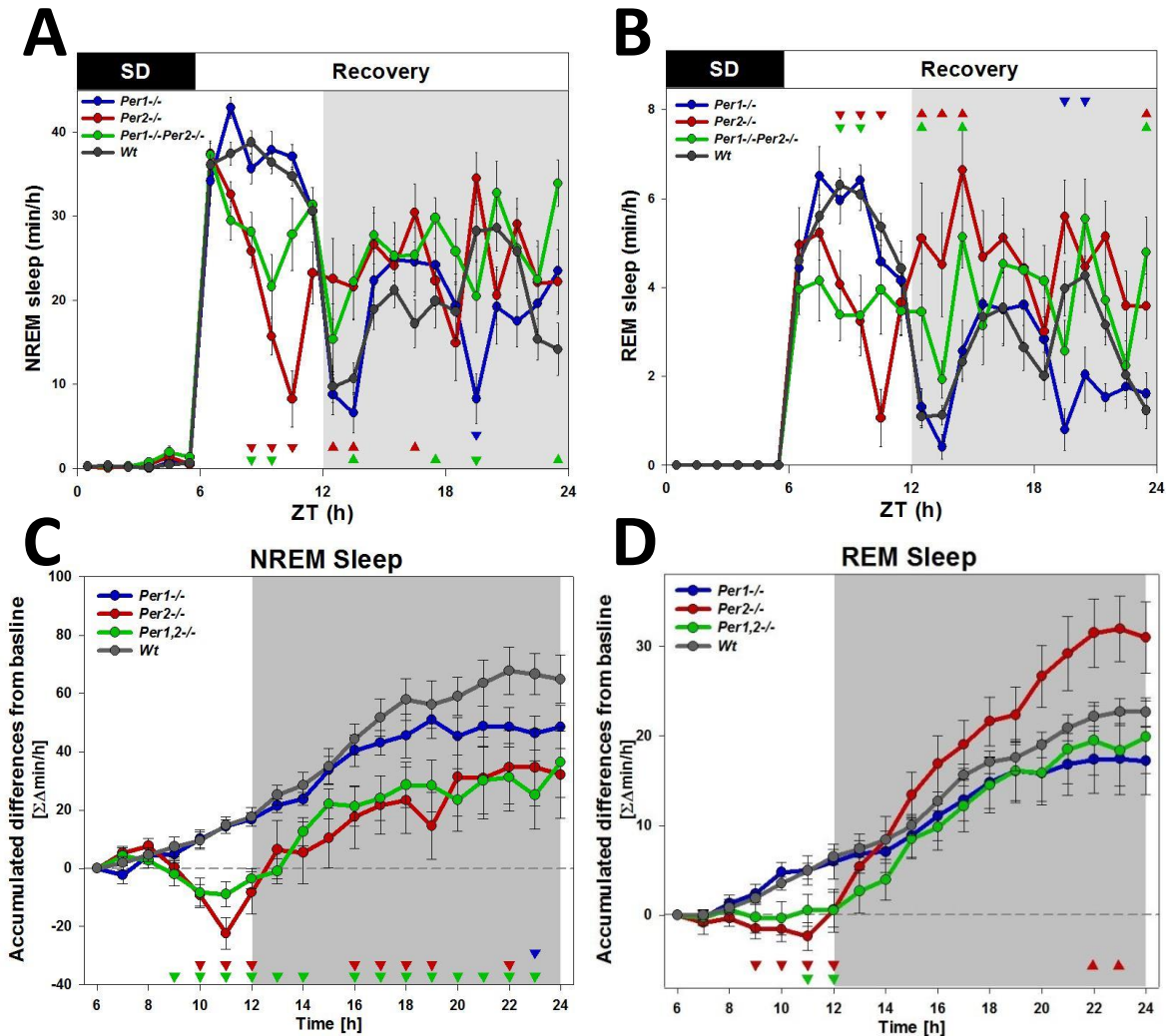


Figure 38 Effect of 6 hours of sleep deprivation (SD) on sleep in *Per* knock-out mice. **A,B.** Effects of SD on NREM sleep (A) and REM sleep (B) in *Per1*^{-/-}, *Per2*^{-/-}, *Per1,2*^{-/-} and Wt mice. Each point is the mean value in minute \pm SEM for 1h intervals. 2-way ANOVA, factors 'genotype' and 'ZT'; interaction: $p < 0.001$. \blacktriangle or \blacktriangledown : $p < 0.05$ with Holm-Sidak as post-hoc test between knock-out and Wt mice. **C,D.** Accumulation of recovery-baseline differences in NREM sleep (C) and REM sleep (D) starting at ZT6 (the end of the SD) and calculated with 1h increments for 18h. Each point is the mean difference \pm SEM. \blacktriangledown : $p < 0.05$ by t-test between knock-out and Wt mice. Number of used mice: *Per1*^{-/-} (blue, $n=10$), *Per2*^{-/-} (red, $n=9$), *Per1,2*^{-/-} (green, $n=10$) and Wt (dark grey, $n=21$).

Lack of *Per2* did affect the recovery dynamics of time spent asleep. In the first 5h of recovery sleep *Per2*^{-/-} and *Per1,2*^{-/-} mice accrued *less* NREM and REM sleep compared to corresponding hours in baseline or, in other words, during the recovery light period animals further increased their sleep debt. For instance at ZT11 *Per2*^{-/-} mice accumulated an extra deficit of $22.4\text{min} \pm 5.5$ of NREM sleep compared to their own baseline and $35.9\text{min} \pm 4.1$ compared to Wt mice (Fig.38C). This was confirmed by smaller total amount of NREM and REM sleep both in *Per2*^{-/-} and *Per1,2*^{-/-} mice compared to Wt mice ($p < 0.001$; table 8) during the light recovery period. From ZT11 onwards, *Per2*^{-/-} and *Per1,2*^{-/-}

		<i>Per1</i> ^{-/-}	<i>Per2</i> ^{-/-}	<i>Per1,2</i> ^{-/-}	Wt
light period recovery	Wake [min]	110 (4)	195 (8) ↗	162 (6) ↗	114 (3)
	NREM [min]	218 (5)	143 (7) ↘	176 (5) ↘	214 (3)
	REM [min]	32 (2)	22 (3) ↘	22 (2) ↘	32 (1)
dark period recovery	Wake [min]	476 (15)	374 (11) ↘	368 (7) ↘	461 (12)
	NREM [min]	219 (14)	291 (9) ↗	307 (8) ↗	228 (10)
	REM [min]	26 (2)	56 (4) ↗	46 (3) ↗	31 (2)
all recovery period	Wake [min]	586 (15)	567 (15)	530 (9) ↘	575 (11)
	NREM [min]	437 (15)	433 (13)	482 (9)	442 (10)
	REM [min]	58 (4)	78 (6) ↗	68 (4)	63 (2)

Table 8 Summary table of sleep-wake state amounts during the recovery (in min) for the 6h light period, 12h dark period, and 18h for all genotypes. The mean of two days was used (SEM). 1-way ANOVA: factor 'genotype' for Wake, NREM sleep and REM sleep: p<0.001. ↘ or ↗: p<0.05 with Holm-Sidak as post-hoc test between knock-out and Wt. Number of mice used: *Per1*^{-/-} (n=10), *Per2*^{-/-} (n=9), *Per1,2*^{-/-} (n=10) and Wt (n=21).

mice gain extra NREM sleep but the recovery curves ran largely in parallel to that of Wt mice indicating that this initial extra loss was not compensated for thereafter. Moreover, both *Per2*^{-/-} and *Per1,2*^{-/-} mice expressed higher levels of NREM and REM sleep amount compared to Wt mice in the dark recovery period (p<0.001 ; table 8). Interestingly, REM sleep seemed to be compensated to a larger extent in *Per2*^{-/-} mice specifically with significant difference reaching at ZT22-23. In absolute terms *Per2*^{-/-} mice spent 1.8-fold more REM sleep in the recovery dark period as compared to Wt mice. This increase was so large that REM amount of all recovery period remained higher *Per2*^{-/-} compared to Wt mice (p=0.01 ; table 8). These results support the notion that *Per2* is needed to adequately compensate the loss of NREM sleep after SD.

i. Homeostatic control of EEG delta power seems not affected by a lack of *Per2*

Above I showed that mice lacking *PER2* had impaired homeostatic regulation of NREM sleep duration. Here, I analyzed the impact of the SD on another aspect of NREM sleep homeostasis; i.e., the sleep intensity. I quantified the intensity or depth of NREM sleep by calculating EEG delta power. Most of the variance in the changes in EEG delta power can be explained by the sleep-wake distribution [48]. EEG delta power during NREM sleep is high after periods of extended waking and SD, and decreased during intervals where NREM sleep is prevalent [46]. In all four genotypes, EEG delta power decreased progressively from the beginning of the light period at ZT0 in baseline to the light-dark transition and then increased to reach the maximum level during the dark period (Fig.39). After the SD, EEG delta power reached the highest level and then decreased in an exponential manner. Despite the general similarity among genotypes, the time course of EEG delta power (2-way ANOVA, factors 'genotype' and 'ZT'; interaction: p<0.001) as well as the EEG delta power quantified immediately dur-

ing the first 20min after the SD differed, among genotypes (1-way ANOVA, factor 'genotype', $p=0.027$). Small but significant changes ($p<0.05$ with Holm-Sidak as post-hoc, Fig.39) were observed in $Per1^{-/-}$ mice compared to Wt mice for the last two intervals the both dark periods. These statistical differences could be explained by difference sleep/wake distribution because Wt mice obtained more NREM sleep during the preceding 3h (i.e. the 'nap'; Fig.38A).

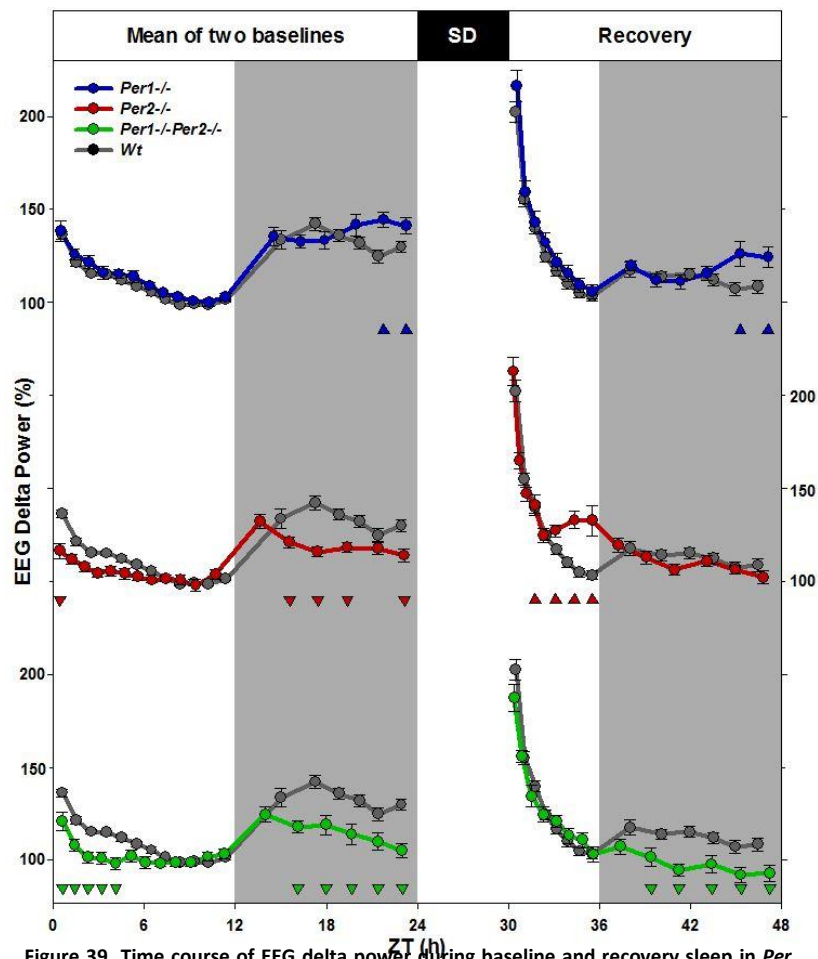


Figure 39 Time course of EEG delta power during baseline and recovery sleep in *Per* knock-out mice. Mean time course of delta power (1-4Hz) in $Per1^{-/-}$ (blue, $n=10$), $Per2^{-/-}$ (red, $n=9$), $Per1,2^{-/-}$ (green, $n=10$) and Wt (dark grey, $n=21$) mice in baseline (ZT0-24, average of 2 baseline days), SD (between 24-30h) and in the recovery (from 30-48h). Values represent mean absolute values \pm SEM calculated over 12-, 6-, 8- NREM sleep-time percentiles in the baseline light period, both dark periods, and recovery light period, respectively. 2-way ANOVA, factors 'genotype' - 'ZT'; interaction: $p<0.001$. ▲ or ▼: $p<0.05$ with Holm-Sidak as post-hoc test between knock-out and Wt mice.

A previous study done with same $Per1$ knock-out mice on the same genetic background showed that after 6h of SD, EEG delta power of $Per1^{-/-}$ in the first hour of the recovery was lower than Wt mice (Fig.40) [203]. In opposite, another study under 129S4/SvJae background seemed to have an higher delta power in $Per1^{-/-}$ compared with Wt mice, however no statistic was done to confirm (Fig.40)

[201]. Changes in delta power of *Per1*^{-/-} mice were not observed after SD in the current experiment. Moreover, the EEG delta power during the first 20min after the SD did not differ from the Wt mice (p=0.4 with Holm-Sidak as post-hoc test).

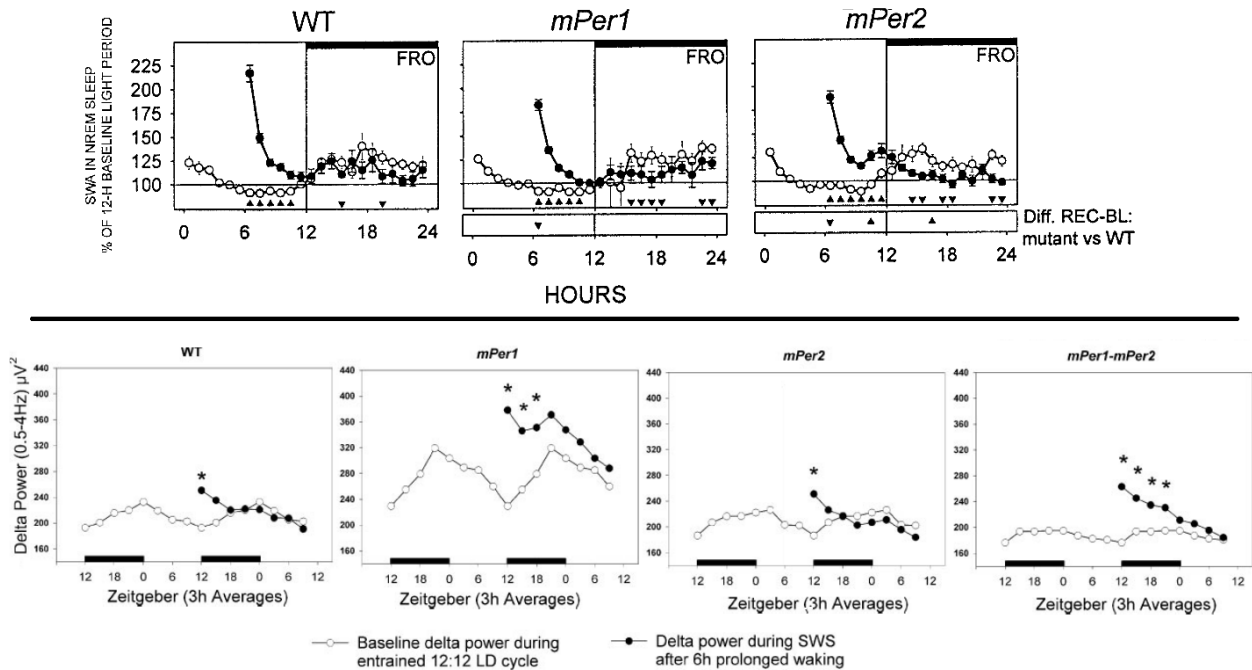


Figure 40 Upper panel: Effects of 6-h sleep deprivation (SD) on slow-wave activity in NREM sleep (SWA in NREM sleep; mean EEG power density in the 0.75±4.0 Hz band) in the frontal (FRO) for the baseline (BL) and recovery (REC) for *mPer1* mutants (n = 10), *mPer2* mutants (n = 12) and WT (n = 7). Mean 1-h values ± SEM. In the 6-h interval of recovery in the light period, rANOVA interaction between factors 'condition' (BL, REC) and '1-h interval' (1-6) was P < 0.0001 in frontal derivations for all genotypes. Triangles below the curves indicate significant differences between conditions for the corresponding interval (P < 0.05, two-tailed paired t-test). ANOVA interaction between factors 'genotype' (*mPer1* mutants, *mPer2* mutants, WT) and '1-h interval' (1-6) for the effect of sleep deprivation (difference REC-BL) was P < 0.05 for both derivations. Triangles in the lower panels indicate significant differences between mutant and WT mice in the frontal derivation (P < 0.05, Duncan test). Adapted from Kopp C. *et al.* (2002) [203] **Upper panel:** Electroencephalogram (EEG) delta power (0.1–3 Hz) during SWS in WT and *mPer* mice. Delta power during the entrained LD cycle (white dots) is double-plotted to illustrate the rise and fall of delta power during the dark and light periods, respectively. Black dots, Delta power after 6-h prolonged waking. In all of the genotypes, there was a significant increase in delta power after the 6-h prolonged waking compared with their respective entrained values. *P < 0.05 vs. white dots. Adapted from Shiromani P.J. *et al.* (2004) [201]

EEG delta power in both *Per2*^{-/-} and *Per1,2*^{-/-} mice was lower than Wt mice over most of the baseline dark period. Again this likely to be consequence of the difference in the sleep-wake distribution because mice lacking *Per2* how sleep more during this period (Fig.38A). *Per2* knock-out mice as well as the double knock-out mice responded as Wt mice in the first hours of the recovery following the SD, contrasting with a previous study showing a lower delta power for *Per2*^{m/m} (Fig.40) [203]. Additionally, EEG delta power quantified during the first 20min after the SD did not differ from both *Per2*^{-/-} and *Per1,2*^{-/-} mice as compared to the Wt mice (p=0.722 and p=0.052, respectively with Holm-Sidak as post-hoc test). However, the higher delta power in *Per2*^{-/-} mice at the end of the light recov-

ery period was found in both the previous [203] and the present study and can be explained by the pronounced difference of 71min in NREM sleep in the recovery light period as compared to Wt mice (table 8). These results suggest that the homeostatic sleep intensity was not affected by PER2.

j. Missing a central clock gene, *Per2*^{-/-} react in the same way to a sleep deprivation at molecular level in the cerebral cortex

Above I have presented and discussed the effects of the lack of *Per* genes on the behavioral and electrophysiological aspects of sleep homeostasis. Here I focus on the molecular aspects of sleep homeostasis in mice lacking *Per2* by quantifying steady state mRNA levels in the cerebral cortex of the clock genes *Per1*, *Per2*, and *Cry1* as well as a widely used clock controlled gene *Dbp*. The mRNA levels of these four genes are known to be activated by the BMAL1::CLOCK/NPAS2 and inhibited by CRY::PER [158]. Moreover *Per1*, *Per2* and *Dbp* are known to be altered by sleep loss [26, 250-252]. I also quantified *Homer1a* expression which reliable reflects the sleep homeostat at a molecular level [45, 48]. Expression levels were quantified at ZT6 in animals that were kept awake in the 6 preceding hours and in animals that were left undisturbed and could sleep *ad lib* (Fig.41).

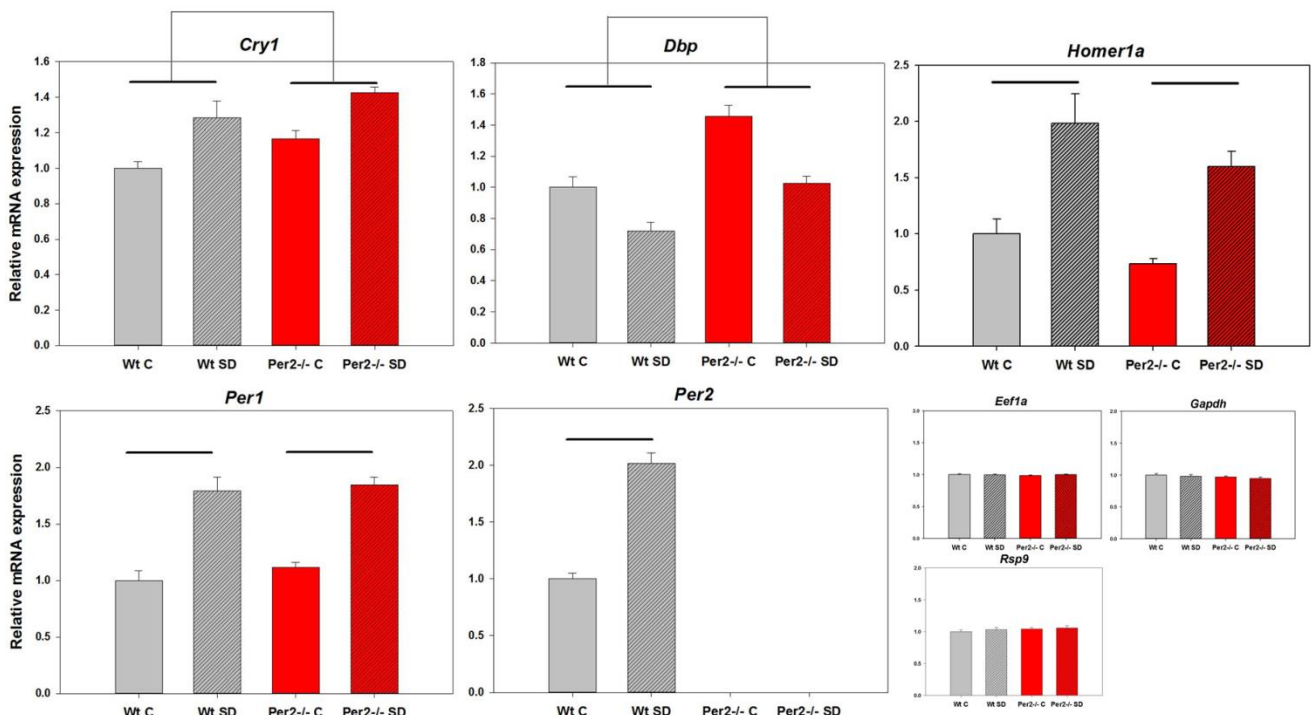


Figure 41 Effect of 6 h sleep deprivation (SD) on mRNA level in the cortex of *Per2*^{-/-} and Wt mice. Relative expression of *Cry1*, *Dbp*, *Per1*, *Per2*, *Homer1a* and the house-keeping genes *Eef1a*, *Gapdh* and *Rsp9* in the cerebral cortex of *Per2*^{-/-} (in red) and Wt (in grey) mice measured by qPCR at ZT6 in control condition (C, open bars) or after 6h of SD at ZT6 (hatched bars), n=5 for each group expect for Wt SD that n=4. 2-way ANOVA, factors 'genotype' and 'SD'. There was a genotype effect for *Cry1* ($p < 0.01$) and *Dbp* ($p < 0.001$). SD revealed a significantly increase of *Cry1*, *Per1*, *Per2* and *Homer1a* expression, and a decrease for *Dbp* ($p < 0.01$ with Tukey as post-hoc test). There was no significant difference for the house-keeping genes.

Wt mice showed the expected response to the SD: *Per1*, *Per2* and *Homer1a* increased, while *Dbp* decreased [48, 192]. The effects of SD on *Cry1* were none or modest according to the literature [48, 195], however we found a statistically increase. The relative change after SD did not differ with genotype (no interaction with 2-way ANOVA, factors 'genotype' and 'SD/C'). SD had the same effect on *Per2*^{-/-} mice; i.e., an increase for *Cry1* ($p < 0.01$ with Tukey as post-hoc test), *Per1* ($p < 0.001$) and *Per2* ($p < 0.001$); and a decrease for *Dbp* ($p < 0.008$). As expected, *Per2* was not detected in *Per2*^{-/-} mice, while *Homer1a* ($p < 0.01$) increased independently of the genotypes after the SD. So, both the electrophysiological (EEG delta power) and the molecular correlates of sleep homeostasis seem not to depend on PER2. These data represent the time-point collected immediately after SD, however maybe long-term effects could be revealed such as NREM sleep time homeostasis showed before.

A genotype effect between Wt and *Per2*^{-/-} mice for *Cry1* and *Dbp*, (respectively $p < 0.01$ and $p < 0.001$ with 2-way ANOVA, factors 'genotype' and 'SD/C') was observed. The general level expression was higher independently of the condition for these genes in *Per2*^{-/-} mice compared to Wt mice. These higher levels in gene expression could be due to the absence of PER2 which acts as a suppressor of BMAL1::CLOCK/NPAS2 induced transcription. Alternatively, the analyses presented above show that under LD12:12 conditions clock gene expressions were advanced by *circa* 2h (Fig.32). However that would predict higher levels for *Per1* too, which we did not observe here as well as in the previous results at ZT6 in the figure 32. This is perhaps due to the reduction in the amplitude of *Per1* transcript oscillation in mice lacking functional PER2 [197, 199].

In parallel to this experience, I tested if food had an impact on the RNA expression in the cerebral cortex because during sleep deprivation animals might eat more and feeding is known to change the timing of clock gene expression at least in the liver and also in the brain [103]. To analyze this effect I sleep deprived mice with and without access to food that I compared them to their non-sleep deprived control mice (Fig.42).

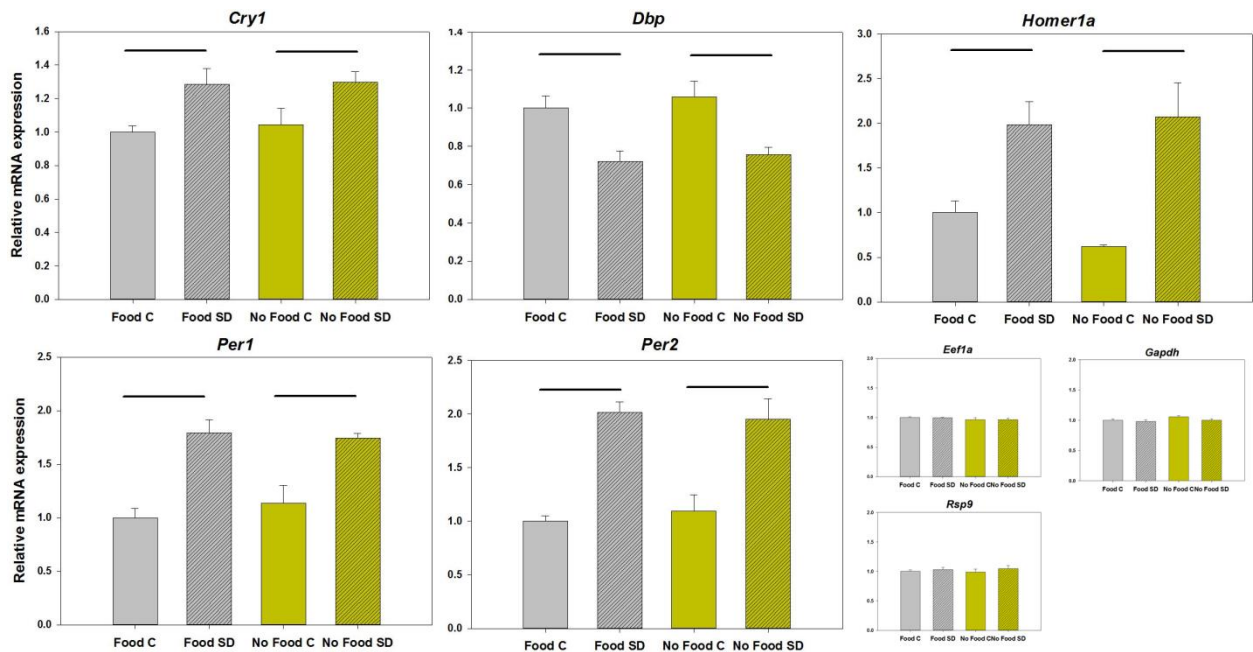


Figure 42 Effect of 6 hours of sleep deprivation (SD) on mRNA level in the cortex of Wt mice with or without access to food. Relative expression of *Cry1*, *Dbp*, *Per1*, *Per2*, *Homer1a* and the house-keeping genes *Eef1a*, *Gapdh* and *Rsp9* in the cerebral cortex of Wt mice with food ad libitum (in grey) or without food (in yellow) measured by qPCR at ZT6 in control condition (C, in blank) or after 6h of SD at ZT6 (in hatched), n=5 for Food C, n=3 for No Food C and n=4 for both Food and No Food SD. 2-way ANOVA, factors 'Food/No Food' and 'SD/C'. There was no food effect between the conditions, however there is a SD effect for *Cry1* ($p < 0.05$ with Tukey as post-hoc test), *Dbp* ($p < 0.01$), *Per1* ($p < 0.01$), *Per2* ($p < 0.001$), and *Homer1a* ($p < 0.02$). There was not significantly effect on the control genes.

Food availability did not modify the effect of SD (with 2-way ANOVA, factors 'genotype' and 'Food availability', no interaction); *Cry1*, *Per1*, *Per2* and *Homer1a* increase ($p < 0.05$, $p < 0.01$, $p < 0.001$, $p < 0.02$, respectively) and *Dbp* decreased ($p < 0.01$) after the SD in both conditions. Thus food seems to do not play a role in the effects of sleep loss on clock gene expression.

4. Conclusions and perspectives

In this section of my doctoral work we first performed a in depth characterization of circadian rhythmicity at the behavioral level using locomotor activity recordings and the molecular level quantifying clock gene expression in the cerebral cortex in *Per2*^{-/-} mice, and *Per1*^{-/-} mice, as well as their double knock-out offspring (*Per1,2*^{-/-}) and littermate wild-type (Wt) mice. The second and main aim of this project was to analyze the effects of these two Period genes on the homeostatic regulation of sleep at the behavioral (sleep and waking), electrophysiological (EEG) and molecular levels. I will discuss the results according these two main aims; i.e., circadian characterization and sleep regulation.

a. Circadian characterization

Under constant dark (DD) condition we showed that *Per1*^{-/-} mice had a somewhat shorter period compared to Wt, while 94% *Per2*^{-/-} and all *Per1,2*^{-/-} mice became immediately arrhythmic. While in previous reports *Per2*^{-/-} mice remained initially rhythmic under DD but then lost rhythms in locomotor activity we here, surprisingly observed the opposite; *Per2*^{-/-} female mice rhythmicity could be reinstated by an event not yet fully understood both with respect to the triggering event and to the sex specificity of this event. These results suggested that PER2 was able in large part to substitute the lack of PER1 with minor changes, while PER1 can substitute PER2 only under very specify condition. This instability in the clock machinery, place *Per2*^{-/-} mice at the border of arrhythmicity depending on conditions and sex. We also showed that under LD12:12 conditions, earlier onset were noted in *Per2*^{-/-} mice at behavioral (i.e., wake onset), physiological (i.e., corticosterone levels) and molecular levels (i.e., clock gene and *Homer1a* expression). We demonstrated that this earlier onset is probably not reflecting a true circadian entrainment but, instead, results from a light-driven rhythm of short period that is reset each day and linked to light onset.

Per2 construct comparison

Our findings demonstrate that our full null-*Per2* knock-out (*Per2*^{-/-}; i.e., *Per2*^{tm1Ccl}) mice had a stronger circadian phenotype as previous *Per2* mutant (*Per2*^{tm1Brd} and *Per2*^{tm1Drw}) mice studies [197, 199]. Indeed we observed an immediate arrhythmicity when put in DD, than *Per2*^{tm1Brd} mice on a

129S7/SvEvBrd x C57BL6 mixed background from 2-18 days to lose its circadian rhythm [199], while *Per2^{tm1Drw}* on a C57BL/6J background had a circadian rhythm with a period similar to Wt mice [312]. Moreover the triple *Per1,2,3^{tm1Drw}* knock-out mice on a C57BL/6J background possessed also an early activity onset of about 2h under standard LD12:12, as well as an early activity onset of about 5h before the dark onset in LD18:6 and were immediately arrhythmic under DD [313]. This phenotype was strikingly similar to our *Per2^{-/-}* mice. Given the fact that the *Per2^{tm1Drw}* and *Per1,2,3^{tm1Drw}* lines were backcrossed to the same genetic background than ours, we can conclude that it is a difference in the *Per2* construction. *Per2^{tm1Drw}* mice are a widely used appearing in 26 studies, and the last published example dates from June 2013 [314]. However, *Per2^{tm1Drw}* mice have the least severe phenotype compared to both *Per2^{tm1Ccl}* and *Per2^{tm1Brd}* mice, and might express a truncated PER2 lacking only 107 residues (corresponding to a fragment of the PAS domain). Therefore, *Per2^{tm1Drw}* mice cannot be considered as a true knock-out, and the statements on PER2's function reported in the literature using this strain are likely not accurate. Concerning the phenotype differences between *Per2^{tm1Brd}* and our mice could be explained by both differences in the construct and genetic background.

Early onset at behavioral, molecular and physiological level in *Per2^{-/-}* mice

Another obvious and reproducible feature unique to the *Per2^{-/-}* genotype concerned their entrainment under LD12:12 conditions. The onset of both waking and activity was earlier than in the other 3 genotypes and occurred 2.0h and 1.4h prior to dark onset, respectively. We revealed using EEG analysis that wakefulness onset for *Per2^{-/-}* mice occurred at ZT9.9±0.2 under LD12:12, while activity onset 43min later. It's possible that this difference in onsets is due to a partial masking effect of the light. Other genotypes did not show a statistical difference between wakefulness and activity onset. *Per2^{-/-}* mice waking state seems to be more pronounced and differently timed than the locomotor activity and this difference could be even more important when relying on running wheels, because mice could be awake and active (such as feeding, drowsing, grooming) without using wheels. Thus activity onset does not imply that subject was not awake before, and circadian researchers that usually associated wake with activity had to take into account. It is important to note that waking is more accu-

rate measure reflecting SCN effects on behavior, while locomotor activity is just one behavior expressed during waking.

We also revealed that gene expression of *Bmal1*, *Npas2*, *Per1*, *Cry1*, *Cry2*, *Dbp* and *Homer1a* as well as plasma corticosterone levels in *Per2*^{-/-} mice were advanced by 2h. We showed that if *Per2*^{-/-} data curves were delayed by 2h, surprisingly almost RNA curves and corticosterone fitted statistically with those obtained in the Wt mice. In addition, it seemed that the changes in *Per1*, *Cry1* and corticosterone in *Per2*^{-/-} mice were lower in amplitude compared to Wt. To confirm this assumption, a complete 24h time-course should be performed. Nevertheless, a smaller amplitude of the *Per1* oscillation was also observed in *Per2*^{tm1Brd} mice on a 129S7/SvEvBrd x C57BL6 background [199], and both *Per1* and *Cry1* as well as PER1 and CRY1 oscillation were attenuated in *Per2*^{tm1Drw} in 129S4/SvJae background [197]. However in these studies, both genes and proteins expression were not delayed in SCN. Conversely, another study showed that *Per1* was advanced by about 3-6h in the SCN of *Per2*^{tm1Brd} mice on a 129S7/SvEvBrd x C57BL6 mixed background [315]. An interesting follow-up experiment would be to quantify core clock gene expression in SCN of our *Per2*^{-/-} mice to know if *Per2* is involved in phase advancing at the SCN level too. This raises the possibility to study the link at the molecular level between masterclock and peripheral clock.

A method to verify if light-driven oscillations are regulated through the SCN would be to put *Per2*^{-/-} mice under DD, and then put them back in LD. Clock gene expression in both SCN and peripheral tissues as cerebral cortex could be quantified in a time-course manner, expecting that clock gene expression will be flat before the light onset. Such experience could confirm the role of *Per1* in the light-induction and tell us more about where and which others genes are first induced.

Entrainment or masking effect

The apparent rhythmicity observed in our *Per2*^{-/-} mice at both behavioral and molecular levels under LD12:12, raises the issue whether to use “entrainment” or “masking effect”. Masking refers to disruption in the expression of overt rhythms caused by an external agent such as light without a directly effect on the period underlying the circadian pacemaker. For instance, a nocturnal animal avoids

moving under light, then if lights-off were to be delayed, the activity onset of this animal will be delayed too [101]. On the other hand, a short period of darkness during the light period will induce wakefulness [316]. These are thought to be direct effects of light that are not thought to be mediated by the circadian clock. In our case, this masking effect seem not to be applicable, in fact, there is no need to assume the locomotor behavior was driven by factors other than the clock mechanism. After all, we showed that other clock gene expression in *Per2*^{-/-} mice continues to change in a circadian-like manner. Moreover, they became active despite the light. However, the entrainment term (synchronization of a self-sustaining oscillation by a forcing Zeitgeber oscillation) also seems inappropriate because behavioral rhythmicity was totally abolished in *Per2*^{-/-} mice under DD. Then the more appropriate term is “light-driven”. It was shown that light exposure is able to induce expression of *Per1* and *Per2* (but not *Per3*) in the SCN [214, 215, 317], then probably trigger the molecular rhythmicity. Our experiment showed that *Per1,2*^{-/-} mice seems not to be light-driven, because they just follow the light dark cycle and all of them became directly arrhythmic under DD suggesting the absence of functional molecular rhythm. Given the fact that *Per1* is directly induced in the SCN after a light pulse of 5-15min [128], and that *Per1* induction in the SCN is required for light-induced phase shifting in mice [127], we thought that light-driven rhythm is mediated through *Per1*. To summarize, it seems that *Per1* is sufficient to initiate the molecular oscillation *via* light induction in our *Per2*^{-/-} mice, but *Per2* is needed to maintain rhythmicity over more cycle.

Cry1,2^{-/-} mice share several phenotypes with our *Per2*^{-/-} mice. They possessed an early onset at about ZT9 under LD12:12 [318] and are behaviorally and molecularly arrhythmic when kept under DD [164, 196]. To my knowledge Vitaterna and colleagues were the first to propose the concept of a light-driven rhythm [196]. Given the fact that both *Per2* and *Cry1,2* genes act at the same level as negative regulator of the clock machinery at the molecular level, the similar circadian phenotype between them are striking. Additionally, they noted that *Cry1,2* genes differentially influenced *Per1* and *Per2* transcription and suggested that then these two genes have non-redundant functions [196]. Surprisingly, *Cry1,2*^{-/-} mice on *Per2*^{-/-} and *Per1,2*^{-/-} animals had diametrically opposed sleep pheno-

types; *Cry1,2^{-/-}* mice had altered EEG delta power and increased consolidation of NREM sleep [191].

Entrainment under LD11:11

We showed that *Per2^{-/-}* mice are incapable of generating self-sustained rhythms under LD12:12. We then raised the question whether *Per2^{-/-}* mice might be able to stably entrain to a short 22h day schedule (11h light, 11h dark; LD11:11) better matching the period observed in one male (21.1h), seven females (21.9h±0.2), and the short period reported in the literature [199]. An ongoing experiment using running wheel showed that *Per2^{-/-}* mice (n=13) adapted perfectly to the new schedule with an activity onset set at ZT12.15±0.0, i.e., 10min after the dark onset, while four Wt mice had a large variability in activity onset (ZT13.02±1.33) and two free-ran under these conditions. More surprising, *Per2^{-/-}* mice remained rhythmic when released into DD, while majority of these mice (n=5/6) became subsequently arrhythmic under DD following LD12:12 as in the main experiment. This suggests that an entrainment corresponding to the period 22h could have a lasting impact on the stability of the *Per2^{-/-}* mice molecular clock, whereas a T-cycle with too long period has a destabilizing effect. A following experiment to confirm this T-cycle influence on the clock machinery would be to compare clock gene expression under LD12:12 and LD11:11 and also when release under DD.

*Red dim light, a potential factor of the rhythmicity reinstatement in *Per2^{-/-}* female*

In contrast to males, *Per2^{-/-}* females rhythmicity can be triggered under DD but the key trigger is unknown. A first possibility is the short exposure (max. 5min) to red dim light associated with opening the recording cabinets during DD for health status verification although mice are considered 'blind' to red light. Several publications have shown that dim red light can impact locomotor activity rhythms in mice adapted to DD conditions [101, 319]. Moreover, it was shown that arrhythmic *Per2^{tm1Brd}* mice in 129S7/SvEvBrd x C57BL6 mixed background under DD could have similar rhythmicity reinstatement using 6h white light pulse [199]. Taken together, that let us suppose that dim red light could be the triggering factor of this circadian reinstatement in our *Per2^{-/-}* female mice. It is well

known that there are differences between male and female concerning the vigilance state (e.g. higher locomotor activity in the females, different regulation of REM sleep time and NREM sleep need) [194]. However to be able to sustain circadian rhythm in DD, females have something more than male, perhaps it is due to an effective color vision in females as in human [320] or more probably due to the estrus cycle phase and its specific hormones in females. However, primary female sex hormone estrogen was able to delay the phase and increased the amplitude of *Per1* in liver and kidney only but not in SCN and in the cerebral cortex [210]. Maybe the estrogen effect on the reinstatement of the circadian rhythmicity did not pass through *Per* induction, but by other way such as *Cry*. In fact, it was show that in rats that estrogen was able to modify *Cry2* expression (but not *Cry1*) in the SCN [321].

Rhythmicity reinstatement under DD

By chance we found that an event could trigger establishment of rhythmicity that was associated with checking the mice while kept under DD. The key trigger could be one of many; e.g., fresh food, noise, odor, dim red light. In some ways this triggering of rhythmicity is reminiscent of serum shock cultured cells which induced and synchronized rhythms in gene expression [322]. We are currently systematically investigating the effects of a dim red light pulse (625-30nm, 5min). We choose 5min, because it was the maximum time required in the previous experiment to verify the health status under DD using red dim light. Because mice do not have red cones like human, it is assumed that they are not able to respond to the red light input [323]. Moreover, several studies analyzed in depth the spectral sensitivity of the photoreceptors in mice and predicted no or minimal response to red light [324-326]. For these reason red dim light is widely used during DD to permit to easily check the mice, without disturbing them. Conversely, an impact of red light on rodent's circadian rhythmicity was shown in the 1980's. For instance, circadian running activity and luteinizing hormone secretion were shifted by a 2h red light pulse (> 650 nm) in rats under DD [327]. More recently, it was shown that constant dim red light (with a *light-emitting diode* (LED) at 652 nm) lengthens circadian period compared to constant darkness [319]. Thus although mice are not thought to see in the red wave-

length range, when adapted to for a long time to DD, they seem to be able to detect it. It is still unclear what cell type is responsible for responding to dim red light.

In a previous experiment using arrhythmic *Per2^{tm1Brd}* mice in 129S7/SvEvBrd x C57BL6 mixed background under DD, it was found similar rhythmicity reinstatement using 6h white light pulse [199]. The fact that only 5min of an “invisible” light has the same effect is very surprising. We hypothesize that after the red dim pulse *Per2^{-/-}* female mice will free-run with a short period of about 22h, while males will remain arrhythmic. Preliminary results indicate that our hypothesis is partially correct; following a 5min red light pulse, three arrhythmic female *Per2^{-/-}* mice regained rhythmicity with a short period ($21.5\text{h}\pm 0.2$), while two *Per2^{-/-}* mice were not affected. However, contrary to what we hypothesized, exposure to red light had the same effect on *Per2^{-/-}* males. Rhythmicity was established in three arrhythmic male mice with a period similar to the female ($21.6\text{h}\pm 0.1$), while two *Per2^{-/-}* mice were not affected. While more experiments need to be performed.

Sex difference effect on circadian rhythmicity strengths

Despite the fact that a lot of phenotypes (such as activity onset under LD, arrhythmicity under DD, period length as far as could be determined, etc.) were shared between *Per2^{-/-}* female and male mice, it seems that rhythmicity could be reinstated specifically in female suggesting a more robust circadian rhythm in females compared to males. This sex-effect deserves further investigation. The obvious physiological differences found between males and females are of course sexual hormones. Estrogens are a family of female sex hormones with an exceptionally wide spectrum of effects. To better study the effect of these hormone on mice, ovariectomy has commonly been performed to suppress the rapidly cycling hormone production from the estrous cycle and could be replaced by 17β -estradiol exogenously administrated [328]. Estrogen hormone could have also an impact on circadian rhythm through *Per* or *Cry* genes as it was shown that 17β -estradiol treatment in ovariectomized female rats was able to advance the peak of *Per2* expression in the SCN and to delay the phase and increased the amplitude of *Per1* specifically in liver and kidney, suggesting that estrogen effect on *Per* genes was tissue specific [210]. It has also been shown that 17β -estradiol modified *Cry2* ex-

pression, but not *Cry1* in SCN of ovariectomized female rats [321]. An interesting project would be to investigate if the sex differences in the circadian reinstatement behavior found in our *Per2*^{-/-} female were still present after ovariectomy and if 17β-estradiol administration could rescue the phenotype in female and could make more robust circadian rhythms in *Per2*^{-/-} male.

b. Sleep regulation analysis

Lack of *Per2* affected several aspects of sleep both under baseline and during recovery from a 6h sleep deprivation. In baseline the most salient feature was the increased NREM sleep fragmentation. In addition, and consistent with our main hypotheses concerning a role of *Per2* in sleep homeostasis, we observed a profound deficit in the compensatory response in NREM sleep duration during the first 5h of recovery from SD during which *Per2*^{-/-} mice expressed less sleep than during baseline. However, other aspects of sleep homeostasis such as EEG delta power its molecular correlate *Homer1a* were not altered.

Baseline

Quantification and consolidation analysis of NREM and REM sleep during baseline revealed that PER1 is not needed to maintain a normal sleep distribution and sleep integrity. On the other hand PER2 is required, because in both *Per2*^{-/-} and *Per1,2*^{-/-} mice NREM sleep is more fragmented, and *Per1,2*^{-/-} mice expressed more NREM sleep. This alteration in the sleep integrity was also found in other clock gene mutant mice such as *Bmal1*^{-/-} [190] and *Clock*^{m/m} mice [193]. While double *Cry1,2*^{-/-} knock-out mice had more consolidated sleep, more NREM sleep and longer NREM sleep episodes than Wt mice [191]. This suggests that several clock genes are involved in a specific manner in sleep consolidation. It was previously shown that animals rendered arrhythmic by lesioning the SCN had more fragmented sleep [22]. An intact circadian system is probably required to consolidate sleep. Moreover a human study shown that sleep at the wrong circadian phase decreased its quality [21]. From an evolutionary view, enabling sleep-wake consolidation represents then an adaptive advantage provided by the circadian system [329]. However more investigations were needed to understand this relationship.

What role could clock gene have in sleep homeostasis

Several studies demonstrated that clock genes play a role in sleep homeostasis [26]. Two previous studies assessed in mice lacking *Per1* and/or *Per2* gene concluded that knock-out mice did not show a homeostatic phenotype [201, 203]. Kopp and colleagues found a lower EEG delta power rebound in *Per1* and *Per2* single mutant mice 6h SD, but they proposed that EEG differences between mutants and Wt mice reflects behavioral differences during the extended waking episode rather than changes in the homeostatic sleep process [203]. Although not commented on by Shiromani and collaborators, *Per1,2* double-mutant mice EEG delta power seemed enhanced to a greater extent after sleep deprivation compared to Wt mice [201]. These results suggest an eventual functional implication of Period genes in sleep homeostasis. Because of the disparate results we here re-assessed this question using a null-mutant *Per2* mouse line. We quantified 3 different aspects of sleep homeostasis sleep duration, sleep intensity, and at the molecular level by clock gene quantification.

We observed the amount of NREM and REM sleep in the recovery are similar between *Per1*^{-/-} and Wt mice, while both *Per2*^{-/-} and *Per1,2*^{-/-} mice had a distinct phenotype. In the first 5h of recovery sleep these mice slept less than during baseline and thus further increase their sleep loss. Their actual recovery started in the last hour of the light period (ZT11) but the extra sleep obtained during the following dark did not make up for this later onset of recovery sleep indicating that this initial extra loss was not compensated for. Thus PER2 is necessary to adequately compensate for the loss of NREM sleep suggesting that PER2 at some level is needed to sense sleep need or to translate increased sleep need into the appropriate behavior; i.e., sleep. Interestingly, although initially also for REM sleep extra loss was accrued *Per2*^{-/-} mice subsequently compensated to a larger extent with significant difference reaching at ZT22-23. Higher REM sleep amount during baseline and its REM sleep over compensation during recovery was only found in *Per2*^{-/-} mice, suggesting a particular link between REM sleep regulation and PER2. Given the fact that double knock-out and *Per1*^{-/-} mice didn't show this phenotype, we can speculate that it is not a direct effect of PER2 but, instead, an effect of the shorter non-functional clock machinery present in *Per2*^{-/-} mice under LD12:12. To verify, this hy-

pothesis, sleep-wake distribution could be analyzed under LD11:11 conditions, where *Per2*^{-/-} mice seemed to be correctly entrained.

We observed that expression of *Cry1*, *Per1*, *Dbp* and *Homer1a* genes in both *Per2*^{-/-} and Wt mice respond in the same way to a sleep deprivation suggesting that the absence of PER2 did not modify the circadian machinery at the molecular level in response to higher sleep pressure. Moreover, quantification of the sleep-wake dependent dynamics of EEG delta power revealed that lack of *Period* gene had no influence on homeostatic sleep intensity. The time course of EEG delta power during baseline and recovery periods seemed to reliably follow the sleep-wake distribution within each genotype. Moreover, EEG delta power levels reached immediately after the end of the SD did not vary among genotypes. This let us conclude that EEG delta power dynamic is not altered by the lack of *Per1*, and/or *Per2*.

Another way to confirm that observed EEG delta power in our knock-out mice did not result in a more rapid or slow build-up of homeostatic sleep need during wakefulness compared to Wt mice, would be to perform a simulation analyze, a mathematical method that quantifies the relationship between the changes observed in delta power and the sleep-wake distribution for each genotype [46]. This method permits to separate the effects of sleep-wake patterns, which varied between genotypes, from the effects of different dynamics of EEG delta power [46]. Thereafter we could compare the simulated EEG delta power dataset *versus* the empirical EEG delta power dataset.

Many other clock mutant mice had impairment in the EEG delta power dynamics, such as *Bmal1*^{-/-} mice which EEG delta power just after 6h SD was lower than the Wt mice [190], or *Npas2*^{-/-} mice which dynamic of delta power increased slower than Wt mice [194] or *Cry1,2*^{-/-} mice in which the the need for sleep increased at a faster rate than Wt mice [191]. In contrast, despite the fact that EEG delta power of the *Clock*^{m/m} mice was lower than Wt mice in baseline, this mutant mice responded similarly to SD suggesting that homeostatic regulation of sleep intensity was not affected [193]. Contrasting with the almost of these sleep studies, our data revealed that lack of either PER1 and PER2 did not affect the dynamics of EEG delta power.

Usually sleep deprivation was performed between ZT0-6 in Wt mice corresponding to 1st half of the man sleep period, which SD have the larger impact on the sleep homeostasis. Perhaps this starting time-point from SD is not optimal for mice with early activity onset such as *Per2*^{-/-} mice. Thus an experience would be to initiate SD when delta power is at its maximum under baseline for *Per2*^{-/-} mice at about ZT15.

Although both *Per1* and *Per2* did not modulate the sleep-wake distribution dynamics of EEG delta power, we demonstrated that PER2 is involved in REM sleep regulation, NREM sleep consolidation and in the ability to adequately compensate a lack of both REM and NREM sleep. Then PER2, in contrast to PER1, seems to be implicated in these aspects of sleep homeostasis. This report shows that a modification on clock gene alters the sleep homeostasis specifically in term of duration, such as *Clock*^{m/m} and *Dbp*^{-/-} mice [193, 248]. Other clock mutant studies showed modification in term of sleep intensity or both. Although clock genes have a non-circadian role in sleep homeostasis, the story appears to be more complicated. All aspects of sleep homeostasis are not equally affected by an altered clock gene. Moreover these effects cannot be categorized for instance by mutation in clock gene of the positive (e.g. *Bmal1*, *Npas2*) or negative regulator (e.g. *Cry*, *Per*) of the circadian machinery. Both *Cry1,2*^{-/-} and *Per1,2*^{-/-} mice had similar circadian phenotype (see above), but with a specific altered sleep homeostasis.

c. Others remarks

Food effect

Food availability is thought to be a strong Zeitgeber in rodents. When food is offered *ad libitum*, mice and rats feed usually at night. However when food is restricted to a short period during light, they will adapt to the new condition developing an anticipatory locomotor activity before the food availability even in the light period. This food anticipatory phenomenon is effective even in mice with SCN lesions, demonstrating that it not depend on the SCN [330]. It was shown in C57BL/6 mice that food restriction confined to light period during several weeks altered *Bmal1*, *Clock* and *Per2* gene expression in the liver but had no effect in the hypothalamus [103, 331]. Same alteration was found in kid-

ney, heart, pancreas and cortex, but not in SCN [332, 333]. In short food intake at specific time could modify core clock gene oscillation in tissue specific manner [331, 334]. Then we raised the question if modification of gene expression after 6h of sleep deprivation is a direct effect of this sleep loss or a result of food availability, i.e., during SD mice could eat more compared to the sleeping control mice. Here we showed that food availability during SD had no impact on the changes in *Per1*, *Per2*, *Cry1* and *Dbp* gene expression in the cerebral cortex. These results did not call into question our sleep deprivation protocol and suggest maybe that it is not food intake that synchronizes circadian rhythm but hunger.

Background effect

A very general important point to highlight is the genetic background that had an influence on both sleep and circadian behavior. It was shown that genetic background in mice has a strong impact on the NREM sleep need. It was shown that both the dynamics of NREM sleep intensity (delta power) and NREM sleep duration are regulated with a large strain differences in mice [46]. The genetic background has an impact on the circadian phenotype too. For instance, as it was previously reported, *Per1*^{-/-} mice in 129S7/SvEvBrd background had a shorter period (22.6h ±0.2) [26] than in C57BL6/J background (23.4h ±0.1) shown in the present study. Another example is the *Per2*^{tm1Drw} on a 129S4/SvJae background that initially displayed a short period (23.0h±0.3) and became arrhythmic under DD condition [197]. This strong phenotype completely disappear when backcrossed onto a C57BL6/J background, these mice remained rhythmic with a normal period (data not shown) throughout DD [200]. That demonstrates that the genetic background could have a more important impact on the circadian phenotype and could modify the penetrance of a clock gene mutation. For these reasons, I would like to warn the reader to take particular attention to genetic background before to compare results between different studies, an important point often overlooked in the literature.

C57BL6/J is a widely used particular inbred strain that do not produce melatonin hormone [335, 336]. Melatonin is produced in the pineal gland with high day/night amplitude can be consid-

ered as a neuroendocrine hand of the clock. In fact, melatonin may provide a feedback loop to the circadian clock in the SCN and may serve the synchronization of peripheral oscillators. In the SCN, melatonin interacts with PACAP, a neuropeptide of the retinohypothalamic tract and suppresses indirectly the transcription factor CREB that activate *Per* transcription [336]. Mice with melatonin such as C3H/HeJ could affect a knock-out, and perhaps change the phenotype. A relevant example is the hypomorphic mutant *Clock^{m/m}* mice that a longer period in a C57BL6/J background [193], while this phenotype completely disappeared in a C3H/HeJ background [337]. Then an intriguing project implying very long period of backcrossing would be to put our *Per2^{-/-}* mutation on a C3H/HeJ background to study if melatonin could rescue our phenotype and improve the knowledge between this hormone the *Per* genes regulation. Another easier idea would be to directly administrate melatonin at about ZT24 (maximum plasma concentration [335]) to our mice.

VIII. Concluding remarks

Sleep is regulated by a homeostatic process that is activated by the loss of sleep and by a circadian process that determines the time-of-day when sleep occurs. These two processes are functionally and anatomically separated. However, this work underlines the idea that clock genes, which generate the circadian rhythm, are also involved in sleep homeostasis. My research is of both fundamental and clinically relevant, as many disorders are sleep associated.

In first part of my doctoral work, we presented the first and thus far only study that asses the changes in DNA-binding pattern of clock genes following sleep-deprivation. DNA-binding of NPAS2 and BMAL1 to *Per2* and *Dbp* E-box and E'-box elements was decreased after sleep deprivation suggesting that the sleep-wake state contributes to the circadian changes in DNA-binding and clock gene expression. However, the precise dynamic relationship between DNA-binding and mRNA expression, especially for *Per2*, remains elusive. Our results also suggest that part of the reported circadian changes in DNA-binding of core clock components in tissues peripheral to the suprachiasmatic nuclei could, in fact, be sleep-wake driven. In the second part of my doctoral work, we demonstrated that PER2 is involved in REM sleep regulation, NREM sleep consolidation and in the ability to adequately compensate a lack of both REM and NREM sleep after sleep deprivation. This last finding strongly suggests that sleep homeostasis, in term of duration, was in part regulated by PER2, while PER1 seems not to be involved. However, it was shown that at the molecular level PER1 could partially replace PER2, because even in the absence of PER2 all other clock genes were expressed in a circadian fashion. Given the fact that behavioral rhythmicity was totally abolished in *Per2*^{-/-} mice from the first day under DD, we proposed that *Per2*^{-/-} rythms under LD12:12 conditions are light-driven in a fashion different from masking.

Sleep and circadian rhythms are closely interconnected. Their subtle interaction allows us to stay awake and alert, despite the increase of sleep need accumulated throughout the day. Minor changes in only one of these two processes are enough to significantly decrease performance and clinically disrupt the quality of sleep. Disrupted or insufficient sleep those are wide-spread in our hectic modern society represent a serious public health problem. Chronic disturbances in sleep can have profound adverse physiological effects. For instance, epidemiological and experimental evidence reveals that poor sleep hygiene increases the risk for metabolic disorders such as type-2 diabetes and obesity [338]. Experimental studies also demonstrates that only 6 consecutive nights of 5h sleep are enough to increase levels of free fatty acids, beta-cell dysfunction, and insulin sensitivity. Moreover, the circadian system is tightly associated with metabolism at the molecular, cellular and system levels [339]. Mice with mutated or lack of some core clock genes such as *Bmal1* and *Clock* were responsible of metabolic syndrome with obesity, hyperglycemia, and hypoinsulinemia, while lack of *Per2* promote *inter alia* lymphomas [120], hyperinsulinemia [340], altered glucose homeostasis [341] and suppression of glucocorticoid rhythm [342]. It important to note that etiology of both chronic sleep loss and disrupted circadian rhythmicity might be through clock genes.

Strikingly, patients suffering of FASPS (human familial advanced sleep phase syndrome) have been found to have a mutation in PER2 [141] or in the kinase responsible for PER2 phosphorylation [144]. This syndrome is characterized by a very short circadian period with early sleep and early morning awakening time [140]. These patients have blood melatonin level and the body core temperature rhythm phase advanced by about 3-4 hours. Our work helps understanding this disease by strengthening the implication of *Per2* in the sleep-wake distribution and in sleep regulation. *Our results provide new knowledge on this gene which will help to design treatments for FASPS.* Moreover, the use of *Per* knock-out mice as model, allow to better understand their genes implication in many metabolic and physiological pathway as well in behavior.

IX. References

1. Hesiod, *Hesiod, the Homeric Hymns, and Homeric*. 1914. ll. 758-766.
2. Schopenhauer, A., *The Wisdom of Life and Counsels and Maxims*. 2011: Neeland Media LLC. 87.
3. Haas, L.F., *Hans Berger (1873-1941), Richard Caton (1842-1926), and electroencephalography*. *J Neurol Neurosurg Psychiatry*, 2003. **74**(1): p. 9.
4. Davis, H., et al., *Changes in Human Brain Potentials during the Onset of Sleep*. *Science*, 1937. **86**(2237): p. 448-50.
5. Aserinsky, E. and N. Kleitman, *Regularly occurring periods of eye motility, and concomitant phenomena, during sleep*. *Science*, 1953. **118**(3062): p. 273-4.
6. Jouvet, M., F. Michel, and J. Courjon, *Comptes rendus des séances de l'Académie des Science*. Vol. CLIII n° 6. 1959. p.1024.
7. Iber, C., et al., *The AASM manual for the scoring and sleep and associated events: rules, terminology and technical specification* American Academy of Sleep Medicine, 2007.
8. Everson, C.A., B.M. Bergmann, and A. Rechtschaffen, *Sleep deprivation in the rat: III. Total sleep deprivation*. *Sleep*, 1989. **12**(1): p. 13-21.
9. Pilcher, J.J. and A.I. Huffcutt, *Effects of sleep deprivation on performance: a meta-analysis*. *Sleep*, 1996. **19**(4): p. 318-26.
10. Benington, J.H. and H.C. Heller, *Restoration of brain energy metabolism as the function of sleep*. *Prog Neurobiol*, 1995. **45**(4): p. 347-60.
11. Scharf, M.T., et al., *The energy hypothesis of sleep revisited*. *Prog Neurobiol*, 2008. **86**(3): p. 264-80.
12. Tononi, G. and C. Cirelli, *Sleep function and synaptic homeostasis*. *Sleep Med Rev*, 2006. **10**(1): p. 49-62.
13. Ramanathan, L., et al., *Sleep deprivation decreases superoxide dismutase activity in rat hippocampus and brainstem*. *Neuroreport*, 2002. **13**(11): p. 1387-90.
14. Havekes, R., C.G. Vecsey, and T. Abel, *The impact of sleep deprivation on neuronal and glial signaling pathways important for memory and synaptic plasticity*. *Cell Signal*, 2012. **24**(6): p. 1251-60.
15. Hopfield, J.J., D.I. Feinstein, and R.G. Palmer, *Unlearning Has a Stabilizing Effect in Collective Memories*. *Nature*, 1983. **304**(5922): p. 158-159.
16. Luppi, P.H., et al., *The neuronal network responsible for paradoxical sleep and its dysfunctions causing narcolepsy and rapid eye movement (REM) behavior disorder*. *Sleep Med Rev*, 2011. **15**(3): p. 153-63.
17. Pace-Schott, E. and J. Hobson, *The neurobiology of sleep: genetics, cellular physiology and subcortical networks*. *Nat Rev Neurosci*, 2002. **3**(8): p. 591-605.
18. McCarley, R. and J. Hobson, *Neuronal excitability modulation over the sleep cycle: a structural and mathematical model*. *Science (New York, N.Y.)*, 1975. **189**(4196): p. 58-60.
19. Saper, C., T. Chou, and T. Scammell, *The sleep switch: hypothalamic control of sleep and wakefulness*. *Trends Neurosci*, 2001. **24**(12): p. 726-731.
20. Borbély, A., *A two process model of sleep regulation*. *Hum Neurobiol*, 1982. **1**(3): p. 195-204.
21. Dijk, D.J. and C.A. Czeisler, *Contribution of the circadian pacemaker and the sleep homeostat to sleep propensity, sleep structure, electroencephalographic slow waves, and sleep spindle activity in humans*. *J Neurosci*, 1995. **15**(5 Pt 1): p. 3526-38.
22. Edgar, D.M., W.C. Dement, and C.A. Fuller, *Effect of SCN lesions on sleep in squirrel monkeys: evidence for opponent processes in sleep-wake regulation*. *J Neurosci*, 1993. **13**(3): p. 1065-79.
23. Xu-Guang, L.I.U., et al., *Lesions of suprachiasmatic nucleus modify sleep structure but do not alter the total amount of daily sleep in rats*. *Sleep and Biological Rhythms*, 2012. **10**.
24. Larkin, J., et al., *Homeostatic regulation of sleep in arrhythmic Siberian hamsters*. *Am J Physiol Regul Integr Comp Physiol*, 2004. **287**(1): p. 11.

25. Easton, A., et al., *The suprachiasmatic nucleus regulates sleep timing and amount in mice*. *Sleep*, 2004. **27**(7): p. 1307-18.
26. Franken, P. and D.J. Dijk, *Circadian clock genes and sleep homeostasis*. *The European journal of neuroscience*, 2009. **29**(9): p. 1820-1829.
27. Eban-Rothschild, A. and G. Bloch, *Social influences on circadian rhythms and sleep in insects*. *Adv Genet*, 2012. **77**: p. 1-32.
28. Eiland, M.M., O.I. Lyamin, and J.M. Siegel, *State-related discharge of neurons in the brainstem of freely moving box turtles, *Terrapene carolina major**. *Arch Ital Biol*, 2001. **139**(1-2): p. 23-36.
29. Siegel, J.M., *Sleep viewed as a state of adaptive inactivity*. *Nat Rev Neurosci*, 2009. **10**: p. 747-753.
30. Lesku, J.A., N.C. Rattenborg, and C.J. Amlaner, *Sleep: A Comprehensive Handbook*. 2006. 1136.
31. Mang, G.M., et al. *Piezoelectric system as an alternative for electroencephalography in animal sleep experiments*. in *Congress of the European Sleep Research Society*. 2012. Paris, France.
32. Mang, G.M. and P. Franken, *Sleep and EEG Phenotyping in Mice*. *Current Protocols in Mouse Biology*, 2012: p. 55–74.
33. Osselton, J.W., *Acquisition of EEG data by bipolar, unipolar and average reference methods: a theoretical comparison*. *Electroencephalogr Clin Neurophysiol*, 1965. **19**(5): p. 527-8.
34. Brown, R.E., et al., *Control of sleep and wakefulness*. *Physiol Rev*, 2012. **92**(3): p. 1087-187.
35. Datta, S. and R. Maclean, *Neurobiological mechanisms for the regulation of mammalian sleep-wake behavior: reinterpretation of historical evidence and inclusion of contemporary cellular and molecular evidence*. *Neurosci Biobehav Rev*, 2007. **31**(5): p. 775-824.
36. Franken, P., A. Malafosse, and M. Tafti, *Genetic variation in EEG activity during sleep in inbred mice*. *Am J Physiol*, 1998. **275**(4 Pt 2): p. R1127-37.
37. Carskadon, M.A. and W. Dement, *Principles and Practice of Sleep Medicine*. 4 ed. Normal human sleep: An overview. 2005.
38. Espiritu, J.R., *Aging-related sleep changes*. *Clin Geriatr Med*, 2008. **24**(1): p. 1-14, v.
39. Hasan, S., et al., *Age-related changes in sleep in inbred mice are genotype dependent*. *Neurobiol Aging*, 2012. **33**(1): p. 195 e13-26.
40. Duncan, M., et al., *Effects of aging and genotype on circadian rhythms, sleep, and clock gene expression in APPxPS1 knock-in mice, a model for Alzheimer's disease*. *Exp Neurol*, 2012. **236**(2): p. 249-258.
41. Achermann, P., *EEG analysis applied to sleep*. *Epileptologie*, 2009. **26**: p. 28-33.
42. Bertini, M., et al., *Directional information flows between brain hemispheres during presleep wake and early sleep stages*. *Cereb Cortex*, 2007. **17**(8): p. 1970-8.
43. Kitaoka, K., et al., *Vitamin A deficiency induces a decrease in EEG delta power during sleep in mice*. *Brain Res*, 2007. **1150**: p. 121-30.
44. Purves, D., et al., *Neurosciences*. 4 ed. 2008.
45. Maret, S., et al., *Homer1a is a core brain molecular correlate of sleep loss*. *Proc Natl Acad Sci U S A*, 2007. **104**(50): p. 20090-20095.
46. Franken, P., D. Chollet, and M. Tafti, *The homeostatic regulation of sleep need is under genetic control*. *J Neurosci*, 2001. **21**(8): p. 2610-2621.
47. Tobler, I. and A.A. Borbely, *Sleep EEG in the rat as a function of prior waking*. *Electroencephalogr Clin Neurophysiol*, 1986. **64**(1): p. 74-6.
48. Curie, T., et al., *Homeostatic and circadian contribution to EEG and molecular state variables of sleep regulation*. *Sleep*, 2013. **36**(3): p. 311-23.
49. Werth, E., et al., *Dynamics of the sleep EEG after an early evening nap: experimental data and simulations*. *Am J Physiol*, 1996. **271**(3 Pt 2): p. R501-10.
50. Perlis, M., et al., *Beta EEG activity and insomnia*. *Sleep Med Rev*, 2001. **5**(5): p. 363-374.

51. Tafti, M., et al., *Deficiency in short-chain fatty acid beta-oxidation affects theta oscillations during sleep*. Nat Genet, 2003. **34**(3): p. 320-325.
52. Aston-Jones, G. and J.D. Cohen, *An integrative theory of locus coeruleus-norepinephrine function: adaptive gain and optimal performance*. Annu Rev Neurosci, 2005. **28**: p. 403-50.
53. Burdakov, D., et al., *Tandem-pore K⁺ channels mediate inhibition of orexin neurons by glucose*. Neuron, 2006. **50**(5): p. 711-22.
54. Billiard, M. and Y. Dauvilliers, *Les troubles du sommeil*. 2 ed. 2011.
55. Andretic, R., P. Franken, and M. Tafti, *Genetics of sleep*. Annu Rev Genet, 2008. **42**: p. 361-88.
56. Peyron, C., et al., *Neurons containing hypocretin (orexin) project to multiple neuronal systems*. J Neurosci, 1998. **18**(23): p. 9996-10015.
57. Saper, C.B., T.E. Scammell, and J. Lu, *Hypothalamic regulation of sleep and circadian rhythms*. Nature, 2005. **437**(7063): p. 1257-63.
58. Chemelli, R.M., et al., *Narcolepsy in orexin knockout mice: molecular genetics of sleep regulation*. Cell, 1999. **98**(4): p. 437-51.
59. de Lecea, L., et al., *The hypocretins: hypothalamus-specific peptides with neuroexcitatory activity*. Proc Natl Acad Sci U S A, 1998. **95**(1): p. 322-7.
60. Lin, L., et al., *The sleep disorder canine narcolepsy is caused by a mutation in the hypocretin (orexin) receptor 2 gene*. Cell, 1999. **98**(3): p. 365-76.
61. Sakurai, T., et al., *Orexins and orexin receptors: a family of hypothalamic neuropeptides and G protein-coupled receptors that regulate feeding behavior*. Cell, 1998. **92**(5): p. 1 page following 696.
62. Gélinau, J.-B.E., *De la narcolepsie*. 1881: Surgères.
63. Jones, B.E., *From waking to sleeping: neuronal and chemical substrates*. Trends Pharmacol Sci, 2005. **26**(11): p. 578-86.
64. McCormick, D.A., *Cholinergic and noradrenergic modulation of thalamocortical processing*. Trends Neurosci, 1989. **12**(6): p. 215-21.
65. Gervasoni, D., et al., *Role and origin of the GABAergic innervation of dorsal raphe serotonergic neurons*. J Neurosci, 2000. **20**(11): p. 4217-25.
66. Gaus, S.E., et al., *Ventrolateral preoptic nucleus contains sleep-active, galaninergic neurons in multiple mammalian species*. Neuroscience, 2002. **115**(1): p. 285-94.
67. Szymusiak, R., *Magnocellular nuclei of the basal forebrain: substrates of sleep and arousal regulation*. Sleep, 1995. **18**(6): p. 478-500.
68. Gallopin, T., et al., *Identification of sleep-promoting neurons in vitro*. Nature, 2000. **404**(6781): p. 992-5.
69. Chamberlin, N.L., et al., *Effects of adenosine on gabaergic synaptic inputs to identified ventrolateral preoptic neurons*. Neuroscience, 2003. **119**(4): p. 913-8.
70. Landolt, H.P., *Sleep homeostasis: a role for adenosine in humans?* Biochem Pharmacol, 2008. **75**(11): p. 2070-9.
71. Porkka-Heiskanen, T., et al., *Adenosine: a mediator of the sleep-inducing effects of prolonged wakefulness*. Science (New York, N.Y.), 1997. **276**(5316): p. 1265-1268.
72. Gallopin, T., et al., *The endogenous somnogen adenosine excites a subset of sleep-promoting neurons via A2A receptors in the ventrolateral preoptic nucleus*. Neuroscience, 2005. **134**(4): p. 1377-1390.
73. Schwierin, B., A.A. Borbely, and I. Tobler, *Effects of N6-cyclopentyladenosine and caffeine on sleep regulation in the rat*. Eur J Pharmacol, 1996. **300**(3): p. 163-71.
74. Jouvet, M., *[Research on the neural structures and responsible mechanisms in different phases of physiological sleep]*. Arch Ital Biol, 1962. **100**: p. 125-206.
75. Carli, G. and A. Zanchetti, *A study of pontine lesions suppressing deep sleep in the cat*. Arch Ital Biol, 1965. **103**(4): p. 751-88.
76. Webster, H.H. and B.E. Jones, *Neurotoxic lesions of the dorsolateral pontomesencephalic tegmentum-cholinergic cell area in the cat. II. Effects upon sleep-waking states*. Brain Res, 1988. **458**(2): p. 285-302.

77. Lu, J., et al., *A putative flip-flop switch for control of REM sleep*. *Nature*, 2006. **441**(7093): p. 589-94.
78. Vetrivelan, R., et al., *Medullary circuitry regulating rapid eye movement sleep and motor atonia*. *J Neurosci*, 2009. **29**(29): p. 9361-9.
79. Luppi, P.H., et al., *Brainstem mechanisms of paradoxical (REM) sleep generation*. *Pflugers Arch*, 2012. **463**(1): p. 43-52.
80. Dijk, D.J. and D.G. Beersma, *Effects of SWS deprivation on subsequent EEG power density and spontaneous sleep duration*. *Electroencephalogr Clin Neurophysiol*, 1989. **72**(4): p. 312-20.
81. Dijk, D.J. and R.E. Kronauer, *Commentary: models of sleep regulation: successes and continuing challenges*. *J Biol Rhythms*, 1999. **14**(6): p. 569-73.
82. Daan, S., D. Beersma, and A. Borbély, *Timing of human sleep: recovery process gated by a circadian pacemaker*. *Am J Physiol*, 1984. **246**(2 Pt 2): p. 83.
83. Achermann, P., *The two-process model of sleep regulation revisited*. *Aviat Space Environ Med*, 2004. **75**(3 Suppl): p. 43.
84. Hursh, S.R., et al., *Fatigue models for applied research in warfighting*. *Aviat Space Environ Med*, 2004. **75**(3 Suppl): p. A44-53; discussion A54-60.
85. Akerstedt, T., S. Folkard, and C. Portin, *Predictions from the three-process model of alertness*. *Aviat Space Environ Med*, 2004. **75**(3 Suppl): p. A75-83.
86. Moore-Ede, M., et al., *Circadian alertness simulator for fatigue risk assessment in transportation: application to reduce frequency and severity of truck accidents*. *Aviat Space Environ Med*, 2004. **75**(3 Suppl): p. A107-18.
87. Belyavin, A.J. and M.B. Spencer, *Modeling performance and alertness: the QinetiQ approach*. *Aviat Space Environ Med*, 2004. **75**(3 Suppl): p. A93-103; discussion 104-6.
88. Borbély, A.A. and P. Achermann, *Sleep Homeostasis and Models of Sleep Regulation*, in *Principles and practice of sleep medicine*, D.W.C. Roth T.Kryger M.H., Editor. 2011. p. 431-444.
89. Van Dongen, H., et al., *The cumulative cost of additional wakefulness: dose-response effects on neurobehavioral functions and sleep physiology from chronic sleep restriction and total sleep deprivation*. *Sleep*, 2003. **26**(2): p. 117-126.
90. Dinges, D. and P. Achermann, *Commentary: future considerations for models of human neurobehavioral function*. *J Biol Rhythms*, 1999. **14**(6): p. 598-601.
91. Dunlap, J.C., J.J. Loros, and P.J. Decoursey, *Chronobiology: Biological Timekeeping*. 2003.
92. Blatter, K. and C. Cajochen, *Circadian rhythms in cognitive performance: methodological constraints, protocols, theoretical underpinnings*. *Physiol Behav*, 2007. **90**(2-3): p. 196-208.
93. Asher, G. and U. Schibler, *Crosstalk between components of circadian and metabolic cycles in mammals*. *Cell Metab*, 2011. **13**(2): p. 125-137.
94. Hastings, M., A. Reddy, and E. Maywood, *A clockwork web: circadian timing in brain and periphery, in health and disease*. *Nat Rev Neurosci*, 2003. **4**(8): p. 649-661.
95. Dortous de Mairan, J.J., *Observation botanique in Histoire de l'academie royale des Sciences*. 1729. p. 35-36.
96. Moore, R.Y. and V.B. Eichler, *Loss of a circadian adrenal corticosterone rhythm following suprachiasmatic lesions in the rat*. *Brain Res*, 1972. **42**(1): p. 201-6.
97. Pittendrigh, C.S., *Circadian rhythms and the circadian organization of living systems*. *Cold Spring Harb Symp Quant Biol*, 1960. **25**: p. 159-84.
98. Aschoff, J., *Zeitgeber der tierischen Tagesperiodik*, in *Naturwissenschaften*. 1954. p. 49-56.
99. Balsalobre, A., *Resetting of Circadian Time in Peripheral Tissues by Glucocorticoid Signaling*. *Science*, 2000. **289**.
100. King, M.A., et al., *The validation of a new actigraphy system for the measurement of periodic leg movements in sleep*. *Sleep Med*, 2005. **6**(6): p. 507-13.
101. Jud, C., et al., *A guideline for analyzing circadian wheel-running behavior in rodents under different lighting conditions*. *Biol Proced Online*, 2005. **7**: p. 101-16.

102. Morin, L.P. and C.N. Allen, *The circadian visual system*, 2005. *Brain Res Rev*, 2006. **51**(1): p. 1-60.
103. Dudley, C., et al., *Altered patterns of sleep and behavioral adaptability in NPAS2-deficient mice*. *Science* (New York, N.Y.), 2003. **301**(5631): p. 379-383.
104. Waterhouse, J., et al., *Jet lag: trends and coping strategies*. *Lancet*, 2007. **369**(9567): p. 1117-29.
105. Schernhammer, E.S., et al., *Night-shift work and risk of colorectal cancer in the nurses' health study*. *J Natl Cancer Inst*, 2003. **95**(11): p. 825-8.
106. Dijk, D.J. and S.W. Lockley, *Integration of human sleep-wake regulation and circadian rhythmicity*. *J Appl Physiol*, 2002. **92**(2): p. 852-62.
107. Bradshaw, W. and C. Holzapfel, *What season is it anyway? Circadian tracking vs. photoperiodic anticipation in insects*. *J Biol Rhythms*, 2010. **25**(3): p. 155-165.
108. Schultz, T. and S. Kay, *Circadian clocks in daily and seasonal control of development*. *Science* (New York, N.Y.), 2003. **301**(5631): p. 326-328.
109. Stirland, J.A., *The tau mutation in the Syrian hamster alters the photoperiodic responsiveness of the gonadal axis to melatonin signal frequency*. *Endocrinology*, 1996. **137**.
110. Shimomura, K., et al., *Photoperiodic time measurement in tau mutant hamsters*. *J Biol Rhythms*, 1997. **12**(5): p. 423-430.
111. Ikeno, T., et al., *Photoperiodic diapause under the control of circadian clock genes in an insect*. *BMC biology*, 2010. **8**: p. 116.
112. Bradshaw, W. and C. Holzapfel, *Circadian clock genes, ovarian development and diapause*. *BMC biology*, 2010. **8**: p. 115.
113. Froy, O., et al., *Illuminating the Circadian Clock in Monarch Butterfly Migration*. *Science*, 2003. **300**.
114. Wiltschko, R., M. Walker, and W. Wiltschko, *Sun-compass orientation in homing pigeons: compensation for different rates of change in azimuth?* *The Journal of experimental biology*, 2000. **203**(Pt 5): p. 889-894.
115. Rana, S. and S. Mahmood, *Circadian rhythm and its role in malignancy*. *J Circadian Rhythms*, 2010. **8**: p. 3.
116. Filipinski, E., et al., *Host circadian clock as a control point in tumor progression*. *J Natl Cancer Inst*, 2002. **94**(9): p. 690-7.
117. Kondratov, R.V., et al., *Early aging and age-related pathologies in mice deficient in BMAL1, the core component of the circadian clock*. *Genes Dev*, 2006. **20**(14): p. 1868-73.
118. Gauger, M.A. and A. Sancar, *Cryptochrome, circadian cycle, cell cycle checkpoints, and cancer*. *Cancer Res*, 2005. **65**(15): p. 6828-34.
119. Ozturk, N., et al., *Loss of cryptochrome reduces cancer risk in p53 mutant mice*. *Proc Natl Acad Sci U S A*, 2009. **106**(8): p. 2841-2846.
120. Fu, L., et al., *The circadian gene Period2 plays an important role in tumor suppression and DNA damage response in vivo*. *Cell*, 2002. **111**(1): p. 41-50.
121. Takahashi, J.S., et al., *The genetics of mammalian circadian order and disorder: implications for physiology and disease*. *Nat Rev Genet*, 2008. **9**(10): p. 764-75.
122. Reppert, S.M. and D.R. Weaver, *Coordination of circadian timing in mammals*. *Nature*, 2002. **418**(6901): p. 935-41.
123. Lall, G.S., et al., *Distinct contributions of rod, cone, and melanopsin photoreceptors to encoding irradiance*. *Neuron*, 2010. **66**(3): p. 417-28.
124. Hattar, S., et al., *Melanopsin and rod-cone photoreceptive systems account for all major accessory visual functions in mice*. *Nature*, 2003. **424**(6944): p. 76-81.
125. Hannibal, J., *Neurotransmitters of the retino-hypothalamic tract*. *Cell Tissue Res*, 2002. **309**(1): p. 73-88.
126. Tischkau, S.A., et al., *Ca²⁺/cAMP response element-binding protein (CREB)-dependent activation of Per1 is required for light-induced signaling in the suprachiasmatic nucleus circadian clock*. *J Biol Chem*, 2003. **278**(2): p. 718-23.

127. Akiyama, M., et al., *Inhibition of light- or glutamate-induced mPer1 expression represses the phase shifts into the mouse circadian locomotor and suprachiasmatic firing rhythms.* J Neurosci, 1999. **19**(3): p. 1115-21.
128. Shigeyoshi, Y., et al., *Light-induced resetting of a mammalian circadian clock is associated with rapid induction of the mPer1 transcript.* Cell, 1997. **91**(7): p. 1043-53.
129. Allen, G., et al., *Oscillating on borrowed time: diffusible signals from immortalized suprachiasmatic nucleus cells regulate circadian rhythmicity in cultured fibroblasts.* J Neurosci, 2001. **21**(20): p. 7937-7943.
130. Buhr, E., S.-H. Yoo, and J. Takahashi, *Temperature as a universal resetting cue for mammalian circadian oscillators.* Science (New York, N.Y.), 2010. **330**(6002): p. 379-385.
131. Underwood, H., C. Steele, and B. Zivkovic, *Circadian organization and the role of the pineal in birds.* Microsc Res Tech, 2001. **53**(1): p. 48-62.
132. Watanabe, N., et al., *Circadian pacemaker in the suprachiasmatic nuclei of teleost fish revealed by rhythmic period2 expression.* Gen Comp Endocrinol, 2012. **178**(2): p. 400-7.
133. Bertolucci, C., et al., *Role of suprachiasmatic nuclei in circadian and light-entrained behavioral rhythms of lizards.* Am J Physiol Regul Integr Comp Physiol, 2000. **279**(6): p. R2121-31.
134. Paul, K.N., T.B. Saafir, and G. Tosini, *The role of retinal photoreceptors in the regulation of circadian rhythms.* Rev Endocr Metab Disord, 2009. **10**(4): p. 271-8.
135. Czeisler, C.A., et al., *Stability, precision, and near-24-hour period of the human circadian pacemaker.* Science, 1999. **284**(5423): p. 2177-81.
136. DeBruyne, J., D. Weaver, and S. Reppert, *CLOCK and NPAS2 have overlapping roles in the suprachiasmatic circadian clock.* Nat Neurosci, 2007. **10**(5): p. 543-545.
137. Dudley, C.A., et al., *Altered patterns of sleep and behavioral adaptability in NPAS2-deficient mice.* Science, 2003. **301**(5631): p. 379-83.
138. Skene, D. and J. Arendt, *Circadian rhythm sleep disorders in the blind and their treatment with melatonin.* Sleep Med, 2007. **8**(6): p. 651-655.
139. Lockley, S.W., et al., *Melatonin administration can entrain the free-running circadian system of blind subjects.* J Endocrinol, 2000. **164**(1): p. R1-6.
140. Sack, R.L., et al., *Entrainment of free-running circadian rhythms by melatonin in blind people.* N Engl J Med, 2000. **343**(15): p. 1070-7.
141. Gooley, J., *Treatment of circadian rhythm sleep disorders with light.* Annals of the Academy of Medicine, Singapore, 2008. **37**(8): p. 669-676.
142. Jones, C., et al., *Familial advanced sleep-phase syndrome: A short-period circadian rhythm variant in humans.* Nat Med, 1999. **5**(9): p. 1062-1065.
143. Toh, K., et al., *An hPer2 phosphorylation site mutation in familial advanced sleep phase syndrome.* Science (New York, N.Y.), 2001. **291**(5506): p. 1040-1043.
144. Xu, Y., et al., *Functional consequences of a CK1delta mutation causing familial advanced sleep phase syndrome.* Nature, 2005. **434**(7033): p. 640-644.
145. Takano, A., et al., *A missense variation in human casein kinase I epsilon gene that induces functional alteration and shows an inverse association with circadian rhythm sleep disorders.* Neuropsychopharmacology, 2004. **29**(10): p. 1901-1909.
146. Ebisawa, T., et al., *Association of structural polymorphisms in the human period3 gene with delayed sleep phase syndrome.* EMBO reports, 2001. **2**(4): p. 342-346.
147. Gallego, M. and D. Virshup, *Post-translational modifications regulate the ticking of the circadian clock.* Nature reviews. Molecular cell biology, 2007. **8**(2): p. 139-148.
148. Roenneberg, T., A. Wirz-Justice, and M. Meroz, *Life between clocks: daily temporal patterns of human chronotypes.* J Biol Rhythms, 2003. **18**(1): p. 80-90.
149. Roenneberg, T., et al., *Social jetlag and obesity.* Curr Biol, 2012. **22**(10): p. 939-43.
150. Konopka, R. and S. Benzer, *Clock mutants of Drosophila melanogaster.* Proc Natl Acad Sci U S A, 1971. **68**(9): p. 2112-2116.

151. Reddy, P., et al., *Molecular analysis of the period locus in Drosophila melanogaster and identification of a transcript involved in biological rhythms*. Cell, 1984. **38**(3): p. 701-710.
152. Bargiello, T., F. Jackson, and M. Young, *Restoration of circadian behavioural rhythms by gene transfer in Drosophila*. Nature, 1984. **312**(5996): p. 752-754.
153. Hardin, P., J. Hall, and M. Rosbash, *Feedback of the Drosophila period gene product on circadian cycling of its messenger RNA levels*. Nature, 1990. **343**(6258): p. 536-540.
154. Feldman, J.F. and M.N. Hoyle, *Isolation of circadian clock mutants of Neurospora crassa*. Genetics, 1973. **75**(4): p. 605-13.
155. Millar, A., et al., *Circadian clock mutants in Arabidopsis identified by luciferase imaging*. Science, 1995.
156. Vitaterna, M., et al., *Mutagenesis and mapping of a mouse gene, Clock, essential for circadian behavior*. Science (New York, N.Y.), 1994. **264**(5159): p. 719-725.
157. Dunlap, J.C., *Molecular bases for circadian clocks*. Cell, 1999. **96**(2): p. 271-90.
158. Buhr, E. and J. Takahashi, *Molecular components of the Mammalian circadian clock*. Handbook of experimental pharmacology, 2013. **217**: p. 3-27.
159. Zhou, Y., et al., *Molecular characterization of two mammalian bHLH-PAS domain proteins selectively expressed in the central nervous system*. Proc Natl Acad Sci U S A, 1997. **94**(2): p. 713-718.
160. Gekakis, N., et al., *Role of the CLOCK protein in the mammalian circadian mechanism*. Science (New York, N.Y.), 1998. **280**(5369): p. 1564-1569.
161. Ripperger, J. and U. Schibler, *Rhythmic CLOCK-BMAL1 binding to multiple E-box motifs drives circadian Dbp transcription and chromatin transitions*. Nat Genet, 2006. **38**(3): p. 369-374.
162. Ko, C. and J. Takahashi, *Molecular components of the mammalian circadian clock*. Human molecular genetics, 2006. **15 Spec No 2**: p. 7.
163. Bunger, M., et al., *Mop3 is an essential component of the master circadian pacemaker in mammals*. Cell, 2000. **103**(7): p. 1009-1017.
164. van der Horst, G., et al., *Mammalian Cry1 and Cry2 are essential for maintenance of circadian rhythms*. Nature, 1999. **398**(6728): p. 627-630.
165. Zheng, B., et al., *Nonredundant roles of the mPer1 and mPer2 genes in the mammalian circadian clock*. Cell, 2001. **105**(5): p. 683-94.
166. Guillaumond, F., et al., *Differential control of Bmal1 circadian transcription by REV-ERB and ROR nuclear receptors*. J Biol Rhythms, 2005. **20**(5): p. 391-403.
167. Cho, H., et al., *Regulation of circadian behaviour and metabolism by REV-ERB- α and REV-ERB- β* . Nature, 2012. **485**(7396): p. 123-127.
168. Liu, A., et al., *Redundant function of REV-ERB α and beta and non-essential role for Bmal1 cycling in transcriptional regulation of intracellular circadian rhythms*. PLoS genetics, 2008. **4**(2).
169. Sato, T., et al., *A functional genomics strategy reveals Rora as a component of the mammalian circadian clock*. Neuron, 2004. **43**(4): p. 527-537.
170. Akashi, M. and T. Takumi, *The orphan nuclear receptor ROR α regulates circadian transcription of the mammalian core-clock Bmal1*. Nature structural & molecular biology, 2005. **12**(5): p. 441-448.
171. Preitner, N., et al., *The orphan nuclear receptor REV-ERB α controls circadian transcription within the positive limb of the mammalian circadian oscillator*. Cell, 2002. **110**(2): p. 251-260.
172. Etchegaray, J.-P., et al., *Rhythmic histone acetylation underlies transcription in the mammalian circadian clock*. Nature, 2003. **421**(6919): p. 177-182.
173. Aguilar-Arnal, L. and P. Sassone-Corsi, *The circadian epigenome: how metabolism talks to chromatin remodeling*. Current opinion in cell biology, 2013. **25**(2): p. 170-176.
174. Katada, S. and P. Sassone-Corsi, *The histone methyltransferase MLL1 permits the oscillation of circadian gene expression*. Nature structural & molecular biology, 2010. **17**(12): p. 1414-1421.

175. Etchegaray, J.P., *The Polycomb Group Protein EZH2 Is Required for Mammalian Circadian Clock Function*. Journal of Biological Chemistry, 2006. **281**.
176. Feng, D., et al., *A circadian rhythm orchestrated by histone deacetylase 3 controls hepatic lipid metabolism*. Sci Signal, 2011. **331**(6022): p. 1315.
177. Belden, W. and J. Dunlap, *SIRT1 is a circadian deacetylase for core clock components*. Cell, 2008. **134**(2): p. 212-214.
178. Vielhaber, E., et al., *Nuclear entry of the circadian regulator mPER1 is controlled by mammalian casein kinase I epsilon*. Molecular and cellular biology, 2000. **20**(13): p. 4888-4899.
179. Eide, E., et al., *Control of mammalian circadian rhythm by CKIepsilon-regulated proteasome-mediated PER2 degradation*. Molecular and cellular biology, 2005. **25**(7): p. 2795-2807.
180. Akashi, M., et al., *Control of intracellular dynamics of mammalian period proteins by casein kinase I epsilon (CKIepsilon) and CKIdelta in cultured cells*. Molecular and cellular biology, 2002. **22**(6): p. 1693-1703.
181. Busino, L., et al., *SCFFbxl3 Controls the Oscillation of the Circadian Clock by Directing the Degradation of Cryptochrome Proteins*. Science, 2007. **316**.
182. Takano, A., et al., *Cloning and characterization of rat casein kinase 1epsilon*. FEBS Lett, 2000. **477**(1-2): p. 106-112.
183. Iitaka, C., et al., *A role for glycogen synthase kinase-3beta in the mammalian circadian clock*. J Biol Chem, 2005. **280**(33): p. 29397-29402.
184. Isojima, Y., et al., *CKIepsilon/delta-dependent phosphorylation is a temperature-insensitive, period-determining process in the mammalian circadian clock*. Proc Natl Acad Sci U S A, 2009. **106**(37): p. 15744-15749.
185. Brown, S., et al., *Rhythms of mammalian body temperature can sustain peripheral circadian clocks*. Curr Biol, 2002. **12**(18): p. 1574-1583.
186. Klaus, H., *Die relative Wirksamkeit von Zeitgebern*. Oecologia, 1969. **3**.
187. Morf, J., et al., *Cold-inducible RNA-binding protein modulates circadian gene expression posttranscriptionally*. Science (New York, N.Y.), 2012. **338**(6105): p. 379-383.
188. Rutter, J., et al., *Regulation of clock and NPAS2 DNA binding by the redox state of NAD cofactors*. Science (New York, N.Y.), 2001. **293**(5529): p. 510-514.
189. Reppert, S. and D. Weaver, *Molecular analysis of mammalian circadian rhythms*. Annu Rev Physiol, 2001. **63**: p. 647-676.
190. Laposky, A., et al., *Deletion of the mammalian circadian clock gene BMAL1/Mop3 alters baseline sleep architecture and the response to sleep deprivation*. Sleep, 2005. **28**(4): p. 395-409.
191. Wisor, J., et al., *A role for cryptochromes in sleep regulation*. BMC Neurosci, 2002. **3**: p. 20.
192. Franken, P., et al., *A non-circadian role for clock-genes in sleep homeostasis: a strain comparison*. BMC Neurosci, 2007. **8**: p. 87.
193. Naylor, E., et al., *The circadian clock mutation alters sleep homeostasis in the mouse*. J Neurosci, 2000. **20**(21): p. 8138-8143.
194. Franken, P., et al., *NPAS2 as a transcriptional regulator of non-rapid eye movement sleep: genotype and sex interactions*. Proc Natl Acad Sci U S A, 2006. **103**(18): p. 7118-7123.
195. Wisor, J., et al., *Sleep deprivation effects on circadian clock gene expression in the cerebral cortex parallel electroencephalographic differences among mouse strains*. J Neurosci, 2008. **28**(28): p. 7193-7201.
196. Vitaterna, M., et al., *Differential regulation of mammalian period genes and circadian rhythmicity by cryptochromes 1 and 2*. Proc Natl Acad Sci U S A, 1999. **96**(21): p. 12114-12119.
197. Bae, K., et al., *Differential functions of mPer1, mPer2, and mPer3 in the SCN circadian clock*. Neuron, 2001. **30**(2): p. 525-536.
198. Cermakian, N., et al., *Altered behavioral rhythms and clock gene expression in mice with a targeted mutation in the Period1 gene*. The EMBO journal, 2001. **20**(15): p. 3967-3974.

199. Zheng, B., et al., *The mPer2 gene encodes a functional component of the mammalian circadian clock*. Nature, 1999. **400**(6740): p. 169-173.
200. Xu, Y., et al., *Modeling of a human circadian mutation yields insights into clock regulation by PER2*. Cell, 2007. **128**(1): p. 59-70.
201. Shiromani, P., et al., *Sleep rhythmicity and homeostasis in mice with targeted disruption of mPeriod genes*. Am J Physiol Regul Integr Comp Physiol, 2004. **287**(1): p. 57.
202. Shearman, L., et al., *Targeted disruption of the mPer3 gene: subtle effects on circadian clock function*. Molecular and cellular biology, 2000. **20**(17): p. 6269-6275.
203. Kopp, C., et al., *Homeostatic sleep regulation is preserved in mPer1 and mPer2 mutant mice*. The European journal of neuroscience, 2002. **16**(6): p. 1099-1106.
204. Hasan, S., et al., *Altered sleep and behavioral activity phenotypes in PER3-deficient mice*. Am J Physiol Regul Integr Comp Physiol, 2011. **301**(6): p. 30.
205. Mang, G.M., et al. *Altered sleep homeostasis in Rev-erb(alpha) knock-out mice*. in Congress of the European Sleep Research Society. 2012. Paris, France.
206. Franken, P., A. Malafosse, and M. Tafti, *Genetic determinants of sleep regulation in inbred mice*. Sleep, 1999. **22**(2): p. 155-169.
207. Zhang, C., et al., *Prokineticin 2 is a target gene of proneural basic helix-loop-helix factors for olfactory bulb neurogenesis*. J Biol Chem, 2007. **282**(10): p. 6917-6921.
208. Mongrain, V., et al., *Separating the contribution of glucocorticoids and wakefulness to the molecular and electrophysiological correlates of sleep homeostasis*. Sleep, 2010. **33**(9): p. 1147-1157.
209. Kiessling, S., G. Eichele, and H. Oster, *Adrenal glucocorticoids have a key role in circadian resynchronization in a mouse model of jet lag*. J Clin Invest, 2010. **120**(7): p. 2600-2609.
210. Nakamura, T., et al., *Estrogen differentially regulates expression of Per1 and Per2 genes between central and peripheral clocks and between reproductive and nonreproductive tissues in female rats*. J Neurosci Res, 2005. **82**(5): p. 622-630.
211. Cheon, S., et al., *Glucocorticoid-mediated Period2 induction delays the phase of circadian rhythm*. Nucleic Acids Res, 2013.
212. Travnickova-Bendova, Z., et al., *Bimodal regulation of mPeriod promoters by CREB-dependent signaling and CLOCK/BMAL1 activity*. Proc Natl Acad Sci U S A, 2002. **99**(11): p. 7728-7733.
213. Cirelli, C. and G. Tononi, *Differential expression of plasticity-related genes in waking and sleep and their regulation by the noradrenergic system*. J Neurosci, 2000. **20**(24): p. 9187-9194.
214. Takumi, T., et al., *A light-independent oscillatory gene mPer3 in mouse SCN and OVL*. The EMBO journal, 1998. **17**(16): p. 4753-4759.
215. Albrecht, U., et al., *A differential response of two putative mammalian circadian regulators, mper1 and mper2, to light*. Cell, 1997. **91**(7): p. 1055-1064.
216. Yamajuku, D., et al., *Cellular DBP and E4BP4 proteins are critical for determining the period length of the circadian oscillator*. FEBS Lett, 2011. **585**(14): p. 2217-2222.
217. Zwilling, S., A. Annweiler, and T. Wirth, *The POU domains of the Oct1 and Oct2 transcription factors mediate specific interaction with TBP*. Nucleic Acids Res, 1994. **22**(9): p. 1655-1662.
218. Yang, C., et al., *Prevalence of the initiator over the TATA box in human and yeast genes and identification of DNA motifs enriched in human TATA-less core promoters*. Gene, 2007. **389**(1): p. 52-65.
219. Albrecht, U., et al., *The multiple facets of Per2*. Cold Spring Harb Symp Quant Biol, 2007. **72**: p. 95-104.
220. Ripperger, J.A. and U. Albrecht, *The circadian clock component PERIOD2: from molecular to cerebral functions*. Prog Brain Res, 2012. **199**: p. 233-45.
221. Yagita, K., et al., *Nucleocytoplasmic shuttling and mCRY-dependent inhibition of ubiquitylation of the mPER2 clock protein*. EMBO J, 2002. **21**(6): p. 1301-14.
222. Yagita, K., et al., *Dimerization and nuclear entry of mPER proteins in mammalian cells*. Genes Dev, 2000. **14**(11): p. 1353-63.

223. McIntosh, B., J. Hogenesch, and C. Bradfield, *Mammalian Per-Arnt-Sim proteins in environmental adaptation*. *Annu Rev Physiol*, 2010. **72**: p. 625-645.
224. Hefti, M., et al., *The PAS fold. A redefinition of the PAS domain based upon structural prediction*. *Eur J Biochem*, 2004. **271**(6): p. 1198-1208.
225. Ishida, M., T. Ueha, and I. Sagami, *Effects of mutations in the heme domain on the transcriptional activity and DNA-binding activity of NPAS2*. *Biochem Biophys Res Commun*, 2008. **368**(2): p. 292-7.
226. Kitanishi, K., et al., *Heme-binding characteristics of the isolated PAS-A domain of mouse Per2, a transcriptional regulatory factor associated with circadian rhythms*. *Biochemistry*, 2008. **47**(23): p. 6157-68.
227. Kaasik, K. and C.C. Lee, *Reciprocal regulation of haem biosynthesis and the circadian clock in mammals*. *Nature*, 2004. **430**(6998): p. 467-71.
228. Albrecht, U., et al., *MPer1 and mper2 are essential for normal resetting of the circadian clock*. *J Biol Rhythms*, 2001. **16**(2): p. 100-4.
229. Schmutz, I., et al., *The mammalian clock component PERIOD2 coordinates circadian output by interaction with nuclear receptors*. *Genes & development*, 2010. **24**(4): p. 345-357.
230. Ozber, N., et al., *Identification of two amino acids in the C-terminal domain of mouse CRY2 essential for PER2 interaction*. *BMC molecular biology*, 2010. **11**: p. 69.
231. Ohno, T., Y. Onishi, and N. Ishida, *The negative transcription factor E4BP4 is associated with circadian clock protein PERIOD2*. *Biochem Biophys Res Commun*, 2007. **354**(4): p. 1010-5.
232. Koike, N., et al., *Transcriptional architecture and chromatin landscape of the core circadian clock in mammals*. *Science (New York, N.Y.)*, 2012. **338**(6105): p. 349-354.
233. Franken, P., *A role for clock genes in sleep homeostasis*. *Curr Opin Neurobiol*, 2013.
234. Etchegaray, J.P., et al., *Rhythmic histone acetylation underlies transcription in the mammalian circadian clock*. *Nature*, 2003. **421**(6919): p. 177-82.
235. Rey, G., et al., *Genome-wide and phase-specific DNA-binding rhythms of BMAL1 control circadian output functions in mouse liver*. *PLoS Biol*, 2011. **9**(2): p. e1000595.
236. Ripperger, J.A. and U. Schibler, *Rhythmic CLOCK-BMAL1 binding to multiple E-box motifs drives circadian Dbp transcription and chromatin transitions*. *Nat Genet*, 2006. **38**(3): p. 369-74.
237. Stratmann, M., et al., *Flexible phase adjustment of circadian albumin D site-binding protein (DBP) gene expression by CRYPTOCHROME1*. *Genes Dev*, 2010. **24**(12): p. 1317-28.
238. Franken, P., et al., *NPAS2 as a transcriptional regulator of non-rapid eye movement sleep: genotype and sex interactions*. *Proc Natl Acad Sci U S A*, 2006. **103**(18): p. 7118-23.
239. Mongrain, V., et al., *Separating the contribution of glucocorticoids and wakefulness to the molecular and electrophysiological correlates of sleep homeostasis*. *Sleep*, 2010. **33**(9): p. 1147-57.
240. Travnickova-Bendova, Z., et al., *Bimodal regulation of mPeriod promoters by CREB-dependent signaling and CLOCK/BMAL1 activity*. *Proc Natl Acad Sci U S A*, 2002. **99**(11): p. 7728-33.
241. Graves, L., et al., *Genetic evidence for a role of CREB in sustained cortical arousal*. *J Neurophysiol*, 2003. **90**(2): p. 1152-1159.
242. Mongrain, V., et al., *Sleep loss reduces the DNA-binding of BMAL1, CLOCK, and NPAS2 to specific clock genes in the mouse cerebral cortex*. *PLoS One*, 2011. **6**(10).
243. Reynolds, A.C. and S. Banks, *Total sleep deprivation, chronic sleep restriction and sleep disruption*. *Prog Brain Res*, 2010. **185**: p. 91-103.
244. Borbely, A.A., *A two process model of sleep regulation*. *Hum Neurobiol*, 1982. **1**(3): p. 195-204.
245. Ko, C.H. and J.S. Takahashi, *Molecular components of the mammalian circadian clock*. *Hum Mol Genet*, 2006. **15 Spec No 2**: p. R271-7.
246. Gekakis, N., et al., *Role of the CLOCK protein in the mammalian circadian mechanism*. *Science*, 1998. **280**(5369): p. 1564-9.

247. Lee, C., et al., *Posttranslational mechanisms regulate the mammalian circadian clock*. Cell, 2001. **107**(7): p. 855-67.
248. Franken, P., et al., *The transcription factor DBP affects circadian sleep consolidation and rhythmic EEG activity*. J Neurosci, 2000. **20**(2): p. 617-25.
249. Naylor, E., et al., *The circadian clock mutation alters sleep homeostasis in the mouse*. J Neurosci, 2000. **20**(21): p. 8138-43.
250. Wisor, J.P., et al., *A role for cryptochromes in sleep regulation*. BMC Neurosci, 2002. **3**: p. 20.
251. Franken, P., et al., *A non-circadian role for clock-genes in sleep homeostasis: a strain comparison*. BMC Neurosci, 2007. **8**: p. 87.
252. Wisor, J.P., et al., *Sleep deprivation effects on circadian clock gene expression in the cerebral cortex parallel electroencephalographic differences among mouse strains*. J Neurosci, 2008. **28**(28): p. 7193-201.
253. Franken, P., et al., *Sleep deprivation in rats: effects on EEG power spectra, vigilance states, and cortical temperature*. Am J Physiol, 1991. **261**(1 Pt 2): p. R198-208.
254. Cai, W., et al., *Expression levels of estrogen receptor beta are modulated by components of the molecular clock*. Molecular and cellular biology, 2008. **28**(2): p. 784-793.
255. Guillaumond, F., et al., *Kruppel-like factor KLF10 is a link between the circadian clock and metabolism in liver*. Molecular and cellular biology, 2010. **30**(12): p. 3059-3070.
256. Haque, R., et al., *CLOCK and NPAS2 have overlapping roles in the circadian oscillation of arylalkylamine N-acetyltransferase mRNA in chicken cone photoreceptors*. J Neurochem, 2010. **113**(5): p. 1296-1306.
257. Fustin, J.M., et al., *Cry1 circadian phase in vitro: wrapped up with an E-box*. J Biol Rhythms, 2009. **24**(1): p. 16-24.
258. Bendova, Z., A. Sumova, and J.D. Mikkelsen, *Circadian and developmental regulation of N-methyl-d-aspartate-receptor 1 mRNA splice variants and N-methyl-d-aspartate-receptor 3 subunit expression within the rat suprachiasmatic nucleus*. Neuroscience, 2009. **159**(2): p. 599-609.
259. Hao, H., et al., *A fast carrier chromatin immunoprecipitation method applicable to microdissected tissue samples*. J Neurosci Methods, 2008. **172**(1): p. 38-42.
260. Taylor, P. and P.E. Hardin, *Rhythmic E-box binding by CLK-CYC controls daily cycles in per and tim transcription and chromatin modifications*. Mol Cell Biol, 2008. **28**(14): p. 4642-52.
261. Maret, S., et al., *Homer1a is a core brain molecular correlate of sleep loss*. Proc Natl Acad Sci U S A, 2007. **104**(50): p. 20090-5.
262. Hampp, G., et al., *Regulation of monoamine oxidase A by circadian-clock components implies clock influence on mood*. Curr Biol, 2008. **18**(9): p. 678-83.
263. Ramsey, K.M., et al., *Circadian clock feedback cycle through NAMPT-mediated NAD+ biosynthesis*. Science, 2009. **324**(5927): p. 651-4.
264. Menet, J.S., et al., *Dynamic PER repression mechanisms in the Drosophila circadian clock: from on-DNA to off-DNA*. Genes Dev, 2010. **24**(4): p. 358-67.
265. Yu, W., et al., *PER-dependent rhythms in CLK phosphorylation and E-box binding regulate circadian transcription*. Genes Dev, 2006. **20**(6): p. 723-33.
266. DeBruyne, J.P., D.R. Weaver, and S.M. Reppert, *CLOCK and NPAS2 have overlapping roles in the suprachiasmatic circadian clock*. Nat Neurosci, 2007. **10**(5): p. 543-5.
267. Zhou, Y.D., et al., *Molecular characterization of two mammalian bHLH-PAS domain proteins selectively expressed in the central nervous system*. Proc Natl Acad Sci U S A, 1997. **94**(2): p. 713-8.
268. Yamamoto, T., et al., *Acute physical stress elevates mouse period1 mRNA expression in mouse peripheral tissues via a glucocorticoid-responsive element*. J Biol Chem, 2005. **280**(51): p. 42036-43.
269. Petrzilka, S., et al., *Clock gene modulation by TNF-alpha depends on calcium and p38 MAP kinase signaling*. J Biol Rhythms, 2009. **24**(4): p. 283-94.

270. Patel, S.R., et al., *Sleep duration and biomarkers of inflammation*. Sleep, 2009. **32**(2): p. 200-4.
271. Hu, J., et al., *Sleep-deprived mice show altered cytokine production manifest by perturbations in serum IL-1ra, TNFa, and IL-6 levels*. Brain, Behavior, and Immunity, 2003. **17**.
272. Baracchi, F. and M.R. Opp, *Sleep-wake behavior and responses to sleep deprivation of mice lacking both interleukin-1 beta receptor 1 and tumor necrosis factor-alpha receptor 1*. Brain Behav Immun, 2008. **22**(6): p. 982-93.
273. Takahashi, S., et al., *Inhibition of tumor necrosis factor attenuates physiological sleep in rabbits*. Neuroreport, 1996. **7**(2): p. 642-6.
274. Bertolucci, C., et al., *Evidence for an overlapping role of CLOCK and NPAS2 transcription factors in liver circadian oscillators*. Mol Cell Biol, 2008. **28**(9): p. 3070-5.
275. DeBruyne, J.P., D.R. Weaver, and S.M. Reppert, *Peripheral circadian oscillators require CLOCK*. Curr Biol, 2007. **17**(14): p. R538-9.
276. Doi, M., J. Hirayama, and P. Sassone-Corsi, *Circadian regulator CLOCK is a histone acetyltransferase*. Cell, 2006. **125**(3): p. 497-508.
277. Nader, N., G.P. Chrousos, and T. Kino, *Circadian rhythm transcription factor CLOCK regulates the transcriptional activity of the glucocorticoid receptor by acetylating its hinge region lysine cluster: potential physiological implications*. FASEB J, 2009. **23**(5): p. 1572-83.
278. Ueda, H.R., et al., *System-level identification of transcriptional circuits underlying mammalian circadian clocks*. Nat Genet, 2005. **37**(2): p. 187-92.
279. Kondratov, R.V., et al., *Dual role of the CLOCK/BMAL1 circadian complex in transcriptional regulation*. FASEB J, 2006. **20**(3): p. 530-2.
280. Nakashima, A., et al., *DEC1 modulates the circadian phase of clock gene expression*. Mol Cell Biol, 2008. **28**(12): p. 4080-92.
281. Katada, S. and P. Sassone-Corsi, *The histone methyltransferase MLL1 permits the oscillation of circadian gene expression*. Nat Struct Mol Biol, 2010. **17**(12): p. 1414-21.
282. Maywood, E.S., et al., *Rapid down-regulation of mammalian Period genes during behavioral resetting of the circadian clock*. Proceedings of the National Academy of Sciences, 1999. **96**.
283. Abarca, C., U. Albrecht, and R. Spanagel, *Cocaine sensitization and reward are under the influence of circadian genes and rhythm*. Proc Natl Acad Sci U S A, 2002. **99**(13): p. 9026-30.
284. Garcia, J.A., et al., *Impaired cued and contextual memory in NPAS2-deficient mice*. Science, 2000. **288**(5474): p. 2226-30.
285. Wang, L.M., et al., *Expression of the circadian clock gene Period2 in the hippocampus: possible implications for synaptic plasticity and learned behaviour*. ASN Neuro, 2009. **1**(3).
286. Donlea, J.M., N. Ramanan, and P.J. Shaw, *Use-dependent plasticity in clock neurons regulates sleep need in Drosophila*. Science, 2009. **324**(5923): p. 105-8.
287. Sakai, T., et al., *A clock gene, period, plays a key role in long-term memory formation in Drosophila*. Proc Natl Acad Sci U S A, 2004. **101**(45): p. 16058-63.
288. Franken, P. and D.J. Dijk, *Circadian clock genes and sleep homeostasis*. Eur J Neurosci, 2009. **29**(9): p. 1820-9.
289. Mackiewicz, M., et al., *Macromolecule biosynthesis: a key function of sleep*. Physiol Genomics, 2007. **31**(3): p. 441-57.
290. Thompson, C.L., et al., *Molecular and anatomical signatures of sleep deprivation in the mouse brain*. Front Neurosci, 2010. **4**: p. 165.
291. Asher, G., et al., *SIRT1 regulates circadian clock gene expression through PER2 deacetylation*. Cell, 2008. **134**(2): p. 317-28.
292. Hirayama, J., et al., *CLOCK-mediated acetylation of BMAL1 controls circadian function*. Nature, 2007. **450**(7172): p. 1086-90.
293. Dijk, D.J. and P. Franken, *Interaction of sleep homeostasis circadian rhythmicity: dependent or independent systems?*, in *Principles and Practice of Sleep Medicine*, E. Saunders, Editor. 2005. p. 418-434.

294. Schlosser, A., J. Vanselow, and A. Kramer, *Mapping of phosphorylation sites by a multi-protease approach with specific phosphopeptide enrichment and NanoLC-MS/MS analysis*. *Anal Chem*, 2005. **77**(16): p. 5243-5250.
295. Zar, J.H., *Biostatistical analysis*. 5th ed. 2009: Pearson.
296. Sokolove, P.G. and W.N. Bushell, *The chi square periodogram: its utility for analysis of circadian rhythms*. *J Theor Biol*, 1978. **72**(1): p. 131-60.
297. Vandesompele, J., et al., *Accurate normalization of real-time quantitative RT-PCR data by geometric averaging of multiple internal control genes*. *Genome Biol*, 2002. **3**(7): p. RESEARCH0034.
298. Hellemans, J., et al., *qBase relative quantification framework and software for management and automated analysis of real-time quantitative PCR data*. *Genome Biol*, 2007. **8**(2): p. R19.
299. Baird, A.L., et al., *Daily methylphenidate and atomoxetine treatment impacts on clock gene protein expression in the mouse brain*. *Brain Res*, 2013. **1513**: p. 61-71.
300. Godinho, S.I., et al., *The after-hours mutant reveals a role for Fbxl3 in determining mammalian circadian period*. *Science*, 2007. **316**(5826): p. 897-900.
301. Gallagher, S.R., *One-dimensional SDS gel electrophoresis of proteins*. *Curr Protoc Mol Biol*, 2012. **Chapter 10**: p. Unit 10 2A.
302. Reick, M., et al., *NPAS2: an analog of clock operative in the mammalian forebrain*. *Science*, 2001. **293**(5529): p. 506-9.
303. Wyse, C. and A. Coogan, *Impact of aging on diurnal expression patterns of CLOCK and BMAL1 in the mouse brain*. *Brain Res*, 2010. **1337**: p. 21-31.
304. Abe, H., et al., *Circadian rhythms in behavior and clock gene expressions in the brain of mice lacking histidine decarboxylase*. *Brain Res Mol Brain Res*, 2004. **124**(2): p. 178-87.
305. Oishi, K., et al., *Clock mutation affects circadian regulation of circulating blood cells*. *J Circadian Rhythms*, 2006. **4**: p. 13.
306. Corbalán-Tutau, D., et al., *Daily profile in two circadian markers "melatonin and cortisol" and associations with metabolic syndrome components*. *Physiol Behav*, 2012.
307. James, F.O., N. Cermakian, and D.B. Boivin, *Circadian rhythms of melatonin, cortisol, and clock gene expression during simulated night shift work*. *Sleep*, 2007. **30**(11): p. 1427-36.
308. Steriade, M. and R.R. Llinas, *The functional states of the thalamus and the associated neuronal interplay*. *Physiol Rev*, 1988. **68**(3): p. 649-742.
309. Vertes, R.P. and B. Kocsis, *Brainstem-diencephalo-septohippocampal systems controlling the theta rhythm of the hippocampus*. *Neuroscience*, 1997. **81**(4): p. 893-926.
310. Vinogradova, O.S., *Expression, control, and probable functional significance of the neuronal theta-rhythm*. *Prog Neurobiol*, 1995. **45**(6): p. 523-83.
311. Buzsáki, G., *Theta oscillations in the hippocampus*. *Neuron*, 2002. **33**(3): p. 325-340.
312. Pendergast, J.S., K.D. Niswender, and S. Yamazaki, *The complex relationship between the light-entrainable and methamphetamine-sensitive circadian oscillators: evidence from behavioral studies of Period-mutant mice*. *Eur J Neurosci*, 2013.
313. Pendergast, J., et al., *Period determination in the food-entrainable and methamphetamine-sensitive circadian oscillator(s)*. *Proc Natl Acad Sci U S A*, 2012. **109**(35): p. 14218-14223.
314. Maywood, E.S., et al., *Analysis of core circadian feedback loop in suprachiasmatic nucleus of mCry1-luc transgenic reporter mouse*. *Proc Natl Acad Sci U S A*, 2013. **110**(23): p. 9547-52.
315. Steinlechner, S., et al., *Robust circadian rhythmicity of Per1 and Per2 mutant mice in constant light, and dynamics of Per1 and Per2 gene expression under long and short photoperiods*. *J Biol Rhythms*, 2002. **17**(3): p. 202-9.
316. Tsai, J.W., et al., *Melanopsin as a sleep modulator: circadian gating of the direct effects of light on sleep and altered sleep homeostasis in Opn4(-/-) mice*. *PLoS Biol*, 2009. **7**(6): p. e1000125.
317. Okamura, H., et al., *Photic induction of mPer1 and mPer2 in cry-deficient mice lacking a biological clock*. *Science*, 1999. **286**(5449): p. 2531-4.

318. Honma, S., et al., *Circadian behavioral rhythms in Cry1/Cry2 double-deficient mice induced by methamphetamine*. J Biol Rhythms, 2008. **23**(1): p. 91-94.
319. Hofstetter, J.R., et al., *Intermittent long-wavelength red light increases the period of daily locomotor activity in mice*. J Circadian Rhythms, 2005. **3**: p. 8.
320. Abramov, I., et al., *Sex and vision II: color appearance of monochromatic lights*. Biol Sex Differ, 2012. **3**(1): p. 21.
321. Nakamura, T., et al., *Effect of estrogen on the expression of Cry1 and Cry2 mRNAs in the suprachiasmatic nucleus of female rats*. Neurosci Res, 2001. **41**(3): p. 251-255.
322. Balsalobre, A., F. Damiola, and U. Schibler, *A serum shock induces circadian gene expression in mammalian tissue culture cells*. Cell, 1998. **93**(6): p. 929-937.
323. Nathans, J., *The evolution and physiology of human color vision: insights from molecular genetic studies of visual pigments*. Neuron, 1999. **24**(2): p. 299-312.
324. Hattar, S., et al., *Melanopsin and rod-cone photoreceptive systems account for all major accessory visual functions in mice*. Nature, 2003. **424**(6944): p. 76-81.
325. Provencio, I. and R. Foster, *Circadian rhythms in mice can be regulated by photoreceptors with cone-like characteristics*. Brain Res, 1995. **694**(1-2): p. 183-190.
326. Yoshimura, T. and S. Ebihara, *Spectral sensitivity of photoreceptors mediating phase-shifts of circadian rhythms in retinally degenerate CBA/J (rd/rd) and normal CBA/N (+/+)mice*. J Comp Physiol A, 1996. **178**(6): p. 797-802.
327. McCormack, C. and C. Sontag, *Entrainment by red light of running activity and ovulation rhythms of rats*. Am J Physiol, 1980. **239**(5): p. 3.
328. Strom, J.O., et al., *Ovariectomy and 17beta-estradiol replacement in rats and mice: a visual demonstration*. J Vis Exp, 2012(64): p. e4013.
329. Rusak, B. and I. Zucker, *Neural regulation of circadian rhythms*. Physiol Rev, 1979. **59**(3): p. 449-526.
330. Marchant, E. and R. Mistlberger, *Anticipation and entrainment to feeding time in intact and SCN-ablated C57BL/6j mice*. Brain Res, 1997. **765**(2): p. 273-282.
331. Jang, H., et al., *Feeding period restriction alters the expression of peripheral circadian rhythm genes without changing body weight in mice*. PLoS One, 2012. **7**(11).
332. Damiola, F., et al., *Restricted feeding uncouples circadian oscillators in peripheral tissues from the central pacemaker in the suprachiasmatic nucleus*. Genes & development, 2000. **14**(23): p. 2950-2961.
333. Wakamatsu, H., Y. Yoshinobu, and R. Aida..., ... *activity rhythm is associated with a phase-shift of the expression of mPer1 and mPer2 mRNA in the cerebral cortex and hippocampus but not in the suprachiasmatic European Journal of ...*, 2001.
334. Wu, T., et al., *Regulation of circadian gene expression in the kidney by light and food cues in rats*. Am J Physiol Regul Integr Comp Physiol, 2010. **298**(3): p. 41.
335. Kasahara, T., et al., *Genetic variation of melatonin productivity in laboratory mice under domestication*. Proc Natl Acad Sci U S A, 2010. **107**(14): p. 6412-7.
336. Korf, H. and C. Von Gall, *Mice, melatonin and the circadian system*. Mol Cell Endocrinol, 2006. **252**(1): p. 57-68.
337. Shimomura, K., et al., *Genetic suppression of the circadian Clock mutation by the melatonin biosynthesis pathway*. Proc Natl Acad Sci U S A, 2010. **107**(18): p. 8399-403.
338. Spiegel, K., et al., *Effects of poor and short sleep on glucose metabolism and obesity risk*. Nat Rev Endocrinol, 2009. **5**(5): p. 253-61.
339. Bass, J. and J.S. Takahashi, *Circadian integration of metabolism and energetics*. Science, 2010. **330**(6009): p. 1349-54.
340. Zhao, Y., et al., *Loss of mPer2 increases plasma insulin levels by enhanced glucose-stimulated insulin secretion and impaired insulin clearance in mice*. FEBS Lett, 2012. **586**(9): p. 1306-1311.

341. Carvas, J.M., et al., *Period2 gene mutant mice show compromised insulin-mediated endothelial nitric oxide release and altered glucose homeostasis*. *Front Physiol*, 2012. **3**: p. 337.
342. Yang, S., et al., *The role of mPer2 clock gene in glucocorticoid and feeding rhythms*. *Endocrinology*, 2009. **150**(5): p. 2153-2160.